Characterization of SPFH domain containing proteins in *Bacillus subtilis*

Dissertation

zur Erlangung des Doktorgrades der Naturwissenschaften
(Dr. rer. nat.)
an der Fakultät für Biologie der
Ludwig-Maximilians-Universität München

vorgelegt von

Abigail Savietto Scholz

aus Jundiaí (São Paulo, Brasilien)

München, 2023

Printed and/or published with the support of the

German Academic Exchange Service

Diese Dissertation wurde angefertigt unter der Leitung von Prof. Dr. Marc Bramkamp im Bereich der Mikrobiologie an der Ludwig-Maximilians-Universität München, jetzt Christian-Albrechts-Universität zu Kiel.

Erster Gutachter:	Prof. Dr. Marc Bramkamp
Zweiter Gutachter:	Prof. Joerg Nickelsen

Datum der Abgabe: 02.10.2023

Datum der mündlichen Prüfung: 19.03.2024

EIDESSTATTLICHE ERKLÄRUNG

Ich versichere hiermit an Eides statt, dass die vorgelegte Dissertation von mir selbständig und ohne unerlaubte Hilfsmittel angefertigt worden ist. Die vorliegende Dissertation wurde weder ganz, noch in wesentlichen Teiler einer anderen Prüfungskommission vorgelegt. Ich habe noch zu keinem früheren Zeitpunkt versucht, eine Dissertation einzureichen oder mich der Doktorprüfung zu unterziehen.

I hereby confirm that I have written the accompanying thesis by myself without contribution from any sources other than those cited in the text. Moreover, I declare that I have not submitted or defended a dissertation previously without success. This thesis has not been presented to any other examining board.

Hanau, den 02 October 2023

Abigail Savietto Scholz

Abigail Savietto Scholz

"Everything flows and nothing abides,
everything gives way and nothing stays fixed."
Heraclitus

TABLE OF CONTENTS

SUMMARY

Every living cell is enclosed by a flexible and dynamic membrane made of phospholipids and proteins. The bacterial plasma membrane and its proteins play a central role throughout the bacterial life cycle, promoting membrane compartmentalization for specific biochemical and molecular processes to occur in a correct time and place. The membrane also shields the cell from harmful chemicals and other threats. In bacteria and some eukaryotic organisms, a rigid structure known as the cell wall sits outside of the membrane and determines the cellular shape. The membrane adapts its composition and fluidity through a series of molecular interactions, which are critical for downstream cellular processes like membrane surveillance, repair, cell growth and division to work properly. Here, we aimed to describe and characterize aspects of membrane biology and bacterial membrane fluidity homeostasis, with focus on the characterization of the three known Stomatin-Prohibitin, Flotillin, HflK/C (SPFH)-domain proteins in *Bacillus subtilis*, namely the two flotillin proteins FloT and FloA, and YdjI. These proteins are genetically regulated by the ECF sigma factor σ^w which is triggered by membrane stressors such as alkaline shock, high salt concentrations, and phage infection. These proteins have been shown to be involved in membrane protection and direct regulation of membrane fluidity.

This thesis describes in the Chapter 2.1 a direct influence of membrane fluidity on MreB dynamics. Absence of flotillins reduces membrane fluidity, thereby altering MreB velocity and as consequences, in peptidoglycan synthesis. When bacterial cells lacking flotillins were treated with a membrane fluidizer, these phenotypes were suppressed. Further experiments revealed that flotillin FloT has an important impact on the ordering parameter along the entire acyl chain of phospholipids in model membranes, increasing dynamics of these molecules and, as consequence, increasing the membrane's fluidity. Fluidity in that sense, is a key physical parameter of the membrane that changes rapidly depending on the environment. Altogether, the results suggest a direct role of flotillins in maintenance of membrane's fluidity homeostasis, rather than for the formation of lipid scaffolds for other proteins to take place (bacterial "lipid rafts"), as previously thought. The proteins containing the SPFH domain in *B. subtilis*, including bacterial flotillins, have been shown to be involved in

membrane protection and membrane fluidity regulation, since they have the same genetic regulation by σ^w. Therefore, we further characterized a third bacterial SPFH-domain protein YdjI that is part of a stress induced complex in *B. subtilis.*

In the Chapter 2.2, we show that YdjI requires the help of two membrane integral proteins, YdjG/H, to localize the ESCRT-III homolog PspA to the membrane. Moreover, YdjI, unlike classical flotillins, was found in fluid membrane regions and was not enriched in detergent-resistant membrane fractions. However, deletion of YdjI reduced membrane fluidity, similarly to FloA and FloT deletion in *B. subtilis*. Our findings show that the membrane repair performed by phage-shock response system and the regulation of membrane fluidization and homeostasis driven by SPFH-domain proteins are closely intertwined.

ZUSAMMENFASSUNG

Lebende Zellen sind umgeben von flexiblen, dynamischen Membranen, die aus Phospholipiden und Proteinen bestehen. Die Bakterienmembran und ihre Proteine spielen während des gesamten bakteriellen Lebenszyklus eine zentrale Rolle: Sie fördern die Kompartimentierung der Membran, damit spezifische biochemische und molekulare Prozesse zur rechten Zeit am richtigen Ort ablaufen können. Die Membran schützt die Zelle auch vor schädlichen Chemikalien und anderen Bedrohungen. Bei Bakterien und einigen eukaryotischen Organismen befindet sich außerhalb der Membran eine starre Struktur, die als Zellwand bezeichnet wird und die Form der Zelle bestimmt. Die Membran hält die Homöostase durch eine Reihe von molekularen Wechselwirkungen aufrecht, die für das ordnungsgemäße Funktionieren nachgelagerter zellulärer Prozesse wie Membranintegrität, Reparatur, Zellwachstum und Zellteilung von entscheidender Bedeutung sind. Die in dieser Arbeit vorgestellten Ergebnisse beschreiben und charakterisieren Aspekte der Membranbiologie und der bakteriellen Membranhomöostase, wobei der Schwerpunkt auf der Charakterisierung der drei bekannten Stomatins-Prohibitins-Flotillins-HflK/C (SPFH)-Domänenproteine in *B. subtilis* liegt. Dieses sind die beiden Flotillin-Proteine FloT und FloA, sowie YdjI, welche nachweislich am Membranschutz und der direkten Regulierung der Membranfluidität beteiligt sind.

In der ersten Veröffentlichung zeigten wir mit Hilfe von Mikroskopietechniken, dass sich MreB in Gegenwart von Flotillinen schneller durch die Membran bewegt, als wenn keine Flotilline vorhanden sind: ein Hinweis darauf, dass Peptidoglycan-Synthese aktiver ist. Ähnliche Ergebnisse wurden nach Gabe eines Membranfluidisators auf Bakterienzellen erzielt, denen Flotilline fehlten. Weitere Experimente zeigten, dass die Flotilline es den Phospholipidmolekülen in einer künstlichen Membran ermöglichten, sich freier zu bewegen, was die Fluidität der Membran erhöhte. Insgesamt deuten die Ergebnisse auf eine direkte Rolle der Flotilline bei der Aufrechterhaltung der Membranfluiditäthomöostase hin, und nicht - wie bisher angenommen - auf die Bildung von Membrandomäne (sogenannten bakteriellen "Lipid Rafts") über direkte Protein-Lipid-Wechselwirkungen. Da sich zeigte, dass die Proteine mit der SPFH-Domäne - einschließlich der bakteriellen Flotilline - am

Membranschutz und an der Regulierung der Membranfluidität beteiligt sind, charakterisierten wir ein drittes bakterielles Protein mit SPFH-Domäne: YdjI. Dieses Protein ist Teil eines stressinduzierten Komplexes in *B. subtilis*. In einer zweiten Veröffentlichung zeigten wir, dass YdjI die Hilfe von zwei membranintegralen Proteinen YdjG/H benötigt, um das ESCRT-III-Homolog PspA an der Membran zu lokalisieren. Darüber hinaus ist YdjI im Gegensatz zu den klassischen Flotillinen in flüssigen Membranregionen zu finden und wird nicht in detergenzienresistenten Membranfraktionen angereichert. Die Deletion von YdjI reduziert die Membranfluidität, ebenso wie die Deletion von FloA und FloT aus *B. subtilis*. Unsere Ergebnisse zeigen, dass Membranreparatur durch das Phagen-Schock-System und die Regulierung der Membranfluidisierung und homöostase, durch SPFH-Domänenproteine eng miteinander verwoben sind.

ABBREVIATIONS

Abbreviation	Definition
B. subtilis	*Bacillus subtilis*
B2H	Bacterial two-hybrid
AMP	Antimicrobial Peptide
BnOH	Benzyl Alcohol
CESR	Cell envelop stress response
CL	Cardiolipin
DRM	Detergent Resistant Membrane (fraction)
DSM	Detergent Sensitive Membrane (fraction)
E. coli	*Escherichia coli*
ECF	Extracytoplasmic function (sigma) factor
GL	Glycolipids
GPI	Glycosylphosphatidylinositol
HADA	7-hydroxycoumarin 3-carboxylic acid-amino-D-alanine
HOPs	Hopanoids
IM30	Inner membrane associated protein of 30KDa
Laurdan	6-Dodecanoyl-2-Dimethylaminonaphthalene
Ld	Liquid disordered
Lo	Liquid ordered
LPG	Lysylphosphatidylglycerol
mNG	mNeonGrren (Monomeric fluorescent green/yellow fluorescent protein)
MOA	Mechanism of action
PA	Phosphatidic acid
PE	Phosphatidylethanolamine
PG	Phosphatidylglycerol
PI	Phosphatidylinositol
PS	Phosphatidylserine
RIF	Region of increased (membrane) fluidity
SPFH	Stomatins-Prohibitins-Flotillins-HflK/C (domain)
TCS	Two Component System
TIRF	Total internal reflection fluorescence (microscopy)

LIST OF PUBLICATIONS

I. **Flotillin-mediated membrane fluidity controls peptidoglycan synthesis and MreB movement.**

Zielińska A*, **Savietto A***, de Sousa Borges A, Martinez D, Berbon M, Roelofsen JR, Hartman AM, de Boer R, Van der Klei IJ, Hirsch AK, Habenstein B, Bramkamp M, Scheffers DJ. **eLife**. 14th July 2020; doi: 10.7554/eLife.57179.

**Authors contributed equally to this work.*

II. **An Stomatin, Prohibitin, Flotillin, and HflK/C-Domain Protein Required to Link the Phage-Shock Protein to the Membrane in *Bacillus subtilis.***

Scholz AS, Baur SSM, Wolf D and Bramkamp M. **Frontiers in Microbiology**. 28th October 2021; doi: 10.3389/fmicb.2021.754924

DECLARATION OF CONTRIBUTIONS

I. Zielińska A*, **Savietto A***, de Sousa Borges A, Martinez D, Berbon M, Roelofsen JR, Hartman AM, de Boer R, Van der Klei IJ, Hirsch AK, Habenstein B, Bramkamp M, Scheffers DJ. **Flotillin-mediated membrane fluidity controls peptidoglycan synthesis and MreB movement.** eLife. 2020 Jul 14;9:e57179. doi: 10.7554/eLife.57179. PMID: 32662773; PMCID: PMC7360373.

**Authors contributed equally to this work.*

Abigail Savietto Scholz contributed to the conceptualization of the paper, performed complete experimental design, data acquisition, statistical analysis and graphical editing of the main figures 2, 3, 4, figure 2 supplement 4, and all videos supplements to figure 4. She contributed with data acquisition and statistical analysis of main figure 1, specifically performing microscopy with DiI-C12 and cell length analysis, figure 2 supplement 1, performing cell length analysis, and additionally with graphical abstract and editing of main figure 5. Abigail Savietto Scholz contributed to writing of original draft, writing of the review response to editors and editing the final version of the paper.

II. **Scholz AS**, Baur SSM, Wolf D and Bramkamp M (2021). **An Stomatin, Prohibitin, Flotillin, and HflK/C-Domain Protein Required to Link the Phage-Shock Protein to the Membrane in *Bacillus subtilis*.** Front. Microbiol. 12:754924. doi: 10.3389/fmicb.2021.754924

Abigail Savietto Scholz contributed to the paper conceptualization, complete experimental design, strains construction, performed experiments and data acquision, data analysis and design of all figures, except figure 4E and supplements (experiments done by Sarah Baur) and Figure 6E (experiment done by Thomas Huber). The original manuscript was written by Abigail Savietto Scholz and Marc Bramkamp.

Abigail Savietto Scholz

Abigail Savietto Scholz

Prof. Dr. Marc Bramkamp

1. INTRODUCTION

1.1 Introductory note

Performing cell envelope and membrane organization studies can be relatively challenging, however the importance of such research is highlighted by the fact that one third of the genes from a bacterial genome encode membrane proteins (Wallin and Von Heijne, 1998; Liu *et al.*, 2002). The plasma membrane serves as a barrier between the cell and the outside environment, playing crucial physiological roles. Membrane proteins are essential for a wide range of biological functions, from transport to energy generation and signalling. Therefore, they are a major category of drug targets, since most drugs achieve the therapeutic effects via interacting with membrane proteins (Wallin and Von Heijne, 1998; Jamshad *et al.*, 2011). It is no surprise that the membrane's integrated function with its proteins is critical: through combined molecular interactions, the membrane maintain homeostatic modulation of key parameters such as thickness or fluidity, which is of utmost importance for downstream cellular processes such as cell growth and division to occur correctly, maintaining cellular integrity and allowing cellular life.

The results that comprise this thesis deal with the impact of various aspects of membrane biology with focus on the characterization of the so called Stomatin-Prohibitin-Flotillin-HflK/C (SPFH)-domain containing proteins in the gram-positive model bacterium *Bacillus subtilis*, namely FloT, FloA and YdjI – here demonstrated to be important for the control of cell wall synthesis and fluidity homeostasis, and cell envelope stress response.

1.2 Biological membranes and their physiological function

Every living cell and organelles are surrounded by viscoelastic layers of lipids and proteins. These layers are collectively known as cell membranes. The membrane acts as a physical and electrical barrier, preventing exogenous material from entering the cell and avoiding cellular contents from flowing out. The plasma membrane, as the main interface between the cell and its milieu, mediates communication with nearby cells as well as the extracellular matrix through a number of proteins found on this cellular structure. A multitude of

external signals that mediate important cellular activities are transmitted by distinct classes of membrane-bound proteins and lipids, and therefore, the plasma membrane also acts as a center for extremely dynamic and complex cellular biochemistry (Escribá and Nicolson, 2014), allowing energy generation in the form of ion gradients, transport ions, proteins, nucleic acids, nutrients and metabolites (Remaut and Fronzes, 2014). Integral membrane proteins take part in many crucial functions, such as nutrient uptake, antibiotic extrusion, ATP synthesis, stress transduction, conjugation, and protein secretion (Remaut and Fronzes, 2014).

Additionally, it controls the mechanical and physical properties of the cell assuming a conformation in response to the organization of cytoskeletal structures inside the cell, which determines the cell's shape and assists in cell movement by undergoing remodeling simultaneously with cytoskeletal rearrangements (Keren, 2011). Furthermore, cell membranes play a role in compartmentalization, ensuring that the appropriate molecular components are recruited to distinct regions to perform their specific functions. Therefore, membrane expansion must keep up with overall cell growth in a defined manner in time and space.

1.3 Bacterial envelope

1.3.1 Bacterial cell wall

The cell wall is a critical structural component of bacteria, with exception of Mollicutes (*Spiroplasma*, *Mycoplasma* and *Acholeplasma*), a class of bacteria distinguished by the absence of a cell wall (Trachtenberg, 2005). The cell wall sits just outside the cytoplasmic membrane, and together they form the cell envelope. Bacterial cell envelope is structurally diverse and functionally complex, allowing bacteria to survive and cope with an often dynamic and hostile environment (Rajagopal and Walker, 2015; Siegel *et al.*, 2016; Shrivastava, 2019). The integrity of the cell wall is of utmost importance for cell viability, since it determines the bacterial cell shape and confers resistance to the osmotic pressure generated by the cell turgor. Bacterial envelopes are classified into two broad types, Gram-positive or Gram-negative, depending on whether it retains the Gram stain (Gram, 1884; Bartholomew and Mittwer, 1952). Both cell

envelopes surround a phospholipid bilayer plasma membrane (PM), also known as inner membrane (IM). The scaffolding of the cell wall consists of the cross-linked polymer peptidoglycan (PG), in both Gram-positive and Gram-negative bacteria. Gram-negative bacteria, have only 1 to 3 peptidoglycan layers, making up a 5-10 nm structure, and a lipid bilayer called the outer membrane (7.5-10 nm thick) composed mainly of lipopolysaccharides. The cell wall lies in the periplasmic space between the outer membrane and the inner membrane. The bacterium *Escherichia coli* is the most researched Gram-negative bacterium (Milton R.J. Salton *et al.*, 1996).

Gram-positive bacteria, such as *B. subtilis*, lack an outer membrane and therefore the cell wall is the direct contact area with the external environment. The PM is encased by a thick (20-80 nm) cell wall composed of 10 to 30 layers of peptidoglycan and covalently linked teichoic, teichuronic acid polymers, as well as proteins. The Gram-positive cell wall is composed of two major structural components, the peptidoglycan and anionic polymers that are covalently linked to the PG or to the cytoplasmic membrane via acyl chain membrane anchors. *B. subtilis* proteome analysis revealed 11 proteins that are associated to the cell wall (Antelmann *et al.*, 2002).

Peptidoglycan (PG) or murein, is a macromolecule composed of long glycan chains cross-linked by peptide bridges forming strong but flexible polymer structures that confers resistance to the underlying protoplast against the internal osmotic pressure (Vollmer and Seligman, 2010). The glycan chains are formed by alternating β-1,4-linked, N-acetylglucosamine (GlcNAc) and N-acetylmuramic acid (MurNAc) subunits. An organization model on PG architecture was first published in 1964, where the authors concluded that the glycan strands run parallel to the plasma membrane (Weidel and Pelzer, 1964). Although sophisticated techniques have made substantial progress in the field, our understanding of how cell wall is structured is still far from complete. Advanced methods such as electron cryo-tomography, molecular dynamics simulations, atomic force microscopy studies and solid-state NMR experiments still support the classical model of parallel PG organization in *Bacillus* (Hayhurst *et al.*, 2008; Turner *et al.*, 2010; Beeby *et al.*, 2013; Pasquina-Lemonche *et al.*, 2020a). The cell wall has a rough surface on the outside, but on the interior, where the PG is synthesized, cables of around 50 nm in width runs parallel to the short axis of the cell (Hayhurst *et al.*, 2008). In *S. aureus*, nascent PG is deposited in concentric rings at the septum, also arguing for a parallel

organization of the glycan strands (Turner *et al.*, 2010). In *Bacillus*, PG strands are arranged as circumferential furrows rather than coiled cables, and peptide crosslinks are placed parallel to the cell's long axis that increase in length but not in width when peptide crosslinks are broken (Beeby *et al.*, 2013). Recent AFM data revealed that the cell wall of *B. subtilis* is decorated with large and deep pores on the outside surface and that the polymer-like structure from the inside is a much denser material when compared to the outside portion (Pasquina-Lemonche *et al.*, 2020b).

The cell wall is overall negatively charged due to the presence of anionic PG-linked polymers that in majority are wall teichoic acids (WTA) and lipoteichoic acids (LTA) (Neuhaus and Baddiley, 2003). They have functions in controlling porosity of the cell wall as consequences of cation binding, anchoring of wall associated proteins, phage binding, autolysin activity regulation, mediation of DNA binding during competence and regulation of cell division dependent on their distribution on the cell surface (Swoboda *et al.*, 2010; Brown *et al.*, 2013; Mirouze *et al.*, 2018).

Synthesis of cell wall precursor components occurs in the cytoplasm and must be subsequently flipped across the cytoplasmic membrane to be assembled into the cell wall. To promote the translocation of a hydrophilic substrate from one aqueous environment to another across the hydrophobic barrier, a disaccharide precursor must be coupled to a lipid molecule, therefore all PG, WTA and teichuronic acid precursors link to the lipid carrier undecaprenyl-phosphate (bactoprenol) to be flipped across the membrane. Different translocases have been found to act as particular translocases or flippases for Lipid II (GlcNAc-β-(1,4)-MurNAc-(pentapeptide)-pyrophosphoryl-undecaprenol) (Scheffers and Tol, 2015).

FtsW/RodA homologues, members of Shape, Elongation, Division and Sporulation (SEDS) protein family were firstly proposed as candidate translocases. Recent reports suggested RodA and likely also FtsW to have their primary function as glycan strand elongation factors, acting as glycosyltransferases in combination with their cognate transpeptidases PBP2 and FtsI (Class B PBP – penicillin binding protein B) (Meeske *et al.*, 2016; Emami *et al.*, 2017; Taguchi *et al.*, 2019; Sjodt *et al.*, 2020; Li *et al.*, 2021). However, these findings do not exclude the possibility that FtsW/RodA might simultaneously flip Lipid II and then use it to elongate the glycan strands. The MurJ Lipid II

flippase is considered a to be part of the multidrug-oligosaccaridyl-lipid-polysaccharide exporter superfamily (MOP) (Hvorup 2003). MurJ was firstly identified in a genomic study specific for bacteria with cell wall. Depletion of MurJ levels causes defects in cell shape maintenance (Ruiz, 2008).

PBPs catalyze the transglycosylation and transpeptidation reactions that result in the formation of the PG's glycosidic and peptide bonds. In the transglycosylation reaction, the glycan chain is elongated by the formation of a glycosidic bond between Lipid II and the lipid-linked PG strand. The terminal D-Ala-D-Ala of one stem peptide is attached to the active site of the enzyme during the transpeptidation reaction by binding of the penultimate D-Ala to the catalytic serine in the protein, which occurs concurrently with the release of the terminal D-Ala. The PBPs are a class of acyl serine transferases divided in high (HMW > 60 KDa), low molecular weight (LMW < 60 KDa) and β-lactamases. LMW PBPs catalyze carboxypeptidases and endopeptidase reactions whereas β-lactamases cleave β-lactam rings and thereby facilitate resistance to penicillin and analogous antibiotics (Ghuysen, 1991). HMW PBPS catalyze transglycosylation and transpeptidation reactions, are attached to the cytoplasmic membrane via transmembrane helixes. They are further subdivided in classes A and B PBPs, based on their primary structure and N-terminal domain catalytic-activity (Goffin and Ghuysen, 1998). *B. subtilis* has four genes that encode class A PBPs. The *ponA* gene produces both PBP1a and PBP1b, which are differentiated by the C-terminal protein processing (Popham and Setlow, 1995). PBP1 has non-essential functions in cell division, is involved in pole maturation, cell elongation and have localization shuttling between division site and lateral wall (Popham and Setlow, 1995; Claessen *et al.*, 2008).

During cell elongation and division, the cell wall is continuously turned over, with PG being constantly hydrolyzed and synthesized on the cell wall in a very controlled manner, without causing disruptions in the polymer structure during insertion of new synthesized PG strands in the meshwork. This process involves a principle called “make-before-break”, where it is proposed that biochemical reactions catalyzed by multi-enzyme complexes, synthesized the new material that will be inserted close to the membrane where the PBPPs are (Höltje, 1998). PG is displaced outwards as a result of the incorporated new material. On moving out, the PG is stretched and becomes stress-bearing, but also more susceptible to the activity of autolysins (Koch, 2000). In 2001, the discovery of

the bacterial cytoskeletal proteins and their control of cell shape led to the suggestion that the multi-enzyme complexes that synthesize the cell wall are controlled by the cytoskeleton (Jones *et al.*, 2001).

To enable cell multiplication with optimum cell length and width, septal and lateral cell wall synthesis must be coordinated and controlled. The elongasome is a multi-protein complex that is involved in PG synthesis at the lateral wall during cell elongation. It is linked to the cytoskeleton protein MreB (Carballido-López and Formstone, 2007; Hussain *et al.*, 2018). MreB is assumed to be composed of short membrane associated filaments that autonomously move across the cell width on the inner surface of the cytoplasmic membrane (Jones *et al.*, 2001). The majority of rod-shaped bacteria have at least one *mreB* homologue. MreB, a bacterial actin homologue, is closely connected with cell shape, and loss of MreB results in spherical cells rather than rod-shaped cells (Wachi *et al.*, 1987; Jones *et al.*, 2001). MreB controls and regulates cell shape by affecting cell wall production dynamics in the following ways: a) MreB interacts with PBPs and enzymes involved in the synthesis of Lipid II and PG hydrolysis (Carballido-López *et al.*, 2006; Kawai *et al.*, 2009; Rueff *et al.*, 2014); b) MreB naturally organizes the membrane into regions of increased fluidity (RIFs) that can incorporate more Lipid II (Strahl *et al.*, 2014; Scheffers and Tol, 2015); c) Ongoing cell wall synthesis and presence of Lipid II control MreB dynamics and membrane association (Domínguez-Escobar *et al.*, 2011; Garner *et al.*, 2011; Van Teeffelen *et al.*, 2011; Schirner *et al.*, 2015).

1.3.2 Cytoplasmic membrane

One of the first accepted model of the plasma membrane organization was proposed by Singer and Nicolson in their landmark paper from 1972 (Singer and Nicolson, 1972a), where they postulated the Fluid-Mosaic Membrane Model (F-MMM) that has shaped our knowledge on the structure and function of biological membranes since then. The model was proposed based on thermodynamic principals of organization of membrane lipids and proteins and the forehead available evidence of asymmetry and lateral mobility within the membrane matrix. In their model, they postulated that:

> *"the proteins […] are a heterogeneous set of globular molecules, each arranged in an amphipathic structure, that is, with the ionic and highly polar groups protruding from the membrane*

> *into the aqueous phase, and the nonpolar groups largely buried in the hydrophobic interior of the membrane. These globular molecules are partially embedded in a matrix of phospholipid. The bulk of the phospholipid is organized as a discontinuous, fluid bilayer, although a small fraction of the lipid may interact specifically with the membrane proteins. The fluid mosaic structure is therefore formally analogous to a two-dimensional oriented solution of integral proteins (or lipoproteins) in the viscous phospholipid bilayer solvent."*

This model depicts membranes as two-dimensional fluids composed of lipid bilayers interspersed with proteins in a mosaic-like pattern. The lipid molecules' hydrophilic phosphate head groups are in contact with the aqueous environment at the bilayer's outer surface, whilst the two hydrophobic lipid chains are confined to the inner side of the bilayer, away from any interaction with the fluidic environment. The fluid mosaic model considers the dynamic character of bilayer membrane architecture, which happens as a result of the continual rotational and lateral mobility of the integral lipid and protein molecules (Singer and Nicolson, 1972b). While lipids supply the fundamental structure of membranes, proteins perform a wide range of specialized functions, from ion and small molecule transport to signaling pathway regulation.

The authors considered that the cytoplasmic membrane was a two-dimensional liquid structure with free lateral diffusion of lipids and associated proteins, resulting in an idea that the plasma membrane was a relatively homogeneous structure. However, the fluid mosaic model has been refined in the past years to account for the complexity and high organization that cytoskeletal structures give to the membrane. Later reports claimed that lipid distribution *in vitro* was more heterogeneous than previously thought, contradicting the aspect of free diffusion within the membrane proposed by the F-MMM (Karnovsky *et al.*, 1982). This is due to the ability of certain lipid species to cluster into domains based on their vary physicochemical properties (Vereb *et al.*, 2003). Early studies of membrane lipid-protein heterogeneity revealed quite defined lipid domains, which are more rigid, surrounded by freely dispersed lipid molecules, which are more fluid (Wunderlich *et al.*, 1975). Studies about membrane compartmentalization and the formation of membrane microdomains account for the presence of large protein domains or complexes,

for example, due to protein-protein interaction, as well as a wide-ranging membrane thickness due to diversity of fatty acids. Recent membrane compartmentalization studies, in that sense, brings new insights to the classical fluid mosaic model.

1.4 Membrane Composition

The physiochemical properties of cell membranes are determined by their molecular composition. The types of lipids and their densities present in the membrane, for example, determine a multitude of membrane features such as phase behaviour, viscosity (ability to flow like a liquid), rigidity and thickness (Holthuis and Menon, 2014). Similarly, the accumulation of distinct curvature-sensing lipids and proteins causes curvature in limited parts of the membrane, which dictates its form on a broader scale (McMahon and Boucrot, 2015). The distribution of these molecular components in the bilayer is influenced by dynamic lipid-protein interactions on the cell membrane, resulting in the formation of distinct membrane domains with specialized functions. The lipidome and membrane protein abundance or crowding have important impact on various aspects of the physicochemical properties of bacterial membranes leading to changes in the membrane composition and regulation (Saxton and Jacobson, 1997).

The cytoplasmic membrane of bacteria is composed of proteins and lipids. While the exact composition may vary between different bacterial species, there is a great diversity and complexity in the lipids and synthetic pathways that contribute to the formation and characteristics of the membrane. In order to understand further the concept of membrane compartmentalization, it is important to look at the architecture and composition of membranes and how the diversity of its components impact important aspects of membrane biology.

1.4.1 Membrane lipids

Lipids are a structurally diverse group of compounds with the property of being highly soluble in nonpolar solvents (e.g., methanol, chloroform) but relatively insoluble in water. Essentially most of the lipids in prokaryotes are in the membranes. Phospholipids, which consist of fatty acids esterified to glycerol phosphate derivatives are the major membrane lipids in bacteria and Eukaryotes.

Membranes are composed by amphiphilic lipids which are mainly glycerophospholipids, composed of two fatty acids, a glycerol moiety, a phosphate group and a variable head group (Sohlenkamp and Geiger, 2016). In aqueous solutions, phospholipids are driven by hydrophobic interactions, which result in the fatty acid tails aggregating to minimize interactions with the water, resulting in an energy-efficient phospholipid bilayer of oppositely oriented phospholipid molecules. The lipid molecules' hydrophilic head groups face the bilayer's outer sides, shielding the hydrophobic tail from hydrophilic moieties (Green, David E., 1971).

The most frequently membrane-forming lipids in bacteria are zwitterionic phosphatidylethanolamine (PE), phosphatidylglycerol (PG), cardiolipin (CL), lysyl-phosphatidylglycerol (LPG), phosphatidylinositol (PI), phosphatidic acid (PA) and phosphatidylserine (PS) (Sohlenkamp and Geiger, 2016). Exponentially growing *Escherichia coli* cells contain a lipidome composed of primary 75 % PE, 20 % PG and 5 % CL (Raetz and Dowhan, 1990; Sohlenkamp and Geiger, 2016); whereas in the Gram-positive bacterium *B. subtilis,* the lipidome of exponentially growing cells comprises ~50 % PE, ~25 % PG, ~17 % LPG and ~8% CL (López *et al.*, 2006). Studies on simplified membranes in *B. subtilis*, with lipid biosynthesis enzymes mutants, have shown that cells can grow similarly to wild type rates when the membrane is formed predominantly by phosphatidylglycerol, suggesting that PG is the only essential phospholipid in *B. subtilis* (Salzberg and Helmann, 2008; Nickels *et al.*, 2017). In addition to the dominant phospholipids and glycolipids, bacteria can also synthesize membrane lipids that are free of phosphorus. These are membranes that contain ornithine lipids (OLs), sulfolipids, diacyl glyceryl-N,N,N- trimethyl homoserine (DGTS), glycolipids (GLs), diacylglycerol (DAG), hopanoids (HOPs) in their composition (Sohlenkamp and Geiger, 2016).

Aside from the phospholipid family, biological membranes contain a wide range of lipids with different physicochemical properties that helps the membrane to adapt to different conditions (Sohlenkamp and Geiger, 2016), suggesting that the lipidome of a cell contributes to special functions of membranes. Despite the fact that membranes have a complex and adaptive lipidome, cells are greatly resistant to genetic deletion of lipid synthetic pathways (Sohlenkamp and Geiger, 2016; Chwastek *et al.*, 2020). Other lipids associated with the membrane include isoprenoids and their derivatives such as hopanoids and carotenoids. Unlike Eukaryotic cells, where cholesterol and sphingolipids represent the major components of membrane, bacteria are uncapable to produce either of these

lipids. Instead, several bacterial species produce hopanoids, with physicochemical properties similar to that sterol compound. Analogous to cholesterol, hopanoids are classified as terpenoids or isoprenoids and have vastly diverged lipid synthesis pathways, based on the conversion of isoprene-based precursors – such as farnesyl pyrophosphate – into cyclic or non-cyclic terpenoids. Cholesterol is synthesized by condensation of isoprenoid precursors head-to-head to produce acyclic squalene, which is subsequently cyclized to its final state. Although prokaryotes lack the mechanism to convert squalene precursors to cholesterol, bacteria cyclize squalene precursors into hopanoids (e.g. sporulenes, diplopterol) (Bosak *et al.*, 2008; Kontnik *et al.*, 2008). Importantly, hopanoid synthesis does not require molecular oxygen, and hopanoids have been reported in sediments predating the enrichment of oxygen in the atmosphere (Brocks *et al.*, n.d.; Ohtomo *et al.*, 2014). Therefore, it was proposed that they might serve as sterol surrogates in bacteria, especially since hopanoids and sterols share structural features and are cyclized by similar related cyclase enzymes (Sáenz *et al.*, 2015).

Hopanoids are found in several bacterial species and in similarity with eukaryotic sterols, hopanoids are membrane lipids with a planar geometry, are polycyclic hydrocarbons with five rings instead of four rings as sterols, including a variety of polar and nonpolar side chains (Rohmer *et al.*, 1979; Sáenz *et al.*, 2012). The structural analogy resembles their functional similarities: both sterols and hopanoids modulate the fluidity and permeability, are related to lateral segregation and tendency for membranes to bind and integrate other biomolecules (Van Meer *et al.*, 2008). This membrane features contribute for their propensity to constrain and order lipid bilayers, promoting lipid ordering at the rotational freedom of motion and lateral packing of lipids within the bilayer's plane.

Hopanoids are thought to intercalate into phospholipid bilayers and control membrane fluidity by interacting with their lipid components. In model membranes, diplopterol produces phase separation and enhances lipid packing while maintaining membrane fluidity and compressibility similarly as eukaryotic sterols such as cholesterol, stigmasterol, and ergosterol (Sáenz *et al.*, 2012; Sáenz *et al.*, 2015; Mangiarotti *et al.*, 2019). Hopanoids are also crucial in lowering membrane permeability, including oxygen diffusion (Fischer *et al.*, 2005; Härtner *et al.*, 2005; Belin *et al.*, 2018). They also allow bacteria to adapt to stress induced by extreme environmental conditions such as high

temperatures, low pH, detergents, and antibiotics. Hopanoids have been found in “exposed” membranes that requires additional stability: the plasma membrane and outer membranes of Gram-negative bacteria, as well as the outer membrane and thylakoid membranes of cyanobacteria. There, they interact with glycolipids to form a highly ordered bilayer, similar to how sterols interact with sphingolipids to form raft-like microdomains in eukaryotic plasma membranes (Rexroth *et al.*, 2011). Hopanoids typically make up 1 to 5% of total lipids in cells, but their percentage can rise significantly in response to stress. *Bacillus acidocaldarius*, for instance, produces nearly seven times more hopanoids at 65 ˚C than it does at 60 ˚C (Poralla *et al.*, 1984), likely to counteract for the increased membrane fluidity, therefore, maintaining its homeostasis.

Carotenoids, which are acyclic terpenoids made from the same precursor as hopanoids (namely farnesyl diphosphate), are another form of isoprenoid-based lipid. Ubiquitously present in bacterial species, carotenoids have a wide range of biological functions, including pathogenicity (Liu and Nizet, 2009), bacterial cell pigmentation and colour, as well as neutralization of oxygen radicals to confer resistance to oxidative stress (Alexander, 1999). Moreover, carotenoids have been shown to reduce bilayer fluidity similarly to sterol compounds (Taylor, 1984; Subczynski *et al.*, 1992; Gabrielska and Gruszecki, 1996; Seel *et al.*, 2020).

It is worth noting that the composition of lipids in bacterial membranes varies not only between species, but also within species, depending on the conditions in which the cells are cultivated (López *et al.*, 2006; Sohlenkamp *et al.*, 2020). Moreover, highly regulated pathways of lipid synthesis influence the molecular composition of lipids in different locations as well as within the different leaflets of the same bilayer, which determines its physicochemical properties, and thus, its biological functions. For example, the effect of temperature on bacterial membrane lipids has been extensively studied (Suutari and Laakso, 1994; Shivaji and Prakash, 2010; Barria *et al.*, 2013). Bacteria can adapt their membranes increasing the amount of unsaturated fatty acids (FAs), short chain FAs and branched chain FAs as well as the incorporation of carotenoids and glycolipids, in order to lower the phase-transition temperature below a range where the membrane changes from a “fluid” (liquid-crystalline) to a “rigid” phase (Shivaji and Prakash, 2010; Siliakus *et al.*, 2017). The formation

of different lipid membrane phases will be explained later in more detail, in the section *Membrane Compartmentalization.*

1.4.2 Membrane proteins

Originally, it was thought that proteins only formed a small portion of biological membranes, however, recent studies showed that more than a quarter of all putative genes in some bacteria code for membrane proteins (Liu *et al.*, 2002). In recent decades, it has been established that proteins play significant roles in biological functionality of membranes (Engelman, 2005), and that the interaction between lipids and proteins within the membrane is crucial for cell viability. One of the functions of biological membranes is to prevent the unregulated flow of proteins and other macromolecules that are synthesized in the cytoplasm but will perform their metabolic or structural functions within the membrane itself or outside of the cell. Various transport and localization mechanisms have evolved to allow proteins to penetrate the cytoplasmic membrane without impairing their structures and functions. After protein synthesis, protein components are present at the correct place and adequate concentration for subcellular activities to take place (Blobel, 1980; Emanuelsson *et al.*, 2007; Chou and Shen, 2007; Ramamurthi *et al.*, 2009). A number of models have been proposed to explain the subcellular localization of proteins (Collier and Shapiro 2007; Thanbichler and Shapiro 2008).

Proteins contain portions in the polypeptide chain called signal peptide that directs the proteins to be transferred outside the cell or to other intracellular membranes, locations or compartments (Blobel, 1980). A cellular sorting and translocation machinery recognizes and decodes this signal, targeting the protein for translocation across the plasma membrane in prokaryotes (Emanuelsson *et al.*, 2007). After protein delivery to the correct subcellular location, the signal peptide is removed by specialized signal peptidases. In general, soluble targeting factors identify a preprotein before transporting it to the target membrane, where it is coupled with a translocation machinery. A proteinaceous channel is then used to convey the polypeptide chain. In most cases, a translocation motor that binds and hydrolyses nucleoside triphosphates drives the transport process. Finally, the signal peptide is eliminated, enabling the full protein to be released from the translocase. If the protein is translocated in an unfolded state, it will fold into its native

conformation after being released from the translocase. Several integral membrane proteins maintain their signal-like peptides and diffuse laterally from the translocase (Pohlschröder *et al.*, 1997). Although different, signal peptides tend to be quite similar in general structure, apparently small differences between individual signal peptides can cause cleavage by different signal peptidases, export via different pathways, and transport to different destinations.

B. subtilis employs two highly conserved pathways for protein export, namely the general secretion (Sec) pathway and the twin-arginine (Tat) pathway. Both pathways are ubiquitously distributed in all domains of life (Pohlschröder *et al.*, 1997). The twin-arginine translocation pathway is specialized in export of fully folded proteins (Palmer *et al.*, 2005; Yuan *et al.*, 2010; Fröbel *et al.*, 2012; Frain *et al.*, 2019). Often, the proteins translocated by the Tat-pathway contains a consensus motif that contain cofactors including the so called “twin-arginine” residues, in the N-terminal signal peptides (Berks, 1996). In *B. subtilis*, the Tat pathway is composed by only two components TatA and TatC (a core translocase TatAyCy and a complementarily translocase TatAdCd) to perform activity, whereas in *E. coli* a third component known as TatB is present (Eijlander *et al.*, 2009). In the Gram-positvie bacterium, the core translocase TatAyCy is built by the constitutively expressed TatAy and TatCy proteins and it has functions in transporting the protein QcrA (iron-sulphur protein) into the cytoplasm (Goosens *et al.*, 2014b), the metallophosphoestearase YkuE to the cell wall (Monteferrante *et al.*, 2012; Goosens *et al.*, 2014a), and the haemoprotein EfeB to the interface between cell wall and plasma membrane, as well as extracellularly (Miethke *et al.*, 2013; Goosens *et al.*, 2014a). Moreover, biochemical studies have shown that in *B. subtilis* the TatAyCy translocase is functionality influenced by the LiaH expression levels (Bernal-Cabas *et al.*, 2020). The second translocase TatAdCd is expressed under low phosphate conditions when secretion of the phosphodiesterase protein PhoD occurs (Pop *et al.*, 2002). The Sec-pathway translocates unfolded proteins across the membrane and besides the Sec pathway being well conserved in bacteria, it has been best characterized in the Gram-negative model *E. coli* (De Keyzer *et al.*, 2003; Du Plessis *et al.*, 2011). It is composed of a multi-protein complex with a peripheral motor domain SecA, ancillary proteins SecDF, YidC, and a membrane-embedded protein conducting channel SecYEG with functions in accommodating the protein to be inserted or translocated (Prabudiansyah and Driessen 2017).

In the diffusion and capture model, the proteins are randomly inserted into all membranes or the cytoplasm, diffuse to their correct localization, and are then captured at the place where they finally reside (Rudner et al. 2002; Deich et al. 2004; Thanbichler and Shapiro 2008; Shapiro et al. 2009; Komeili 2012).

Geometric or physical cues are also a mechanism used by bacteria to localize proteins to certain membrane areas. Shape-sensing proteins identify particular membrane topographies and insert into concave or convex membranes. More precisely, the structure of a particular protein allows it to translocate more robustly and efficiently on membranes with certain geometries. For instance, DivIVA localizes to specific regions of the bacterial plasma membrane by binding to cardiolipin, which is enriched in the membrane at the cell poles. Once localized to the membrane, DivIVA recruits other proteins involved in cell division, to form the division septum and complete cell division (Ramamurthi *et al.*, 2009; Lenarcic *et al.*, 2009). Another example, SpoVM localizes to a specific region of the plasma membrane that will eventually become the outer surface of the spore in *B. subtilis* (Levin *et al.*, 1993). SpoVM contains a hydrophobic region that allows it to bind to the membrane, and it also interacts with other proteins, such as SpoIVA and CotE, to ensure proper localization and assembly of the spore-coat (Van Ooij and Losick, 2003; Henriques and Moran, 2007). Given the diversity of membrane forms in biology, subcellular localization of macromolecular molecules may be a broadly shared method in a range of cell types. The current challenge is to identify the molecular mechanism through which bacteria carry out this process. Nonetheless, certain bacteria develop positively curved membrane organelles, such as photosynthetic vesicles and magnetosomes (Komeili *et al.*, 2006).

1.5 Membrane homeoviscous adaptation

Cell viability is dependent on the functionality of biological membranes and despite their critical role in cell function, our knowledge in membrane physiology and homeostasis is far behind that of most other topics in cell biology. The functionality of membranes is associated with the activity of membrane proteins, as they perform a diverse range of roles from signaling to transport. The function of these proteins is, in turn, critically dependent on membrane physical parameters such as viscosity, fluidity, thickness, curvature and bilayer asymmetry (Ernst *et al.*, 2016a), which are determined by membrane

lipid composition. The lipid composition determines the dynamics and interactions of lipid molecules, which in turn determine the barrier and permeability properties of the membrane and influence the topology, interactions and functions of the membrane proteins (Coskun and Simons, 2011; Quinn, 2012), thereof, underlying mechanisms that guarantee membrane adaptation.

The preservation of the aforementioned membrane parameters in the face of environmental stress depends on mechanisms that sense and respond, conferring homeostasis and adaptation to the membrane lipidome in a constantly changing environment. Temperature in that sense is a critical environmental variable for microorganism because it quickly equilibrates with their reduced volumes, therefore affecting the reaction rates and equilibria that drive cellular biochemistry (De Mendoza *et al.*, 1983; Zhang and Rock, 2008). Membrane bilayer undergoes a series of transitional states as a function of temperature. At low temperatures, there is a reversible change from a fluid (disordered) to a non-fluid (ordered) state of the fatty acyl chains. However, a liquid-gel transition occurs as the temperature rises and the temperature at which this transition begins is called the transition temperature (T_m). T_m is a function of membrane lipid composition and, in low-cholesterol species, is primarily determined by the fatty acid content of membrane lipids (Cronan and Gelmann, 1975; De Mendoza *et al.*, 1983)

The balance of esterified saturated (SFAs) and unsaturated fatty acids (UFAs), for example, is an important component in influencing lipid packing, water permeability, and membrane fluidity. Unsaturated or terminally branched fatty acids create a disordered state, in contrast to the densely packed orderly arrangement of the lipid bilayer provided by straight chain-saturated acyl chains. Long-chain saturated fatty acids such as hexadecanoic acid ($C_{16:0}$) are linear and pack tightly together to form a bilayer with a high T_m and low permeability. The *cis* unsaturated fatty acids (UFAs) induce a bend in the acyl chain, altering the order of the bilayer rendering the membrane more permeable and with a lower T_m. This membrane lipid homeostasis that self-guard the biophysical properties of membrane is called homeoviscous adaptation and is considered a mechanism by which the permeability of phospholipid bilayer is modified in an energy dependent manner (Zhang and Rock, 2008). To this end, cells need to recognize temperature signal to regulate enzymatic activities or genes required for a proper adaptation to the new temperature (Sengupta and

Garrity, 2013). In that sense, bacteria possess a set of proteins and biomolecules with functions in sensing changes in lipid bilayer trigged by temperature.

DesK was identified as the sensor protein of a two-component system (TCS) in *B. subtilis*, with both kinase and phosphatase activity. DesK is encoded in an operon containing also its cognate response regulator, DesR (Aguilar *et al.*, 1998; Aguilar *et al.*, 1999). When the temperature decreases below 30 ºC, the *Pdes* promoter is activated, inducing Δ5 desaturase expression, which uses existing phospholipids as substrates to introduce a *cis*-double bond at the fifth position of the fatty acyl chain (Altabe *et al.*, 2003). Consequently, helping to restore appropriate membrane fluidity in the new environment, leading to membrane adaptation. The resultant unsaturated fatty acids increase bilayer fluidity, which restores DesK phosphatase activity in a negative feedback loop. A series of *in vivo* and *in vitro* studies on full-length DesK and truncated constructs in its transmembrane domain suggested that DesK detects membrane thickness as a cue for cold sensing (Cybulski *et al.*, 2010; Porrini *et al.*, 2014). However, it is important to note that acyl chain lengths not only affect membrane thickness, but also other membrane properties such as permeability to water, fluidity/rigidity, especially when fluid-to-gel phase transitions are caught in the relevant temperature range. Therefore, it is difficult to determine which biophysical aspects of the membrane are sensed by the protein. Anyhow, it is clear that DesK senses membrane state as a proxy of decrease in temperature.

On the other hand, bacteria also need to adapt the membrane in response to increased membrane fluidity. It was reported by Kingston and colleagues that the σ^W promoter existing within the *fabHA-fabF* operon have functions in modulating membrane homeostasis. Detergents, antibiotics, and bacteriocins active on the membrane triggers the response of the ECF factor W in *B. subtilis.* By activating σ^W response, FabHA levels decrease, consequently increasing dependence on FabHB which in turn, increase ratio in straight chain FA from a range up to 30 % higher. Overexpression of FabF, an elongation enzyme, leads to increased FA chain length, rendering the membrane with longer acyl chains and decreased ratio of BCFA. Consequently, there is increase in membrane rigidification, believed to be important, in this case, to adapt the membrane against the effects of antimicrobial peptides and detergents (Kingston *et al.*, 2011).

To better understand how heterogeneity of fatty-acid affect membrane properties, Nickels and collaborators utilized a *B. subtilis* with a chemically simple membrane for incorporation of exogenous FAs. They suppressed the *de novo* synthesis of fatty-acids by using cerulenin and a mutation that inhibited FA degradation. They found out that only two FA species were necessary to rescue the growth arrest: a straight-chain C16 fatty-acid (high melting), and an anteiso-C15 FA (low melting). Cells counteract this reduced FA complexity by varying the distribution of phospholipid headgroups, inducing the DesRK system, downregulating the σ^W stress response, and increasing ratio of isoprenoid lipids (Nickels *et al.*, 2020).

In a recent report from the laboratories of Strahl and Deckers-Hebestreit, it was demonstrated *in vivo* that reduction in membrane fluidity resulted in a remarkable lipid phase separation into gel-phase and segregation of membrane proteins into fluid-lipid domains, and that this processes drastically interfere with essential cellular processes such as morphogenesis and maintenance of membrane potential. They demonstrated that by constructing mutants of *B. subtilis* and *E. coli* cells in which the lipid composition of the membrane could be controlled by externally adding FA precursors. With this, they demonstrated the importance of lipid homeostasis for critical cellular functions (Gohrbandt *et al.*, 2022). This altogether demonstrated a high degree of adaptability of bacteria for maintenance of homeostasis and functionality of membranes.

1.6 Membrane compartmentalization

For nearly half a century, understanding plasma membrane organization has been a significant interest in cell biology, biophysics and mechanobiology. Membranes are not an amorphous aggregation of proteins and phospholipids. Instead, biological membranes are composed of distinct compartments which enhances the efficiency of several membrane-bound processes though concentration of the necessary components inside a small region within this structure. When a specific condition is necessary to enable a specific subcellular activity, it may be locally isolated so that it does not interfere with the function of other subcellular compartments. Different lipids tend to associate together in the membrane depending on their individual physicochemical properties, resulting in a heterogeneous distribution of domains containing lipids. Early reports on membrane heterogeneity proposed an organizational model of

'*quasicrystallin*" rigid lipid regions surrounded by more freely dispersed lipid molecules, depending on the temperature and molecular structure of the lipids present in the system (Hjort Ipsen *et al.*, 1987).

This model proposed that when the temperature of the membrane rises over a certain point – known as the transition temperature – the lipids transition from a solid-ordered to a disordered liquid-crystalline state.

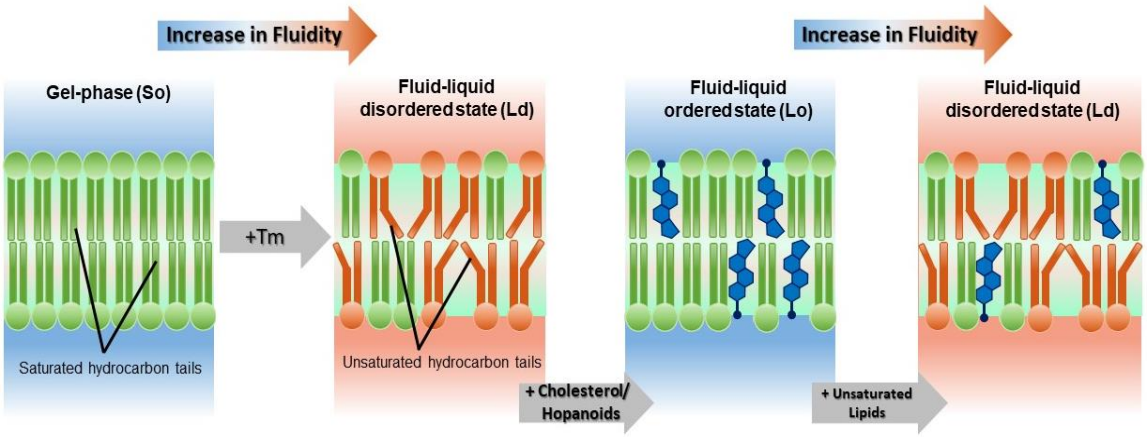

Figure 1. Different states of lipid bilayers depending on the composition and temperature. At higher temperatures the membrane changes from gel solid-ordered state (So) to a more fluid and less dense liquid state (Ld), going through the transition temperature (Tm). In the presence of cholesterol (in Eukaryotes) or hopanoids (in Bacteria) the temperature effect is stabilized rendering the membrane a more dense packing and an increased rigidity. Presence of unsaturated phospholipids renders the membrane an impaired packing and a higher state of fluidity. The double bounds in the lipids results in bends in the fatty chains causing repulsing and steric hindrance between the lipids.

This lipid organization principle subsequently evolved, and in 1982, the notion of lipid domains was introduced, in which lipids were suggested to cluster into a so-called 'more ordered state', with cholesterol playing a key role in the formation of those lipid domains (Karnovsky *et al.*, 1982). Later, findings in model membranes showed the coexistence of liquid-disordered and liquid-ordered membrane areas, with the later having lower diffusivity with greater molecular packing, and subsequently a relatively low membrane fluidity (Simons and Vaz, 2004; Kaiser *et al.*, 2009; Lingwood and Simons, 2010).

It was postulated that the liquid-ordered domain may play a significant role in the sorting of lipids and proteins between interior organelle membranes and this finding, then, gained biological significance. In 1997, these domains were named "lipid rafts" by Simons and Ikonen (Simons and Ikonen, 1997).

In their model, they imply that distinct membrane microdomains are enriched in sphingolipids, cholesterol and proteins and since then, eukaryotic

lipid rafts have been broadly studied. One of the very first *in vivo* evidences for the membrane heterogeneity, which also gave rise to the idea of the existence of lipid microdomains, was to explain why the apical membrane of epithelial cells are enriched in glycolipids (Simons and Van Meer, 1988). The cells had clear differences in protein and lipid composition between the apical and basolateral membranes and it was suggested that a lipid sorting mechanism specifically drives sphingolipids from the Golgi complex to the apex of the epithelial cell, with their assembly being restricted via tight junctions (Simons and Van Meer, 1988; Rodriguez-Boulan and Nelson, 1989). Later, it was reported that GPI-anchored proteins are recruited to this specialized lipid enriched domains in apical membranes (Brown and Rose, 1992a). Therefore, it was assumed that heterogeneity of membrane organization is not an exclusive feature conferred by lipids, but also proteins, and the concept of lipid raft was proposed (Simons and Ikonen, 1997). Later reports revealed that eukaryotic lipid rafts are highly enriched in sphingolipids and cholesterol (Pike, 2003). The model has been polished over the years and in the Keystone Symposium on Lipid Rafts and Cell Function (2006, Colorado), a definition for lipid rafts was brought into a consensus, as following:

> *"Membrane rafts are small (10-200 nm), heterogeneous, highly dynamic, sterol- and sphingolipid-enriched domains that compartmentalize cellular processes. Small rafts can sometimes be stabilized to form larger platforms through protein-protein and protein-lipid interactions."* (Pike, 2006).

Going back to the initial lipid raft hypothesis, it is important to highlight that it was developed in an attempt to explain the biochemical and microscopical results that glycosylphosphatidylinositol (GPI-anchored) and other membrane-bound signaling proteins are resistant to extraction using cold non-ionic detergents (Brown and Rose, 1992a; Simons and Ikonen, 1997; Lang *et al.*, 1998). Because of the close packing of sphingolipids, GPI-anchored proteins and cholesterol would be resistant to treatment to detergent, thus, being experimentally isolated in a membrane fraction that is insoluble in non-ionic detergents (Simons and Ikonen, 1997), namely the DRM (detergent resistant membrane fraction). In the early years of lipid raft research, this method was considered the best approach. However, some reports suggested that treatment with non-ionic detergent, such as Triton-X100, resulted in unspecific aggregation (London and Brown, 2000). With it, a lot of skepticism and unclear

observations called the theory into question and even the existence of such lipid domains was brought into discussion. Later on, some reports using other methods, including detergent-free techniques (Schuck *et al.*, 2003), showed that the whole eukaryotic raft proteome was comparable to that enriched by methods containing detergent (Foster *et al.*, 2003).

However, despite all the different attempts mentioned, the *in vivo* role of lipid raft remains unclear and the discussion seems to be multifaceted. Some arguments against the existence of this domains and their physiological role in *in vivo* membranes include (a) the existence of many lipid species, (b) continuous lipid and protein turn over, (c) association with cytoskeleton structures, (d) no consensus on lipid raft size and (e) the time scale that they might occur may be irrelevant to biological processes. Additionally, it must be emphasized that the detergent resistant membrane fraction (DRM) where proteins thought to scaffold lipid rafts are enriched, *does not equal lipid rafts* (Bramkamp and Lopez, 2015) and any protein candidates co-purified with the DRM should be explored in further experiments, for instance whether it co-localizes with known raft markers such as flotillins (Bramkamp and Lopez, 2015).

1.6.1 Eukaryotic flotillins and the SPFH-domain

A class of non-GPI-anchored proteins consistently enriched in DRM fractions was discovered in 1997, and due to their ability to float in low-density fractions of a sucrose gradient after Triton-X100 extraction, they were named *flotillins* (Bickel *et al.*, 1997). Coincidently, genes encoding for flotillins were also reported to be upregulated after axon regeneration of goldfish retinal ganglion cells, and were named “reggie” proteins due to its importance in this process (Schulte *et al.*, 1997; Lang *et al.*, 1998). Flotillins/reggie-like proteins were since then considered lipid-raft markers in Eukaryotes (Langhorst *et al.*, 2005).

The most studied flotillin proteins are Flotillin-1 and Flotillin-2, two homologous membrane-associated cytoplasmic proteins that shares around 50 % of amino acid sequence identity (Morrow and Parton, 2005). They assemble in almost equal amounts at the plasma membrane creating microdomains that bud into the cell (Riento *et al.*, 2009). They are ubiquitous, being expressed in mammals, plants and prokaryotes. They are evolutionary conserved with 64 % homology amino acid sequence between fly and man (Zhao *et al.*, 2011),

although absent in yeast cells and in the nematode *Caenorhabditis elegans* (Morrow and Parton, 2005). Flotillins were described to associate N-terminally with the inner leaflet of the membrane by three different modes: (a) via hairpin loop, that penetrates the membrane without crossing it; (b) via a transmembrane helix or; (c) via post-translational modifications by myristylation or palmitoylation; making both N- and C- terminus cytoplasmic (Salzer and Prohaska, 2001; Neumann-Giesen *et al.*, 2004; Bach and Bramkamp, 2013). The C-terminus of flotillin proteins has several coiled-coil motifs, called flotillin repeats, which are believed to have a role in the formation of homo and hetero-oligomers (Solis *et al.*, 2007; Langhorst *et al.*, 2007).

Flotillins belong to the Stomatin, Prohibitin, Flotillin, HflK/C (SPFH) protein family – synonym to PHB domain (prohibitin homology domain), a class of proteins that shares homology at their N-terminus region (Tavernarakis *et al.*, 1999). Members of the SPFH domain superfamily can be found in all domains of life including bacteria, Archaea and Eukaryotes, and are mostly absent in endosymbionts or endoparasites (Hinderhofer *et al.*, 2009). SPFH domain was initially thought to be evolutionarily conserved. A study showed that they emerged independently in different proteins through convergent evolution (Rivera-Milla *et al.*, 2006a) and after that a report concluded, based on their operon structure and functional similarities, that their diverse phylogenetic distribution in prokaryotes would better be explained by lateral gene transfer (Hinderhofer *et al.*, 2009).

The SPFH domain has a highly conserved structure, suggested to be responsible for binding the protein to lipid moieties and to contribute to protein self-oligomerization into large membrane spanning or membrane-anchored complexes (Morrow and Parton, 2005; Rivera-Milla *et al.*, 2006b; Browman *et al.*, 2007b). In addition, many SPFH proteins are implicated in highly specific processes occurring on the membrane, including a potential scaffolding role for the formation and organization of membrane compartments. However, a detailed molecular mechanism remains unclear.

Despite their high degree of evolutionarily conservation and distribution, flotillins' precise biological function remains unknown and somewhat controversial. However, several studies link eukaryotic flotillins to T-lymphocyte activation, insulin signalling, endocytosis, axon regeneration, neuronal differentiation, and progression of some diseases and tumours (Zhao *et al.*, 2011). Flotillins are thought to function as scaffold or recruiters for other

membrane-associated proteins, facilitating protein-protein interaction, clustering, association and oligomerization for their correct activity (Morrow and Parton, 2005; Zhao *et al.*, 2011). Nonetheless, as stated above, the precise molecular mechanism by which flotillins arbitrate those interactions, and if and how they interact with membrane lipids, remains elusive and further research is necessary to unravel the precise mechanisms.

1.6.2 Lateral membrane heterogeneity in bacteria

Despite the fact that much research on lateral membrane organization has been conducted in Eukaryotes, membrane heterogeneity is not a concept exclusive to this domain of life. While historically considered to be simple cells with low degree of lateral differentiation, bacteria also have a high level of complexity in terms of membrane arrangement. Lipids and proteins in bacterial membranes are heterogeneously distributed and have been found to localize and perform their activity in specific regions of the membrane. For instance, in the model organism *B. subtilis*, lipid species are enriched at the polar regions and many proteins are localized into distinct foci or have preferences to localize in membranes with negative curvature or at the septum (Mileykovskaya and Dowhan, 2000; Kawai *et al.*, 2004; Lenarcic *et al.*, 2009; Rudner and Losick, 2010; Bach and Bramkamp, 2013; Meeske *et al.*, 2015; van Tilburg *et al.*, 2021).

It has been shown that membrane patches with higher fluidity exist most likely due to the accumulation of unsaturated fatty acids, and have a higher concentration of proteins with distinct roles in organizing the membrane, such as the cytoskeleton related MreBH complex, PlsX and MurG (Strahl, Bürmann, and Hamoen, 2014; Müller et al., 2016). These data altogether add to the idea of an intricate and complex membrane organization in bacteria.

As already described in the section 1.4, bacterial membranes are primarily composed of phosphatidylglycerol (PG), cardiolipin (CL) and phosphatidylethanolamine (PE) and their ratios vary depending on the species. For example, in *B. subtilis* cardiolipin is relatively abundant and makes up to one quarter of the membrane composition. In contrast to eukaryotic lipid domains, where cholesterol and sphingolipids are major components, bacteria are unable to synthesize either of those lipids, and only a few selective species, such as *Borrelia burgdorferii*, *Ehrlichia chaffeensis*, *Anaplasma phagocytophilum*, or

Mycoplasma spp., have been found to be capable to incorporate exogenous cholesterol into their own membranes. Reports on lateral membrane organization in bacteria highlights, however, that several bacterial species produce distinct hopanoids that could contribute to similar physicochemical properties to bacterial membranes as to eukaryotic cholesterol and sphingolipids. Therefore, these lipid species are considered to serve as cholesterol surrogates in bacteria. The ordering properties of hopanoids in some bacteria could potentially confer the ability to subcompartmentalize their membranes into functions domains.

Sterols, as the main membrane-ordering lipids, provide a dilemma as sterol biosynthesis involves molecular oxygen, although life existed on Earth for at least a billion years before cyanobacteria first enriched the atmosphere with oxygen (Ohtomo *et al.*, 2014). Therefore, the question whether lipids influenced membrane organization before sterol synthesis was raised. All three domains of life have isoprenoid synthesis pathways, which produce a diverse range of structurally homologous lipids such as sterols and hopanoids (e.g., diplopterol). Hopanoids are among the most common cyclic isoprenoid lipids found in sedimentary rocks, and they have been exploited as molecular markers for ancient microbial life (Ourisson and Albrecht, 1992). Notably, hopanoid synthesis does not need molecular oxygen, and hopanoids have been found in sediments prior to the enrichment of oxygen in the atmosphere (Kannenberg and Poralla, 1999; Briggs and Summons, 2014). Because hopanoids and sterols share structural properties and are cyclized by closely similar enzymes (Wendt *et al.*, 1997; Frickey and Kannenberg, 2009), it was suggested that they may function as sterol surrogates in bacteria (Ourisson *et al.*, 1987).

Cholesterol is synthesized from the head-to-head condensation of isoprenoid precursors to acyclic squalene, which is then cyclized to its final state. Although prokaryotes lack a mechanism for converting squalene precursors to cholesterol, bacteria can cyclize squalene precursors into hopanoids (e.g., sporulenes) (Bosak *et al.*, 2008; Kontnik *et al.*, 2008). Hopanoids have comparable physicochemical properties to cholesterol and are thought to function as sterol surrogates in bacteria (Sáenz *et al.*, 2012; Sáenz *et al.*, 2015; Chwastek *et al.*, 2020). Additionally, carotenoids, which are acyclic terpenoids derived from the same precursor as hopanoids, are another form of isoprenoid-based lipid (namely farnesyl diphosphate). Carotenoids are found in all bacterial species and have a wide range of biological activities, including pathogenicity

(Liu and Nizet, 2009), pigmentation of bacterial cells, and neutralization radicals to counteract oxidative stress (Alexander, 1999). Recently, it has been reported in a study with *Methylobacterium extorquens*, that hopanoids are essential for growth at high temperatures and the outer membrane lipids of the hopanoid knockout strains were less packed as compared to the wild type strain, rendering the membrane more fluid (Rizk *et al.*, 2021). Moreover, the same study suggested that disruption of carotenoid or hopanoid synthesis caused opposing effect on the outer membrane, suggesting complementary roles on stabilizing membrane for these two major bacterial lipids (Rizk *et al.*, 2021). These findings suggest a role for these bacterial lipids towards the membrane organization.

The lipid domains in Eukaryotes have relatively low membrane fluidity and are related with the presence or accumulation of flotillin proteins. Because the closest homologue of the eukaryotic flotillins in bacteria is found in the genus *Bacillus*, most investigations on lateral membrane heterogeneity in bacteria have been conducted in the Gram-positive model organism *B. subtilis*. This bacterium encodes two flotillin homologues, *floA* (formerly *yqfA*) and *floT* (formerly *yuaG*).

In 2010, a functional membrane microdomain (FMM) or what the authors called “bacterial-raft”, was proposed as a membrane microdomain involved in the coordination of cellular signaling pathways (López and Kolter, 2010). This work suggested that the *B. subtilis* membrane-bound sensor kinase KinC, involved in biofilm formation, could have functions in membrane compartmentalization, however lacking the data that prove an altered lipid composition that would justify their model. The same study originally proposed the protein YisP to be a putative squalene synthase without actually identifying its product (López and Kolter, 2010). It was demonstrated that when YisP was absent in *B. subtilis*, the bacterium was deficient in biofilm formation, suggesting a role of squalene for this differentiation process. This, together with the discovery that FloT localizes into distinct foci in the membrane and investigations with chemicals that impact sterol production, led to the conclusion that bacteria actually possess FMMs (Bramkamp and Lopez 2015; Wagner, Kricks, and Lopez 2017). Later on, further research about the crystal structure of YisP revealed that one of the aspartate-rich motifs consistently found in all squalene synthases was missing in YisP protein (Hu *et al.*, 2013).

Following research found that YisP is in fact a farnesyl-diphosphate phosphatase and its product is the long chain alcohol farnesol rather than squalene (Feng *et al.*, 2014). It was reported that farnesol alone rescue the *yisP*

mutant's biofilm deficient phenotype, indicating that farnesol may have a role in stabilizing FMMs in a similar way that hopanoids and carotenoids do in other systems (Bell and Chappell, 2014; Feng *et al.*, 2014; Chwastek *et al.*, 2020; Rizk *et al.*, 2021). However, no direct involvement of farnesol as part of FMMs formation and function nor its participation in lipid species synthesis pathways has been described so far. Moreover, a report from 2016 describes the molecular mechanism of farnesol in inhibiting growth, inducing membrane disordering and eventual disruption of the cytoplasmic membrane of *S. aureus*, by promoting potassium leakage. The effects of farnesol decreases the insertion of carotenoid, which is a membrane stabilizing agent (Inoue *et al.*, 2016).

Nonetheless, as pointed above, lateral membrane heterogeneity is an important feature of bacterial membranes as several membrane processes are localized to specific membrane areas. Identifying and characterizing proteins associated to the existence of FMMs, also named “protein cargo”, is critical for understanding the molecular mechanisms related to bacterial membrane organization.

1.7 Bacterial Flotillins

Bacterial flotillin homologues were first described more than 20 years ago (Tavernarakis *et al.*, 1999) and just like their eukaryotic counterparts, they belong to the so called Stomatin, Prohibitin, Flotillin, and HflK/C (SPFH) domain superfamily. They are found in all life kingdoms, but evolved via convergent evolution which leads to the conclusion that the molecular setup is a crucial and restricted feature for the functionality of flotillins (Tavernarakis *et al.*, 1999). *B. subtilis* DRM fractions contain two homologues of the eukaryotic flotillins (FloA and FloT) (López and Kolter, 2010; Bach and Bramkamp, 2013). In *Staphylococcus aureus*, FloA colocalizes with staphyloxanthin, a candidate for FMM-formation lipid, since its chemical structure resembles eukaryotic lipid rafts (Foster *et al.*, 2003; García-Fernández *et al.*, 2017).

In other systems, flotillins and FMMs are linked to a plethora of roles, from flagellar function and chemotaxis in *E. coli* and *Vibrio cholera* respectively (Padilla-Vaca et al., 2019; Takekawa et al., 2019), to type VII secretion (Mielich-Suss et al., 2017), signaling (Wagner et al., 2017), and host contact during infection (Wagner et al., 2017) (Hutton et al., 2017) in *S. aureus*.

In *B. subtilis*, FloA and FloT are oligomeric, integral membrane proteins thought to be involved in the formation and function of FMMs (López and Kolter, 2010; Bach and Bramkamp, 2013; Bramkamp and Lopez, 2015; Lopez and Koch, 2017). FloT was described as capable of oligomerizing via the SPFH domain (Bach and Bramkamp, 2015).

Initially, it was proposed that FloT and FloA would interact *in vivo* with each other, justified by their similar structure that could colocalize in a defined and dynamic foci along the cell membrane (Schneider *et al.*, 2015). The bacterial membrane was assumed to be partitioned into low fluidity FMM regions that are spatially separated from the more fluid regions, by FloA and FloT. However, this direct role for flotillins in FMM formation has been put into question, due to a report showing by super resolution microscopy that *B. subtilis* FloA and FloT do not always colocalize, and form separated foci of approximately 100 nm in diameter - appearing spatially distinct and with different dynamics from the formerly described FMMs (Dempwolff *et al.*, 2016), with FloA being more mobile than FloT. The same report also shows colocalization of FloT with NfeD2, apparently FloT recruits NfeD2 into the focal assembly, leading to a conclusion that flotillins and NfeD proteins have a close interaction in bacteria (Dempwolff *et al.*, 2012a). Not surprisingly, both FloT and FloA are encoded in operons containing *nfeD* genes, *nfeD2* upstream of *floT* and *nfeD1B* upstream of *floA*. Some reports also characterize several proteins associated with DRM fractions from *B. subtilis* and attempted to draw a direct protein-protein interaction with bacterial flotillins. Since DRM fractions are functionally distinct from FMMs, not every protein in the DRM fraction necessarily have functions in stabilizing or promoting membrane compartmentalization.

Both FloA and FloT are not essential in *B. subtilis,* but overexpression or deletions (single or double) of *floA* and *floT* are associated with perturbations in cell shape (Mielich-Süss *et al.*, 2013), motility (Dempwolff *et al.*, 2012a), biofilm formation (Yepes *et al.*, 2012; Mielich-Süss and Lopez, 2015), sporulation (Donovan and Bramkamp, 2009), cell division and natural competence efficiency (Koch *et al.*, 2017), and regulation of membrane fluidity and transport (Bach and Bramkamp, 2013).

Flotillins are also described to be genetically linked to the membrane associated-GTPase DynA (Dempwolff *et al.*, 2012b; Dempwolff and Graumann, 2014), which is associated with functions in membrane remodeling, membrane lipid content mixing, and fission (Guo and Bramkamp, 2019). DynA may

contribute to the recovery of damaged membrane areas while also contributing to resistance to antibiotics that bind membrane components such as nisin, bacitracin or daptomycin (Sawant *et al.*, 2016). FloT, in that sense, was thought to play a non-redundant role with dynamin-like protein A, in membrane dynamics and control of cell shape (Dempwolff *et al.*, 2012b). Recently, it has been shown that the presence of DynA may have roles in defense by delaying cell lysis following phage infection, limiting the release of phage offspring from host cells (Guo *et al.*, 2022).

These findings contribute to a general role of the aforementioned proteins in membrane stress response, and points to functions related to membrane homeostasis maintenance for flotillins. They are related to a plethora of membrane-bound roles, indirect related to membrane organization. Our knowledge of bacterial flotillin, as well as their molecular functions in bacterial physiology, is currently limited but in rapid development.

1.8 The role of SPFH-domain proteins in stress response

All living organisms have to defend and protect their environmental niches against competing species in order to establish themselves in their natural environment. bacteria have developed a variety of strategies to surpass competition, including the production of antibiotics, bacteriocins and antimicrobial peptides (AMPs) (Czárán *et al.*, 2002). AMPs, which typically target cell envelope integrity via a number of different modes of action (MOA), are one significant antibiotic family that is particularly relevant for Gram-positive bacteria (Malanovic and Lohner, 2016).

Even with a great difference in their specific MOA, AMPs share common structural properties such as a significant number of hydrophobic residues and are overall positively charged (Guilhelmelli *et al.*, 2013). Since bacteria generally have a negatively charged surface due to the presence of wall teichoic acids, AMPs can easily bind to the bacterial surface and disrupt cytoplasmic membrane homeostasis, leading to envelope damage and cell lyses (Jordan *et al.*, 2008a; Teixeira *et al.*, 2012; Malanovic and Lohner, 2016). Therefore, bacteria evolved several mechanisms such as peptide antibiotic sensing and detoxification modules, to closely monitor their cell envelope and detect the presence of such threats in order to execute defensive counteractions as quickly as possible (Staroń *et al.*, 2011; Guilhelmelli *et al.*, 2013; Radeck *et al.*, 2016). This means that

bacterial survival is dependent on their capacity to recognize and respond to threats to the cell envelope, which they execute via signal transduction mechanisms called cell envelope stress responses (CESRs).

These CESRs initiate a protective and/or corrective reaction by modulating some aspects of membrane composition, when alterations in cell envelope homeostasis are recognized. These alterations in membrane composition and structure are regulated by activation of extracytoplasmic function sigma factors (ECF σ factors) (Eiamphungporn and Helmann, 2008; Kingston *et al.*, 2013; Helmann, 2016) also referred to as an σ ECF *stress response sigma factors* (Radeck *et al.*, 2017).

CESRs induces proteins that function in membrane protection and remodelling in addition to altering membrane lipid content. The bacterium *B. subtilis* has a sophisticated cell envelope stress response network that is regulated by at least four ECFs, a comparable number of two component systems (TCSs) and detoxification modules (Jordan *et al.*, 2008a; Helmann, 2016; Radeck *et al.*, 2017). This network includes the two bacterial flotillin homologs (FloA and FloT) and two *E. coli's* PspA homologues (PspA and LiaH), members of the phage shock protein family (Kobayashi *et al.*, 2007; Flores-Kim and Darwin, 2016).

The PspA proteins were originally identified in *E. coli*, as part of the phage-shock protein response (Brissette *et al.*, 1991). They are members of a conserved family that includes the inner-membrane associated protein of 30 KDa (IM30), also known as vesicle inducing protein in plastids (Vipp1) (Heidrich *et al.*, 2017). These proteins are essential for proper biogenesis of thylakoid membranes in chloroplasts and cyanobacteria (Manganelli and Gennaro, 2017). Together with PspA proteins, they are part of the ancient ESCRT-III protein superfamily (endosomal sorting complexes required for transport), ubiquitously distributed in both pro- and eukaryotes (Isono, 2021; Siebenaller and Schneider, 2023) with roles in membrane remodeling and stabilization (McCullough *et al.*, 2015; Thurotte *et al.*, 2017; Liu *et al.*, 2021). Hence, Psp proteins belong to a widely conserved polymer-forming protein superfamily found in all domains of life and share roles in membrane remodeling and repair - processes direct interlinked with membrane stress response (Junglas *et al.*, 2021; Liu *et al.*, 2021). For instance, the recruitment and accumulation of ESCRT-III proteins in eukaryotes have been observed at sites of damaged membranes, persisting there until the closure of the membrane (Jimenez *et al.*, 2014).

Structurally PspA proteins feature a conserved N-terminal amphipathic helix that is necessary for membrane binding (McDonald et al., 2015, 2017) and Vipp1 oligomerizes itself in dynamic rings with vary symmetries that, when stacked, create a dome-like structure that binds to damaged membrane areas (Thurotte *et al.*, 2017; Junglas and Schneider, 2018; Gupta *et al.*, 2021). Recently, it has been shown that the monomers dissociated from the ring-like structure can interact with the membrane, forming a membrane "carpet" with functions in protecting the membrane against proton leakage (Junglas *et al.*, 2020).

The stress response via Psp system has been extensively studied in *E. coli* (Flores-Kim and Darwin, 2016). When cells sense threats such as phage infection, changes in osmolarity, heat or proton leakage, the *pspABCDE* operon, the activator *pspF* and the effector *pspG* are activated. Transcription of the *psp* genes is initiated in a σ^{54} (sigma-54) dependent manner. Under non-stressed conditions, PspF is associated with PspA, inhibiting its activity. Under stressed conditions, PspF dissociates from PspA, and PspA is recruited to the membrane through two stress-sensors and membrane associated proteins PspB and PspC, where it counteracts membrane damaged areas (Joly *et al.*, 2010). A similar Psp stress response cascade is also found in the bacterium *Yersinia enterocolitica* (Maxson and Darwin, 2006; Darwin, 2007; Gueguen *et al.*, 2009; Yamaguchi and Darwin, 2012), with additionally data showing that the Psp system in this bacterium is of utmost importance for bacterial survival, since deletion of the component *pspC* results in reduced virulence and growth defect (Darwin and Miller, 2001). Recent studies on phylogenetic diversity of Psp systems, however, demonstrated that there is no archetypal Psp network architecture (Popp *et al.*, 2022). It is accepted though, that the Psp system is intrinsically regulated by temporary protein interaction arranged around PspA.

As stated above, the genome of the model organism *B. subtilis* encodes two PspA homologues – PspA and LiaH – and despite their sequence homology, they differ significantly from the *E. coli* / *Y. enterocolitica* regulation network (Manganelli and Gennaro, 2017). While the expression of *pspA* in *B. subtilis* is governed by the ECF sigma factor σ^{W} , which is strongly induced by alkaline shock (Wiegert *et al.*, 2001), LiaH is encoded in a operon controlled by the LiaRS two-component system (Mascher *et al.*, 2004; Jordan *et al.*, 2008b). However, this TCS also strongly responds to a variety of cell envelope stress conditions, including cell envelope perturbing chemicals such as AMPs, cell wall antibiotics such as bacitracin, nisin or vancomycin, as well as abiotic stressors such as heat

and osmotic shock (Mascher *et al.*, 2004; Wolf *et al.*, 2010; Domínguez-Escobar *et al.*, 2014; Radeck *et al.*, 2016). Furthermore, it is weakly induced by detergents, ethanol, alkaline shock and secretion stress (Wiegert *et al.*, 2001; Mascher *et al.*, 2004).

The PspA protein is encoded in an operon composed of *pspA-ydjGHI*. YdjI, a third protein containing the SPFH-domain was recently discovered in *B. subtilis.* At first, YdjI was thought to be a flotillin (Cozy *et al.*, 2012; Ravi *et al.*, 2021; Popp *et al.*, 2022). However, unlike FloA and FloT, topological protein prediction indicated that YdjI lacks the N-terminal transmembrane structure that would bind the protein to the membrane and the flotillin domain behind the SPFH domain, typical of this protein class. In that sense, YdjI membrane interaction may be conceivable via positively charged N-terminal residues. Given that the genetic structure and regulation of SPFH-domain proteins (FloA, FloT and YdjI) in *B. subtilis* is responsive to environmental stress, a realistic role for SPFH-domain proteins in stress response pathways appears to be likely. The specific and direct molecular mechanisms of these proteins in stress response is still to be elucidated, however their roles in membrane stabilization and repair are becoming more recognized.

1.9 Thesis outline

Currently, our understanding of bacterial SPFH-domain proteins and their roles in bacterial physiology is rapidly evolving. The commonly accepted hypothesis was that bacterial SPFH-domain proteins described so far (FloA and FloT) exist in liquid-ordered membrane domains and serve primarily as scaffold proteins, allowing spatial and temporal membrane compartmentalization. However, following research by our lab and others have indicated different roles for the bacterial SPFH-domain proteins toward membrane modulation responsive to stress (Dempwolff *et al.*, 2012b; Dempwolff and Graumann, 2014; Sawant *et al.*, 2016; Zielińska *et al.*, 2020).

In the present thesis, we aimed to unravel the molecular mechanism by which bacterial flotillins stabilize the membrane of *Bacillus subtilis* by regulating membrane homeostasis and modulating an important physical aspect of membrane, the fluidity. Furthermore, we intended to characterized the downstream effects of flotillins in membrane bound processes such as control of cellular shape and peptidoglycan synthesis.

This project also had as objectives the characterization of the putative third SPFH domain protein in *B. subtilis*, the YdjI protein. Since the genetic regulation of the classical flotillins – FloA and FloT – and YdjI is similar and related to stress (please see section 1.7 of Introduction for detailed explanation), we decided to further investigate the SPFH-domain protein YdjI in detail. We aimed to assess the subcellular distribution of YdjI protein and its possible localization with FloT. We further dissected the interactions of YdjI with the other proteins encoded in the *pspA-ydjGHI* operon, in order to reveal the dependency of the proteins encoded in this operon for correct membrane association and functionality.

2. RESULTS

1.1 Publication I

(link to online publication)

Zielińska A*, Savietto A*, de Sousa Borges A, Martinez D, Berbon M, Roelofsen JR, Hartman AM, de Boer R, Van der Klei IJ, Hirsch AK, Habenstein B, Bramkamp M, Scheffers DJ. **Flotillin-mediated membrane fluidity controls peptidoglycan synthesis and MreB movement.** eLife. 2020 Jul 14;9:e57179. doi: 10.7554/eLife.57179. PMID: 32662773; PMCID: PMC7360373.
*These authors contributed equally to this work.

Abstract

The bacterial plasma membrane is an important cellular compartment. In recent years it has become obvious that protein complexes and lipids are not uniformly distributed within membranes. Current hypotheses suggest that flotillin proteins are required for the formation of complexes of membrane proteins including cell-wall synthetic proteins. We show here that bacterial flotillins are important factors for membrane fluidity homeostasis. Loss of flotillins leads to a decrease in membrane fluidity that in turn leads to alterations in MreB dynamics and, as a consequence, in peptidoglycan synthesis. These alterations are reverted when membrane fluidity is restored by a chemical fluidizer. In vitro, the addition of a flotillin increases membrane fluidity of liposomes. Our data support a model in which flotillins are required for direct control of membrane fluidity rather than for the formation of protein complexes via direct protein-protein interactions.

RESEARCH ARTICLE

Flotillin-mediated membrane fluidity controls peptidoglycan synthesis and MreB movement

Aleksandra Zielińska[1†], Abigail Savietto[2,3†], Anabela de Sousa Borges[1], Denis Martinez[4], Melanie Berbon[4], Joël R Roelofsen[1], Alwin M Hartman[5,6,7], Rinse de Boer[8], Ida J Van der Klei[8], Anna KH Hirsch[5,6,7], Birgit Habenstein[4], Marc Bramkamp[2,3]*, Dirk-Jan Scheffers[1]*

[1]Molecular Microbiology, Groningen Biomolecular Sciences and Biotechnology Institute, University of Groningen, Groningen, Netherlands; [2]Biozentrum, Ludwig-Maximilians-Universität München, München, Germany; [3]Institute for General Microbiology, Christian-Albrechts-University, Kiel, Germany; [4]Institute of Chemistry & Biology of Membranes & Nanoobjects (UMR5248 CBMN), IECB, CNRS, Université Bordeaux, Institut Polytechnique Bordeaux, Pessac, France; [5]Department of Drug Design and Optimization (DDOP), Helmholtz-Institute for Pharmaceutical Research Saarland (HIPS) - Helmholtz Centre for Infection Research (HZI), Saarbrücken, Germany; [6]Department of Pharmacy, Saarland University, Saarbrücken, Germany; [7]Stratingh Institute for Chemistry, University of Groningen, Groningen, Netherlands; [8]Molecular Cell Biology, Groningen Biomolecular Sciences and Biotechnology Institute, University of Groningen, Groningen, Netherlands

***For correspondence:** bramkamp@ifam.uni-kiel.de (MB); d.j.scheffers@rug.nl (D-JS)

[†]These authors contributed equally to this work

Competing interests: The authors declare that no competing interests exist.

Funding: See page 18

Received: 24 March 2020
Accepted: 12 June 2020
Published: 14 July 2020

Reviewing editor: Tâm Mignot, CNRS-Aix Marseille University, France

Abstract The bacterial plasma membrane is an important cellular compartment. In recent years it has become obvious that protein complexes and lipids are not uniformly distributed within membranes. Current hypotheses suggest that flotillin proteins are required for the formation of complexes of membrane proteins including cell-wall synthetic proteins. We show here that bacterial flotillins are important factors for membrane fluidity homeostasis. Loss of flotillins leads to a decrease in membrane fluidity that in turn leads to alterations in MreB dynamics and, as a consequence, in peptidoglycan synthesis. These alterations are reverted when membrane fluidity is restored by a chemical fluidizer. In vitro, the addition of a flotillin increases membrane fluidity of liposomes. Our data support a model in which flotillins are required for direct control of membrane fluidity rather than for the formation of protein complexes via direct protein-protein interactions.

Introduction

The shape of a bacterium is predominantly defined by the structure of its peptidoglycan. Although there is a great variety in bacterial shapes, the overall chemistry of peptidoglycan is very similar between bacteria and thus the shape of peptidoglycan is primarily determined by the temporal and spatial regulation of peptidoglycan synthesis. In rod-shaped bacteria, peptidoglycan synthesis is thought to be mediated by two protein assemblies, the elongasome and the divisome, that synthesise peptidoglycan along the long axis and across the division plane of the cell, respectively (***Typas et al., 2012***; ***Zhao et al., 2017***). These complexes contain a set of proteins required for the final steps of synthesis and translocation of the peptidoglycan precursor, LipidII, from the inner to the outer leaflet of the cytoplasmic membrane, and proteins that incorporate LipidII into peptidoglycan. These include SEDS (Shape, Elongation, Division and Sporulation) proteins that can perform

eLife digest Every living cell is enclosed by a flexible membrane made of molecules known as phospholipids, which protects the cell from harmful chemicals and other threats. In bacteria and some other organisms, a rigid structure known as the cell wall sits just outside of the membrane and determines the cell's shape.

There are several proteins in the membrane of bacteria that allow the cell to grow by assembling new pieces of the cell wall. To ensure these proteins expand the cell wall at the right locations, another protein known as MreB moves and organizes them to the appropriate place in the membrane and controls their activity. Previous studies have found that another class of proteins called flotillins are involved in arranging proteins and phospholipid molecules within membranes. Bacteria lacking these proteins do not grow properly and are unable to maintain their normal shape. However, the precise role of the flotillins remained unclear.

Here, Zielińska, Savietto et al. used microscopy approaches to study flotillins in a bacterium known as *Bacillus subtilis*. The experiments found that, in the presence of flotillins, MreB moved around the membrane more quickly (suggesting it was more active) than when no flotillins were present. Similar results were observed when bacterial cells lacking flotillins were treated with a chemical that made membranes more 'fluid' – that is, made it easier for the molecules within the membrane to travel around. Further experiments found that flotillins allowed the phospholipid molecules within an artificial membrane to move around more freely, which increases the fluidity of the membrane.

These findings suggest that flotillins make the membranes of bacterial cells more fluid to help cells expand their walls and perform several other processes. Understanding how bacteria control the components of their membranes will further our understanding of how many currently available antibiotics work and may potentially lead to the design of new antibiotics in the future.

glycosyl transferase reactions (***Cho et al., 2016***; ***Meeske et al., 2016***; ***Taguchi et al., 2019***), and Penicillin Binding Proteins (PBPs) that are divided in class A PBPs (aPBPs) that catalyse both glycosyl transferase and transpeptidase reactions, class B PBPs (bPBPs) that only catalyse transpeptidase reactions and low molecular weight PBPs that modify peptidoglycan, as well as hydrolases (***Zhao et al., 2017***; ***Morales Angeles and Scheffers, 2017***).

Coordination of these complexes is linked to cytoskeletal elements, MreB (-like proteins) for the elongasome and FtsZ for the divisome. In models, the cytoplasmic membrane is often depicted as a passive environment in which these machineries are embedded. However, it is becoming clear that the structure of the membrane plays a critical role in the coordination of peptidoglycan synthesis (***Strahl and Errington, 2017***). Inward membrane curvature serves as a localisation trigger for MreB and the elongasome, and enhanced local synthesis at bulges straightens out the membrane sufficient to convert spherical cells to a rod shape (***Hussain et al., 2018***; ***Ursell et al., 2014***). In *Bacillus subtilis,* the motion of MreB along the membrane is associated with elongasome activity (***Domínguez-Escobar et al., 2011***; ***Garner et al., 2011***), and the velocity of MreB patches is related to growth rate (***Billaudeau et al., 2017***), indicating that MreB motion can be used as a marker for elongasome activity. Interestingly, MreB localises to and organises regions of increased membrane fluidity (RIF) (***Strahl et al., 2014***), which in turn is linked to the presence of LipidII, which favours a more fluid membrane and promotes local membrane disorder (***Ganchev et al., 2006***; ***Witzke et al., 2016***). Inhibition of LipidII synthesis by genetic or chemical means results in a dissolution of membrane structures observed with the dye FM 4–64 and release of MreB from the membrane (***Domínguez-Escobar et al., 2011***; ***Garner et al., 2011***; ***Muchová et al., 2011***; ***Schirner et al., 2015***).

Next to RIFs, membrane regions of decreased fluidity have been identified in bacteria (***Strahl and Errington, 2017***; ***Bramkamp and Lopez, 2015***; ***Lopez and Koch, 2017***). These so-called functional membrane microdomains (FMMs) are thought to be organised by the bacterial flotillin proteins, are enriched in isoprenoid lipids (***García-Fernández et al., 2017***; ***López and Kolter, 2010***), and can be found in so-called Detergent Resistant Membrane (DRM) fractions of the membrane. Since the formulation of the FMM hypothesis, FMMs have been linked to many processes, such as protein secretion, biofilm formation, competence and cell morphology (***Mielich-Süss and Lopez, 2015***; ***Mielich-***

Süss et al., 2013; *Bach and Bramkamp, 2013*; *Dempwolff et al., 2012*). Cell morphology defects are linked to cell wall synthesis, and analysis of the protein content of *Bacillus subtilis* DRMs identified several PBPs, MreC and other proteins involved in cell wall metabolism as well as the two flotillins, FloA and FloT (*López and Kolter, 2010*; *Bach and Bramkamp, 2013*; *Yepes et al., 2012*). FloA is constitutively expressed, whereas FloT is expressed primarily during stationary growth, cell wall stress and sporulation (*Schneider et al., 2015a*; *Huang et al., 1999*; *Nicolas et al., 2012*). Super resolution microscopy showed that the flotillins and other proteins found in DRMs do not colocalise and have different dynamics (*Dempwolff et al., 2016*), so it is unlikely that FMMs are regions in the membrane that offer a favourable environment in which these membrane proteins are continuously present and active. Recently, the hypothesis has been put forward that FMMs/flotillins form a platform for the formation of functional protein oligomers, as work in *Staphylococcus aureus* showed that multimerisation of Type 7 secretion systems and PBP2a depends on FMMs (*Lopez and Koch, 2017*; *García-Fernández et al., 2017*; *Mielich-Süss et al., 2017*).

Here, we have analysed the role of flotillins in peptidoglycan synthesis in *B. subtilis*. Our results show that, at high growth rates, flotillins control membrane fluidity in a manner that is critical for peptidoglycan synthesis and MreB dynamics, but have no effect on PBP oligomerisation. This results in a new model for flotillin function in the physical organisation of membranes during fast growth.

Results

Absence of flotillins shifts peptidoglycan synthesis to division Septa

In previous studies, a double deletion of *floA/floT* was either reported to suffer severe shape defects and perturbed membrane structure (*Dempwolff et al., 2012*), or to not have strong shape defects but with a change in the overall lipid ordering of the membrane (*Bach and Bramkamp, 2013*). We grew wild type and Δ*floAT* strains and analysed exponentially growing cells. We did not observe striking shape defects but did see an increase in median cell length and distribution of cell lengths in the absence of flotillins (*Figure 1A,G*). To look at effects on peptidoglycan synthesis, we labelled cells with HADA, a fluorescent D-Alanine analogue that reports on sites of active peptidoglycan synthesis (*Kuru et al., 2012*), and with fluorescent vancomycin (Van-FL), which labels LipidII and peptidoglycan containing pentapeptide side chains (*Daniel and Errington, 2003*; *Morales Angeles et al., 2017*). This revealed a significant accumulation of peptidoglycan synthesis stains at division septa in the Δ*floAT* strain (*Figure 1A–C*). To look at membrane structure, cells were labelled with FM4-64, Nile-Red and DiI-C12, which are lipid dyes that accumulate in zones enriched in fluid lipids (*Strahl et al., 2014*). Again, the stains accumulated at the septa in the Δ*floAT* strain, which also showed some accumulation of FM4-64 and DiI-C12 in patches, suggesting that the more fluid regions of the membrane are coalescing into larger regions (*Figure 1A,D–F*). The HADA, FM4-64 and Nile-Red measurements were repeated using a wild type strain expressing endogenous GFP, allowing simultaneous imaging of both strains on the same slide, and gave similar results, confirming that the observed signal increase is not due to variation between microcopy experiments (*Figure 1—figure supplement 1A,B*). In this mixed-strain experiment, Nile-Red labelling at the lateral membrane was the same between wild type and Δ*floAT* strains, indicating that there is no difference in dye diffusion between the strains (*Figure 1—figure supplement 1D*). Inspection of the septa by electron microscopy revealed that there was no difference between the thicknesses of the septa between the wild type and Δ*floAT* strain, ruling out that the increase in signal was due to formation of thicker septa (*Figure 1—figure supplement 1C*). The shift of peptidoglycan synthesis to the division site could hint at stress in the overall peptidoglycan synthesis route. This was confirmed by growing cells at a sublethal concentration of fosfomycin, which limits synthesis of LipidII (*Kahan et al., 1974*), but that does not impact growth rate at the concentration used. This resulted in bulging cells and some lysis, which was exacerbated in the Δ*floAT* strain (*Figure 1—figure supplement 1F,G*). It should be noted that the peptidoglycan synthesis stress caused by fosfomycin is not the same as the stress caused by the absence of flotillins, as the phenotypes of wild type cells with sublethal fosfomycin are quite distinct from Δ*floAT* cells without fosfomycin.

We ruled out that the peptidoglycan synthesis stress was caused by a change in the folding or complex formation by PBPs in the absence of flotillins, as there were no differences in the overall PBP-profiles of Bocillin-FL labelled wild type or flotillin deletion strains (*Figure 1—figure*

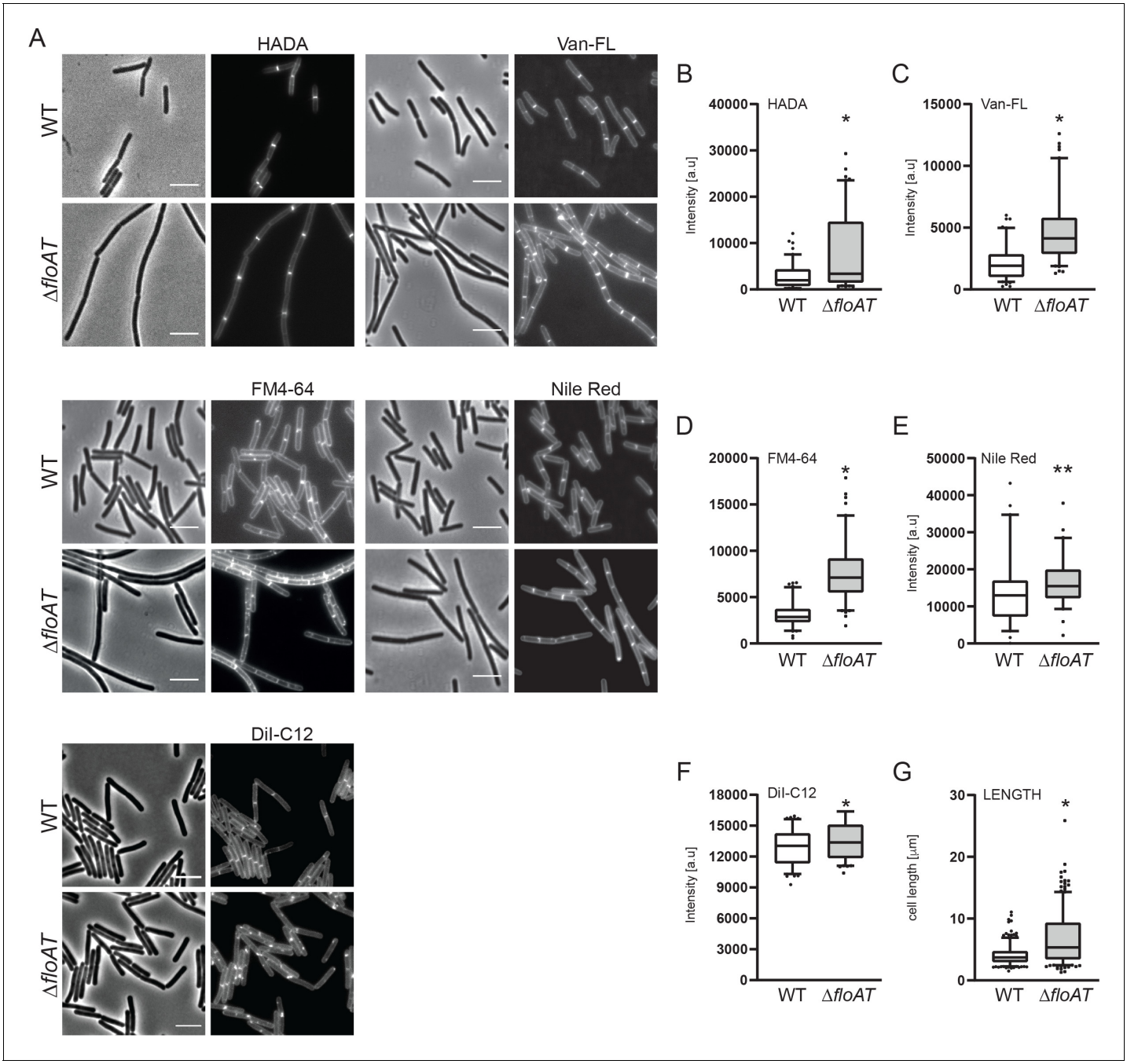

Figure 1. Accumulation of peptidoglycan synthesis and membrane material at division sites in a flotillin mutant. (**A**) Morphology of the exponentially growing wild type (WT) and Δ*floAT* strains labelled with HADA, fluorescent Vancomycin (Van-FL), FM 4–64, Nile Red, and DiI-C12. Scale bar: 5 µm. (**B–F**) Peak intensity of HADA (**B**), Van-FL (**C**), Nile Red (**D**), FM4-64 (**E**) and DiI-C12 (**F**) labelled division sites of the cells shown in (**A**). Cells from each strain ($n \geq 100$, except E, n = 60) were analysed using the ObjectJ macro tool PeakFinder followed by statistical analysis with Prism. Significant differences are based on the two-tailed Mann-Whitney test (*p<0.05; **p<0.01). (**G**) Distribution of the cell length of the strains analysed in (**A**). Statistical analysis of the data (n = 100, two tailed Mann-Whitney test, *p<0.05) was performed with Prism, resulting in box plot graphs.

The online version of this article includes the following source data and figure supplement(s) for figure 1:

Source data 1. Fluorescence intensity and cell length measurements.

Figure supplement 1. Control experiments showing that differences in septal labeling intensity are not due to microscopy settings, septum thickness, or dye diffusion.

Figure supplement 1—source data 1. Growth data plotted in FS1F.

Figure supplement 1—source data 2. Data plotted in F1F1Sb, F1FS1C, F1FS1.

Figure 1 continued on next page

Figure 1 continued

Figure supplement 2. Absence of flotillins does not affect expression, oligomerisation or localisation of PBPs.

supplement 2A). PBP complex formation was analysed using a combination of Native-PAGE and SDS-PAGE with Bocillin-labelled membrane fractions (***Trip and Scheffers, 2016***) and showed that various PBPs can be found in a high-MW complex (notably PBPs 1, 2, 3 and 4), but that complex formation is similar in the Δ*floAT* strain (***Figure 1—figure supplement 2B***). Also, none of the five functional GFP-PBPs examined changed their localisation in the Δ*floAT* strain (***Figure 1—figure supplement 2C***). Overall, the data suggest that in the absence of flotillins, peptidoglycan synthesis is affected and relatively increased at division septa, with a concomitant accumulation of membrane dyes that are indicative of higher membrane fluidity.

The absence of both flotillins and PBP1 causes a severe phenotype, linked to a loss of membrane fluidity

We reasoned that a non-lethal defect in septal peptidoglycan synthesis could reveal more about the role of flotillins and constructed a flotillin mutant that lacks PBP1, a bifunctional glycosyl transferase/transpeptidase that is required for efficient cell division (***Scheffers and Errington, 2004***). Simultaneous deletion of *pbp1*, *floA*, and *floT* resulted in strong filamentation and delocalisation of peptidoglycan synthesis as well as membrane dyes to patches (***Figure 2A***, ***Figure 2—figure supplement 1A***). Deletion of single flotillin genes and PBP1 had similar, albeit less severe effects (***Figure 2—figure supplement 1B,C***). To exclude the possibility that an alteration of peptidoglycan modification resulted in the delocalisation of HADA and Van-FL, we used D-Alanine-D-Propargylglycine (D-Ala-D-Pra), a clickable dipeptide analogue which is exclusively incorporated into peptidoglycan via LipidII (***Sarkar et al., 2016***). D-Ala-D-Pra incorporation was delocalised in the Δ*pbp1*Δ*floAT* strain, indicating that peptidoglycan synthesis itself is delocalised (***Figure 2—figure supplement 1D***). So far, our experiments were done with fast growing cells and Lysogeny Broth (LB) as the growth medium. Strikingly, none of the mutant strains had an apparent phenotype when cultivated in Spizizen's minimal medium (SMM, ***Figure 2B***), and peptidoglycan synthesis and lipid dyes were no longer accumulating at division sites in the Δ*floAT* strain (***Figure 2—figure supplement 2***). SMM has a higher Mg^{2+} concentration, which is known to rescue various cell shape mutations by inhibition of cell wall hydrolysis (***Dajkovic et al., 2017***). However, the increase in Mg^{2+} was not sufficient to explain the reversal of phenotype as cells grown on LB supplemented with Mg^{2+} (6 mM, concentration in SMM, or 20 mM) still displayed the elongated phenotype with delocalised peptidoglycan synthesis (***Figure 2—figure supplement 3***). This indicated that the phenotypes associated with the absence of flotillins are growth-rate and/or nutrient related.

Next, we determined lipid packing order in the different strains using the fluorescent dye Laurdan, a reporter for flotillin-mediated lipid ordering (***Bach and Bramkamp, 2013***). LB-grown cells lacking flotillins displayed an increased generalised polarisation (GP) (***Bach and Bramkamp, 2013***), indicative of an overall increase in ordered lipid packing in the membrane, but the effect of flotillins on membrane ordering completely disappeared when cells were grown on SMM (***Figure 3***). The resolution obtained with Laurdan does not allow the detection of local differences in fluidity between the lateral membrane and the septa, but does report on overall lipid ordering. Overall, lipid order was increased in cells grown on SMM compared to LB (***Figure 3***), whereas the absence of PBP1 had no significant effect on membrane fluidity, also not when combined with flotillin deletions (***Figure 3***). The changes in lipid ordering were not due to changes in the overall fatty acid composition of the membranes - the ratios of C17/C15 side chains and *iso/anteiso* fatty acids, which are indicative of fluidity (***Strahl et al., 2014***), were identical for wild type and Δ*floAT* strains grown on LB, and very similar for cells grown on SMM (***Figure 3—figure supplement 1***).

Restoring membrane fluidity rescues normal peptidoglycan synthesis

The GP values indicated that membranes are more ordered when cells are grown on minimal medium, and this suggests that the flotillin-associated increase in overall membrane fluidity is important for cell shape control at high growth rates. This was tested by growing the strains lacking flotillins and PBP1 on LB in the presence of benzyl alcohol, an extensively used membrane fluidiser that

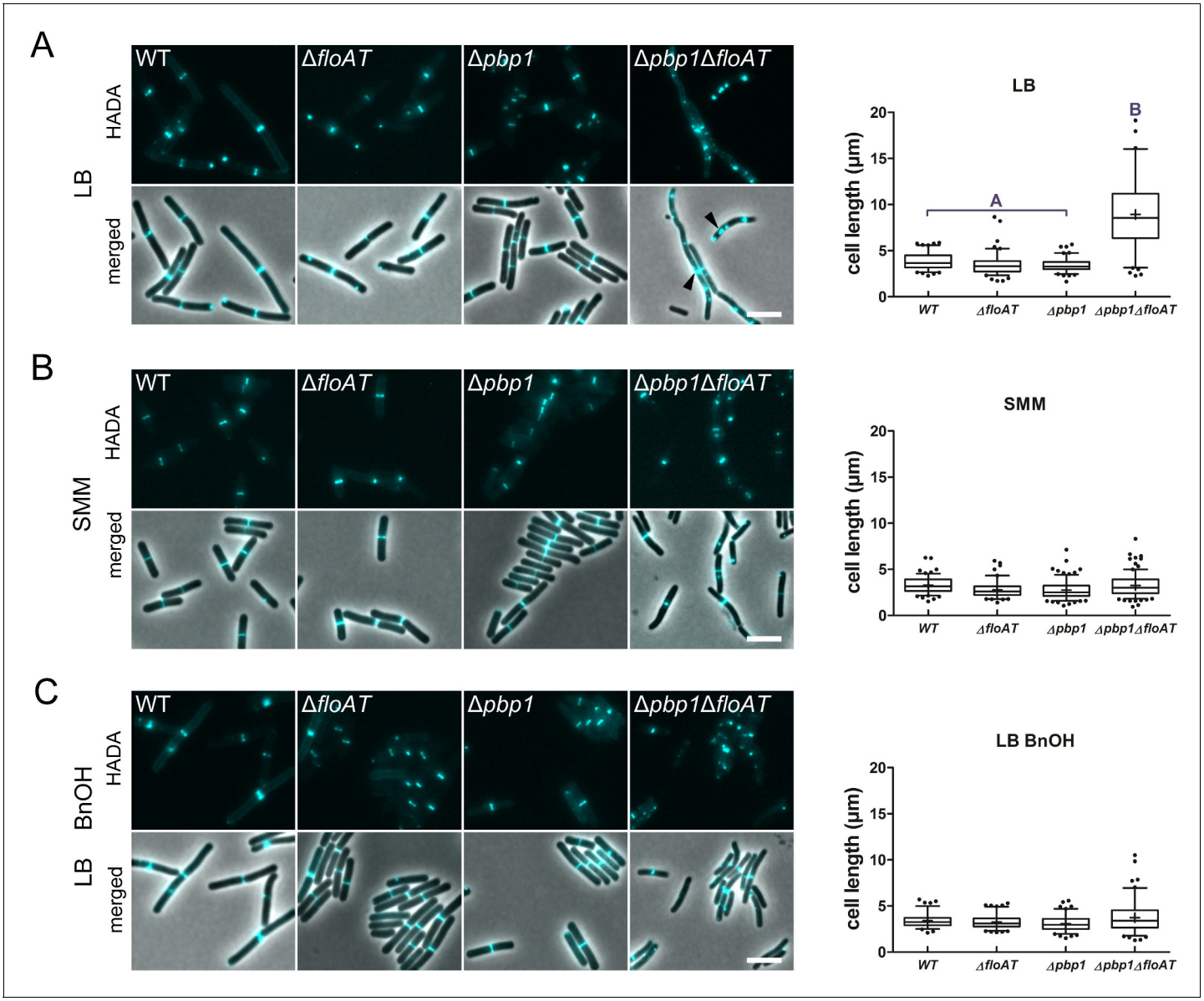

Figure 2. Cell morphology and cell wall synthesis localisation is dependent on growth conditions. Morphology of the *WT*, Δ*floAT*, Δ*pbp1*, and Δ*pbp1*Δ*floAT* strains grown in (**A**) rich (LB), (**B**) minimal (SMM) medium, and in (**C**) rich medium with membrane fluidising conditions (0.1% benzyl alcohol, LB+BnOH). Cells were labelled with HADA, and aberrant cell shape and peptidoglycan synthesis are indicated with arrowheads. Panels on the right indicate corresponding cell length distributions ($n \geq 100$). Distributions were analysed using Dunn's multiple comparison tests after Kruskal–Wallis. Statistically significant cell length distribution classes ($p<0.001$) are represented as letters above each graph – in B and C there were no significant differences. Scale bar: 4 μm.

The online version of this article includes the following source data and figure supplement(s) for figure 2:

Source data 1. Cell length measurements.

Figure supplement 1. Deletion of both flotillins and PBP1 induces filamentation and delocalisation of peptidoglycan synthesis.

Figure supplement 1—source data 1. Cell length measurements plotted in F2F1C.

Figure supplement 2. Septum labelling of wild type and flotillin mutant cells grown on minimal medium.

Figure supplement 2—source data 1. Fluorescence intensity measurements plotted in F2FS2.

Figure supplement 3. Filamentation and delocalisation of peptidoglycan synthesis in the absence of flotillins and PBP1 is not rescued by the addition of magnesium.

Figure supplement 4. Growth curves and growth rates show similar growth for wt, Δ*floAT*, Δ*pbp1*, and Δ*pbp1*Δ*floAT* (as well as Δ*floA*, Δ*floT*, Δ*pbp1*Δ*floA and* Δ*pbp1*Δ*floT)* strains grown on LB or on LB supplemented with BnOH (0.1% (w/v)).

Figure supplement 4—source data 1. Growth curve data.

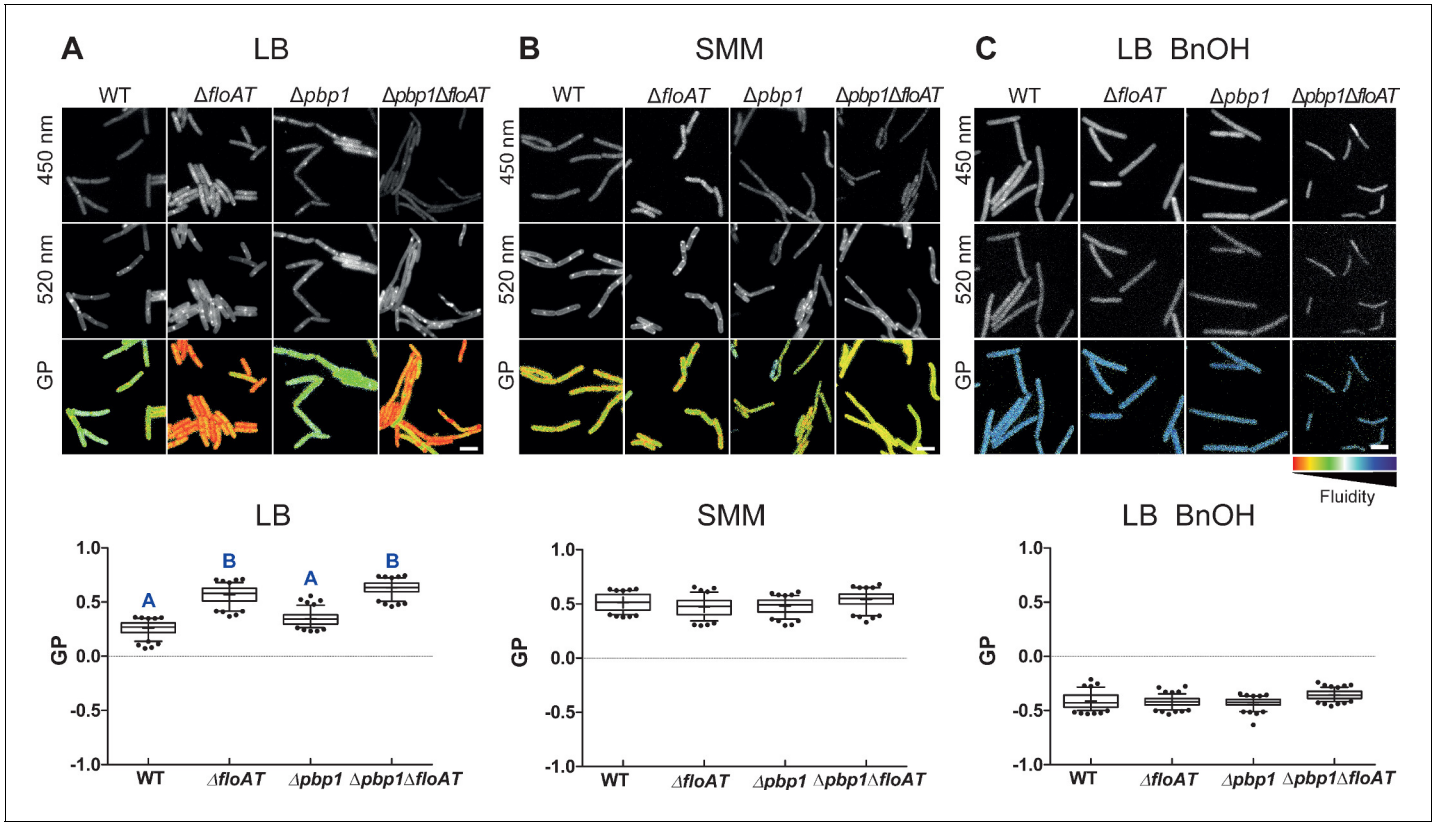

Figure 3. Flotillins increase overall membrane fluidity at high growth rate. Changes in overall membrane fluidity were assessed by Laurdan microscopy in cells grown on LB (**A**), SMM (**B**) and LB+BnOH (**C**). Micrographs show colour-coded generalised polarisation (GP) maps in which red indicates regions of decreased fluidity (scale bar: 4 μm). Correspondent theoretical GP measurements in the graphs vary from −1 (more fluid) to 1 (less fluid). Significant statistical differences according to Dunn's multiple comparison tests after Kruskal–Wallis are represented as letters above each graph in panel (**A**). Data labelled 'A' are significantly different from data labelled 'B'; data with the same letter are not significantly different. No statistically significant difference was observed for the data in panels (**B**) and (**C**) ($p<0.001$; $n \geq 150$, two biological replicates).

The online version of this article includes the following source data and figure supplement(s) for figure 3:

Source data 1. GP measurement.

Figure supplement 1. Fatty acid composition analysis.

Figure supplement 1—source data 1. Fatty acid composition data.

increases membrane hydration due to disordering of membrane structure (***Konopásek et al., 2000***). Notably, the addition of benzyl alcohol increased membrane fluidity to similar extents in the wild-type and the mutant strains (see ***Figure 3C***), but did not affect the growth rates of the strains (***Figure 2—figure supplement 4***). The increase in membrane fluidity restored normal cell length and normal peptidoglycan synthesis patterns to the *pbp1/floA/floT* strain (***Figure 2C***).

In *B. subtilis*, the rate of growth and of peptidoglycan synthesis is linked to the speed of MreB movement – in minimal media, the speed of MreB patches is reduced compared to the speed in rich media (***Billaudeau et al., 2017***). Analysis of the movement of a fully functional mRFPruby-MreB fusion (***Domínguez-Escobar et al., 2011***) by time lapse TIRF (Total Internal Reflection Fluorescence) microscopy, confirmed that MreB patch mobility is higher in cells grown on LB than in cells grown on SMM, with MreB speeds similar to those reported previously (***Billaudeau et al., 2017***; ***Figure 4***, ***Figure 4—videos 1*** and ***2***). Strikingly, in the absence of flotillins, MreB patch mobility was notably decreased in cells grown on LB, while in SMM grown cells MreB patch mobility was independent of the presence of flotillins (***Figure 4***, ***Figure 4—videos 3*** and ***4***). Fluidising the membrane with benzyl alcohol, which does not alter the growth rate, almost completely restored MreB mobility in LB grown cells (***Figure 4***, ***Figure 4—videos 5*** and ***6***). These results indicate that the MreB patch mobility is not only controlled by growth rate, but also by membrane fluidity. Thus, in fast growing cells with decreased membrane fluidity there is a decrease in elongasome mediated peptidoglycan synthesis,

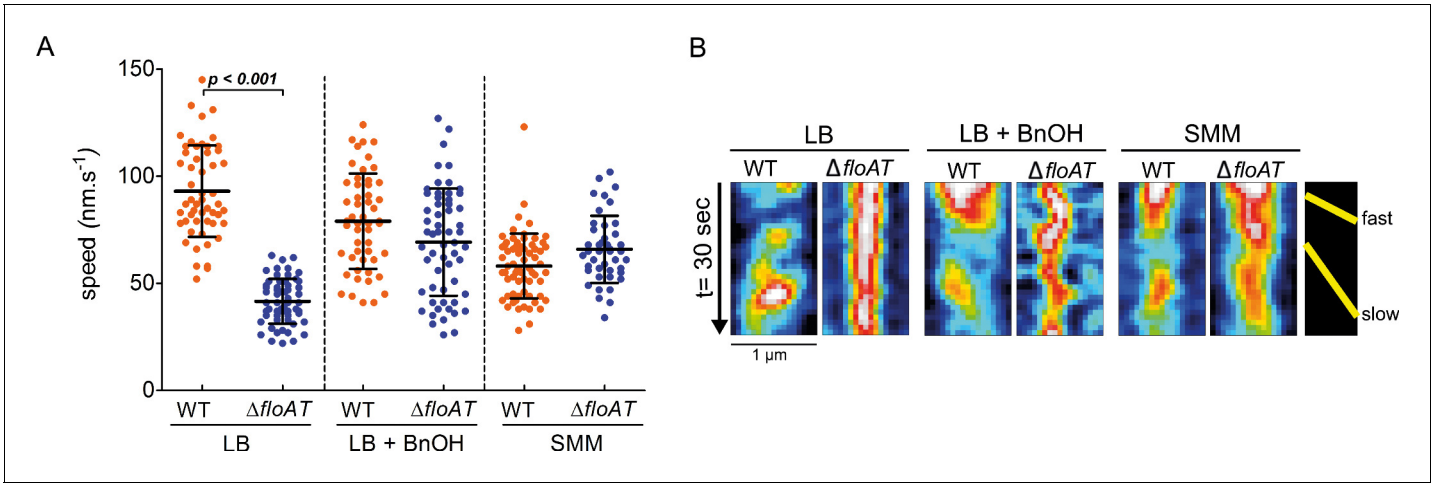

Figure 4. MreB speed is linked to membrane fluidity. (**A**) The MreB speed in different strain backgrounds and growth conditions was analysed by time-lapse TIRF microscopy. Scatter plot of the speed of patches obtained from individual tracks in 5 different cells are represented per fusion and condition. Average speeds are shown; error bars indicate the standard deviation. Significant statistical differences according to Dunn's multiple comparison tests after Kruskal–Wallis are represented ($p<0.001$). (**B**) Representative kymographs showing fast and slow moving patches of mRFPruby-MreB in *B. subtilis* cells lacking endogenous *mreB* (WT) or *mreB* and *floAT* (Δ*floAT*). See ***Figure 4—videos 1–6*** for corresponding raw image series.
The online version of this article includes the following video and source data for figure 4:

Source data 1. MreB patch mobility measurements determined by TIRFM.
Figure 4—video 1. Visualisation of xylose inducible mrfpRuby-MreB patches dynamics (strain 4070) during exponential growth in LB medium at 37˚C by TIRF microscopy.
https://elifesciences.org/articles/57179#fig4video1
Figure 4—video 2. Visualisation of xylose inducible mrfpRuby-MreB patches dynamics (strain 4070) during exponential growth in SMM medium at 37˚C by TIRF microscopy.
https://elifesciences.org/articles/57179#fig4video2
Figure 4—video 3. Visualisation of xylose inducible mrfpRuby-MreB in Δ*floAT* patches dynamics (strain 4076) during exponential growth in LB medium at 37˚C by TIRF microscopy.
https://elifesciences.org/articles/57179#fig4video3
Figure 4—video 4. Visualisation of xylose inducible mrfpRuby-MreB in Δ*floAT* patches dynamics (strain 4076) during exponential growth in SMM medium at 37˚C by TIRF microscopy.
https://elifesciences.org/articles/57179#fig4video4
Figure 4—video 5. Visualisation of xylose inducible mrfpRuby-MreB patches dynamics (strain 4070) during exponential growth in LB medium supplemented with BnOH (0.1%) at 37˚C by TIRF microscopy.
https://elifesciences.org/articles/57179#fig4video5
Figure 4—video 6. Visualisation of xylose inducible mrfpRuby-MreB in Δ*floAT* patches dynamics (strain 4076) during exponential growth in LB medium supplemented with BnOH (0.1%) at 37˚C by TIRF microscopy.
https://elifesciences.org/articles/57179#fig4video6

reflected by the reduction of MreB mobility. This fits with an observed increase in peptidoglycan synthesis at the division site which may act as a compensatory mechanism.

Flotillin increases fluidity of model membranes in vitro

To assess whether the influence of flotillins on membrane fluidity is direct, we determined the membrane fluidity of model membranes with purified flotillin using solid-state NMR (ssNMR). ^{2}H ssNMR is a biophysical tool that assesses lipid mobility in native-like model membranes on the atomic level, by monitoring the carbon-deuterium order parameter of a deuterated lipid along the acyl chain (here POPC-d31) (***Molugu et al., 2017***; ***Legrand et al., 2019***). We purified *B. subtilis* FloT and tested the impact of FloT on the membrane, when reconstituted in POPC-d31 liposomes (Schematically depicted in ***Figure 5A***). FloT decreases the spectral width of the ^{2}H quadrupolar splitting, reflecting an increase in motion on the atomic scale (***Figure 5B***). The ^{2}H spectrum encodes the local order parameter S_{CD} of the carbon-deuterium in absence and in presence of FloT. Strikingly, FloT

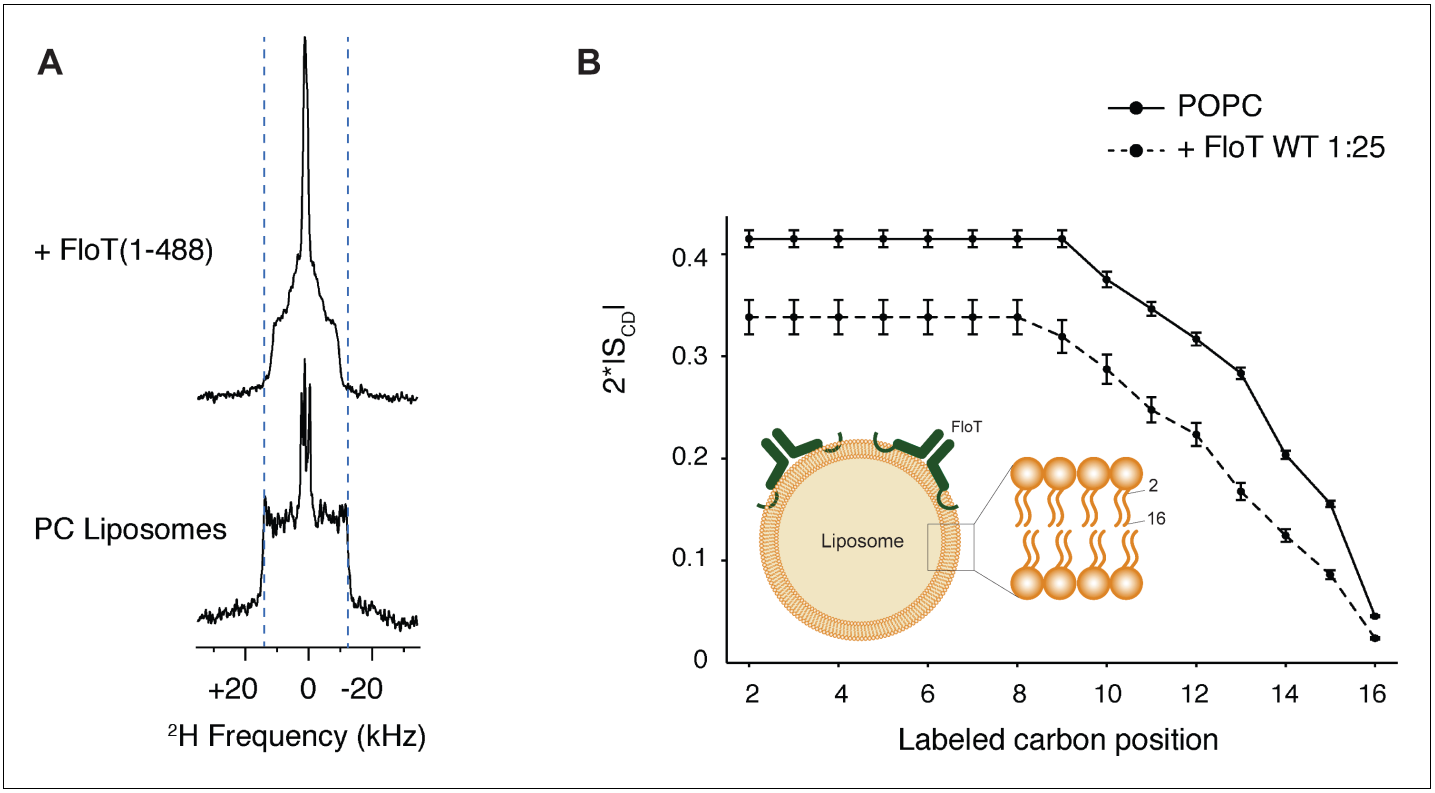

Figure 5. Lipid ordering of FloT probed by ^{2}H solid-state NMR. (**A**) Wide-line ^{2}H spectra of POPC-d31 liposomes with or without FloT at a lipid-to-protein molar ratio of 25:1 acquired at 298 K. (**B**) Effect of FloT on the C-^{2}H order parameters of the PC acyl chain. De-Pake-ing and simulations were applied on the ^{2}H solid-state NMR spectra to determine accurately individual quadrupolar splittings. Order parameters of POPC-d31 acyl chain were derived from experimental quadrupolar splittings and plotted as a function of the labelled carbon position. *Insert:* schematic depiction of a liposome with added FloT which attaches to the membrane via a hairpin loop (***Bach and Bramkamp, 2015***).

The online version of this article includes the following figure supplement(s) for figure 5:

Figure supplement 1. ^{31}P solid-state NMR experiments of POPC liposomes with or without FloT at a lipid-to-protein molar ratio of 25:1.

has an important impact on the order parameter along the entire acyl chain. It is remarkable that the protein significantly decreases the order parameter S_{CD}, reaching even the inner carbon atoms of the acyl chain, indicating a different packing behaviour and increased membrane fluidity upon interaction with FloT (***Figure 5B***). The strong fluidising effect described for FloT is notably different from the effects other proteins have when reconstituted into liposomes, such as plant remorins (***Legrand et al., 2019***) or the membrane binding peptide of the nonreceptor tyrosine kinase Src (***Scheidt and Huster, 2009***). The anisotropic lineshape of the ^{31}P spectra indicates that the membrane is in the lamellar phase as expected for POPC at the chosen temperature (298K) (***Huster, 2014***). Upon interactions with FloT the lamellar phase remains intact with formation of a few smaller objects, indicating that the overall liposome structure is not affected and that its phase is maintained (***Figure 5—figure supplement 1***).

Discussion

Our data provide evidence that flotillins play a direct role in controlling membrane fluidity and that membrane fluidity is critical for peptidoglycan synthesis at certain growth conditions. In vitro, flotillins enhance the fluidity of a model membrane, and in vivo, the membranes of fast growing flotillin-mutant cells are less fluid even though the fatty acid composition in these cells is identical. Therefore, we propose that the effect of flotillins on membrane fluidity is direct, through a change in the packing behaviour of the lipids resulting in an efficient separation of states of liquid ordered and disordered lipid domains in the membrane bilayer (***Bach and Bramkamp, 2013***). We found that

membrane fluidity is not solely a function of temperature, but also of growth conditions. In vivo, flotillins may also recruit specific, more rigid lipids, such as hopanoids and carotenoids (**Bramkamp and Lopez, 2015**; **García-Fernández et al., 2017**; **López and Kolter, 2010**) which have been found in association with FMMs, and whose synthesis could be growth condition dependent. The predominantly physical role in membrane organisation for flotillins fits with our observation that adding a chemical fluidiser is sufficient to restore MreB dynamics and cell shape to fast growing cells that lack flotillins. We propose that in fast-growing cells on rich medium, flotillin-mediated control of membrane fluidity is critical and sufficient to allow essential membrane bound processes, such as peptidoglycan synthesis, to proceed normally.

A sufficiently fluid membrane is necessary for the efficient recruitment and movement of MreB, and provides a more favourable environment for the peptidoglycan precursor LipidII (**Hussain et al., 2018**; **Ursell et al., 2014**; **Schirner et al., 2015**). It has recently been shown that modulation of either MreBCD or PBP1 levels is sufficient to alter the shape of *B. subtilis* cells (**Dion et al., 2019**), underscoring the importance of both systems. In the absence of flotillins, the activity of the MreBCD component is strongly reduced – as evidenced by the reduction of MreB speed – and the overall rigidity of the membrane is increased. This results in a less favourable environment for the peptidoglycan precursor LipidII, which prefers more liquid, disordered membrane phases (**Ganchev et al., 2006**; **Witzke et al., 2016**; **Calvez et al., 2019**). Our data indicate that the reduction in elongasome activity, which does not impact the growth rate itself, is compensated by increased peptidoglycan synthesis activity around division sites in flotillin mutants, which is sufficient to keep the overall cell shape intact, although cells are elongated. The accumulation of lipid dyes indicative of increased fluidity at division sites is in line with a recent study that showed phases of different fluidity in *Streptococcus pneumoniae* membranes, with more fluid membranes and LipidII localising at midcell (**Calvez et al., 2019**) where the membrane is most bent. Our findings are also in agreement with the recent observation that *B. subtilis* cells elongate and lose organisation of MreB when membrane fluidity is decreased by altering the membrane fatty acid composition (**Gohrbandt, 2019**) (H. Strahl, personal communication). It could very well be that the shift of fluidity towards the septum is only relative as the overall fluidity of the membrane is decreased in the absence of flotillins. This is yet to be determined, as the resolution of Laurdan imaging does not allow conclusive statements about local fluidity changes at the septum. The observation that reduced MreB mobility and therefore altered lateral cell wall synthesis lead to accumulation of Van-FL and HADA staining at the septum is not immediately conclusive. Since septal PG synthesis is MreB independent in *B. subtilis*, a direct effect of MreB seems unlikely. Rather, a reduction of overall membrane fluidity in a flotillin knock-out might impair LipidII dynamics within the membrane. MurG is the enzyme that catalyses the final step of LipidII synthesis. There are several reports that MurG localises to the septum in different organisms (**Aaron et al., 2007**; **Mohammadi et al., 2007**). Thus, it seems likely that the septum is a place of increased LipidII synthesis and a change in membrane fluidity would create problems for LipidII molecules to diffuse away from their insertion site, resulting in reduced lateral PG synthesis and MreB mobility. Alternatively, the reduced MreB mobility and reduced lateral PG synthesis lead to a reduced LipidII consumption at the lateral wall, and the excess LipidII is used by the septal PG synthesis machinery, thereby leading to an increase in midcell PG. It remains to be tested which of these possibilities is responsible for the observed phenotype. Nevertheless, in both cases the increase in cell wall staining at the septum would be indicative of a higher local synthesis activity.

It may seem paradoxical that cells elongate when elongasome activity is reduced, but one has to remember that a large amount of the peptidoglycan synthesis contributing to elongation of bacterial cells is actually taking place at midcell, before the ingrowth of the septum (**Aaron et al., 2007**; **Pazos et al., 2018**; **Varma and Young, 2009**). A relative increase in peptidoglycan synthesis at future division sites makes the activity of PBP1 critical and explains why its deletion has such a dramatic effect in cells lacking flotillins. Restoring fluidity using a chemical fluidiser allows the MreBCD component to again efficiently drive peptidoglycan synthesis during elongation, which is sufficient to suppress the flotillin mutant phenotype. The net effect of this is that cells lacking PBP1 and flotillins grown with benzyl alcohol behave as cells that only lack PBP1, which is quite similar to wild type. At low growth rates, there is no difference between wild type cells and cells lacking flotillins with respect to membrane fluidity, and the speed of MreB is similar between the two cell types. Thus the deletion of flotillins does not exacerbate the phenotype of cells lacking PBP1. The reason for the change in membrane fluidity between cells grown on rich or minimal medium is not yet clear – it

does not seem to be caused by a large shift in the fatty acid composition of the membranes. Various factors could play a role, such as the synthesis of specific lipids (hopanoids, isoprenoids) on either type of medium, but also protein crowding, which is higher in membranes of fast-growing cells than in slow-growing cells (**Szenk et al., 2017**). It will be an important future challenge to establish the cause for this difference. An overall rigidification of the membrane may also lead to retardation of processes which require membrane modifications such as division and sporulation, which is indeed observed in *B. subtilis* flotillin mutants (**Dempwolff et al., 2012**; **Donovan and Bramkamp, 2009**).

One of the proposed roles for flotillin proteins is that they form a 'platform' that transiently interacts with membrane proteins that need to oligomerise into functional complexes (**Lopez and Koch, 2017**). We tested this hypothesis for *B. subtilis* PBPs by comparing their localisation and oligomerisation in wild type and flotillin mutant strains. Although we were capable of detecting a high MW complex containing various PBPs (notably PBP1, 2a, 2b, 3 and 4), the complex was not dependent on the presence of flotillins. We also note that PBP1 was present in the complex, as well as present in a large smear in the first dimension native gel, which would explain why PBP1 was detected by mass spectrometry analysis of a native PAGE band containing FloA (**Schneider et al., 2015a**). PBP5, on the other hand, was not part of the high MW complex, which fits with its role in processing of the terminal D-Ala from stem-peptides that have not been cross-linked, which it exercises over the entire surface of the cell (**Kuru et al., 2012**). Although we cannot exclude that flotillins may affect PBPs that are not easily detected by Bocillin-FL, our results do not provide any evidence for a role for flotillins in the oligomerisation of PBPs in *B. subtilis*. This extends the finding of the Graumann lab that found either transient or no colocalisation between flotillins and other proteins present in DRM fractions (**Dempwolff et al., 2016**). Although it is obvious that peptidoglycan synthesis is altered in the absence of flotillins, our data strongly suggest that the basis for this alteration is in the physical organisation of the membrane rather than inefficient formation of divisome or elongasome complexes in the absence of flotillins, because flotillin mutants strains show no synthetic phenotype on minimal medium, and the defects on rich medium can be reverted by chemically fluidising the membrane.

In conclusion, our data provide a new model for flotillin function in the physical organisation of membranes during fast growth. The observation that flotillins differentially affect the membrane in different growth conditions also explains the diversity of phenotypes described for flotillin mutants in the literature.

Materials and methods

Key resources table

Reagent type (species) or resource	Designation	Source or reference	Identifiers	Additional information
Strain, strain background (*Escherichia coli*)	BL21(DE3)	Thermo Fisher Scientific	EC0114	Chemically competent cells
Strain, strain background (*Bacillus subtilis*)	BB001	**Bach and Bramkamp, 2013**	*trpC2 yqfA::tet*	
Strain, strain background (*Bacillus subtilis*)	BB003	**Bach and Bramkamp, 2013**	*trpC2 yuaG::pMUTIN4 yqfA::tet*	
Strain, strain background (*Bacillus subtilis*)	DB003	**Donovan and Bramkamp, 2009**	*trpC2 yuaG::pMUTIN4*	
Strain, strain background (*Bacillus subtilis*)	RWBS5	**Domínguez-Escobar et al., 2011**	*trpC2 amyE::spc* P_{xyl}*-mrfpruby-mreB*	
Strain, strain background (*Bacillus subtilis*)	PS832	**Popham and Setlow, 1995**	Prototrophic revertant of 168	

Continued on next page

Continued

Reagent type (species) or resource	Designation	Source or reference	Identifiers	Additional information
Strain, strain background (*Bacillus subtilis*)	2082	**Scheffers et al., 2004**	*trpC2 pbpD::cat* P_{xyl}*–gfp–pbpD* $^{1–510}$	
Strain, strain background (*Bacillus subtilis*)	2083	**Scheffers et al., 2004**	*trpC2 ponA::cat* P_{xyl}*–gfp–ponA* $^{1–394}$	
Strain, strain background (*Bacillus subtilis*)	2085	**Scheffers et al., 2004**	*trpC2 dacA::cat Pxyl–gfp–dacA* $^{1–423}$	
Strain, strain background (*Bacillus subtilis*)	3105	**Scheffers et al., 2004**	*trpC2 pbpC::cat Pxyl-gfp–pbpC* $^{1–768}$	
Strain, strain background (*Bacillus subtilis*)	3122	**Scheffers et al., 2004**	*trpC2 pbpB::cat* P_{xyl}*-gfp-pbpB* $^{1–825}$	
Strain, strain background (*Bacillus subtilis*)	3511	**Scheffers and Errington, 2004**	*trpC2 ponA::spc*	
Strain, strain background (*Bacillus subtilis*)	4042	**Lages et al., 2013**	*trpC2 pbpA::cat* P_{xyl}*-mkate2-pbpA* $^{1–804}$	
Strain, strain background (*Bacillus subtilis*)	4056	**Morales Angeles et al., 2017**	*trpC2 dacA::kan*	
Strain, strain background (*Bacillus subtilis*)	4059	This work	*trpC2 dacA::cat* P_{xyl}*-gfp–dacA* $^{1–423}$ *yuaG::pMUTIN4 yqfA::tet*	Scheffers lab
Strain, strain background (*Bacillus subtilis*)	4064	This work	*trpC2 dacA::kan yuaG::pMUTIN4 yqfA::tet*	Scheffers lab
Strain, strain background (*Bacillus subtilis*)	4090	This work	*trpC2 ponA::spc yuaG::pMUTIN4*	Scheffers lab
Strain, strain background (*Bacillus subtilis*)	4091	This work	PS832 *ponA::spc yqfA::tet*	Scheffers lab
Strain, strain background (*Bacillus subtilis*)	4092	This work	*trpC2 ponA::spc yuaG::pMUTIN4 yqfA::tet*	Scheffers lab
Strain, strain background (*Bacillus subtilis*)	4095	This work	*trpC2 ponA::cat* P_{xyl}*-gfp–ponA* $^{1–394}$ *yuaG::pMUTIN4 yqfA::tet*	Scheffers lab
Strain, strain background (*Bacillus subtilis*)	4099	This work	*trpC2 pbpB::cat Pxyl-gfp-pbpB* $^{1–825}$ *yuaG::pMUTIN4 yqfA::tet*	Scheffers lab
Strain, strain background (*Bacillus subtilis*)	4102	This work	*trpC2 pbpA::cat Pxyl-mkate2-pbpA* $^{1–804}$ *yuaG::pMUTIN4 yqfA::tet*	Scheffers lab
Strain, strain background (*Bacillus subtilis*)	4108	This work	*trpC2 pbpD::cat* P_{xyl}*-gfp–pbpD* $^{1–510}$ *yuaG::pMUTIN4 yqfA::tet*	Scheffers lab

Continued on next page

Continued

Reagent type (species) or resource	Designation	Source or reference	Identifiers	Additional information
Strain, strain background (*Bacillus subtilis*)	4122	This work	*trpC2 pbpC::cat* P_{xyl}*-gfp–pbpC* $^{1–768}$ *yuaG::pMUTIN4 yqfA::tet*	Scheffers lab
Strain, strain background (*Bacillus subtilis*)	4128	This work	*trpC2 ponA::spc pbpD::cat* P_{xyl}*-gfp–pbpD* $^{1–510}$	Scheffers lab
Strain, strain background (*Bacillus subtilis*)	4129	This work	*trpC2 ponA::spc yuaG::pMUTIN4 pbpD::cat* P_{xyl}*-gfp–pbpD* $^{1–510}$	Scheffers lab
Strain, strain background (*Bacillus subtilis*)	4070	This work	*trpC2 mreB::kan amyE::spc* P_{xyl}*-mrfpruby-mreB*	Scheffers lab
Strain, strain background (*Bacillus subtilis*)	4076	This work	trpC2 *mreB::kan amyE::spc* P_{xyl}*-mrfpruby-mreB yuaG::pMUTIN4 yqfA::tet*	Scheffers lab
Strain, strain background (*Bacillus subtilis*)	4259	This work; **Veening et al., 2009**	*trpC2 amyE::*P_{rrnB}*-gfp*	Scheffers lab
Other	Bocillin	Thermo Fisher Scientific	BOCILLIN FL Penicillin, Sodium Salt	5 µg/ml
Other	HADA	Synthesised as described (**Morales Angeles et al., 2017**)	7-hydroxycoumarin 3-carboxylic acid-amino-D-alanine	50 µM
Other	Vancomycin-FL	Sigma-Aldrich and Molecular Probes (**Zhao et al., 2017**)	Van-FL	1:1 mixture of Vancomycin and BODIPYFL Vancomycin (**Zhao et al., 2017**), final concentration 1 µg/ml
Other	Nile Red	Thermo Fisher Scientific	5H-Benzo[α] phenoxazin-5-one, 9-(diethylamino)-7385-67-3	0.5 µg/ml
Other	16:0-d31-18:1 PC	Avanti	860399	Phospholipids
Other	Laurdan	Sigma-Aldrich	6-Dodecanoyl-N, N-dimethyl-2-naphthylamine	-
Other	Benzyl alcohol	Sigma-Aldrich	Benzyl alcohol	-
Other	DiI-C12	Thermo Fisher Scientific	1,1′-Didodecyl-3,3,3′,3′-Tetramethylindocarbocyanine Perchlorate	2.5 µg/ml
Other	FM4-64	Thermo Fischer Scientific	(N-(3-Triethylammoniumpropyl)–4-(6-(4-(Diethylamino) Phenyl) Hexatrienyl) Pyridinium Dibromide)	0.5 µg/ml, Invitrogen FM 4–64 Dye
Software, algorithm	Prism 5	1992–2010 GraphPad Software	RRID:SCR_002798	-

Continued on next page

Continued

Reagent type (species) or resource	Designation	Source or reference	Identifiers	Additional information
Software, algortithm	ImageJ 1.52p/FIJI	Wayne Rasband – National Institutes of Health, USA	RRID:SCR_002285	Free software
Software, algorithm	SPSS	SPSS	RRID:SCR_002865	software
Software, algorithm	NMR Depaker 1.0rc1 software	[Copyright (C) 2009 Sébastien Buchoux]		software
Software, algorithm	Bruker Topspin 3.2 software	Bruker	RRID:SCR_014227	software

B. subtilis strains and growth conditions

All *B. subtilis* strains used in this study are derived from strain 168 and are listed in the Key resources table. Construction of new strains was based on natural competence of *B. subtilis* (**Harwood and Cutting, 1990**). Gene integration or deletion was validated by colony PCR whereas the expression and localisation of the fluorescent fusions was additionally validated by microscopy. Cells were grown either in LB Lennox (5 g/L yeast extract; 5 g/L NaCl; 10 g/L tryptone) (**Lennox, 1955**) or Spizizen minimal medium (SMM) (**Anagnostopoulos and Spizizen, 1961**) supplemented with 1% glucose, at 37˚C and 200 rpm, unless indicated otherwise. Induction of the P_{xyl} promoter was triggered by addition of 0.2–0.5% xylose. Cell cultures were supplemented with spectinomycin (50 µg/ml), tetracycline (10 µg/ml), chloramphenicol (5 µg/ml), kanamycin (5 µg/ml), erythromycin (1 µg/ml), benzyl alcohol (BnOH, 0.1%) or magnesium sulphate ($MgSO_4$, 6–20 mM) when necessary.

Growth curves

Growth experiments were performed either manually or automatically with a PowerWave 340 microplate reader (BioTek Instruments, U.S.A). Strains were pre-cultured overnight in 3 ml LB or SMM medium at 37˚C with shaking at 200 rpm. Next, stationary or late-exponentially cells were diluted with fresh LB or SMM medium (supplemented when necessary), and cell densities (OD_{600}) were measured every 1 hr when monitored manually or every 10 min when monitored automatically, for a total time of 7–22 hr.

Fluorescence microscopy

For standard fluorescence microscopy, exponentially growing cells were immobilised on microscope slides covered with a thin film of 1% agarose (w/v) in water or the appropriate medium. For TIRFM, agarose pads were mounted using Gene Frames (1.7 × 2.8 cm chamber, 0.25 mm thickness, 125 µL volume) from ThermoScientific. Standard fluorescence microscopy was carried out using an Axio Zeiss Imager M1 fluorescence microscope (EC Plan-Neofluar 100x/1.30 Oil Ph3 objective) equipped with an AxioCam HRm camera and an Nikon-Ti-E microscope (Nikon Instruments, Tokyo, Japan) equipped with Hamamatsu Orca Flash 4.0 camera.

For Laurdan and TIRFM experiments, a Delta Vision Elite microscope (Applied Precision, GE Healthcare) equipped with an Insight SSI Illumination, an X4 Laser module, a CoolSnap HQ (**Zhao et al., 2017**) CCD camera and a temperature-controlled chamber set up at 37 ^{0}C was used. Laurdan images were taken with an Olympus UplanSApo 100x/1.4 oil objective. TIRFM image series were taken using an Olympus UAPO N 100X/1.49 TIRF objective and a 561 nm laser (50 mW, 100% power). Data processing was performed with softWoRx Suite 2.0 Software.

Visualisation of cell wall synthesis

Peptidoglycan (PG) synthesis was assessed by labelling the cells with HADA (7-hydroxycoumarin 3-carboxylic acid-amino-D-alanine) (**Kuru et al., 2015**), Van-FL (**Daniel and Errington, 2003**) or D-Ala-D-Pra (**Sarkar et al., 2016**).

HADA: synthesised as described (**Morales Angeles et al., 2017**). Overnight cultures of *B. subtilis* strains were diluted 1:100 into fresh LB medium or LB medium supplemented with 0.1% (w/v) of

benzyl alcohol (BnOH), a membrane fluidiser. Cells were grown until exponential phase, a sample of 1 ml of culture was spun down for 30 s, 5000 × g and the cell pellet was resuspended in 25 µl of fresh pre-warmed LB or LB containing 0.1% (w/v) BnOH. HADA was added to a 50 µM final concentration. Cells were incubated for 10 min in the dark (37 ^{0}C, 200 rpm) and then washed twice in 1 ml PBS buffer (58 mM Na_2HPO_4, 17 mM NaH_2PO_4, 68 mM NaCl, pH 7.3) to remove the excess of unbounded HADA. Cells were spun down again and resuspended in 25 µl of the appropriate medium and 2 µl of cells were mounted on 1% agarose slides before visualisation. Visualisation of HADA patterns (excitation: 358 nm/emission: 461 nm) under fluorescence microscopy from two biological replicates and cell length measurements were taken from at least 100 cells each strain/treatment.

Van-FL: a 1:1 mixture of vancomycin (Sigma Aldrich) and BODIPYFL Vancomycin (Molecular Probes) at a final concentration 1 µg/ml was used to label cells for 5–10 min at room temperature.

D-Ala-D-Pra: synthesised as described (***Sarkar et al., 2016***). 1 ml of cell cultures was pelleted and resuspended in 50 µl of PBS buffer. Dipeptide was added to a final concentration of 0.5 mM following with 5 min incubation at room temperature. Cells were fixed by adding 70% ethanol and incubated for minimum 2 hr in −20˚C. Next, cells were washed twice with PBS in order to remove unattached peptides, and resuspended in 50 µl of PBS. The D-Ala-D-Pra was subsequently labelled via a click reaction with fluorescent azide (20 µM) that was incubated for 15 min at room temperature with addition of copper sulphate (CuSO4, 1 mM), tris-hydroxypropyltriazolylmethylamine (THPTA, 125 µM) and ascorbic acid (1.2 mM). The sample was washed twice with PBS and resuspended in 50 µl of the same buffer.

Laurdan staining and GP calculations

Laurdan (6-Dodecanoyl-N, N-dymethyl2-naphthylamine, Sigma-Aldrich) was used to detect the liquid ordering in the membrane, as decribed (***Bach and Bramkamp, 2013***), with modifications. Cells were grown in LB or SMM medium until late exponential phase. Laurdan, dissolved in dimethyformamide (DMF), was added at 10 µM final concentration and cells were incubated for 10 min in the dark at 37 ˚C, 200 rpm. Cells were then washed twice in PBS buffer supplemented with 0.2% (w/v) glucose and 1% (w/v) DMF, and resuspended in fresh prewarmed appropriate medium. Laurdan was excited at 360 ± 20 nm, and fluorescence emission was captured at 460 ± 25 nm (exposure time: 500 ms) and at 535 ± 25 nm (exposure time: 1 s) (***Strahl et al., 2014***). The image analysis including the generation of GP maps was carried out using Fiji Software (***Schindelin et al., 2012***) in combination with the macro tool CalculateGP designed by Norbert Vischer (http://sils.fnwi.uva.nl/bcb/objectj/examples/CalculateGP/MD/gp.html). The GP values were measured for at least 100 individual cells after background subtraction, from two biological replicates.

Other fluorescent membrane probes

B. subtilis cell membranes were probed with Nile Red (0.5 µg/ml), FM4-64 (0.5 µg/ml) or DiI-C12 (2.5 µg/ml). To this end, an overnight culture was grown in appropriate antibiotic, diluted 1:100 in LB medium supplemented with DiI-C12 followed by growth until exponential phase. Membranes were probed with Nile Red or FM4-64 for 5 min at room temperature after reaching exponential phase. The stained cells were washed three times in prewarmed LB medium supplemented with 1% DMSO before visualisation under fluorescence microscopy.

TIRF time lapse microscopy

Time-lapse TIRFM movies were taken in two independent experiments for each strain and condition. To this end, overnight cultures of strains grown in LB medium supplemented with the appropriate antibiotic were diluted 1:100 in medium containing 0.5% (w/v) xylose and grown until exponential phase. All experiments were performed inside the incubation chamber set to 37 ˚C, no longer than 10 min after taking the sample. The cells were imaged over 30 s with 1 s inter-frame intervals in a continuous illumination and ultimate focus correction mode. The single particle tracking analyses and kymographs were done using Fiji Software (***Schindelin et al., 2012***) in combination with the MTrackJ (***Meijering et al., 2012***) and MicrobeJ plugins (***Ducret et al., 2016***).

Bocillin labelling

Cells were grown until an OD600 of 0.4–0.5, and washed twice with PBS. Next, samples were resuspended in 50 µl PBS containing Bocillin-FL (5 µg/ml) and incubated at room temperature for 10 min. Subsequently cells were harvested, lysed by sonication and cell-free extracts were prepared. Samples, equalised for culture OD, were prepared with SDS-PAGE sample buffer and run on a 12% SDS-PAGE gel. Fluorescent bands were visualised using a Typhoon Trio (GE Healthcare) scanner.

Isolation of membranes

Membrane isolation was adapted from ***Schneider et al., 2015b***. Briefly, cells were grown until an OD600 of 0.4–0.5, cell fractions were collected and resuspended in PBS with Lysozyme (1 µg/ml), EDTA (5 mM), 1/10 tablet cOmplete protease inhibitor (Roche), and DNAse (5 µg/ml) and incubated for 30 min on ice. Samples were sonicated, cell which did not lyze were spun down (8000 rpm, 2 min, 4˚C), and the supernatant fraction was centrifuged at 4˚C and 40000 rpm for 1 hr. The membrane pellet was dissolved in ACA750 buffer (750 mM aminocaproic acid, 50 mM Bis-Tris, pH 7.0) to a final protein concentration of 1 µg/µl. Membranes were solubilised overnight at 4˚C in 1% (w/v) dodecylmaltoside (DDM) and either used directly or stored at −20˚C.

Blue native PAGE (BN-PAGE)

The experiment was performed as described (***Trip and Scheffers, 2016***). Samples were prepared by mixing sample buffer (0.1% Ponceau S, 42.5% Glycerol) with solubilised membranes in a 1:3 ratio. Samples were resolved on a mini-PROTEAN TGX Stain-Free gradient gel (4–15%, BioRad) using cathode (50 mM Tricine and 15 mM BisTris), and anode (50 mM BisTris pH 7.0) buffers. The Novex NativeMark Unstained Protein Standard marker was used as a Mw marker.

Second dimension SDS PAGE (2D SDS-PAGE)

A lane of interest was excised from the Native-PAGE gel and immobilised horizontally on top of a SDS-PAGE gel (5% stacking, 12% resolving). The excised fragment was flanked with a piece of Whatman paper soaked with PageRuler Prestained Protein Ladder. The gel fragment to be resolved in the second dimension was topped with a mix of 1% (w/v) LowTemperature agarose, 0.5% (w/v) SDS and bromophenol blue. After the agarose had solidified, standard SDS-PAGE electrophoresis was performed.

TEM

Cultures were harvested by centrifugation and a small amount of pellet was placed on a copper dish. A 400 copper mesh grid and a 75 µm aperture grid was placed on top of the cells to create a thin layer. The sandwiched cells were plunged rapidly into liquid propane. Sandwiches were then disassembled and placed on frozen freeze-substitution medium containing 1% osmium tetroxide, 0.5% uranyl acetate and 5% water in acetone. Cells were dehydrated and fixed using the rapid freeze substitution method (***McDonald, 2014***). Samples were embedded in epon and ultrathin sections were collected on formvar coated and carbon evaporated copper grids and inspected using a CM12 (Philips) transmission electron microscope. For each strain 70 random septa were imaged with pixel resolution of 1.2 nm. Using ImageJ the cell wall thickness for each septum was measured at 4 places from which the average was taken.

Statistical analysis

Each set of micrographs to be analysed was imaged with the same exposure time. For the septum intensity analysis of HADA, FM4-64 and Nile Red, the wildtype strain (expressing GFP) and the Δ*floAT strains* were mixed, labelled and imaged on the same agarose pad. Intensity of the fluorescently labelled septa was measured using the ObjectJ macro tool PeakFinder (https://sils.fnwi.uva.nl/bcb/objectj/examples/PeakFinder/peakfinder.html) (***Vischer et al., 2015***). A perpendicular line was drawn across the septal plane, the background intensity was removed resulting in a maximum peak intensity. The number of septa compared was indicated for every individual experiment. Populations were compared using the non-parametric Mann-Whitney test. The null hypothesis was tested with the *p* value of 0.05. The statistical analyses and their graphical representation (box plots) were generated with GraphPad Prism 8.1 (San Diego, California, USA). Box plots show the median and

the interquartile range (box), the 5th and 95th percentile (whiskers). Laurdan fluorescence generalised polarisation, cell length and MreB speed statistical analyses were performed using Kruskal-Wallis with Dunn's multiple comparison *post-hoc* test.

Fatty acid composition analysis

The fatty acid composition of *B. subtilis* wild-type cells and the flotillin/PBP mutants was analysed with gas chromatography as fatty acid methyl esters. Cells for the analyses were grown at 37˚C in LB or SMM until mid-exponential (OD_{600} ~0.5), harvested (6000 rpm, 10 min, 4˚C) and washed with 100 mM NaCl. Next, the cells were freeze dried at −50˚C, 0.012 mbar for a minimum of 18 hr. All analyses were carried out on biological duplicates by the Identification Service of the DSMZ, Braunschweig, Germany.

Sample preparation for solid-state NMR

FloT was essentialy purified as described (***Bach and Bramkamp, 2013***), in solubilised form, and stored in buffer A (50 mM Tris HCl pH 7.5, 150 mM NaCl, 5 mM $MgCl_2$) supplemented with 0.05% Triton X-100.

Liposomes containing POPC-d31 were prepared by mixing appropriate lipid powders in organic solvents (chloroform/methanol, 2:1 ratio). Solvents were evaporated under a flow of N_2 to obtain a thin lipid film. Lipids were rehydrated with ultrapure water before lyophilisation over night. The lipid powder was hydrated with an appropriate amount of buffer A with 10% glycerol and homogenised by three cycles of vortexing, freezing (liquid nitrogen, −196˚C, 1 min) and thawing (40˚C in a water bath, 10 min). This protocol generated a milky suspension of micrometer-sized multilamellar vesicles. FloT was solubilised in Buffer A supplemented with 0.05% Triton X-100 and added to preformed liposomes and incubated for 1 hr at room temperature. A dialysis step was then performed against Buffer A at 4˚C under agitation to remove the detergent. Samples were centrifuged at 100,000 g at 4˚C for 1 hr to pellet the proteoliposomes. ^{2}H solid-state NMR spectra were recorded of liposomes in the presence or absence of FloT at a lipid/protein ratio of 25:1 at 298 K.

Solid-state NMR

^{2}H NMR spectroscopy experiments were performed using a Bruker Avance III 500 MHz WB (11.75 T) spectrometer. They were recorded on ^{2}H-labelled POPC at 76.77 MHz with a phase-cycled quadrupolar echo pulse sequence (90˚x-t-90˚y-t-acq). Acquisition parameters were as follows: spectral window of 500 kHz for 2H NMR spectroscopy, p/2 pulse width of 3.90 ms for ^{2}H, interpulse delays (t) were of 40 µs, recycled delays of 1.3 s for 2H; 3000 and 8000 scans were used for ^{2}H NMR spectroscopy on liposomes and liposomes with FloT, respectively. Spectra were processed using a Lorentzian line broadening of 300 Hz for ^{2}H NMR spectra before Fourier transformation from the top of the echo. Samples were equilibrated for 30 min at a given temperature before data acquisition. All spectra were processed and analysed using Bruker Topspin 3.2 software. Spectral moments were calculated for each temperature using the NMR Depaker 1.0rc1 software [Copyright (C) 2009 Sébastien Buchoux]. Orientational order parameters (SCD) were calculated from experimental quadrupolar splittings (DnQ) as described in ***Huster, 2014***. For ^{31}P ssNMR, we applied a static Hahn spin echo sequence at the ^{31}P frequency of 162 MHz on a 400 MHz (9.4T) Bruker Avance III HD spectrometer, with a 90◦ pulse of 8 µs, a delay of 40 µs, a recycle delay of 5 s, a spectral window of 400 ppm and a number of scans of 4000 and 3400 was used on liposomes and liposomes with FloT, respectively. Spectra were processed using a Lorentzian line broadening of 100 Hz.

Acknowledgements

We thank Henrik Strahl for discussions and sharing of unpublished data, Rut Carballido-Lopez for strain RWBS5 and Luiza Morawska and Oscar Kuipers for the P*rrnB-gfp* plasmid.

This work was funded by NWO grant 864.09.010 (DJS), DFG grants BR 2915/4–1; INST 86/1452–1 (MB), ERC starting grant 757913; NWO grant 721.014.008 (AKHH); PhD fellowships DAAD-GSSP to AS; and SFRH/BD/78061/2011- POPH/FSE/FCT to ASB.

Additional information

Funding

Funder	Grant reference number	Author
Nederlandse Organisatie voor Wetenschappelijk Onderzoek	Vidi 864.09.010	Dirk-Jan Scheffers
Deutsche Forschungsgemeinschaft	BR 2915/7-1	Marc Bramkamp
Deutsche Forschungsgemeinschaft	INST 86/1452-1	Marc Bramkamp
Nederlandse Organisatie voor Wetenschappelijk Onderzoek	721.014.008	Anna KH Hirsch
European Research Council	starting grant 757913	Anna KH Hirsch
Deutscher Akademischer Austauschdienst	PhD fellowship DAAD-GSSP	Abigail Savietto
Fundação para a Ciência e a Tecnologia	PhD fellowship SFRH/BD/78061/2011- POPH/FSE/FCT	Anabela de Sousa Borges

The funders had no role in study design, data collection and interpretation, or the decision to submit the work for publication.

Author contributions

Aleksandra Zielińska, Conceptualization, Data curation, Formal analysis, Supervision, Investigation, Visualization, Methodology, Writing - original draft, Writing - review and editing; Abigail Savietto, Conceptualization, Data curation, Formal analysis, Investigation, Visualization, Methodology, Writing - original draft, Writing - review and editing; Anabela de Sousa Borges, Conceptualization, Funding acquisition, Investigation, Visualization, Methodology; Denis Martinez, Melanie Berbon, Formal analysis, Investigation, Methodology; Joël R Roelofsen, Investigation; Alwin M Hartman, Anna KH Hirsch, Resources; Rinse de Boer, Formal analysis, Investigation; Ida J Van der Klei, Supervision, Investigation; Birgit Habenstein, Conceptualization, Supervision, Investigation, Methodology, Writing - original draft; Marc Bramkamp, Dirk-Jan Scheffers, Conceptualization, Formal analysis, Supervision, Funding acquisition, Writing - original draft, Project administration, Writing - review and editing

Author ORCIDs

Ida J Van der Klei https://orcid.org/0000-0001-7165-9679
Marc Bramkamp http://orcid.org/0000-0002-7704-3266
Dirk-Jan Scheffers https://orcid.org/0000-0002-9439-9168

Decision letter and Author response

Decision letter https://doi.org/10.7554/eLife.57179.sa1
Author response https://doi.org/10.7554/eLife.57179.sa2

Additional files

Supplementary files

- Transparent reporting form

Data availability

All data generated or analysed during this study are included in the manuscript and supporting files.

References

Aaron M, Charbon G, Lam H, Schwarz H, Vollmer W, Jacobs-Wagner C. 2007. The tubulin homologue FtsZ contributes to cell elongation by guiding cell wall precursor synthesis in Caulobacter crescentus. *Molecular Microbiology* **64**:938–952. DOI: https://doi.org/10.1111/j.1365-2958.2007.05720.x, PMID: 17501919

Anagnostopoulos C, Spizizen J. 1961. Requirements for transformation in *Bacillus subtilis*. *Journal of Bacteriology* **81**:741–746. DOI: https://doi.org/10.1128/JB.81.5.741-746.1961, PMID: 16561900

Bach JN, Bramkamp M. 2013. Flotillins functionally organize the bacterial membrane. *Molecular Microbiology* **88**: 1205–1217. DOI: https://doi.org/10.1111/mmi.12252, PMID: 23651456

Bach JN, Bramkamp M. 2015. Dissecting the molecular properties of prokaryotic flotillins. *PLOS ONE* **10**: e0116750. DOI: https://doi.org/10.1371/journal.pone.0116750, PMID: 25635948

Billaudeau C, Chastanet A, Yao Z, Cornilleau C, Mirouze N, Fromion V, Carballido-López R. 2017. Contrasting mechanisms of growth in two model rod-shaped Bacteria. *Nature Communications* **8**:15370. DOI: https://doi.org/10.1038/ncomms15370, PMID: 28589952

Bramkamp M, Lopez D. 2015. Exploring the existence of lipid rafts in Bacteria. *Microbiology and Molecular Biology Reviews* **79**:81–100. DOI: https://doi.org/10.1128/MMBR.00036-14, PMID: 25652542

Calvez P, Jouhet J, Vié V, Durmort C, Zapun A. 2019. Lipid phases and cell geometry during the cell cycle of *Streptococcus pneumoniae*. *Frontiers in Microbiology* **10**:351. DOI: https://doi.org/10.3389/fmicb.2019.00351, PMID: 30936851

Cho H, Wivagg CN, Kapoor M, Barry Z, Rohs PDA, Suh H, Marto JA, Garner EC, Bernhardt TG. 2016. Bacterial cell wall biogenesis is mediated by SEDS and PBP polymerase families functioning semi-autonomously. *Nature Microbiology* **1**:16172. DOI: https://doi.org/10.1038/nmicrobiol.2016.172, PMID: 27643381

Dajkovic A, Tesson B, Chauhan S, Courtin P, Keary R, Flores P, Marlière C, Filipe SR, Chapot-Chartier MP, Carballido-Lopez R. 2017. Hydrolysis of peptidoglycan is modulated by amidation of meso-diaminopimelic acid and Mg(2+) in *Bacillus subtilis*. *Molecular Microbiology* **104**:972–988. DOI: https://doi.org/10.1111/mmi.13673, PMID: 28317238

Daniel RA, Errington J. 2003. Control of cell morphogenesis in Bacteria: two distinct ways to make a rod-shaped cell. *Cell* **113**:767–776. DOI: https://doi.org/10.1016/s0092-8674(03)00421-5, PMID: 12809607

Dempwolff F, Möller HM, Graumann PL. 2012. Synthetic motility and cell shape defects associated with deletions of flotillin/reggie paralogs in *Bacillus subtilis* and interplay of these proteins with NfeD proteins. *Journal of Bacteriology* **194**:4652–4661. DOI: https://doi.org/10.1128/JB.00910-12, PMID: 22753055

Dempwolff F, Schmidt FK, Hervás AB, Stroh A, Rösch TC, Riese CN, Dersch S, Heimerl T, Lucena D, Hülsbusch N, Stuermer CA, Takeshita N, Fischer R, Eckhardt B, Graumann PL. 2016. Super resolution fluorescence microscopy and tracking of bacterial flotillin (Reggie) Paralogs provide evidence for Defined-Sized protein microdomains within the bacterial membrane but absence of clusters containing Detergent-Resistant proteins. *PLOS Genetics* **12**:e1006116. DOI: https://doi.org/10.1371/journal.pgen.1006116, PMID: 27362352

Dion MF, Kapoor M, Sun Y, Wilson S, Ryan J, Vigouroux A, van Teeffelen S, Oldenbourg R, Garner EC. 2019. *Bacillus subtilis* cell diameter is determined by the opposing actions of two distinct cell wall synthetic systems. *Nature Microbiology* **4**:1294–1305. DOI: https://doi.org/10.1038/s41564-019-0439-0, PMID: 31086310

Domínguez-Escobar J, Chastanet A, Crevenna AH, Fromion V, Wedlich-Söldner R, Carballido-López R. 2011. Processive movement of MreB-associated cell wall biosynthetic complexes in Bacteria. *Science* **333**:225–228. DOI: https://doi.org/10.1126/science.1203466, PMID: 21636744

Donovan C, Bramkamp M. 2009. Characterization and subcellular localization of a bacterial flotillin homologue. *Microbiology* **155**:1786–1799. DOI: https://doi.org/10.1099/mic.0.025312-0, PMID: 19383680

Ducret A, Quardokus EM, Brun YV. 2016. MicrobeJ, a tool for high throughput bacterial cell detection and quantitative analysis. *Nature Microbiology* **1**:16077. DOI: https://doi.org/10.1038/nmicrobiol.2016.77, PMID: 27572972

Ganchev DN, Hasper HE, Breukink E, de Kruijff B. 2006. Size and orientation of the lipid II headgroup as revealed by AFM imaging. *Biochemistry* **45**:6195–6202. DOI: https://doi.org/10.1021/bi051913e, PMID: 16681392

García-Fernández E, Koch G, Wagner RM, Fekete A, Stengel ST, Schneider J, Mielich-Süss B, Geibel S, Markert SM, Stigloher C, Lopez D. 2017. Membrane microdomain disassembly inhibits MRSA antibiotic resistance. *Cell* **171**:1354–1367. DOI: https://doi.org/10.1016/j.cell.2017.10.012, PMID: 29103614

Garner EC, Bernard R, Wang W, Zhuang X, Rudner DZ, Mitchison T. 2011. Coupled, circumferential motions of the cell wall synthesis machinery and MreB filaments in *B. subtilis*. *Science* **333**:222–225. DOI: https://doi.org/10.1126/science.1203285, PMID: 21636745

Gohrbandt M. 2019. Low membrane fluidity triggers lipid phase separation and protein segregation in vivo. *bioRxiv*. DOI: https://doi.org/10.1101/852160

Harwood CR, Cutting SM. 1990. *Molecular Biological Methods for Bacillus*. John Wiley and Sons.

Huang X, Gaballa A, Cao M, Helmann JD. 1999. Identification of target promoters for the *Bacillus subtilis* extracytoplasmic function sigma factor, sigma W. *Molecular Microbiology* **31**:361–371. DOI: https://doi.org/10.1046/j.1365-2958.1999.01180.x, PMID: 9987136

Hussain S, Wivagg CN, Szwedziak P, Wong F, Schaefer K, Izoré T, Renner LD, Holmes MJ, Sun Y, Bisson-Filho AW, Walker S, Amir A, Löwe J, Garner EC. 2018. MreB filaments align along greatest principal membrane curvature to orient cell wall synthesis. *eLife* **7**:e32471. DOI: https://doi.org/10.7554/eLife.32471, PMID: 29469806

Huster D. 2014. Solid-state NMR spectroscopy to study protein–lipid interactions. *Biochimica Et Biophysica Acta (BBA) - Molecular and Cell Biology of Lipids* **1841**:1146–1160. DOI: https://doi.org/10.1016/j.bbalip.2013.12.002

Kahan FM, Kahan JS, Cassidy PJ, Kropp H. 1974. The mechanism of action of fosfomycin (phosphonomycin). *Annals of the New York Academy of Sciences* **235**:364–386. DOI: https://doi.org/10.1111/j.1749-6632.1974.tb43277.x, PMID: 4605290

Konopásek I, Strzalka K, Svobodová J. 2000. Cold shock in *Bacillus subtilis*: different effects of benzyl alcohol and ethanol on the membrane organisation and cell adaptation. *Biochimica Et Biophysica Acta (BBA) - Biomembranes* **1464**:18–26. DOI: https://doi.org/10.1016/S0005-2736(99)00240-0, PMID: 10704916

Kuru E, Hughes HV, Brown PJ, Hall E, Tekkam S, Cava F, de Pedro MA, Brun YV, VanNieuwenhze MS. 2012. In Situ probing of newly synthesized peptidoglycan in live bacteria with fluorescent D-amino acids. *Angewandte Chemie International Edition* **51**:12519–12523. DOI: https://doi.org/10.1002/anie.201206749, PMID: 23055266

Kuru E, Tekkam S, Hall E, Brun YV, Van Nieuwenhze MS. 2015. Synthesis of fluorescent D-amino acids and their use for probing peptidoglycan synthesis and bacterial growth in situ. *Nature Protocols* **10**:33–52. DOI: https://doi.org/10.1038/nprot.2014.197, PMID: 25474031

Lages MC, Beilharz K, Morales Angeles D, Veening JW, Scheffers DJ. 2013. The localization of key *Bacillus subtilis* penicillin binding proteins during cell growth is determined by substrate availability. *Environmental Microbiology* **15**:3272–3281. DOI: https://doi.org/10.1111/1462-2920.12206, PMID: 23895585

Legrand A, Martinez D, Grélard A, Berbon M, Morvan E, Tawani A, Loquet A, Mongrand S, Habenstein B. 2019. Nanodomain clustering of the plant protein remorin by Solid-State NMR. *Frontiers in Molecular Biosciences* **6**:00107. DOI: https://doi.org/10.3389/fmolb.2019.00107

Lennox ES. 1955. Transduction of linked genetic characters of the host by bacteriophage P1. *Virology* **1**:190–206. DOI: https://doi.org/10.1016/0042-6822(55)90016-7, PMID: 13267987

Lopez D, Koch G. 2017. Exploring functional membrane microdomains in Bacteria: an overview. *Current Opinion in Microbiology* **36**:76–84. DOI: https://doi.org/10.1016/j.mib.2017.02.001, PMID: 28237903

López D, Kolter R. 2010. Functional microdomains in bacterial membranes. *Genes & Development* **24**:1893–1902. DOI: https://doi.org/10.1101/gad.1945010, PMID: 20713508

McDonald KL. 2014. Out with the old and in with the new: rapid specimen preparation procedures for electron microscopy of sectioned biological material. *Protoplasma* **251**:429–448. DOI: https://doi.org/10.1007/s00709-013-0575-y, PMID: 24258967

Meeske AJ, Riley EP, Robins WP, Uehara T, Mekalanos JJ, Kahne D, Walker S, Kruse AC, Bernhardt TG, Rudner DZ. 2016. SEDS proteins are a widespread family of bacterial cell wall polymerases. *Nature* **537**:634–638. DOI: https://doi.org/10.1038/nature19331, PMID: 27525505

Meijering E, Dzyubachyk O, Smal I. 2012. Methods for cell and particle tracking. *Methods in Enzymology* **504**:183–200. DOI: https://doi.org/10.1016/B978-0-12-391857-4.00009-4, PMID: 22264535

Mielich-Süss B, Schneider J, Lopez D. 2013. Overproduction of flotillin influences cell differentiation and shape in *Bacillus subtilis*. *mBio* **4**:00719-13. DOI: https://doi.org/10.1128/mBio.00719-13

Mielich-Süss B, Wagner RM, Mietrach N, Hertlein T, Marincola G, Ohlsen K, Geibel S, Lopez D. 2017. Flotillin scaffold activity contributes to type VII secretion system assembly in *Staphylococcus aureus*. *PLOS Pathogens* **13**:e1006728. DOI: https://doi.org/10.1371/journal.ppat.1006728, PMID: 29166667

Mielich-Süss B, Lopez D. 2015. Molecular mechanisms involved in *Bacillus subtilis* biofilm formation. *Environmental Microbiology* **17**:555–565. DOI: https://doi.org/10.1111/1462-2920.12527, PMID: 24909922

Mohammadi T, Karczmarek A, Crouvoisier M, Bouhss A, Mengin-Lecreulx D, den Blaauwen T. 2007. The essential peptidoglycan glycosyltransferase MurG forms a complex with proteins involved in lateral envelope growth as well as with proteins involved in cell division in *Escherichia coli*. *Molecular Microbiology* **65**:1106–1121. DOI: https://doi.org/10.1111/j.1365-2958.2007.05851.x, PMID: 17640276

Molugu TR, Lee S, Brown MF. 2017. Concepts and methods of Solid-State NMR spectroscopy applied to biomembranes. *Chemical Reviews* **117**:12087–12132. DOI: https://doi.org/10.1021/acs.chemrev.6b00619, PMID: 28906107

Morales Angeles D, Liu Y, Hartman AM, Borisova M, de Sousa Borges A, de Kok N, Beilharz K, Veening JW, Mayer C, Hirsch AK, Scheffers DJ. 2017. Pentapeptide-rich peptidoglycan at the *Bacillus subtilis* cell-division site. *Molecular Microbiology* **104**:319–333. DOI: https://doi.org/10.1111/mmi.13629, PMID: 28118510

Morales Angeles D, Scheffers DJ. 2017. *Bacillus: Cellular and Molecular Biology*. Freiburg: Caister Academic Press. DOI: https://doi.org/10.21775/9781910190579

Muchová K, Wilkinson AJ, Barák I. 2011. Changes of lipid domains in *Bacillus subtilis* cells with disrupted cell wall peptidoglycan. *FEMS Microbiology Letters* **325**:92–98. DOI: https://doi.org/10.1111/j.1574-6968.2011.02417.x, PMID: 22092867

Nicolas P, Mäder U, Dervyn E, Rochat T, Leduc A, Pigeonneau N, Bidnenko E, Marchadier E, Hoebeke M, Aymerich S, Becher D, Bisicchia P, Botella E, Delumeau O, Doherty G, Denham EL, Fogg MJ, Fromion V, Goelzer A, Hansen A, et al. 2012. Condition-dependent transcriptome reveals high-level regulatory architecture in *Bacillus subtilis*. *Science* **335**:1103–1106. DOI: https://doi.org/10.1126/science.1206848, PMID: 22383849

Pazos M, Peters K, Casanova M, Palacios P, VanNieuwenhze M, Breukink E, Vicente M, Vollmer W. 2018. Z-ring membrane anchors associate with cell wall synthases to initiate bacterial cell division. *Nature Communications* **9**:5090. DOI: https://doi.org/10.1038/s41467-018-07559-2, PMID: 30504892

Popham DL, Setlow P. 1995. Cloning, nucleotide sequence, and mutagenesis of the *Bacillus subtilis* ponA Operon, which codes for penicillin-binding protein (PBP) 1 and a PBP-related factor. *Journal of Bacteriology* **177**:326–335. DOI: https://doi.org/10.1128/JB.177.2.326-335.1995, PMID: 7814321

Sarkar S, Libby EA, Pidgeon SE, Dworkin J, Pires MM. 2016. In vivo probe of lipid II-Interacting Proteins. *Angewandte Chemie International Edition* **55**:8401–8404. DOI: https://doi.org/10.1002/anie.201603441, PMID: 27225706

Scheffers DJ, Jones LJ, Errington J. 2004. Several distinct localization patterns for penicillin-binding proteins in *Bacillus subtilis*. *Molecular Microbiology* **51**:749–764. DOI: https://doi.org/10.1046/j.1365-2958.2003.03854.x, PMID: 14731276

Scheffers DJ, Errington J. 2004. PBP1 is a component of the *Bacillus subtilis* cell division machinery. *Journal of Bacteriology* **186**:5153–5156. DOI: https://doi.org/10.1128/JB.186.15.5153-5156.2004, PMID: 15262952

Scheidt HA, Huster D. 2009. Structure and dynamics of the myristoyl lipid modification of SRC peptides determined by 2H solid-state NMR spectroscopy. *Biophysical Journal* **96**:3663–3672. DOI: https://doi.org/10.1016/j.bpj.2009.02.028, PMID: 19413971

Schindelin J, Arganda-Carreras I, Frise E, Kaynig V, Longair M, Pietzsch T, Preibisch S, Rueden C, Saalfeld S, Schmid B, Tinevez JY, White DJ, Hartenstein V, Eliceiri K, Tomancak P, Cardona A. 2012. Fiji: an open-source platform for biological-image analysis. *Nature Methods* **9**:676–682. DOI: https://doi.org/10.1038/nmeth.2019, PMID: 22743772

Schirner K, Eun YJ, Dion M, Luo Y, Helmann JD, Garner EC, Walker S. 2015. Lipid-linked cell wall precursors regulate membrane association of bacterial actin MreB. *Nature Chemical Biology* **11**:38–45. DOI: https://doi.org/10.1038/nchembio.1689, PMID: 25402772

Schneider J, Klein T, Mielich-Süss B, Koch G, Franke C, Kuipers OP, Kovács ÁT, Sauer M, Lopez D. 2015a. Spatio-temporal remodeling of functional membrane microdomains organizes the signaling networks of a bacterium. *PLOS Genetics* **11**:e1005140. DOI: https://doi.org/10.1371/journal.pgen.1005140, PMID: 25909364

Schneider J, Mielich-Süss B, Böhme R, Lopez D. 2015b. In vivo characterization of the scaffold activity of flotillin on the membrane kinase KinC of *Bacillus subtilis*. *Microbiology* **161**:1871–1887. DOI: https://doi.org/10.1099/mic.0.000137, PMID: 26297017

Strahl H, Bürmann F, Hamoen LW. 2014. The actin homologue MreB organizes the bacterial cell membrane. *Nature Communications* **5**:3442. DOI: https://doi.org/10.1038/ncomms4442, PMID: 24603761

Strahl H, Errington J. 2017. Bacterial membranes: structure, domains, and function. *Annual Review of Microbiology* **71**:519–538. DOI: https://doi.org/10.1146/annurev-micro-102215-095630, PMID: 28697671

Szenk M, Dill KA, de Graff AMR. 2017. Why do Fast-Growing Bacteria enter overflow metabolism? testing the membrane real estate hypothesis. *Cell Systems* **5**:95–104. DOI: https://doi.org/10.1016/j.cels.2017.06.005, PMID: 28755958

Taguchi A, Welsh MA, Marmont LS, Lee W, Sjodt M, Kruse AC, Kahne D, Bernhardt TG, Walker S. 2019. FtsW is a peptidoglycan polymerase that is functional only in complex with its cognate penicillin-binding protein. *Nature Microbiology* **4**:587–594. DOI: https://doi.org/10.1038/s41564-018-0345-x, PMID: 30692671

Trip EN, Scheffers D-J. 2016. A 1 MDa protein complex containing critical components of the *Escherichia coli* divisome. *Scientific Reports* **5**:18190. DOI: https://doi.org/10.1038/srep18190

Typas A, Banzhaf M, Gross CA, Vollmer W. 2012. From the regulation of peptidoglycan synthesis to bacterial growth and morphology. *Nature Reviews Microbiology* **10**:123–136. DOI: https://doi.org/10.1038/nrmicro2677

Ursell TS, Nguyen J, Monds RD, Colavin A, Billings G, Ouzounov N, Gitai Z, Shaevitz JW, Huang KC. 2014. Rod-like bacterial shape is maintained by feedback between cell curvature and cytoskeletal localization. *PNAS* **111**:E1025–E1034. DOI: https://doi.org/10.1073/pnas.1317174111, PMID: 24550515

Varma A, Young KD. 2009. In *Escherichia coli*, MreB and FtsZ direct the synthesis of lateral cell wall via independent pathways that require PBP 2. *Journal of Bacteriology* **191**:3526–3533. DOI: https://doi.org/10.1128/JB.01812-08, PMID: 19346310

Veening JW, Murray H, Errington J. 2009. A mechanism for cell cycle regulation of sporulation initiation in *Bacillus subtilis*. *Genes & Development* **23**:1959–1970. DOI: https://doi.org/10.1101/gad.528209, PMID: 19684115

Vischer NO, Verheul J, Postma M, van den Berg van Saparoea B, Galli E, Natale P, Gerdes K, Luirink J, Vollmer W, Vicente M, den Blaauwen T. 2015. Cell age dependent concentration of *Escherichia coli* divisome proteins analyzed with ImageJ and ObjectJ. *Frontiers in Microbiology* **6**:586. DOI: https://doi.org/10.3389/fmicb.2015.00586, PMID: 26124755

Witzke S, Petersen M, Carpenter TS, Khalid S. 2016. Molecular dynamics simulations reveal the conformational flexibility of lipid II and its loose association with the defensin plectasin in the *Staphylococcus aureus* membrane. *Biochemistry* **55**:3303–3314. DOI: https://doi.org/10.1021/acs.biochem.5b01315, PMID: 27158738

Yepes A, Schneider J, Mielich B, Koch G, García-Betancur JC, Ramamurthi KS, Vlamakis H, López D. 2012. The biofilm formation defect of a *Bacillus subtilis* flotillin-defective mutant involves the protease FtsH. *Molecular Microbiology* **86**:457–471. DOI: https://doi.org/10.1111/j.1365-2958.2012.08205.x, PMID: 22882210

Zhao H, Patel V, Helmann JD, Dörr T. 2017. Don't let sleeping dogmas lie: new views of peptidoglycan synthesis and its regulation. *Molecular Microbiology* **106**:847–860. DOI: https://doi.org/10.1111/mmi.13853, PMID: 28975672

RESEARCH ARTICLE

Figures and figure supplements

Flotillin-mediated membrane fluidity controls peptidoglycan synthesis and MreB movement

Aleksandra Zielińska *et al*

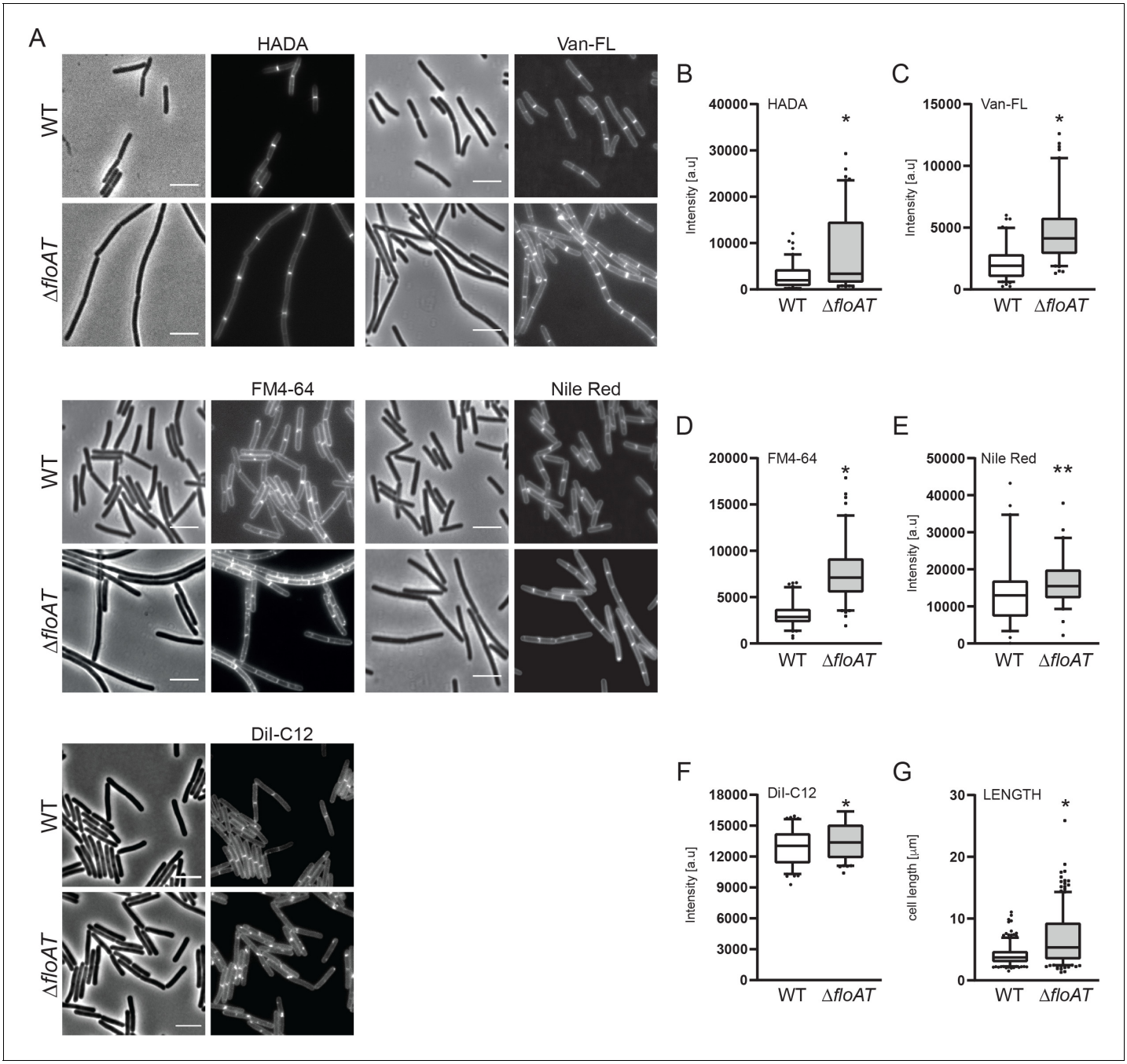

Figure 1. Accumulation of peptidoglycan synthesis and membrane material at division sites in a flotillin mutant. (**A**) Morphology of the exponentially growing wild type (WT) and Δ*floAT* strains labelled with HADA, fluorescent Vancomycin (Van-FL), FM 4–64, Nile Red, and DiI-C12. Scale bar: 5 µm. (**B–F**) Peak intensity of HADA (**B**), Van-FL (**C**), Nile Red (**D**), FM4-64 (**E**) and DiI-C12 (**F**) labelled division sites of the cells shown in (**A**). Cells from each strain ($n \geq 100$, except E, n = 60) were analysed using the ObjectJ macro tool PeakFinder followed by statistical analysis with Prism. Significant differences are based on the two-tailed Mann-Whitney test (*$p<0.05$; **$p<0.01$). (**G**) Distribution of the cell length of the strains analysed in (**A**). Statistical analysis of the data (n = 100, two tailed Mann-Whitney test, *$p<0.05$) was performed with Prism, resulting in box plot graphs.

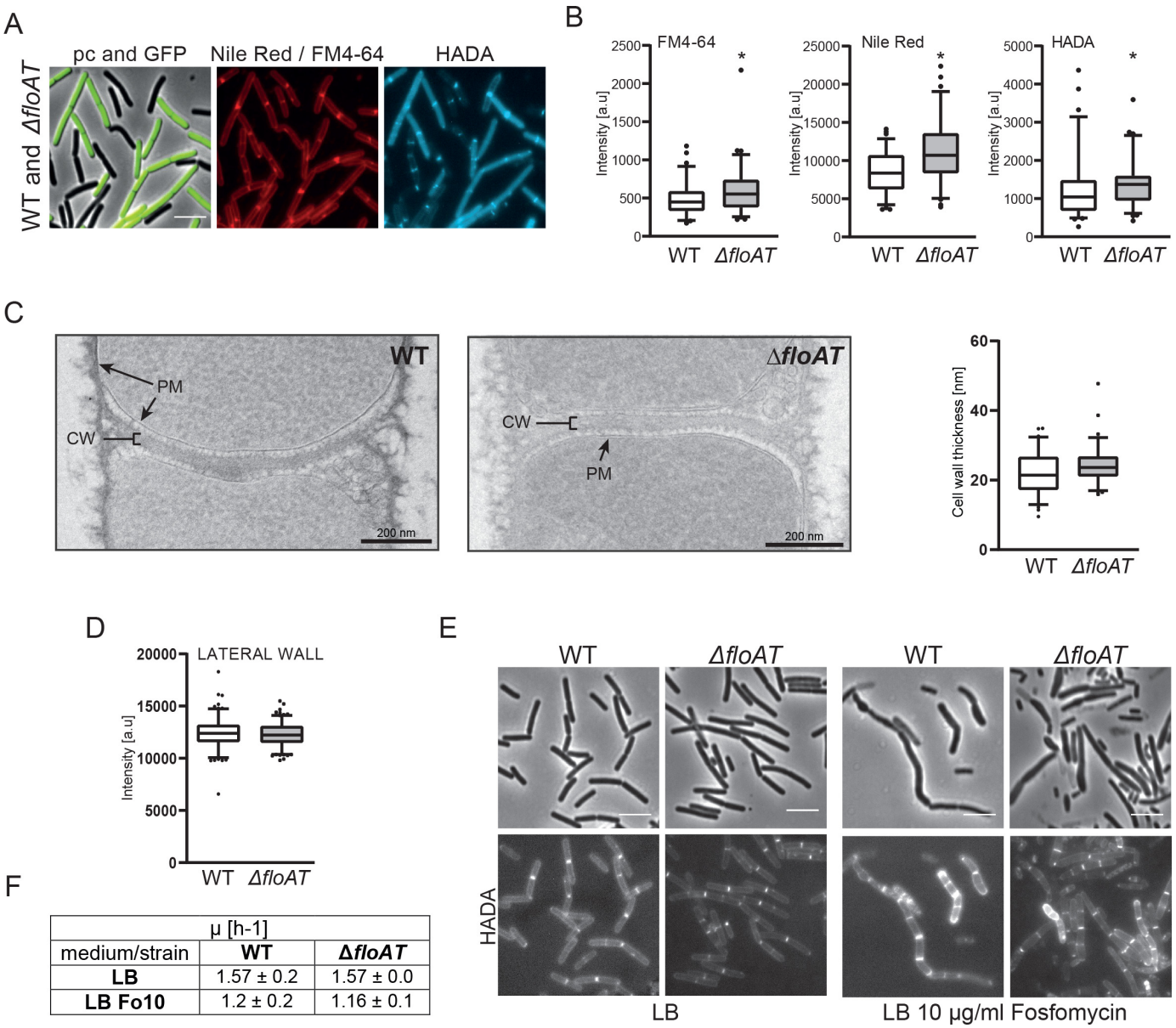

µ [h-1]		
medium/strain	**WT**	**Δ*floAT***
LB	1.57 ± 0.2	1.57 ± 0.0
LB Fo10	1.2 ± 0.2	1.16 ± 0.1

Figure 1—figure supplement 1. Control experiments showing that differences in septal labeling intensity are not due to microscopy settings, septum thickness, or dye diffusion. (**A**) Morphology of the exponentially growing 4259 (WT-GFP) and Δ*floAT* strains labelled simultaneously with Nile Red or FM 4–64 and HADA. (**B**) Septal peak intensity of FM4-64, Nile Red and HADA labelled division sites of the cells shown in (**A**). Cells from each strain (n = 70) were analysed on the same agarose pad using the ObjectJ macro tool PeakFinder followed by statistical analysis with Prism resulting in box plot graphs. Significant differences are based on the two-tailed Mann-Whitney test (*p<0.05). (**C**) Electron micrographs of the septal plane of the exponentially growing 168 (WT) and Δ*floAT* strains alongside with a comparison of their cell wall thickness analysis represented as box plot graphs (n = 70). (**D**) Peak intensities of Nile-Red labelling of the lateral membranes of the WT and Δ*floAT* strains depicted in (**A**). A Mann-Whitney T-test (p<0.05, n ≥ 160), showed no significant statistical difference in intensity between the tested strains. (**E**) Morphology of exponentially growing 168 (WT) and Δ*floAT* strains cultivated in rich (LB) medium grown with or without a sub-lethal concentration of Fosfomycin (LB + 10 µg/ml Fosfomycin) and labelled with HADA. Scale bar 5 µm. (**F**) Growth rate of the cells depicted in (**E**) based on two biological replicates and three technical repetitions.

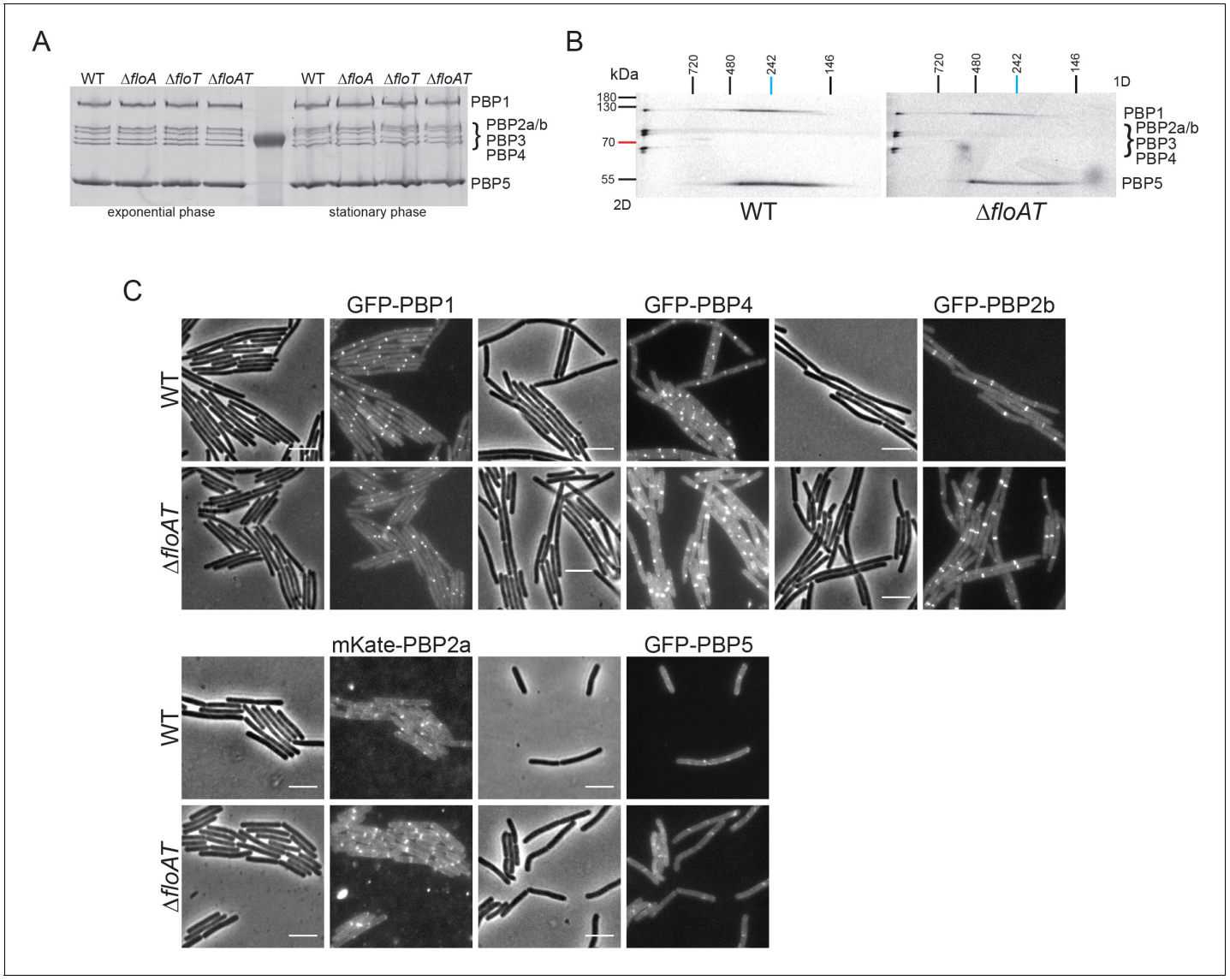

Figure 1—figure supplement 2. Absence of flotillins does not affect expression, oligomerisation or localisation of PBPs. (**A**) Expression pattern of PBPs in wild type and flotillin deficient strains visualised with Bocillin-FL. Membrane fractions isolated from cells (wt, Δ*floA*, Δ*floT* and Δ*floAT*) in exponential and stationary phase of growth were labelled with Bocillin-FL and run on an SDS-PAGE. The fluorescent signal was detected using Typhoon Trio scanner. (**B**) Two-dimensional (2D) BN/SDS-PAGE of PBP membrane oligomers labelled with Bocillin-FL. Membrane fractions of wt and Δ*floAT* strains were isolated, labelled with Bocillin-FL and loaded onto Blue-Native PAGE. The respective lanes were excised, horizontally immobilised on top of the SDS-PAGE gel and resolved. The fluorescent signal was detected using a Typhoon Trio scanner. PBPs 1, 2, 3 and 4 are present in a complex that is not resolved in the native gel, which is resolved at the left of the second dimension gel. PBP5 cannot be found in this complex but runs across a continuum of mass in the second dimension gel. A similar continuum is found for a second fraction of PBP1. This continuum either comes from a second complex that is disintegrating in the first dimension or from various complexes with different but close masses. Although our analysis clearly indicates that several PBPs are part of high Mw complexes, no differences in the patterns of the PBP complexes were found in membranes of the Δ*floAT* strain. (**C**) Localisation patterns of GFP-PBP fluorescent fusions in flotillin deletion strains. Exponentially growing wild-type (wt) and flotillin deletion (Δ*floAT*) strains expressing the indicated GFP-PBP fusions were imaged by phase contrast and fluorescence microscopy. The PBPs chosen were the two main aPBPs 1 and 4, the division associated bPBP 2b, the elongation associated bPBP 2a, and the main D,D-carboxypeptidase PBP5. No obvious differences in the localisation patterns for the PBPs were detected in the absence of flotillins. Scale bar 5 μm.

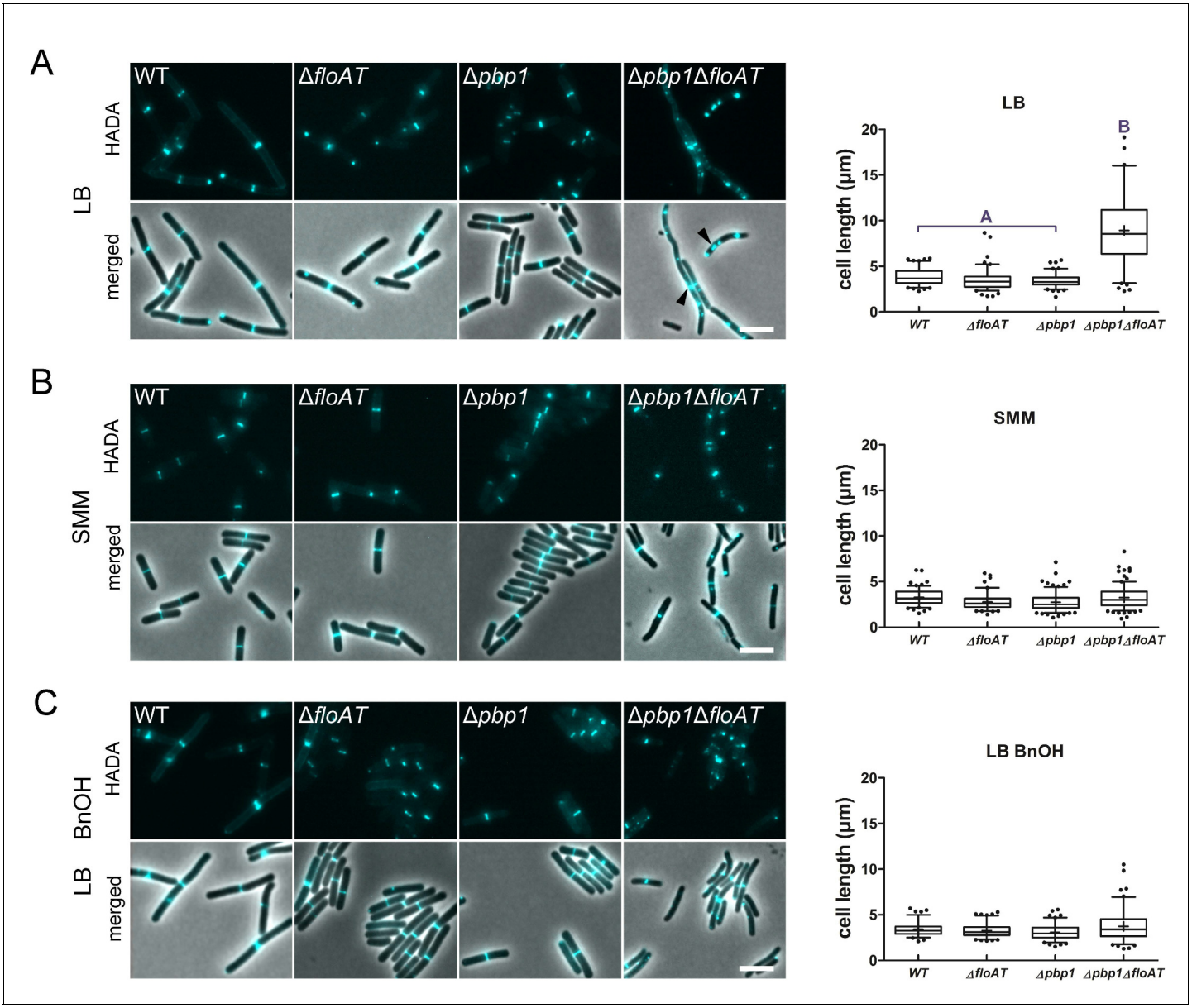

Figure 2. Cell morphology and cell wall synthesis localisation is dependent on growth conditions. Morphology of the *WT*, Δ*floAT*, Δ*pbp1*, and Δ*pbp1*Δ*floAT* strains grown in (**A**) rich (LB), (**B**) minimal (SMM) medium, and in (**C**) rich medium with membrane fluidising conditions (0.1% benzyl alcohol, LB+BnOH). Cells were labelled with HADA, and aberrant cell shape and peptidoglycan synthesis are indicated with arrowheads. Panels on the right indicate corresponding cell length distributions ($n \geq 100$). Distributions were analysed using Dunn's multiple comparison tests after Kruskal–Wallis. Statistically significant cell length distribution classes ($p<0.001$) are represented as letters above each graph – in B and C there were no significant differences. Scale bar: 4 µm.

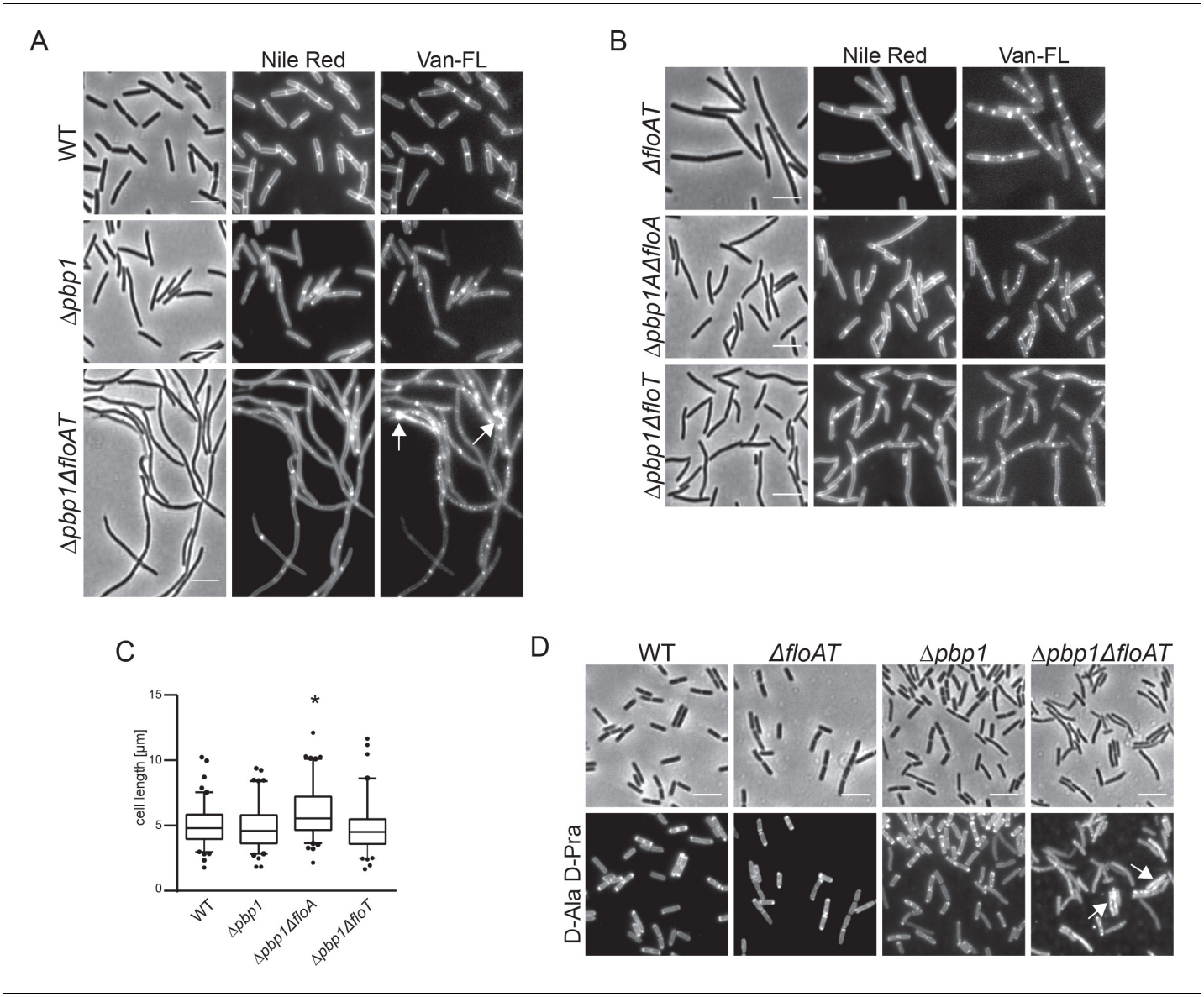

Figure 2—figure supplement 1. Deletion of both flotillins and PBP1 induces filamentation and delocalisation of peptidoglycan synthesis. (**A**) Exponentially growing wt, Δ*pbp1* and Δ*pbp1*Δ*floAT* strains were labelled with Nile Red and Vancomycin-FL (Van-FL). Arrows indicate accumulation of the dye. (**B**) Exponentially growing Δ*floAT*, Δ*pbp1*Δ*floA* and Δ*pbp1*Δ*floT* strains were labelled with membrane stain Nile Red and cell wall dye Vancomycin-FL (Van-FL). (**C**) Distribution of lengths of cells with a combination of deletions of *pbp1* with either *floA or floT*, imaged in A, B. Statistical analysis and generation of box plots was performed with Prism. Significant differences are based on the two-tailed Mann-Whitney test (n = 100, *p<0.05). (**D**) Exponentially growing wt, Δ*floAT*, Δ*pbp1* and Δ*pbp1*Δ*floAT* strains were labelled with fluorescent azide bound to D-Ala-D-Pra dipeptide. Arrows indicate accumulation of the dye. There are less filaments observed in this procedure as some filaments break during the fixation procedure that precedes the click reaction. Scale bar (same for all) 5 μm.

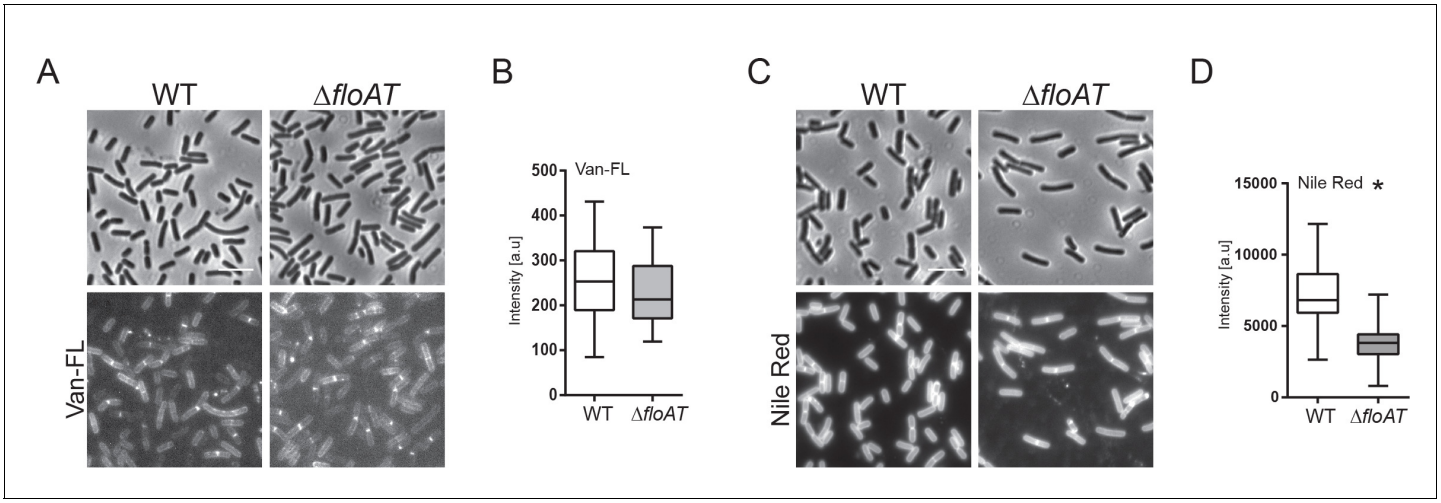

Figure 2—figure supplement 2. Septum labelling of wild type and flotillin mutant cells grown on minimal medium. (**A, C**) Morphology of the exponentially growing wt and Δ*floAT* strains in the minimal medium labelled with fluorescent Vancomycin (Van-FL, (**A**) and Nile Red (**C**). Scale bar 5 μm. (**B, D**) Peak intensity of Van-FL (**B**), and Nile Red (**D**) labelled division sites of the cells shown in (**A and C**). Cells from each strain (n = 50) were analysed using the ObjectJ macro tool PeakFinder followed by statistical analysis with Prism, where the significant difference is based on an unpaired Welch t-test (*p<0.05).

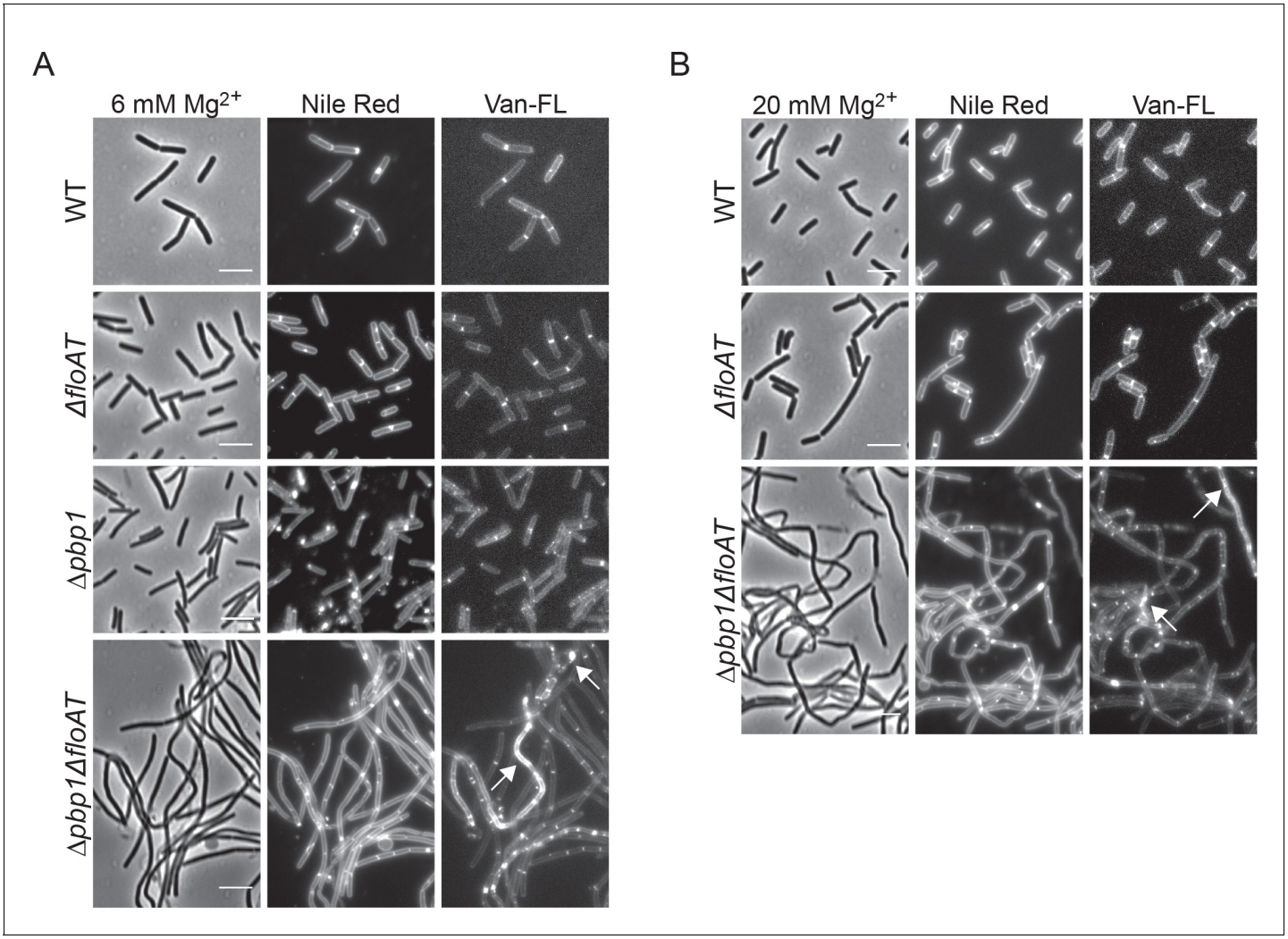

Figure 2—figure supplement 3. Filamentation and delocalisation of peptidoglycan synthesis in the absence of flotillins and PBP1 is not rescued by the addition of magnesium. Cell morphology of wt, Δ*floAT*, Δ*pbp1*, and Δ*pbp1*Δ*floAT* strains grown in LB supplemented with (**A**) 6 mM magnesium (Mg^{2+}) or (**B**) 20 mM magnesium, labelled with Nile Red and Vancomycin-FL (Van-FL). Exponentially growing cells were labelled, and imaged directly with phase contrast and fluorescence microscopy. Arrowheads indicate accumulation of the dye. Scale bar 5 μm.

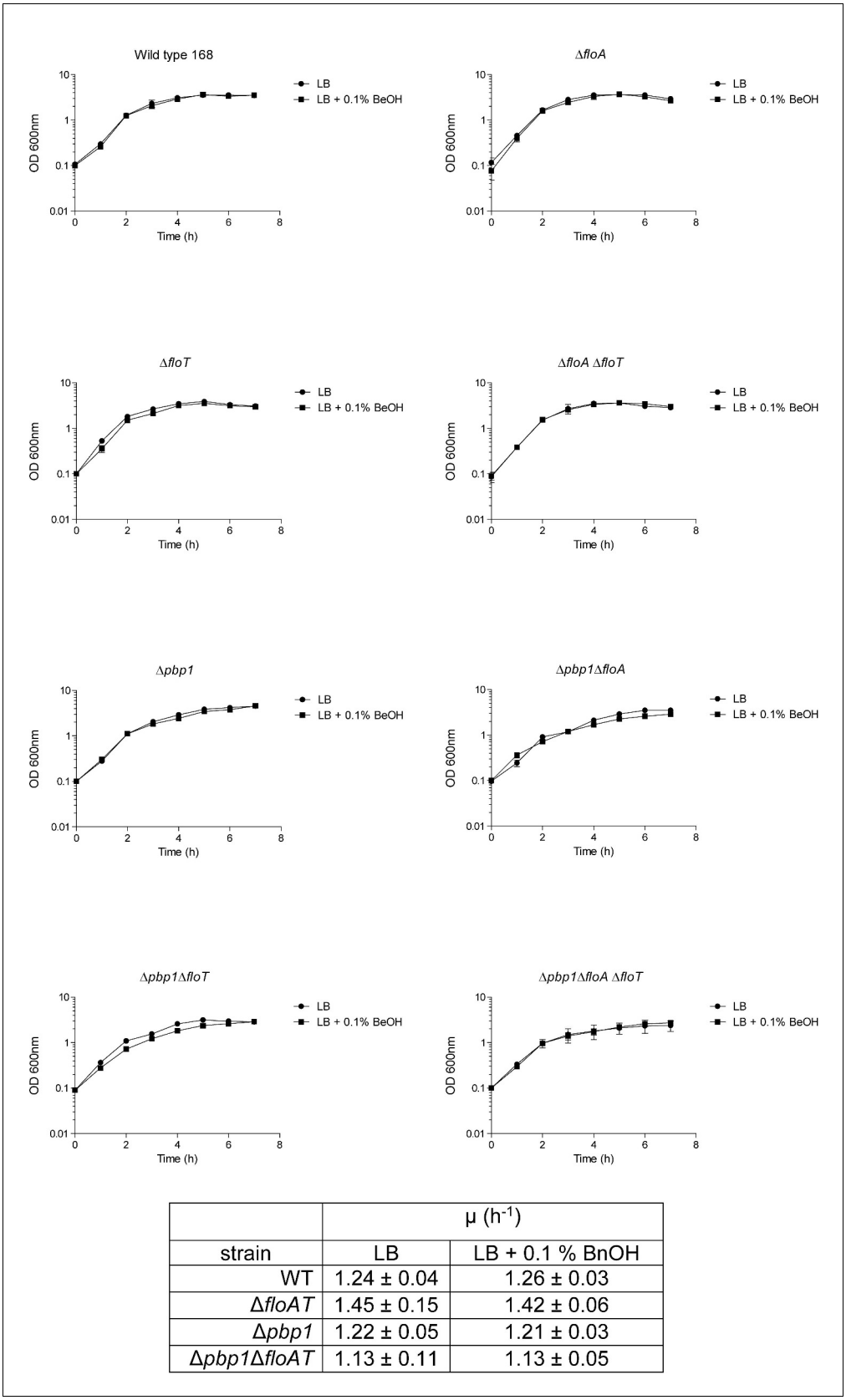

	μ (h^{-1})	
strain	LB	LB + 0.1 % BnOH
WT	1.24 ± 0.04	1.26 ± 0.03
Δ*floAT*	1.45 ± 0.15	1.42 ± 0.06
Δ*pbp1*	1.22 ± 0.05	1.21 ± 0.03
Δ*pbp1*Δ*floAT*	1.13 ± 0.11	1.13 ± 0.05

Figure 2—figure supplement 4. Growth curves and growth rates show similar growth for wt, Δ*floAT*, Δ*pbp1*, and Δ*pbp1*Δ*floAT* (as well as Δ*floA*, Δ*floT*, Δ*pbp1*Δ*floA and* Δ*pbp1*Δ*floT)* strains grown on LB or on LB supplemented with BnOH (0.1% (w/v)). Each datapoint represents the average from biological triplicates and error bars indicate standard deviation.

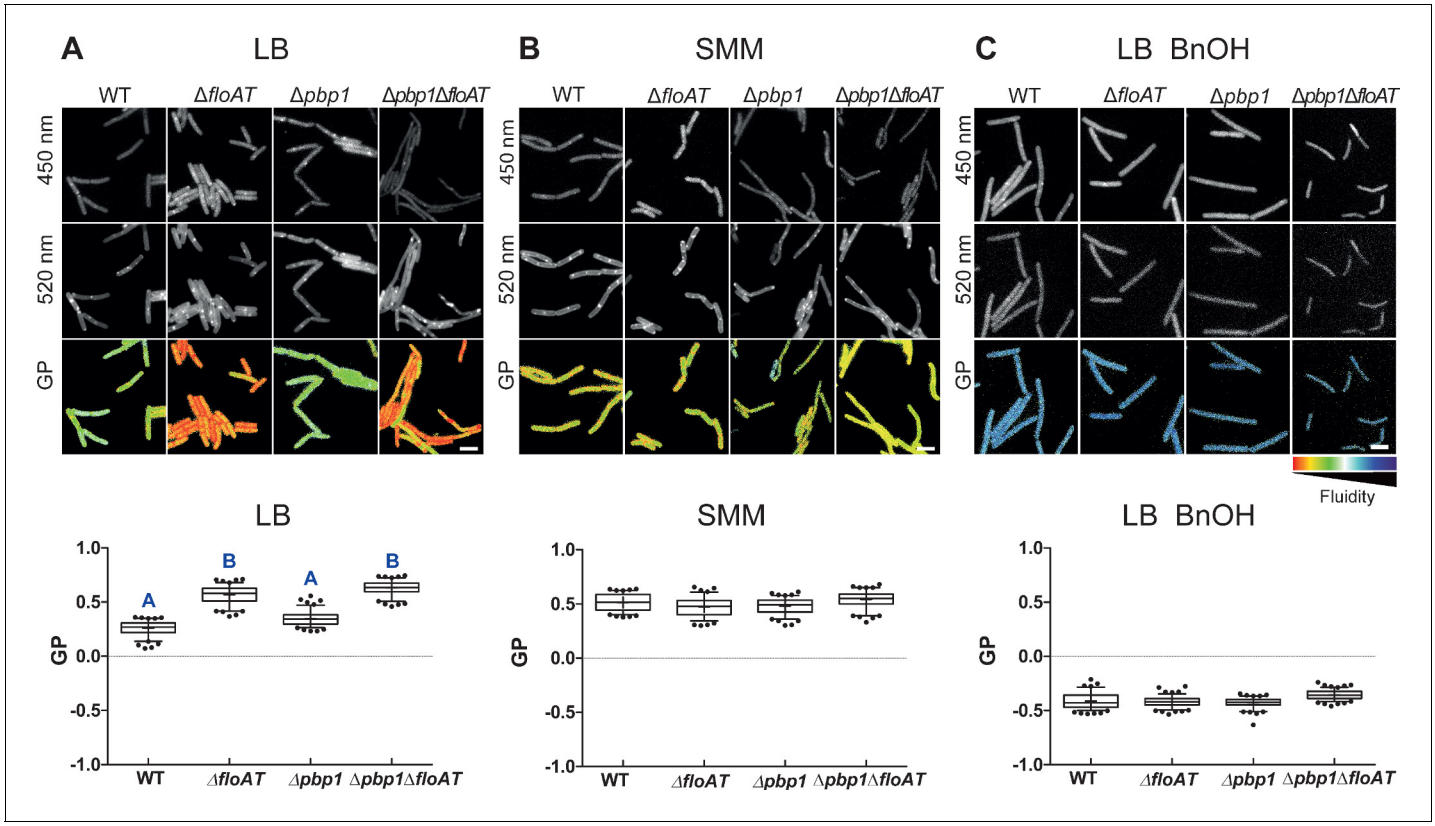

Figure 3. Flotillins increase overall membrane fluidity at high growth rate. Changes in overall membrane fluidity were assessed by Laurdan microscopy in cells grown on LB (**A**), SMM (**B**) and LB+BnOH (**C**). Micrographs show colour-coded generalised polarisation (GP) maps in which red indicates regions of decreased fluidity (scale bar: 4 μm). Correspondent theoretical GP measurements in the graphs vary from −1 (more fluid) to 1 (less fluid). Significant statistical differences according to Dunn's multiple comparison tests after Kruskal–Wallis are represented as letters above each graph in panel (**A**). Data labelled 'A' are significantly different from data labelled 'B'; data with the same letter are not significantly different. No statistically significant difference was observed for the data in panels (**B**) and (**C**) ($p<0.001$; $n \geq 150$, two biological replicates).

A

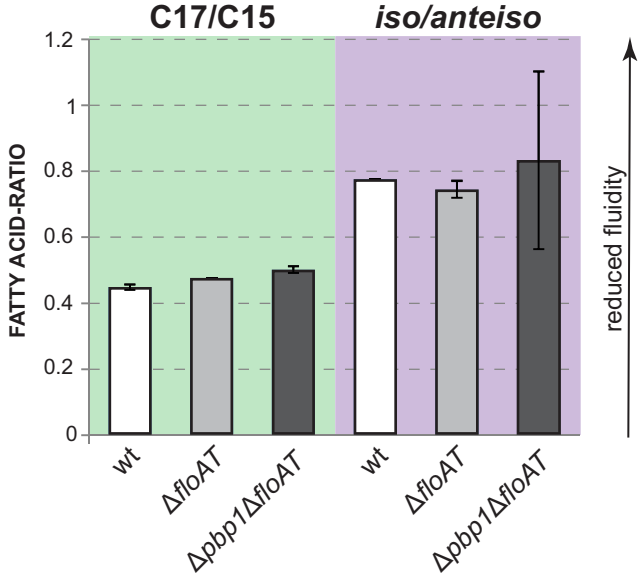

B

FATTY ACID	wt	Δ*floAT*	Δ*pbp1*Δ*floAT*
$C_{14:0}$ *iso*	1.6 ±0.07	1.3 ±0.07	1.8 ±0.48
$C_{15:0}$ *iso*	20.2 ±0.3	19.9 ±0.05	19.0 ±4.09
$C_{15:0}$ *anteiso*	38.1 ±0.76	38.3 ±1.28	36.6 ±4.32
$C_{16:0}$ *iso*	5.3 ±0.02	4.4 ±0.34	5.9 ±1.38
$C_{16:0}$	5.4 ±0.77	5.2 ±0.34	6.2 ±1.25
$C_{17:0}$ *iso*	12.8 ±0.63	13.5 ±0.28	14.2 ±1.87
$C_{17:0}$ *anteiso*	13.4 ±0.32	14.2 ±0.3	13.7 ±2.53

C17/C15	**0.45** ±0.00	**0.48** ±0.00	**0.50** ±0.00
iso/anteiso	**0.77** ±0.00	**0.74** ±0.02	**0.83** ±0.27

C

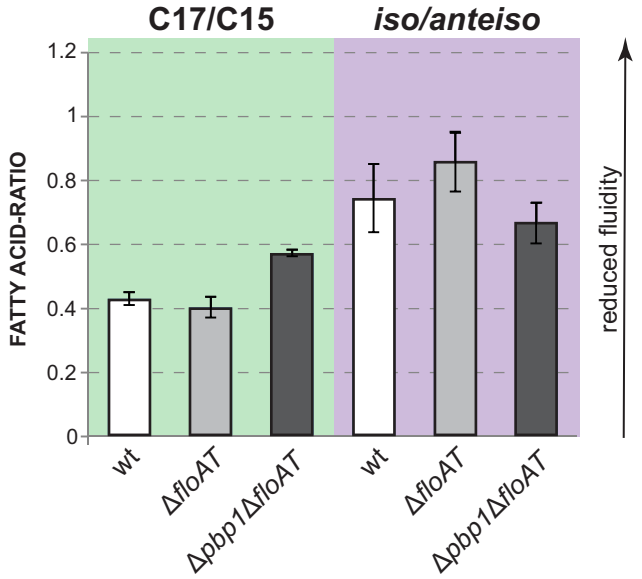

D

FATTY ACID	wt	Δ*floAT*	Δ*pbp1*Δ*floAT*
$C_{14:0}$ *iso*	2.6 ±0.16	3.1 ±0.8	3.3 ±0.14
$C_{15:0}$ *iso*	19.4 ±3.05	21.6 ±1.44	11.3 ±1.2
$C_{15:0}$ *anteiso*	40 ±1.84	38.2 ±1.12	38.9 ±1.38
$C_{16:0}$ *iso*	9.2 ±0.82	9.7 ±0.96	13.6 ±0.19
$C_{16:0}$	2.6 ±0.01	2.4 ±0.02	2.5 ±0.05
$C_{17:0}$ *iso*	9.9 ±1.12	10.2 ±0.53	10.1 ±0.7
$C_{17:0}$ *anteiso*	15.6 ±1.79	13.9 ±1.29	18.7 ±1.31

C17/C15	**0.43** ±0.02	**0.4** ±0.03	**0.57** ±0.01
iso/anteiso	**0.74** ±0.1	**0.86** ±0.09	**0.66** ±0.06

Figure 3—figure supplement 1. Fatty acid composition analysis. (**A, C**) Ratios between chain lengths of the major fatty acids (C17 and C15) and ratios between the *iso* and *anteiso* forms of fatty acids of the exponentially growing wt, Δ*floAT* and Δ*pbp1*Δ*floAT* strains cultivated in LB (**A**) or minimal medium (**C**). (**B**), (**D**) - Corresponding total fatty acid profiles and determination of the ratios in the graphs A and C, respectively. Lipid species contributing more that 1% to overall membrane composition are shown. The charts represent the average value of two independent analyses. Fatty acid ratios remain stable upon deletion of flotillins. Triple deletion of both flotillins and PBP1 causes some variability of the total lipid fractions.

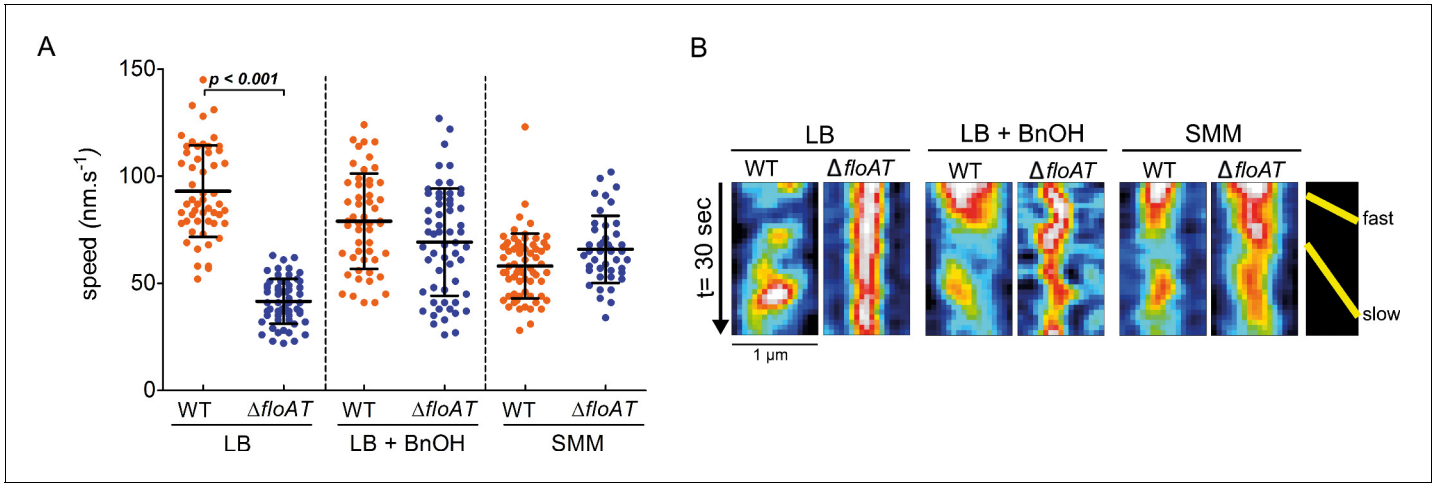

Figure 4. MreB speed is linked to membrane fluidity. (**A**) The MreB speed in different strain backgrounds and growth conditions was analysed by time-lapse TIRF microscopy. Scatter plot of the speed of patches obtained from individual tracks in 5 different cells are represented per fusion and condition. Average speeds are shown; error bars indicate the standard deviation. Significant statistical differences according to Dunn's multiple comparison tests after Kruskal–Wallis are represented ($p<0.001$). (**B**) Representative kymographs showing fast and slow moving patches of mRFPruby-MreB in *B. subtilis* cells lacking endogenous *mreB* (WT) or *mreB* and *floAT* (Δ*floAT*). See ***Figure 4—videos 1–6*** for corresponding raw image series.

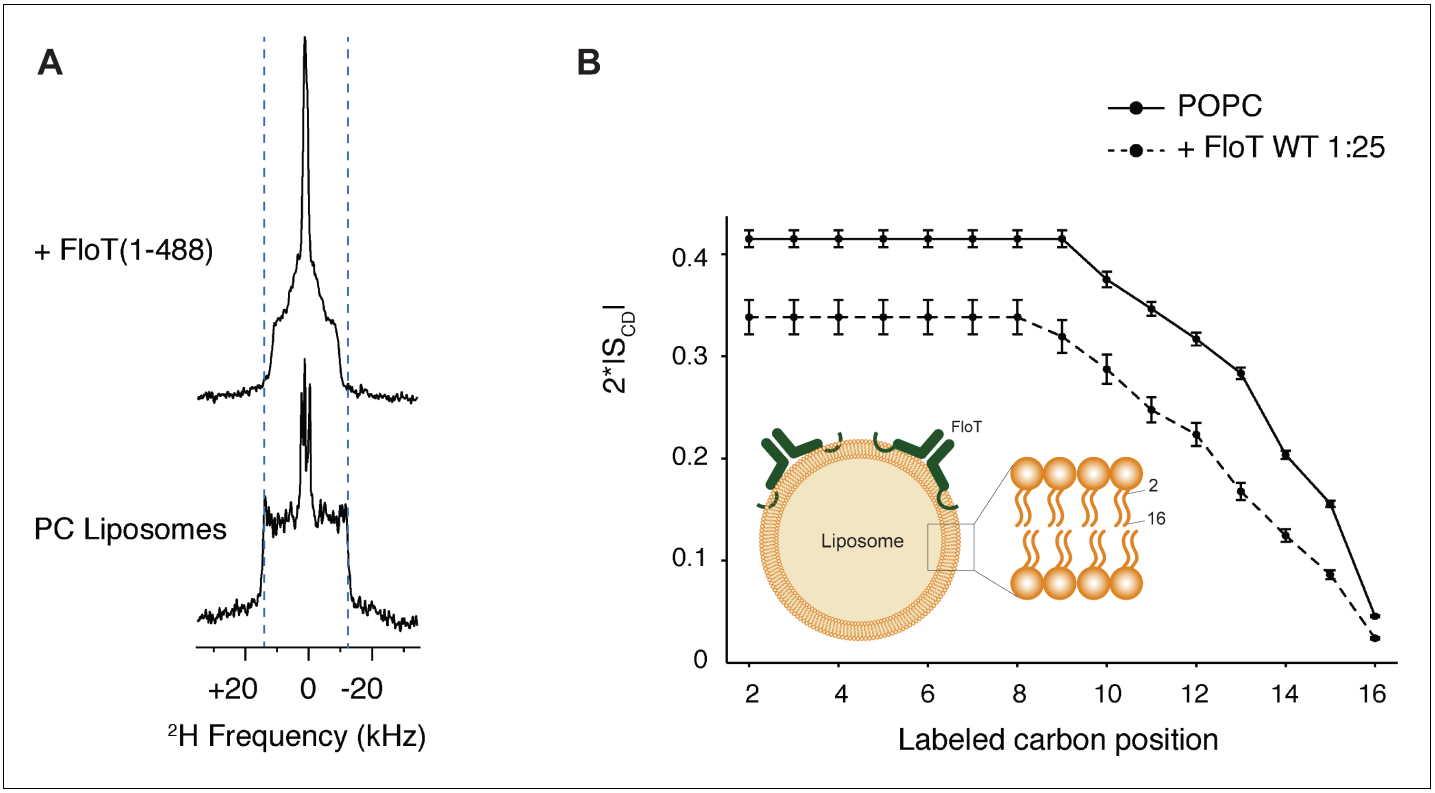

Figure 5. Lipid ordering of FloT probed by ^{2}H solid-state NMR. (**A**) Wide-line ^{2}H spectra of POPC-d31 liposomes with or without FloT at a lipid-to-protein molar ratio of 25:1 acquired at 298 K. (**B**) Effect of FloT on the C-^{2}H order parameters of the PC acyl chain. De-Pake-ing and simulations were applied on the ^{2}H solid-state NMR spectra to determine accurately individual quadrupolar splittings. Order parameters of POPC-d31 acyl chain were derived from experimental quadrupolar splittings and plotted as a function of the labelled carbon position. *Insert:* schematic depiction of a liposome with added FloT which attaches to the membrane via a hairpin loop (***Bach and Bramkamp, 2015***).

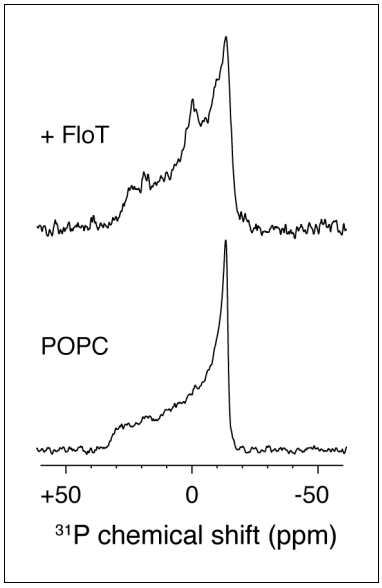

Figure 5—figure supplement 1. ^{31}P solid-state NMR experiments of POPC liposomes with or without FloT at a lipid-to-protein molar ratio of 25:1. All the spectra were acquired at 298 K and a Lorentzian line broadening of 50 Hz was applied before the Fourier transformation.

1.2 Publication II

(link to online publication)

Scholz AS, Baur SSM, Wolf D and Bramkamp M (2021) **An Stomatin, Prohibitin, Flotillin, and HflK/C-Domain Protein Required to Link the Phage-Shock Protein to the Membrane in *Bacillus subtilis*.** Front. Microbiol. 12:754924. doi: 10.3389/fmicb.2021.754924

Abstract

Membrane surveillance and repair is of utmost importance to maintain cellular integrity and allow cellular life. Several systems detect cell envelope stress caused by antimicrobial compounds and abiotic stresses such as solvents, pH-changes and temperature in bacteria. Proteins containing an Stomatin, Prohibitin, Flotillin, and HflK/C (SPFH)-domain, including bacterial flotillins have been shown to be involved in membrane protection and membrane fluidity regulation. Here, we characterize a bacterial SPFH-domain protein, YdjI that is part of a stress induced complex in *Bacillus subtilis*. We show that YdjI is required to localize the ESCRT-III homolog PspA to the membrane with the help of two membrane integral proteins, YdjG/H. In contrast to classical flotillins, YdjI resides in fluid membrane regions and does not enrich in detergent resistant membrane fractions. However, similarly to FloA and FloT from *B. subtilis*, deletion of YdjI decreases membrane fluidity. Our data reveal a hardwired connection between phage shock response and SPFH proteins.

frontiers in Microbiology

ORIGINAL RESEARCH
published: 28 October 2021
doi: 10.3389/fmicb.2021.754924

An Stomatin, Prohibitin, Flotillin, and HflK/C-Domain Protein Required to Link the Phage-Shock Protein to the Membrane in *Bacillus subtilis*

*Abigail Savietto Scholz[1,2], Sarah S. M. Baur[1], Diana Wolf[3] and Marc Bramkamp[1,2]**

[1] Institute for General Microbiology, Christian-Albrechts-Universität zu Kiel, Kiel, Germany, [2] Faculty of Biology, Ludwig-Maximilians-Universität München, Munich, Germany, [3] Institute of Microbiology, Technische Universität Dresden, Dresden, Germany

Membrane surveillance and repair is of utmost importance to maintain cellular integrity and allow cellular life. Several systems detect cell envelope stress caused by antimicrobial compounds and abiotic stresses such as solvents, pH-changes and temperature in bacteria. Proteins containing an Stomatin, Prohibitin, Flotillin, and HflK/C (SPFH)-domain, including bacterial flotillins have been shown to be involved in membrane protection and membrane fluidity regulation. Here, we characterize a bacterial SPFH-domain protein, YdjI that is part of a stress induced complex in *Bacillus subtilis*. We show that YdjI is required to localize the ESCRT-III homolog PspA to the membrane with the help of two membrane integral proteins, YdjG/H. In contrast to classical flotillins, YdjI resides in fluid membrane regions and does not enrich in detergent resistant membrane fractions. However, similarly to FloA and FloT from *B. subtilis*, deletion of YdjI decreases membrane fluidity. Our data reveal a hardwired connection between phage shock response and SPFH proteins.

Keywords: YdjI, SPFH-domain proteins, phage-shock protein, cell envelope stress response, flotillins, *Bacillus subtilis*

OPEN ACCESS

Edited by:
Zhaomin Yang,
Virginia Tech, United States

Reviewed by:
Dirk Schneider,
Johannes Gutenberg University Mainz, Germany
Thomas Brüser,
Leibniz University Hannover, Germany

***Correspondence:**
Marc Bramkamp
bramkamp@ifam.uni-kiel.de

Specialty section:
This article was submitted to Microbial Physiology and Metabolism, a section of the journal Frontiers in Microbiology

Received: *07 August 2021*
Accepted: *27 September 2021*
Published: *28 October 2021*

Citation:
Scholz AS, Baur SSM, Wolf D and Bramkamp M (2021) An Stomatin, Prohibitin, Flotillin, and HflK/C-Domain Protein Required to Link the Phage-Shock Protein to the Membrane in Bacillus subtilis. Front. Microbiol. 12:754924. doi: 10.3389/fmicb.2021.754924

INTRODUCTION

All living cells are surrounded by a membrane barrier that shields them from the outside environment. The cell membrane is a dynamic structure containing a lipid bilayer with membrane integral and associated proteins. An intact membrane is essential to adapt to a changing environment. Thus maintenance of the cell membrane functionality is critical for cell viability. In the model-organism *Bacillus subtilis*, phospholipids such as the neutral lipid phosphatidylethanolamine, the anionic phospholipids phosphatidylglycerol and cardiolipin are the major lipid species in the cell membrane (Nickels et al., 2017), while the membrane proteome comprises proteins with several different functions such as membrane synthesis, remodeling, energy metabolism, as well as transport and signaling.

In eukaryotes, membrane regions with altered lipid composition and ordering are associated with the generation of micro-heterogenous domains referred to as lipid rafts or functional membrane microdomains (FMMs) (Simons and Ikonen, 1997; Jacobson et al., 2007). Lipid rafts

are considered to be enriched in certain lipids such as cholesterol and sphingolipids. This leads to a low membrane fluidity, and a liquid-ordered (Lo-phase) arrangement of phospholipids. Importantly, these domain structures are thought to be short lived and of small size around 10–200 nm (Yuan et al., 2002; Owen and Gaus, 2013; Nickels et al., 2017). Existence and formation of membrane rafts or FMMs are still controversially discussed. Proteins such as flotillins have been considered raft marker proteins (Salzer and Prohaska, 2001; Stuermer and Plattner, 2005), however their involvement in membrane organization remains largely elusive. Early models were based on a detergent extraction method that relied on cold solubilization using Triton X-100. Proteins and lipids were separated into soluble and insoluble fractions after this treatment and, hence, termed detergent resistant membranes (DRMs) and detergent soluble membranes (DSMs). After such a membrane fractionation, flotillins enrich in DRMs, but it is commonly accepted now that DRM extraction is an artificial procedure that does not reflect any native membrane organization (Brown, 2006). Therefore, the molecular role of flotillins in eukaryotic membrane organization remains unclear, despite growing evidence that they are involved in membrane organization and signaling processes.

As their eukaryotic counterparts, *B. subtilis* encodes two flotillin homologs termed FloA and FloT (Donovan and Bramkamp, 2009; Lopez and Kolter, 2010). Bacterial flotillins are thought to help in the spatial organization of the membrane. Deletion of flotillins in *B. subtilis* leads in to an increase in membrane rigidity and Lo regions coalesce into large areas (Bach and Bramkamp, 2013). However, the precise function of flotillins in the organization of FMMs in *B. subtilis* is still unsolved. *B. subtilis* FloA and FloT do not co-localize and form distinct clusters of approximately 100 nm spatially separated (Dempwolff et al., 2016). Recently, it was reported that the lack of flotillins and the subsequent decrease the membrane fluidity (Bach and Bramkamp, 2013) leads to a reduction of MreB-directed elongasome complex activity of the peptidoglycan synthesis machinery (Zielinska et al., 2020). Subcellular localization and molecular function of lateral membrane organization and membrane domains started to be unraveled and several phenotypes were linked to FMMs including biofilm formation, protein secretion, competence and cell morphology (Donovan and Bramkamp, 2009; Dempwolff et al., 2012a; Bach and Bramkamp, 2013; Mielich-Suss et al., 2013; Mielich-Suss and Lopez, 2015). Importantly, the organization, maintenance and function of FMMs in bacterial membranes is still elusive.

The two bacterial flotillins, FloA and FloT, are members of a widely conserved and ancient protein family called Stomatin, Prohibitin, Flotillin, and HflK/C (SPFH) domain proteins (Tavernarakis et al., 1999; Browman et al., 2007). SPFH proteins usually share a tripartite domain core structure with an N-terminal membrane anchor and variable heptad repeat-rich sequences that are predicted to form inter-and/or intramolecular coiled-coil structures, termed the flotillin domain (Langhorst et al., 2005; Rivera-Milla et al., 2006; Hinderhofer et al., 2009). The common SPFH-domain found in all flotillins is likely involved in oligomerization, but alone does not bind the membrane (Bach and Bramkamp, 2015).

Recently, a third protein containing the SPFH-domain, YdjI, was identified in *B. subtilis*. YdjI was considered to be a putative flotillin at first (Cozy et al., 2012; Popp et al., 2021; Ravi et al., 2021). Topological protein prediction, however, revealed that, unlike FloA and FloT, YdjI does not share the N-terminal transmembrane structure that anchors the protein to the membrane (**Figure 1**). Although, YdjI membrane association could be possible through positively charged residues in the N-terminus. When considering that the genetic organization and regulation of SPFH-domain proteins (including FloA and FloT) in *B. subtilis* is responsive to environmental stress, a plausible connection of SPFH-domain proteins in stress response pathways seems likely. Both FloA and FloT, are genetically regulated by an ECF sigma factor σ^W (Huang et al., 1998; Wiegert et al., 2001), which is triggered by membrane stressors such as alkaline shock, high salt concentrations, and phage infection (Petersohn et al., 2001; Wiegert et al., 2001). Likewise, YdjI is part of the *pspA-ydjGHI* operon that is also regulated by σ^W in *B. subtilis* (Wiegert et al., 2001; Cao et al., 2002). PspA and homologous proteins such as IM30/Vipp1 play an important role in cell envelope stress response, supporting membrane remodeling and stability (McDonald et al., 2015; Junglas et al., 2020a,b). They are originally defined as part of the phage shock protein family in *Escherichia coli* (Brissette et al., 1991; Kobayashi et al., 2007). PspA shares homology with conserved eukaryotic proteins including the mammalian ESCRT-III, functioning in stabilizing and remodeling membranes (McCullough et al., 2015), and VIPP1/IM30, essential for proper biogenesis of thylakoid membranes in chloroplasts and cyanobacteria (Manganelli and Gennaro, 2017). Just recently, the structures of several PspA/IM30/Vipp1 proteins have been resolved, confirming their structural similarity to the ESCRT-III proteins (Gupta et al., 2021; Junglas et al., 2021; Liu et al., 2021). In *B. subtilis*, PspA localizes to the membrane under stress conditions and protects the membrane against membrane-targeting antibiotics (Wolf et al., 2010; Kingston et al., 2013; Dominguez-Escobar et al., 2014; Popp et al., 2020). It has been speculated that the PspA/ESCRT-III system is an ancient, ubiquitous membrane repair system (Ravi et al., 2021).

Currently, our understanding of bacterial flotillins and their roles in bacterial physiology is rapidly evolving. The commonly accepted hypothesis was that bacterial SPFH-domain proteins reside in liquid-ordered membrane domains and act mainly as scaffold proteins to allow spatial and temporal membrane compartmentalization. However, further investigations from our group and others have pointed functions for the bacterial SPFH-domain proteins toward membrane modulation responsive to stress (Dempwolff et al., 2012b; Lee et al., 2012; Dempwolff and Graumann, 2014; Sawant et al., 2016; Zielinska et al., 2020).

Since the genetic regulation of FloT and YdjI is similar and stress related, we decided to further investigate the SPFH-domain protein YdjI in detail. Here, we describe the subcellular distribution of the *B. subtilis* YdjI protein and dissect the interaction with the other proteins encoded in the *pspA-ydjGHI*

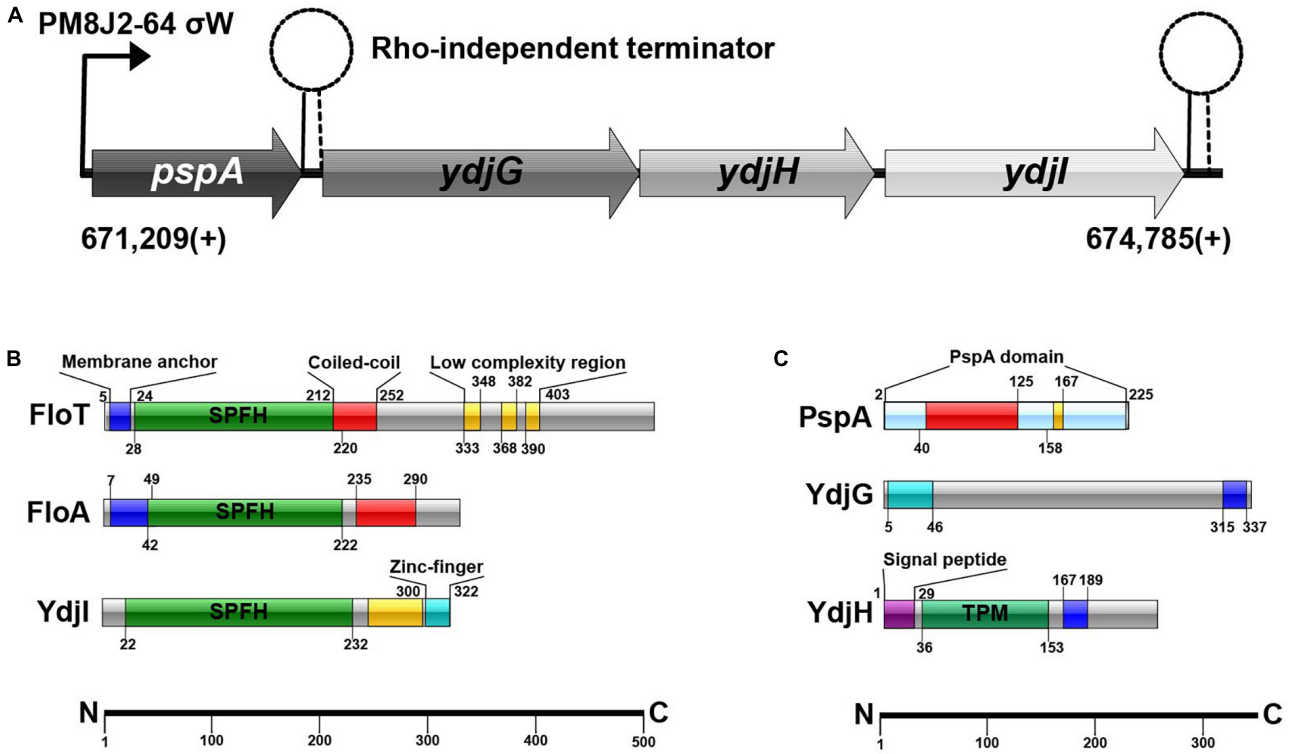

FIGURE 1 | (A) Schematic overview of the *pspA-ydj*-operon. σ^W-dependent promotor PM8J2-64 starts transcription at 671,209(+); transcription starts with *pspA*, continuing with *ydjG*, *ydjH* and subsequently *ydjI*. **(B)** SPFH-proteins in *B. subtilis* and their domains. **(C)** Proteins of the *ydj*-operon and their protein-domains.

operon. We show that YdjI is required in the phage-shock protein response of *B. subtilis* and that the proteins encoded in the σ^w controlled *pspA-ydjGHI* operon are highly interdependent for membrane localization. Contrary to the other SPFH-domain proteins in *B. subtilis* (FloA and FloT), YdjI does reside in fluid membrane region. Membrane complex formation of PspA depends on YdjI and the membrane integral proteins YdjG and YdjH. Unlike in *E. coli*, PspA focus formation and dynamics is independent of MreB in *B. subtilis*. Our data reveal a tight interaction network between YdjI, an SPFH-domain protein, and the phage-shock system in *B. subtilis*.

RESULTS

YdjI Is an Stomatin, Prohibitin, Flotillin, and HflK/C-Domain Protein Localizing Into Liquid Disordered Membrane Regions

Bacillus subtilis 168 encodes a *pspA* (BSU_06180) homolog under control of a σ^w-dependent promoter. Downstream of *pspA*, three structural genes, *ydjGHI* are positioned (**Figure 1A**). This operon is likely controlled via the promoter in front of *pspA*, however there is a Rho-independent terminator between *pspA* and *ydjI*. YdjI is a member of the SPFH-domain proteins. It shares the SPFH-domain with other bacterial flotillins, including FloA and FloT from *B. subtilis* (**Figure 1B**). Topology prediction analysis of YdjI suggests that the protein lacks a hydrophobic domain that could serve as a membrane anchor, consequently rendering YdjI soluble (**Figure 1B**). However, the two genes upstream of *ydjI*, *ydjG*, and *ydjH* encode for proteins that contain transmembrane helices and they are likely membrane integral proteins (**Figure 1C**). YdjI contains a low complexity region and a Zink-finger motif close to its C-terminus.

To study the subcellular localization of the *B. subtilis* YdjI protein, we constructed a translational YdjI-mNeonGreen fusion, replacing the native gene locus and, hence, expression of *ydjI-mNeonGreen* was still under native regulation. Furthermore, we used a PspA-GFP fusion to visualize PspA localization *in vivo*. PspA and YdjI were found to localize in discrete foci at the membrane of *B. subtilis* (**Figures 2A,B**). PspA expression was clearly enhanced under alkaline shock (**Supplementary Figure 1**), as expected since the promotor is known to be strongly induced by the ECF sigma factor σ^W (Huang et al., 1998; Wiegert et al., 2001). Western blotting or in-gel fluorescence revealed that PspA and YdjI fusion proteins were full length and only little degradation was observed (**Supplementary Figure 1**). While the cellular concentration of YdjI did not differ significantly under non-induced and stress induced conditions (stress was applied by addition of 15 mM NaOH), the concentration of PspA was greatly enhanced upon alkaline shock (**Supplementary Figures 1A–C**). These findings are in line with the presence of a Rho-independent terminator between *pspA* and *ydjG* (**Figure 1A**) leading to a

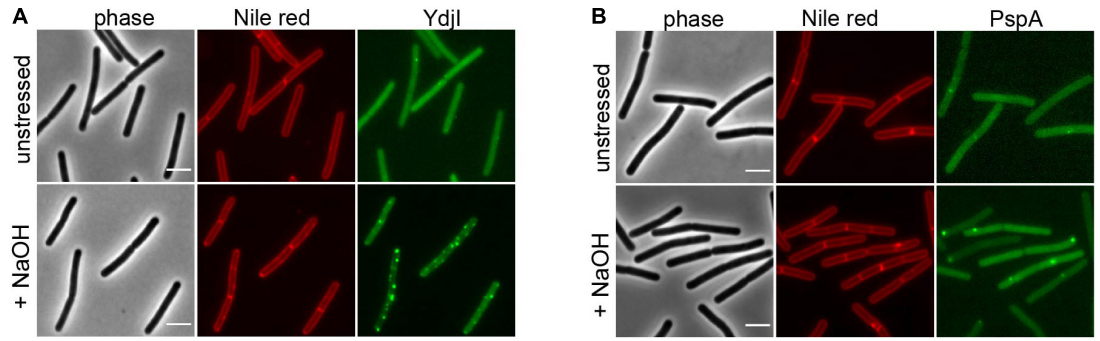

FIGURE 2 | YdjI and PspA intracellular localization. Morphology of the exponentially growing strains labeled with Nile Red in unstressed (upper panel) and in alkali stress conditions (15 mM NaOH), lower panel. **(A)** YdjI-mNeonGreen and **(B)** PspA-GFP. Scale bars: 3 μm.

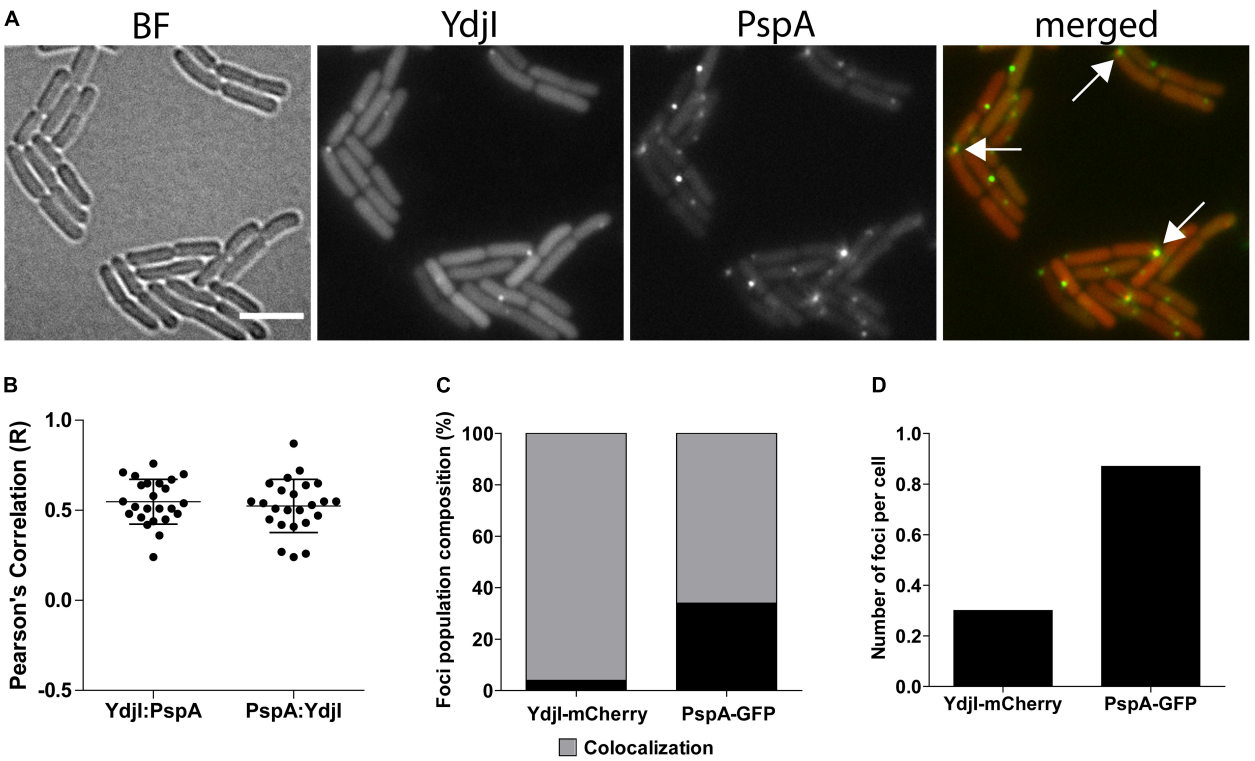

FIGURE 3 | Co-localization analysis of PspA and YdjI proteins. **(A)** Micrographs showing exponentially growing cells of expressing YdjI-mCherry2 and PspA-GFP in alkali stress condition (15 mM NaOH). Arrows indicate co-localized foci. Scale bar: 4 μm. **(B)** Scattered dot plots of Pearson's correlation (*R* values) assessed by Coloc-2 plugin from FIJI. Red to green (YdjI:PspA) and green to red (PspA:YdjI) co-localization analysis are shown. Error bars represent mean and standard deviation of values calculated for 24 cells. **(C)** Foci population composition in percentage of cells (n = 1650). **(D)** Ratio of total number of foci in each channel per total of cells (n = 1650).

substantial difference in the protein concentrations of PspA and YdjGHI after alkaline shock. The majority of YdjI was membrane associated, while the majority of PspA was found in the cytosol and not membrane associated (**Supplementary Figures 1A–C**). Although the PspA concentration was increased in the cell after alkaline shock, cell fractionation experiments show that the ratio of membrane associated and cytosolic PspA remained the same (**Supplementary Figure 1C**). Thus, PspA recruitment to the membrane was not increased after alkaline shock. The addition of 15 mM NaOH was sublethal for all individual deletion strains of *pspA* and the *ydj* genes tested here. In all cases addition of sodium hydroxide only marginally decreased growth rates compared to the unstressed control (**Supplementary Figure 2**). We conclude that alkaline shock with 15 mM NaOH does induce the *pspA-ydjFGHI* operon, but has no deleterious effect on the cells that might compromise localization studies.

In a next attempt we analyzed potential co-localization of PspA and YdjI. Both proteins formed membrane

associated foci under stress conditions induced by 15 mM NaOH shock. We constructed a strain expressing PspA-GFP and YdjI-mCherry2 under control of their native promoters (strain ASB013). Microscopic examination of the cells revealed that PspA and YdjI readily form foci upon alkaline shock. The vast majority of YdjI foci co-localized with PspA foci (**Figures 3A–C**). Cells contained in average more PspA foci (**Figure 3D** and **Table 1**) and therefore not all PspA foci co-localized with a YdjI focus. However, a detailed analysis of co-localization using Pearson's correlation revealed a high degree of co-localization for both proteins (**Figure 3B**).

The subcellular localization pattern of YdjI and PspA was similar to the punctate membrane distribution of other bacterial SPFH-domain proteins, namely FloA and FloT (Donovan and Bramkamp, 2009; Lopez and Kolter, 2010). FloA and FloT were shown to localize into liquid ordered membrane regions (Bach and Bramkamp, 2013). We therefore wanted to address the preferred membrane region to which YdjI is recruited. To assess this, we performed *in vivo* co-localization studies of the YdjI-mNeonGreen fusion strain (strain ASB033) with Dil-C12, a well-known fluorescent probe for fluid membrane regions (Strahl et al., 2014). When *B. subtilis* cells were stained with Dil-C12, strictly punctuated fluorescent foci could be observed that overlapped significantly with the YdjI-mNeonGreen signal, with a Pearson's correlation coefficient of 0.93 ± 0.022 (n = 23 cells) (**Figures 4A,C**). We also analyzed the co-localization pattern of FloT and YdjI by using a doubled tagged strain FloT-mNeonGreen; YdjI-mCherry2 (strain ASB154). In this strain both proteins were under control of their native promoter. YdjI did not co-localize with FloT in neither unstressed, or stressed conditions (**Figures 4B,D**). Fluorescence intensity correlation graphs for alkaline induced conditions in displaying a pixel by pixel correlation between Dil-C12 and YdjI-mNeonGreen (**Figure 4C**) or YdjI-mCherry2 and FloT-mNeonGreen (**Figure 4D**) revealed a clear anti-correlation between FloT and YdjI and a clear correlation between YdjI and Dil-C12.

Classical flotillins such as FloT can be enriched in so-called DRM extractions. We therefore aimed to compare the behavior

TABLE 1 | Number of PspA and YdjI foci per cell under alkaline shock and control conditions.

		Average number of foci per cell (±SD)	No. of cells counted (n)
PspA-GFP	NaOH	1.64 ± 0.18	497
	Control	0.49 ± 0.07	588
Δ*mreB;* PspA-GFP	NaOH	0.68 ± 0.07	539
	Control	0.21 ± 0.05	564
YdjI-mNG	NaOH	1.29 ± 0.05	629
	Control	0.71 ± 0.08	855
Δ*mreB;* YdjI-mNG	NaOH	0.81 ± 0.10	1015
	Control	0.49 ± 0.08	638

Cells were grown in LB medium with supplements where necessary. Alkaline shock was induced by addition of 15 mM NaOH.

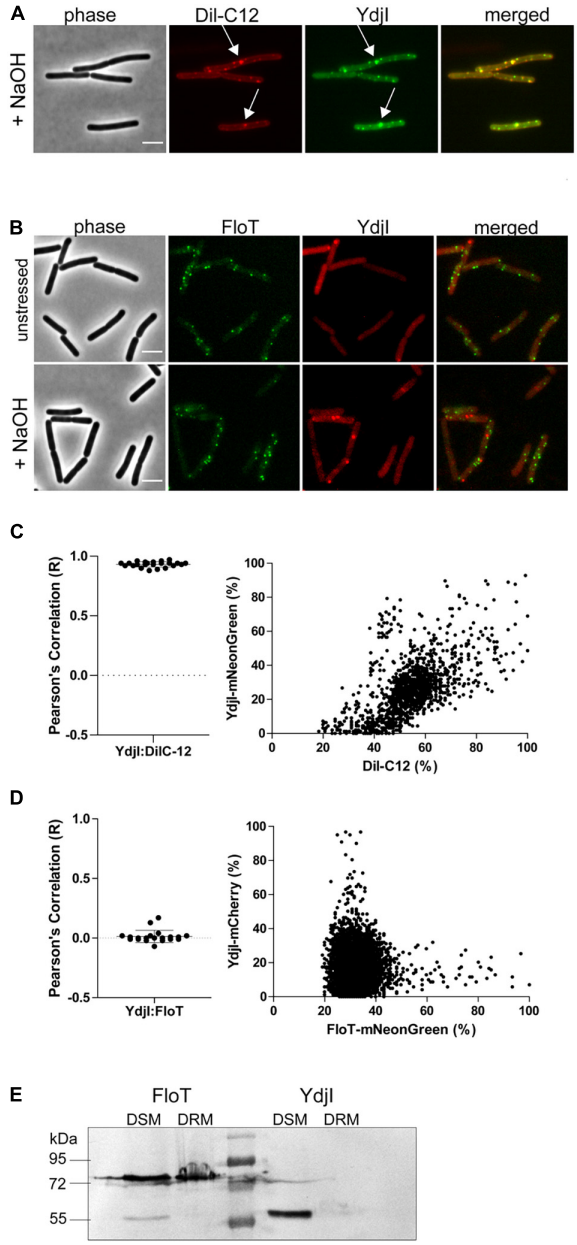

FIGURE 4 | YdjI localizes into fluid membrane regions and does not co-localize with FloT. **(A)** YdjI co-localizes with fluid membrane regions as indicated by co-localization with Dil-C12 staining (arrows). **(B)** Localization of YdjI and FloT are independent. Micrograph show no localization of FloT and YdjI in a double tagged strain *floT-mNeonGreen; ydjI-mcherry*. Cells are in exponentially growing phase under unstressed or alkali stress conditions (15 mM NaOH). Scale bars: 3 μm. **(C)** Pearson's co-localization analysis (n > 20) and fluorescence intensity correlation graphs (right panel) are shown for the YdjI and Dil-C12 localization. The graph displays a pixel by pixel intensity correlation between Dil-C12 and YdjI-mNeonGreen fluorescence. **(D)** Pearson's co-localization analysis (n > 20) and fluorescence intensity correlation graphs are shown for the YdjI-mCherry and FloT-mNeonGreen localization. The graph on the right displays a pixel by pixel intensity correlation between FloT-mNeonGreen and YdjI-mCherry fluorescence. **(E)** Localization of YdjI in the detergent soluble membrane fraction (DSM). DSM/DRM extraction using strains expressing YdjI-mCherry (ASB049) and FloT-mCherry (ASB044) and subsequent immunoblotting using anti-mCherry antibodies is shown.

of YdjI and FloT using DRM and DSM fractionation. Although, DRM/DSM fractionation is not suitable to make predictions about membrane domains in living cells, it allows the specific enrichment of proteins such as classical flotillins. Phase separation of DRM and DSM was achieved using a commercially available kit (see section "Materials and Methods"). Fractionation revealed that FloT is recovered in the DRM fraction as expected (**Figure 4E**). Although, part of the FloT protein was still found in the DSM fraction, a high proportion of the protein was recovered in the DRM fraction. On the contrary, YdjI was found exclusively in the DSM fraction (**Figure 4E**). This is an important difference, since currently, all SPFH-domain proteins have been associated with liquid ordered membrane regions and were thought to enrich in DRM fractions (Bramkamp and Lopez, 2015). In particular, the SPFH-domain itself was supposed to mediate contact and specificity to defined membrane regions. These data, together with the co-localization of YdjI with DilC-12 *in vivo*, confirm that YdjI behaves different compared to classical flotillins and likely resided in fluid membrane domains in the bacterial plasma membrane. Consequently, not all SPFH-domain proteins are associated with Lo domains.

YdjI Is Required for PspA Focus Formation

While FloA and FloT bind autonomously to the membrane, the subcellular localization of YdjI might require other proteins from the PspA-YdjGHI operon for membrane association, as hypothesized by the protein domain prediction analysis of YdjG and YdjH (**Figure 1**). To test this, we used YdjI-mNeonGreen and PspA-GFP fusion strains that lacked the *pspA* and *ydjI* gene, respectively, and analyzed the *in vivo* localization of the tagged proteins. The results revealed that PspA was not recruited to the membrane when YdjI was absent, regardless if the cells were induced or not with alkali-shock (**Figures 5A–D**), showing a strong dependency and interaction between PspA and YdjI for membrane complex formation. Importantly, ectopic expression of YdjI fully complemented this phenotype (**Supplementary Figure 3**). Deletion of *pspA* led to an increase

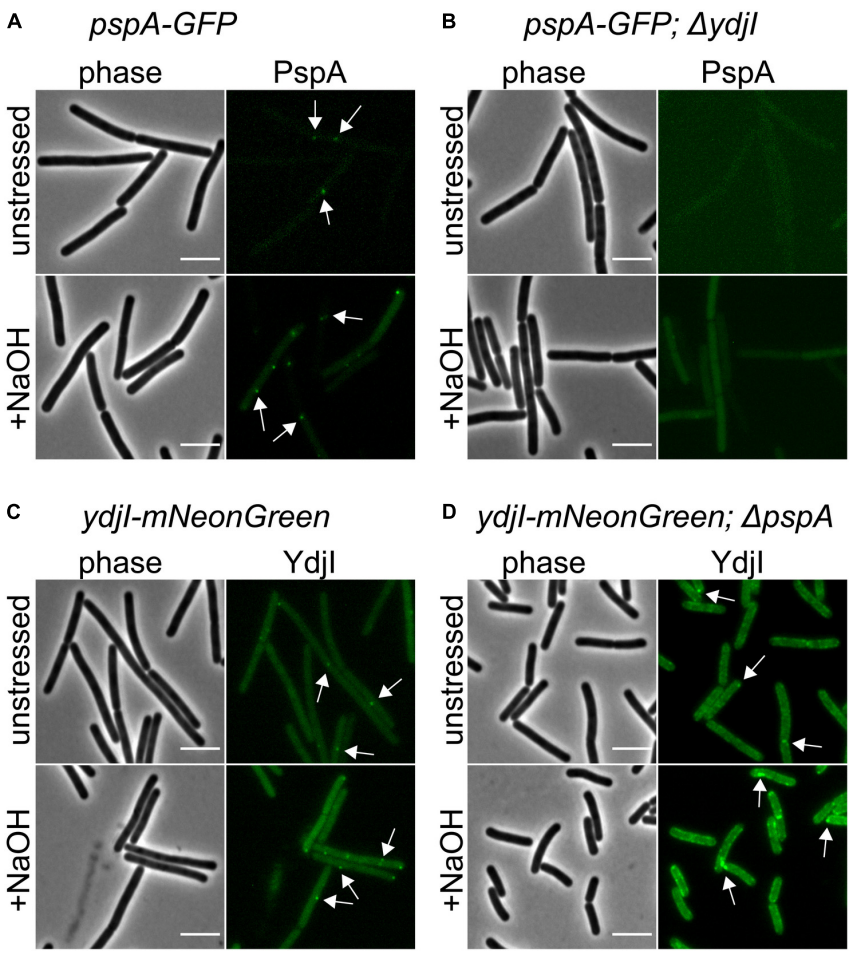

FIGURE 5 | YdjI is required for PspA membrane anchoring and complex formation. **(A)** PspA-GFP foci are shown in unstressed and alkali stress conditions. **(B)** Deletion of *ydjI* delocalize PspA and the cells show no PspA foci in both conditions. Scale bars: 4 μm **(C)** *ydji-mNeonGreen* is shown under unstressed or stressed conditions (15 mM NaOH). **(D)** Deletion of *pspA* leads to YdjI overexpression. YdjI foci are still formed (arrows). Scale bars: 3 μm.

of YdjI expression, due to the removal of the Rho-independent terminator in this strain. In this case we observed YdjI focus formation and conclude that YdjI complex formation does not require PspA (**Figure 5D**).

YdjG and YdjH Are Part of the PspA-YdjI Interaction Network and Are Required for Membrane Localization of PspA and YdjI

Since YdjI is likely a soluble protein its membrane targeting should require an additional factor. We therefore reasoned that the two membrane proteins YdjG and YdjH that are encoded in the *pspA-ydj* operon are potential candidates for this membrane recruitment. Indeed, deletion of either *ydjG* or *ydjH* entirely abolished YdjI and PspA foci formation and membrane recruitment under normal growth and under alkali shock conditions (**Figures 6A–D**), hinting toward a direct interaction between the Ydj proteins. To test this hypothesis, we performed an extensive bacterial two hybrid interaction analysis. To this end, we fused the coding sequences of PspA, YdjI, YdjG, and YdjH to the split adenylate cyclase domains (Karimova et al., 1998). To minimize steric problems of the fusion proteins, we performed all possible combinations of N- and C-terminal fusions (**Figure 6E**). Using a blue-white screen on plate we observed a close interaction network between PspA and the Ydj proteins. PspA, YdjI and YdjH all showed self-interaction. We also detected a strong interaction between PspA and YdjI, corroborating the co-localization studies. Furthermore, we revealed an interaction of the two membrane components YdjG and YdjH with each other. Importantly, we also observed an interaction of YdjH with PspA and with YdjI, indicating that YdjH likely acts as the membrane anchor for the YdjI/PspA complex (**Figure 6E**).

Absence of YdjG and YdjH Causes a Severe Phenotype Linked to Peptidoglycan Synthesis Machinery Delocalization

In strains deleted for either *ydjH* or *ydjG* we observed a severe cell morphological defect under alkali shock conditions. While unstressed cells lacking YdjG or YdjH reveal a normal morphology, these cells showed curved cells and swollen or bulged cell poles upon NaOH addition (**Figures 6A–D**). These aberrant morphologies are reminiscent of certain mutations known from components involved in cell wall synthesis such as a *gpsB* mutation (Claessen et al., 2008) or *mreBH* mutations (Carballido-Lopez et al., 2006). Therefore, we used fluorescent staining of nascent peptidoglycan synthesis, in order to visualize localization of the cell wall synthesis machinery. Strains with clean deletions of either *ydjG* and *ydjH* were stained with HADA (Kuru et al., 2015) and cells were stressed with NaOH (15 mM). HADA localizations were often found at the bulging cell poles and in areas were the cell body seems bent and misshaped (**Supplementary Figures 4A,B**). In wild type *B. subtilis* cells the cell poles are usually inert and do not localize active cell wall synthetic complexes. Cells lacking YdjG show a more pronounced phenotype including occasional branching (**Supplementary Figure 4A**). We conclude that YdjG might couple cell envelope stress signaling and cell wall synthesis. In absence of these proteins, cell wall synthesis becomes deregulated under stress conditions. Interestingly, deletion of YdjI or PspA did not exhibit this strong morphological phenotype and, hence mis-localization of the PspA/YdjI complex might not be the (sole) reason for this cell shape defect in an YdjG/H mutant.

PspA and YdjI Foci Formation Does Not Depend on MreB

Anionic lipids and the cytoskeletal proteins MreB and RodZ define the spatio-temporal distribution and function of PspA in *E. coli* (Jovanovic et al., 2014). Based on these findings and the observed cell shape defect in *ydjG/H* mutants we wanted to analyze a potential involvement of the MreB cytoskeleton on PspA/YdjI complex formation. We constructed strains expressing YdjI-mNeonGreen and PspA-GFP in which we deleted the *mreB* gene (strains ASB155 and ASB123, respectively). In both strains we readily observed PspA and YdjI foci under alkali shock conditions, indicating that MreB is not essential for PspA or YdjI assembly (**Figures 7A–D**). However, a quantification of the PspA and YdjI foci per cell revealed that cells lacking MreB accumulate significant less foci compared to wild type cells (**Table 1**). While wild type cells had on average 1.6 PspA foci per cell, the *mreB* mutant strain had only 0.68 foci per cell. When cells were not stressed with sodium hydroxide we also observed a reduced number of PspA foci (0.21 foci in *mreB* mutant cells and 0.49 foci in wild type cells). Thus, absence of MreB leads to a 2.3-fold reduction of PspA foci formation under stressed and unstressed conditions. Similarly, the number of YdjI foci was reduced in absence of MreB in stressed and unstressed conditions (**Table 1**), lending support to the notion that PspA and YdjI foci formation is tightly connected. We next wanted to analyze whether PspA and YdjI foci are mobile in presence and absence of MreB. Time-lapse analysis revealed that in strains lacking *mreB* PspA and YdjI foci still retain their dynamic behavior (**Supplementary Movies 1–8**). Inspection of all movies revealed that many PspA and YdjI form foci that were mobile while others are rather static. A simple explanation might be that the static foci are acting on the membrane locally, maybe at damaged membrane areas. However, we did not observe a major difference in PspA or YdjI foci dynamics lacking MreB. We conclude that in *B. subtilis*, MreB is not essential for PspA and YdjI foci formation. However, deletion of MreB leads to altered foci numbers. We have shown that deletion of MreB led to a decrease in membrane fluidity (**Figure 7E**). A plausible explanation for the reduced foci number of PspA/YdjI might therefore a change in membrane fluidity.

YdjI Fluidizes the Membrane, Similar to Flotillins

We have shown before that deletion of *mreB* or flotillins has an effect on membrane fluidity. Membrane fluidity can be experimentally addressed by using the generalized polarization (GP) values after a Laurdan staining. Laurdan intercalates into the membrane bilayer and its fluorescent spectra are sensitive

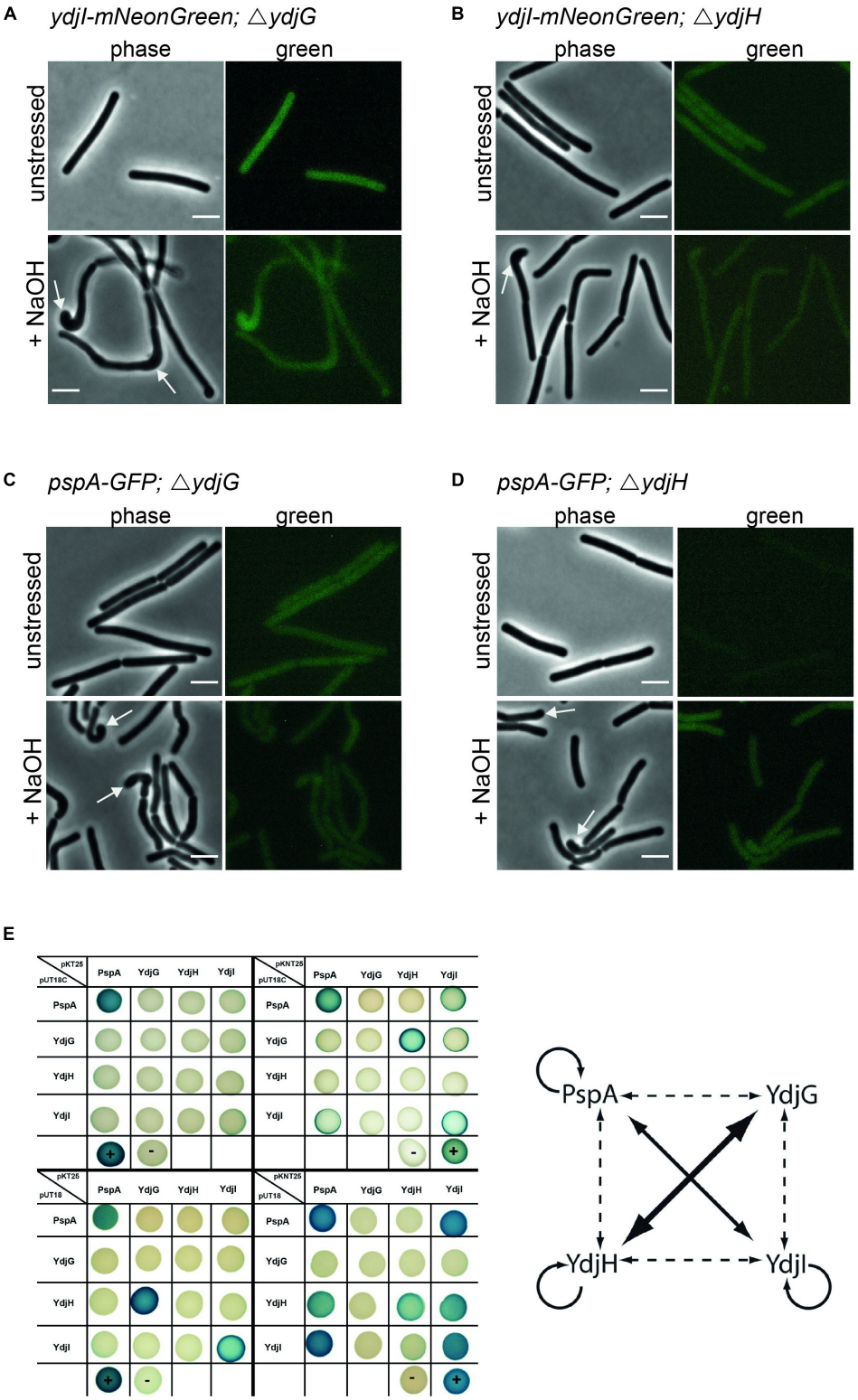

FIGURE 6 | YdjG and YdjH serve as membrane anchor for PspA-YdjI protein complex and seem to have a role in cell-shape maintenance. Deletion of **(A)** *ydjG* and **(B)** *ydjH* delocalize YdjI foci formation under both unstressed and alkali stress conditions. The same is shown for PspA delocalization upon deletion of **(C)** *ydjG* and **(D)** *ydjH*. Arrows indicate a strong cell-shape defect upon deletion of either YdjG or YdjH, under stress conditions. Scale bars: 3 μm. **(E)** Interactions of proteins encoded in the *pspA-ydjGHI* operon via Bacterial-2-Hybrid. Blue colonies indicate protein–protein interaction, while in white colonies the target proteins do not

(Continued)

FIGURE 6 | (Continued)
interact. The positive and negative controls are marked by a plus minus, respectively. In pUT18C and pKT25 plasmids the T18 or T25 fragment of the adenylate cyclase is N-terminally fused to the protein of interest. pUT18 and pKNT25 encode for a C-terminal fusion to the protein of interest. The diagram represents a summary of the B2H analysis. The size of the arrow indicates the intensity of the blue color. Dashed lines indicate weaker protein–protein interactions.

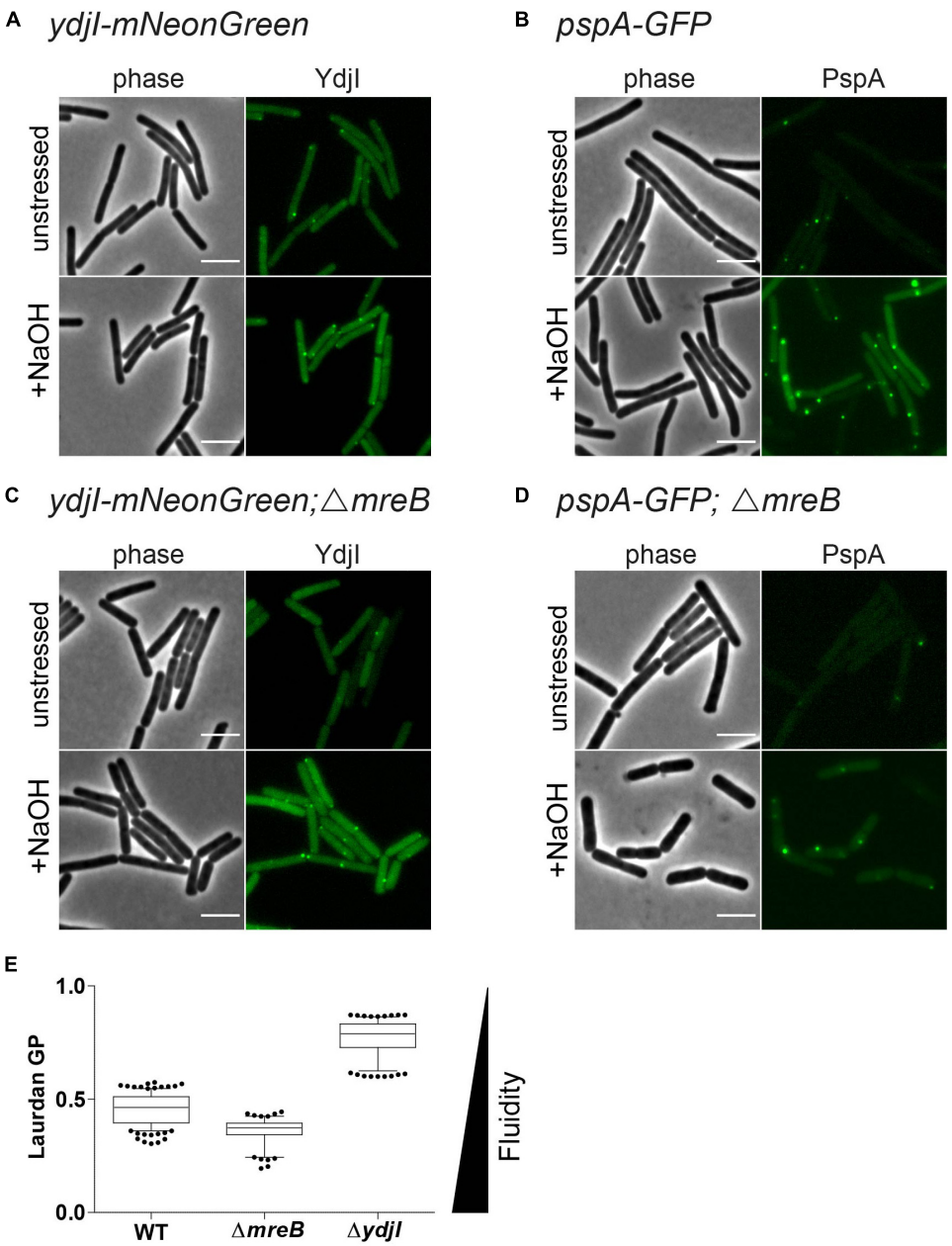

FIGURE 7 | MreB is not required for YdjI and PspA foci formation. **(A)** YdjI localization in unstressed and alkaline stressed conditions. **(B)** PspA localization in unstressed and alkaline stressed conditions. **(C)** YdjI localization in a *mreB* mutant background. Note that in stressed and unstressed conditions YdjI foci are seen. **(D)** Upon deletion of the cytoskeletal protein *mreB*, PspA still localizes in membrane associated foci. Foci numbers in strains lacking *mreB* are reduced (see also **Table 1**). **(E)** Generalized polarization analysis after Laurdan staining of WT 168, MreB, and YdjI mutant strain are shown ($n > 100$); deletion of *mreB* causes increase in membrane fluidity, whereas YdjI deletion increases membrane rigidity. Scale bars 4 μm.

to polarity and dipole dynamics. This allows a correlation of measured GP values and lipid packing in the membrane. Using Laurdan GP analysis we showed that deletion of *mreB* reduced the overall GP, rendering the membrane slightly more fluid. In contrast deletion of YdjI significantly increased the overall GP value. Thus, similar to the situation observed for the deletion of

the flotillins FloA and FloT, deletion of the SPFH domain protein YdjI led to a rigidification of the bacterial membrane (**Figure 7E**).

DISCUSSION

Organization and surveillance of plasma membrane integrity is of vital importance for cellular life. Hence, several systems have been described that are part of membrane organization, stress perception and membrane repair (Willdigg and Helmann, 2021). Many of the involved proteins are ubiquitously distributed in all domains of life. One of the protein families that is widely distributed are the SPFH-domain proteins (Langhorst et al., 2005; Browman et al., 2007; Willdigg and Helmann, 2021). Among these proteins are flotillins, proteins that have been attributed with functional membrane domains in pro- and eukaryotes (Stuermer and Plattner, 2005; Bramkamp and Lopez, 2015). *B. subtilis* encodes two flotillin-like proteins, FloA and FloT (Bramkamp and Lopez, 2015). Both proteins are involved in membrane fluidity regulation (Bach and Bramkamp, 2013; Zielinska et al., 2020). *B. subtilis* encodes a third SPFH-domain protein, YdjI that is encoded in the *pspA-ydjGHI* operon (Popp et al., 2021; Ravi et al., 2021). We show here that YdjI is involved in membrane dynamics and PspA recruitment. The first protein encoded in the operon, PspA, is another ubiquitously found protein that is involved in cell envelope stress response. PspA forms large oligomeric complexes and shares a canonical ESCRT-III type fold (Gupta et al., 2021; Junglas et al., 2021; Liu et al., 2021). *In vitro* analysis shows that PspA proteins bind to membranes and can induce membrane deformation, fusion and fission events (Junglas et al., 2021). PspA homo-oligomeric complexes can be larger than 1 MDa and its donut-shaped arrangement imposes a positive curvature on the membrane (Junglas et al., 2021). Various PspA proteins, including IM30/Vipp1 from *Synechocystis* and PspA from *E. coli* have been shown to localize in foci along the membrane (Engl et al., 2009), similarly to the focus formation described here for the *B. subtilis* PspA and YdjI proteins. However, a main difference is that in *E. coli* the PspA foci are described to enrich at the cell poles and shuttle between poles (Engl et al., 2009), while for *B. subtilis*, we see less overall foci and not a strong bias for polar localization. Foci formation in diffraction limited fluorescence microscopy is in line with oligomerization, however the resolution is not high enough to judge about the molecular architecture. The precise nature of the YdjI or PspA foci remains to be elucidated, however, time-lapse analysis indicates that the complexes are dynamic. Occasionally, we observed static foci, potentially indicating action of YdjI/PspA foci at sites of membrane damage. So far, the best understood PspA system is that of *E. coli* in which PspA has been implicated with membrane repair and protection from proton leakage and subsequent dissipation of the proton motive force (Kleerebezem et al., 1996; Kobayashi et al., 2007). In *B. subtilis* two PspA homologs have been identified, LiaH and PspA. Both proteins are involved in response to cell membrane stress, for example induced by the pore forming antibiotic nisin (Wolf et al., 2010; Dominguez-Escobar et al., 2014). A common theme in PspA mediated stress response is the interaction of the PspA protein with a membrane receptor. In the *E. coli* system PspB and PspC recruit PspA to the membrane (Adams et al., 2003; Maxson and Darwin, 2006; Jovanovic et al., 2010). LiaH interacts with the membrane proteins LiaI and LiaG (Popp et al., 2021). Recent phylogenetic studies suggest a tight genomic connection of PspA with SPFH-domain (also termed Band-7) proteins (Popp et al., 2021; Ravi et al., 2021), however their functional interactions remained speculative. We show here, that the *B. subtilis* PspA requires the SPFH-domain protein YdjI for cluster formation and correct membrane recruitment. SPFH-domain proteins have been described as chaperones for complex formation, indicating a possible function in the oligomerization of PspA. This function is in line with our observation that stressed *B. subtilis* cells have in average more PspA cluster compared to YdjI and that almost all YdjI cluster co-localize with PspA. Thus, an initial interaction of these proteins for cluster formation and a subsequent release of PspA oligomers is plausible. Cluster formation also requires the two transmembrane proteins YdjG and YdjH. Absence of these proteins prevents PspA foci formation *in vivo* and an intricate interaction network has been revealed by bacterial two-hybrid analysis, extending recent studies (Popp et al., 2021; Ravi et al., 2021). Thus, all PspA systems studied so far require a membrane integral receptor complex. The interaction of PspA homologs and SPFH-domain proteins has also been described in other bacteria (Ravi et al., 2021). Although the precise function of SPFH-domain proteins in stress signal perception and membrane integrity is only partially understood, it emerges that membrane protection and surveillance systems are interlinked. Adding to this notion are also reports linking the functions of SPFH-domain proteins and bacterial dynamins (Dempwolff and Graumann, 2014). The latter are involved in membrane fusion and it was shown for the *B. subtilis* dynamin DynA that this protein catalyzes membrane fusion during nisin and phage stress (Burmann et al., 2011; Sawant et al., 2016), suggesting a complex membrane surveillance and repair network.

Stomatin, Prohibitin, Flotillin, and HflK/C-domain proteins that have been characterized so far localize to specific membrane regions (Bach and Bramkamp, 2013; Greenlee et al., 2021). Flotillins from eukaryotic cells have therefore been described as lipid raft marker (Dermine et al., 2001; Yokoyama and Matsui, 2020; Greenlee et al., 2021). Bacterial flotillins, such as FloA and FloT form specific clusters in the bacterial plasma membrane and both proteins are enriched in DRM fractions (Donovan and Bramkamp, 2009; Lopez and Kolter, 2010; Bach and Bramkamp, 2013). Surprisingly, we show here that YdjI localizes in focal assemblies in membrane regions of low fluidity. Consequently, we also recover YdjI only in DSM fractions. DRM fractionation is highly artificial and does not allow to draw conclusions on the native membrane organization. However, it is useful to enrich or separate certain membrane proteins based on the physical properties. Thus, the presence of the name giving SPFH-domain, does not predict *a priori* similar behavior of the proteins within the membrane. An obvious difference between FloA and FloT compared to YdjI is that the flotillins bind autonomously to the membrane by a transmembrane helix or hairpin-loop, respectively (Bach and Bramkamp, 2015). YdjI,

in contrast, requires the membrane integral proteins YdjG and YdjH and transmembrane proteins might favor fluid membrane regions for insertion. So far it is unclear how the stimulus perception via YdjG/H is, but the observed knock-out phenotype of YdjG/H with a mis-localized cell wall synthesis, indicates that there is a tight connection of peptidoglycan synthesis and stress response. Despite the differences between FloA/T and YdjI, a remarkable similarity is the effect of *ydjI* deletion on membrane fluidity. Similar to a deletion of flotillins, loss of YdjI leads to an increase in the overall GP values, indicating that the protein is involved in membrane fluidization. It seems plausible that membrane fluidization might assist membrane repair because in fluid membranes fusion ad fission events occur with higher efficiency. Thus, bacterial cell membrane protection is using several combinations of PspA and SPFH-domain proteins that are hardwired in various combinations. Several of such systems can also act in one species, indicating that they either respond to specific signals or act as redundant systems. Given the importance of membrane integrity for cellular life, this is maybe not surprising.

MATERIALS AND METHODS

Bacillus subtilis Strains and Growth Conditions

All *B. subtilis* strains used in this study are derived from strain 168 and are listed in **Table 2**. Construction of new strains was based on natural competence of *B. subtilis* (Harwood and Cutting, 1990). Gene integration or deletion was validated by colony PCR whereas the expression and localization of the fluorescent fusions were additionally validated by microscopy. Cells were grown in lysogeny broth (5 g/L yeast extract; 5 g/L NaCl; 10 g/L tryptone) at 37°C and 200 rpm. Induction of the *pspA* promoter was triggered by addition of 15 mM NaOH (Wiegert et al., 2001). Cell cultures were supplemented with spectinomycin (50 $\mu g\ ml^{-1}$), chloramphenicol (5 $\mu g\ ml^{-1}$), kanamycin (5 $\mu g\ ml^{-1}$), erythromycin (1 $\mu g\ ml^{-1}$), neomycin (10 $\mu g\ ml^{-1}$), magnesium chloride ($MgCl_2$, 25 mM), and/or sucrose (0.3 M) when necessary.

Strain Constructions

Plasmids were constructed using standard cloning techniques and Golden Gate Cloning Assembly (Engler et al., 2009). For DNA amplification via PCR, Phusion DNA polymerase was used. Restriction enzymes were purchased from New England Biolabs (NEB, Ipswich, MA, United States) and used accordingly with their respective protocols. *E. coli* colonies were checked by colony PCR, using EconoTaq polymerase (Lucigen) and all plasmids were verified by sequencing. All strains, primers and plasmids are listed in **Tables 2–4**, respectively. Plasmid cloning was carried out in *E. coli* DH5α or in DH5α Turbo (New England Biolabs). The strains FloT-PAmCherry and YdjI-mNeonGreen were constructed as follows: PAmCherry fragment was amplified from the plasmid pPAmCherry1-N1 using the primers pamCherry-F and pamCherry-R. The fragment of mNeonGreen was amplified from pNCS-mNeonGreen plasmid using the primers mNeonGreen-F and mNeonGreen-R. The *Bsa*I site in pUC18 plasmid was mutated using the primers pUC18mut-F and pUC18mut-R resulting in the plasmid pUC18mut. YdjI and FloT including their endogenous promoter and ribosomal binding site were amplified from genomic *B. subtilis* DNA using the primers pairs YdjI-GG-F/YdjI-GG-R and FloT-GG-F/FloT-GG-R and cloned into pUC18mut. FloT-PAmCherry construct was done by Golden Gate assembly of the fragments yuaGIN, PAmCherry, cat, yuaGDown and pUC18BsaI, respectively resulting in the plasmid pUC18mut-yuaGIN-PAmCherry-cat-yuaGDown. For the ectopic expression of *ydjI*, we constructed plasmid pJPR1-ydjI. The coding sequence of *ydjI* including its own ribosomal binding site was amplified from genomic *B. subtilis* DNA using the primer pair *Xba*I_RSB_ydjI_UP and *Eag*I_Stop_ydjI_DOWN and subsequently cloned into pJPR1. The final plasmid was transformed into *B. subtilis* and integration into the *amyE* locus was confirmed.

All oligonucleotides resulting in the respective fragments can be found in **Table 4**. All plasmids were transformed into *B. subtilis* was based on natural competence of *B. subtilis* (Harwood and Cutting, 1990) and screened for double cross over. Gene integration or deletion was validated by colony PCR whereas the expression and localization of the fluorescent fusions was additionally validated by microscopy.

Bacterial 2-Hybrid Analysis

Bacterial adenylate cyclase-based two-hybrid (BACTH) assay was performed according the protocol described by Karimova et al. (1998). Strain *E. coli* BTH101 (Euromedex) was co-transformed with plasmids containing genes of interest fused either to T18 or T25 fragments of adenylate cyclase. The adenylate cyclase is divided into two parts, each of them either N- or C-terminal present on the vectors pUT18/pKT25N or pKT25/pUT18C, respectively. Since the interaction of the proteins can be influenced by the position of the adenylate cyclase domains, all plasmid combinations were used (**Table 3**). After transformation, 10 µl of the cell suspensions were spotted on agar plates containing ampicillin (100 $\mu g\ ml^{-1}$), kanamycin (50 $\mu g\ ml^{-1}$), IPTG (0.5 mM), and X-Gal (40 $\mu g\ ml^{-1}$) and incubated at 37°C for approximately 40 h. Blue colonies indicate potential protein-protein interactions. Empty vectors or vectors containing in frame fusions of the leucine zipper of GCN4 to the T18/T25 fragments were used as negative and positive controls, respectively. The plates were stored at 4°C protected from light for at least 4 days to increase contrast and intensity of the colony color.

Detergent Soluble Membrane and Detergent Resistant Membrane Isolation

Detergent resistant membrane and detergent soluble membrane fractions were separated as described previously by Salzer and Prohaska (2001) with modifications. To this end, the kit CelLytic^{TM} MEM Protein Extraction Kit from Sigma-Aldrich was used. Overnight cultures of strains YdjI-mCherry2 and FloT-PAmCherry were diluted (1:100) into 50 ml of LB medium and incubated at 37°C (200 rpm) until an $OD_{600\ nm}$ between 0.5 and

TABLE 2 | Strains used in this study.

Strain	Genotype	Reference/Source
Escherichia coli		
BTH101	*E. coli F-, cya-99, araD139, galE15, galK16, rpsL1 (str^R), hsdR2, mcrA1, mcrB1*	BACTH System Kit (Euromedex)
DH5α	*E. coli F–*Φ80lacZM15 *(lacZYAargF) U169 recA1 endA1 hsdR17(rk–, mk+) phoA supE44 thi-1 gyrA96 relA1*λ.	Invitrogen/Thermo Fisher
NEB Turbo	*F′ proA+ B+ lacIq*Δ *lacZ M15/fhuA2*Δ*(lac-proAB) glnV gal R(zgb210::Tn10)TetS endA1 thi-1*Δ*(hsdS-mcrB)5*	New England Biolabs
25 N F	NEB5α pKNT25-*pspA*	This work
25 N G	NEB5α pKNT25-*ydjG*	This work
25 N H	NEB5α pKNT25-*ydjH*	This work
25 N I	NEB5α pKNT25-*ydjI*	This work
25 C F	NEB5α pKT25-*pspA*	This work
25 C G	NEB5α pKT25-*ydjG*	This work
25 C H	NEB5α pKT25-*ydjH*	This work
25 C I	NEB5α pKT25-*ydjI*	This work
18 N F	NEB5α pUT18-*pspA*	This work
18 N G	NEB5α pUT18-*ydjG*	This work
18 N H	NEB5α pUT18-*ydjH*	This work
18 N I	NEB5α pUT18-*ydjI*	This work
18 C F	NEB5α pUT18C-*pspA*	This work
18 C G	NEB5α pUT18C-ydjG	This work
Bacillus subtilis		
ASB001	trpC2 *Bacillus subtilis*, wild type 168	Laboratory collection
ASB013	trpC2 pspA:pspA-GFP; ydjI:ydjI-mCherry (cat)	This work
ASB023	trpC2 floT::floT-mNeonGreen (spc)	This work
ASB033	trpC2 ydji::ydjI-mNeonGreen (cat)	This work
ASB044	trpC2 floT:: floT-PAmCherry (cat)	This work
ASB049	trpC2 ydjI::ydjI-mCherry2 (cat)	Lab collection
ASB053	trpC2 ydjI::kan	BGSC Knockout collection
ASB054	trpC2 ydjG::kan	BGSC Knockout collection
ASB055	trpC2 ydjH::kan	BGSC Knockout collection
ASB083	trpC2 pspA::kan	BGSC Knockout collection
ASB094	trpC2 mreB::kan amyE::spc Pxyl mrfpRuby-mreB	Zielinska et al., 2020
ASB122	trpC2 mreB::neo	Formstone and Errington, 2005
TSB2351	trpC2 pspA::pspA-GFP (C-term fusion) markerless	Thorsten Mascher/Annika Sprenger (Dresden)
ASB153	trpC2 ydji::ydjI-mNeonGreen cat; pspA::kan	This work (ASB083→ASB033)
ASB154	trpC2 ydjI:ydjI-mCherry2 (cat); floT::floT-mNeonGreen (spc)	This work (ASB023→ASB049)
ASB155	trpC2 ydji::ydjI-mNeonGreen cat; mreB::neo	This work (ASB033→ASB122)
ASB156	trpC2 pspA::pspA-GFP; ydjG::kan	This work (TSB2351→ASB054)
ASB157	trpC2 pspA::pspA-GFP; ydjH::kan	This work (TSB2351→ASB055)
ASB159	trpC2 ydji::ydjI-mNeonGreen cat; ydjG::kan	This work (ASB033→ASB054)
ASB160	trpC2 ydji::ydjI-mNeonGreen cat; ydjH::kan	This work (ASB033→ASB055)
ASB162	trpC2 pspA::pspA-GFP; ydjI::kan	This work (TSB2351→ASB053)
ASB166	trpC2 mreB::neo pspA::pspA-GFP	This work (ASB122→TSB2351)
ASB170	trpC2 pspA::pspA-GFP ydjI::kan amyE::ydjI	This work

Kan = kanamycin; Cat = chloramphenicol; Neo = neomycin; Spc = spectinomycin; Tet = tetracycline.

0.8 was reached. The cells were induced with 15 mM NaOH (final concentration) and incubated for an additional hour under the same conditions. The cells were washed in cold saline phosphate buffer containing 1 mM EDTA and concentrated to a final volume of 1.75 ml. 10 μl of the provided protease inhibitor cocktail was added and the cells were cracked with 7 cycles of sonication (30% amplitude, 0.5 s/pulse ON, 0.5 s/pulse OFF, 30 s total), waiting on ice between the runs. The cell debris was pelleted with a bench top centrifuge (18,000 × *g*, 10 min, 4°C) and 1 ml of the supernatant was transferred into ultracentrifugation tubes. Membranes were pelleted at 235,000 × *g* for 40 min at 4°C. The membrane pellet was resuspended in 600 μl lysis and separation buffer supplemented with protease inhibitor cocktail, and incubated for 10 min on ice. The suspension was centrifuged

TABLE 3 | Plasmids used in this study.

Name/Number	Genotype or Description	Reference/Source
pUT18C	P*lac*, T18 (AA 225 to 399 of ccaA), MCS, *bla*, Ori ColE1	Karimova et al., 1998
pUT18	P*lac*, MCS, T18 (AA 225 to 399 of ccaA), *bla*, Ori ColE1	Karimova et al., 1998
pUT18C-zip	P*lac*, T18 (AA 225 to 399 of ccaA)-leucine zipper of GCN4, MCS, *bla*, Ori ColE1	Karimova et al., 1998
pKNT25-zip	P*lac*, T25 (first 224 AA of ccaA)-leucine zipper of GCN4, MCS, *kan*, Ori p15A	Karimova et al., 1998
pKT25	P*lac*, T25 (first 224 AA of ccaA), MCS, *kan*, Ori p15A	Karimova et al., 1998
pKNT25	P*lac*, MCS T25 (first 224 AA of ccaA) *kan*, Ori p15A	Karimova et al., 1998
pUC18	*OriColE1* MCS CbR; *bla lacZ*	(Yanisch-Perron et al., 1985) Thermo Fisher Scientific
pUC18mut	pUC18 mutated MCS, *bla lacZ*	This work
pPAmCherry1-N1	Amplification of PAmCherry fragment	Subach et al., 2009
pNCS-mNeonGreen	Amplification of mNeonGreen fragment	Shaner et al., 2013
pJPR1-ydjI	*bla amyE3′ cat Pxyl ydjI amyE5′*	This work
pUC18mut-yuaGIN-PAmCherry-cat-yuaGDown	*bla floTIn-PAmCherry-cat-floTDown*	This work
25 N F	pKNT25-*pspA*	This work
25 N G	pKNT25-*ydjG*	This work
25 N H	pKNT25-*ydjH*	This work
25 N I	pKNT25-*ydjI*	This work
25 N F	pKNT25-*pspA*	This work
25 N G	pKNT25-*ydjG*	This work
25 N H	pKNT25-*ydjH*	This work
25 N I	pKNT25-*ydjI*	This work
18 N F	pUT18-*pspA*	This work
18 N G	pUT18-*ydjG*	This work
18 N H	pUT18-*ydjH*	This work
18 N I	pUT18-*ydjI*	This work
18 C F	pUT18C-*pspA*	This work
18 C G	pUT18C-*ydjG*	This work
18 C H	pUT18C-*ydjH*	This work
18 C I	pUT18C-*ydjI*	This work

for an additional 5 min (4°C, 18,000 × *g*). For the separation of the DSM and the DRM fraction the supernatant was heated at 30°C for 3–5 min. Both layers were separated at 3000 × g for 3 min (>20°C). Samples were taken from the upper hydrophilic phase (DSM) and from the lower hydrophilic phase (DRM) and used in Western-blot downstream analysis.

Sample Preparation and Western-Blot Analysis

Overnight cultures containing the appropriate antibiotic and/or supplements were diluted 1:100, incubated at 37°C and induced with 15 mM NaoH when an $OD_{600\ nm}$ between 0.5 and 0.8 was reached. Controls were monitored so that they did not exceed mid-log phase. After 1 h induction, cell densities were normalized, pelleted in a bench centrifuge (max. speed for 10 min, 4°C), and washed with PBS supplemented with 1 mM EDTA. Cell pellets were stored at −80°C for further use. For separation into cytosol and membrane cell pellets, the samples were resuspended in 500 µl of the same buffer (PBS + 1 mM EDTA), supplemented with protease inhibitor cocktail (Sigma Aldrich). The suspensions were homogenized (7 cycles of sonication at 30% amplitude, 0.5 s/pulse ON, 0.5 s/pulse OFF, 30 s total). The cell debris were pelleted in a bench centrifuge (18,000 × *g*, 10 min, 4°C) and 500 µl of the supernatant was transferred into ultracentrifuge tubes. Pellets were washed once and resuspended in same volume as before. Samples of cytosol and membrane were incubated for 20 min at room temperature with 4× SDS loading dye. Samples were subjected to SDS-PAGE through a 10 or 12 % gel and blotted onto a PVDF membrane (Bio-Rad) at 200 mA for 2 h and blocked overnight with 5% milk solution in buffer (50 mM Tris–HCl pH 7.5/150 mM NaCl) supplemented with or without Triton X 100 under slight agitation at 4°C. The blots were incubated with anti-α-mCherry (1:1000) or, anti-mNeonGreen (1:1000) antibodies and incubated at room temperature for at least 1 h with mild shaking. The blots were then washed five times with buffer and incubated with the corresponding secondary antibody (anti-rabbit IgG for α-mCherry and anti-α-GFP; anti-mouse IgG for anti-mNeonGreen) conjugated with the corresponding alkaline phosphatase (1:2000) or horse radish peroxidase conjugate (1:5000, Invitrogen). Immunoblots were again washed with buffer and developed with NBT/BCIP or Pierce™ ECL Western Blotting Substrate (Thermo Scientific) using the Chemi Hi Sensitivity program with signal accumulation of the ChemiDoc™ MP. For in-gel fluorescence of GFP

TABLE 4 | Oligonucleotides used in this study.

Name	Sequence	Restriction site
pUC18mut-F	TTTGGTCTCAGGTTCTCGCGGTATCATTGCAGC	*Bsa*I
pUC18mut-R	TTTGGTCTCAAACCACGCTCACCGGCTCCAG	*Bsa*I
pUC18BsaI-F	GTCGGTCTCAACTAGAATTCGTAATCATG	*Bsa*I
pUC18BsaI-R	CTCGGTCTCATCGGAAGCTTGGCACTGGC	*Bsa*I
pamCherry-F	AATGGTCTCTGGAGGGATGGTGAGCAAGGGCGAGGA	*Bsa*I
pamCherry-R	TTTGGTCTCGCGAATTACTTGTACAGCTC	*Bsa*I
mNeonGreen-F	AATGGTCTCTGGAGGGATGGTGAGCAAGGGCGAGGA	*Bsa*I
mNeonGreen-R	TTTGGTCTCGCGAATTACTTGTACAG CTC	*Bsa*I
mCherry2-F	AACCTCCGGTCTCCAATGGTCAGCAAGGGAGAG	*Bsa*I
mCherry2-R	AACCTCCGGTCTCCAGGATCCTGAGCCGCTTC	*Bsa*I
Cat-GG-F	GGAGGTCTCTTTCGGGCTTTAGATAAAAATTTAGGAGGC	*Bsa*I
Cat-GG-R	CACGGTCTCCCATTTTATAAAAGCCAGTC	*Bsa*I
Spc-GG-F	GGAGGTCTCTTTCGGGGTGAAAGGATGTACTTA	*Bsa*I
Spc-GG-R	CACGGTCTCCCATTTAATTGAGAGAAGTT	*Bsa*I
ydjI-GG-F	CCCTTTAATTATCCTCAAGAGG	*Bsa*I
ydjI-GG-R	TATGGTCTCCCTCCTACAAGCTTCTGGCC	*Bsa*I
*yuaG*IN-GG-F	CTAGGTCTCTCCGAGCCGATGCCAAGAAG	*Bsa*I
*yuaG*INGG-R	TATGGTCTCCCTCCCTCTGATTTTTGGAT	*Bsa*I
*yuaG*DownGG-F	ACGGGTCTCAAATGGGAAAGGGCAGAACCGTATGGT	
*yuaG*DownGG-R	CGGGGTCTCTTAGTTTTCAGGTGAATAGG	
pspA-F-*Bam*HI	AAAGGATCCAATGATGATAATTGGAAGATTTAAAGATATTATG	*Bam*HI
pspA-R-*Kpn*I-stop	AAAGGTACCTTACTTATCGAGCATCATTTTCG	*Kpn*I
pspA-R-*Kpn*I	AAAGGTACCTTATCGAGCATCATTTTCG	*Kpn*I
ydjG-F-*Bam*HI	AAAGGATCCAATGATAATATCTTATAAGTGTCCGAACTGC	*Bam*HI
ydjG-R-*Eco*RI-stop	AAAGAATTCTCAAAATCCGCCTCCCATC	*Eco*RI
ydjG-R-*Eco*RI	AAAGAATTCACAAATCCGCCTCCCATC	*Eco*RI
ydjH-F-*Bam*HI	AAAGGATCCAATGCGTGGATTTTTTGGG	Bam
ydjH-R-*Eco*RI-stop	AAAGAATTCTTAAAAACTGCCCCGGCTCC	*Eco*RI
ydjH-F-*Eco*RI	AAAGAATTCCCAAAACTGCCCCGGCTCC	*Eco*RI
ydjI-F-*Bam*HI	AAAGGATCCAATGTCGTTTTTCAGAAATCAATTAG	*Bam*HI
ydjI-R-*Kpn*I-stop	AAAGGTACCTTATACAAGCTTCTGGCCG	*Kpn*I
ydjI-R-*Kpn*I	AAAGGTACCGCTACAAGCTTCTGGCCGC	*Kpn*I
*Xba*I_RSB_ydjI_UP	GATTCTAGAATAGAGAAAGGGAGAG	*Xba*I
*Eag*I_Stop_ydjI_DOWN	ATCCGGCCGGTATGATTCTTATACAAGC	*Eag*I

fusion proteins, SDS-PAGE gels were rinsed in distilled water and subsequently subjected to Blue Epi illumination in the ChemiDoc^{TM} MP. Emission was detected by a 530/28 filter. For in-gel fluorescence of Δ*mreB pspA-GFP* cultures were sonicated and directly applied to acrylamide gel-electrophoresis. Fluorescence of GFP was visualized in gels using a Bio-Rad ChemiDoc imager.

Sample Preparation for Microscopy

Overnight cultures of the strains were inoculated 1:100 into LB medium with supplements if necessary and grown to $OD_{600\ nm}$ 0.5–0.8. To induce PspA promoter, alkaline shock condition (15 mM NaOH, final concentration) was added. Cells were washed and resuspended in medium supplemented, when appropriate, with Dil-C12 solution (2.5 μg ml^{-1}, final concentration) for staining of fluid membrane regions as described before (Strahl et al., 2014), or with HADA (Kuru et al., 2015), as a peptidoglycan synthesis machinery probe. Exponentially growing cells were immobilized on 1% agarose-pads (w/v) in the appropriate medium mounted onto microscope slides using Gene Frames (1.0 × 1.0 cm chamber, 0.25 mm thickness, from Thermo Scientific) as described before (de Jong et al., 2011). Samples were covered with high precision microscopy cover glasses (170 ± 5 μm, Paul Marienfeld GmbH & Co. KG, Germany) and directly taken for microscopic observations.

Fluorescence Microscopy

Standard fluorescence microscopy was carried out using an Axio Zeiss Imager M1 fluorescence microscope (EC Plan-Neofluar 100×/1.30 Oil Ph3 objective) equipped with an AxioCam HRm camera. For membrane fluidity experiments, a Delta Vision Elite microscope (Applied Precision, GE Healthcare) equipped with an Insight SSI Illumination, an X4 Laser module, a CoolSnap HQ CCD camera and a temperature-controlled chamber set up at 37°C was used. Laurdan images were taken with an

Olympus UplanSApo 100×/1.4 oil objective. Data processing was performed with SoftWoRx Suite 2.0 and FIJI Software's.

Laurdan Microscopy and Generalized Polarization Calculations

Laurdan (6-Dodecanoyl-N, N-dymethyl2-naphthylamine, Sigma-Aldrich) was used to detect the liquid ordering in the membrane, as described (Bach and Bramkamp, 2013), with modifications. Cells were grown in LB until late exponential phase. Laurdan, dissolved in dimethylformamide (DMF), was added at 10 μM final concentration and cells were incubated for 10 min in the dark at 37°C, 200 rpm. Cells were then washed twice in PBS buffer supplemented with 0.2% (w/v) glucose and 1% (w/v) DMF, and resuspended in fresh pre-warmed medium. Laurdan was excited at 360 ± 20 nm, and fluorescence emission was captured at 460 ± 25 nm (exposure time: 500 ms) and at 535 ± 25 nm (exposure time: 1 s) (Strahl et al., 2014). The image analysis including the generation of GP maps was carried out using FIJI Software (Schindelin et al., 2012) in combination with the macro tool CalculateGP designed by Norbert Vischer.[1] The overall GP values were measured for at least 100 individual cells from two biological replicates, after background subtraction.

DATA AVAILABILITY STATEMENT

The original contributions presented in the study are included in the article/**Supplementary Material**, further inquiries can be directed to the corresponding author/s.

[1] http://sils.fnwi.uva.nl/bcb/objectj/examples/CalculateGP/MD/gp.html

AUTHOR CONTRIBUTIONS

AS and SB performed the all experiments and fluorescence microscopy. AS, DW, and MB conceived the study, analyzed the data, and supervised the work. All authors wrote the manuscript.

FUNDING

AS receives a scholarship from Deutscher Akademischer Austauschdienst (Ph.D. fellowship DAAD-GSSP no. 91672248). MB acknowledges a grant by the Deutsche Forschungsgemeinschaft (BR2815/7-1). The authors acknowledge support of the Graduate School Life Science Munich (LSM) for AS.

ACKNOWLEDGMENTS

We thank Juri Bach, Laura Mark, and Nadine Albrecht (all LMU Munich) for help with the construction of strains. We thank Thomas Huber (LMU Munich) for the construction of the B2H plasmids. We also thank Annika Sprenger and Thorsten Mascher (LMU Munich/TU Dresden) for strain TSB2351. The plasmid PAmCherry1-N1 was a gift from Vladislav Verkhusha (Addgene plasmid # 31928; http://n2t.net/addgene:31928; RRID:Addgene_31928).

SUPPLEMENTARY MATERIAL

The Supplementary Material for this article can be found online at: https://www.frontiersin.org/articles/10.3389/fmicb.2021.754924/full#supplementary-material

REFERENCES

Adams, H., Teertstra, W., Demmers, J., Boesten, R., and Tommassen, J. (2003). Interactions between phage-shock proteins in *Escherichia coli*. *J. Bacteriol.* 185, 1174–1180. doi: 10.1128/jb.185.4.1174-1180.2003

Bach, J. N., and Bramkamp, M. (2013). Flotillins functionally organize the bacterial membrane. *Mol. Microbiol.* 88, 1205–1217. doi: 10.1111/mmi.12252

Bach, J. N., and Bramkamp, M. (2015). Dissecting the molecular properties of prokaryotic flotillins. *PLoS One* 10:e0116750. doi: 10.1371/journal.pone.0116750

Bramkamp, M., and Lopez, D. (2015). Exploring the existence of lipid rafts in bacteria. *Microbiol. Mol. Biol. Rev.* 79, 81–100. doi: 10.1128/mmbr.00036-14

Brissette, J. L., Weiner, L., Ripmaster, T. L., and Model, P. (1991). Characterization and sequence of the *Escherichia coli* stress-induced psp operon. *J. Mol. Biol.* 220, 35–48. doi: 10.1016/0022-2836(91)90379-k

Browman, D. T., Hoegg, M. B., and Robbins, S. M. (2007). The SPFH domain-containing proteins: more than lipid raft markers. *Trends Cell Biol.* 17, 394–402. doi: 10.1016/j.tcb.2007.06.005

Brown, D. A. (2006). Lipid rafts, detergent-resistant membranes, and raft targeting signals. *Physiology* 21, 430–439. doi: 10.1152/physiol.00032.2006

Burmann, F., Ebert, N., Van Baarle, S., and Bramkamp, M. (2011). A bacterial dynamin-like protein mediating nucleotide-independent membrane fusion. *Mol. Microbiol.* 79, 1294–1304. doi: 10.1111/j.1365-2958.2011.07523.x

Cao, M., Kobel, P. A., Morshedi, M. M., Wu, M. F., Paddon, C., and Helmann, J. D. (2002). Defining the *Bacillus subtilis* sigma(W) regulon: a comparative analysis of promoter consensus search, run-off transcription/macroarray analysis (ROMA), and transcriptional profiling approaches. *J. Mol. Biol.* 316, 443–457. doi: 10.1006/jmbi.2001.5372

Carballido-Lopez, R., Formstone, A., Li, Y., Ehrlich, S. D., Noirot, P., and Errington, J. (2006). Actin homolog MreBH governs cell morphogenesis by localization of the cell wall hydrolase LytE. *Dev. Cell* 11, 399–409. doi: 10.1016/j.devcel.2006.07.017

Claessen, D., Emmins, R., Hamoen, L. W., Daniel, R. A., Errington, J., and Edwards, D. H. (2008). Control of the cell elongation-division cycle by shuttling of PBP1 protein in *Bacillus subtilis*. *Mol. Microbiol.* 68, 1029–1046. doi: 10.1111/j.1365-2958.2008.06210.x

Cozy, L. M., Phillips, A. M., Calvo, R. A., Bate, A. R., Hsueh, Y. H., Bonneau, R., et al. (2012). SlrA/SinR/SlrR inhibits motility gene expression upstream of a hypersensitive and hysteretic switch at the level of sigma(D) in *Bacillus subtilis*. *Mol. Microbiol.* 83, 1210–1228. doi: 10.1111/j.1365-2958.2012.08003.x

de Jong, I. G., Beilharz, K., Kuipers, O. P., and Veening, J. W. (2011). Live Cell Imaging of *Bacillus subtilis* and Streptococcus pneumoniae using Automated Time-lapse Microscopy. *J. Vis. Exp*. 53:3145.

Dempwolff, F., and Graumann, P. L. (2014). Genetic links between bacterial dynamin and flotillin proteins. *Commun. Integr. Biol.* 7:e970972. doi: 10.4161/cib.29578

Dempwolff, F., Moller, H. M., and Graumann, P. L. (2012a). Synthetic motility and cell shape defects associated with deletions of flotillin/reggie paralogs in *Bacillus subtilis* and interplay of these proteins with NfeD proteins. *J. Bacteriol.* 194, 4652–4661. doi: 10.1128/jb.00910-12

Dempwolff, F., Wischhusen, H. M., Specht, M., and Graumann, P. L. (2012b). The deletion of bacterial dynamin and flotillin genes results in pleiotrophic effects on

cell division, cell growth and in cell shape maintenance. *BMC Microbiol.* 12:298. doi: 10.1186/1471-2180-12-298

Dempwolff, F., Schmidt, F. K., Hervas, A. B., Stroh, A., Rosch, T. C., Riese, C. N., et al. (2016). Super Resolution Fluorescence Microscopy and Tracking of Bacterial Flotillin (Reggie) Paralogs Provide Evidence for Defined-Sized Protein Microdomains within the Bacterial Membrane but Absence of Clusters Containing Detergent-Resistant Proteins. *PLoS Genet.* 12:e1006116. doi: 10.1371/journal.pgen.1006116

Dermine, J. F., Duclos, S., Garin, J., St-Louis, F., Rea, S., Parton, R. G., et al. (2001). Flotillin-1-enriched lipid raft domains accumulate on maturing phagosomes. *J. Biol. Chem.* 276, 18507–18512. doi: 10.1074/jbc.m101113200

Dominguez-Escobar, J., Wolf, D., Fritz, G., Hofler, C., Wedlich-Soldner, R., and Mascher, T. (2014). Subcellular localization, interactions and dynamics of the phage-shock protein-like Lia response in *Bacillus subtilis*. *Mol. Microbiol.* 92, 716–732. doi: 10.1111/mmi.12586

Donovan, C., and Bramkamp, M. (2009). Characterization and subcellular localization of a bacterial flotillin homologue. *Microbiology* 155, 1786–1799. doi: 10.1099/mic.0.025312-0

Engl, C., Jovanovic, G., Lloyd, L. J., Murray, H., Spitaler, M., Ying, L., et al. (2009). In vivo localizations of membrane stress controllers PspA and PspG in *Escherichia coli*. *Mol. Microbiol.* 73, 382–396. doi: 10.1111/j.1365-2958.2009.06776.x

Engler, C., Gruetzner, R., Kandzia, R., and Marillonnet, S. (2009). Golden gate shuffling: a one-pot DNA shuffling method based on type IIs restriction enzymes. *PLoS One* 4:e5553. doi: 10.1371/journal.pone.0005553

Formstone, A., and Errington, J. (2005). A magnesium-dependent mreB null mutant: implications for the role of mreB in *Bacillus subtilis*. *Mol. Microbiol.* 55, 1646–1657. doi: 10.1111/j.1365-2958.2005.04506.x

Greenlee, J. D., Subramanian, T., Liu, K., and King, M. R. (2021). Rafting Down the Metastatic Cascade: the Role of Lipid Rafts in Cancer Metastasis, Cell Death, and Clinical Outcomes. *Cancer Res.* 81, 5–17.

Gupta, T. K., Klumpe, S., Gries, K., Heinz, S., Wietrzynski, W., Ohnishi, N., et al. (2021). Structural basis for VIPP1 oligomerization and maintenance of thylakoid membrane integrity. *Cell* 184, 3643–3659.e23.

Harwood, C. R., and Cutting, S. M. (1990). *Molecular biological methods for Bacillus*. Hoboken: John Wiley & Sons Ltd.

Hinderhofer, M., Walker, C. A., Friemel, A., Stuermer, C. A., Moller, H. M., and Reuter, A. (2009). Evolution of prokaryotic SPFH proteins. *BMC Evol. Biol.* 9:10. doi: 10.1186/1471-2148-9-10

Huang, X., Fredrick, K. L., and Helmann, J. D. (1998). Promoter recognition by *Bacillus subtilis* sigmaW: autoregulation and partial overlap with the sigmaX regulon. *J. Bacteriol.* 180, 3765–3770. doi: 10.1128/jb.180.15.3765-3770.1998

Jacobson, K., Mouritsen, O. G., and Anderson, R. G. (2007). Lipid rafts: at a crossroad between cell biology and physics. *Nat. Cell Biol.* 9, 7–14. doi: 10.1038/ncb0107-7

Jovanovic, G., Engl, C., Mayhew, A. J., Burrows, P. C., and Buck, M. (2010). Properties of the phage-shock-protein (Psp) regulatory complex that govern signal transduction and induction of the Psp response in *Escherichia coli*. *Microbiology* 156, 2920–2932. doi: 10.1099/mic.0.040055-0

Jovanovic, G., Mehta, P., Ying, L., and Buck, M. (2014). Anionic lipids and the cytoskeletal proteins MreB and RodZ define the spatio-temporal distribution and function of membrane stress controller PspA in *Escherichia coli*. *Microbiology* 160, 2374–2386. doi: 10.1099/mic.0.078527-0

Junglas, B., Huber, S. T., Heidler, T., Schlosser, L., Mann, D., Hennig, R., et al. (2021). PspA adopts an ESCRT-III-like fold and remodels bacterial membranes. *Cell* 184, 3674–3688.e18.

Junglas, B., Orru, R., Axt, A., Siebenaller, C., Steinchen, W., Heidrich, J., et al. (2020a). IM30 IDPs form a membrane-protective carpet upon super-complex disassembly. *Commun. Biol.* 3:595.

Junglas, B., Siebenaller, C., Schlosser, L., Hellmann, N., and Schneider, D. (2020b). GTP hydrolysis by Synechocystis IM30 does not decisively affect its membrane remodeling activity. *Sci. Rep.* 10:9793.

Karimova, G., Pidoux, J., Ullmann, A., and Ladant, D. (1998). A bacterial two-hybrid system based on a reconstituted signal transduction pathway. *Proc. Natl. Acad. Sci. U. S. A.* 95, 5752–5756. doi: 10.1073/pnas.95.10.5752

Kingston, A. W., Liao, X., and Helmann, J. D. (2013). Contributions of the sigma(W), sigma(M) and sigma(X) regulons to the lantibiotic resistome of *Bacillus subtilis*. *Mol. Microbiol.* 90, 502–518.

Kleerebezem, M., Crielaard, W., and Tommassen, J. (1996). Involvement of stress protein PspA (phage shock protein A) of *Escherichia coli* in maintenance of the protonmotive force under stress conditions. *EMBO J.* 15, 162–171. doi: 10.1002/j.1460-2075.1996.tb00344.x

Kobayashi, R., Suzuki, T., and Yoshida, M. (2007). *Escherichia coli* phage-shock protein A (PspA) binds to membrane phospholipids and repairs proton leakage of the damaged membranes. *Mol. Microbiol.* 66, 100–109. doi: 10.1111/j.1365-2958.2007.05893.x

Kuru, E., Tekkam, S., Hall, E., Brun, Y. V., and Van Nieuwenhze, M. S. (2015). Synthesis of fluorescent D-amino acids and their use for probing peptidoglycan synthesis and bacterial growth in situ. *Nat. Protoc.* 10, 33–52.

Langhorst, M. F., Reuter, A., and Stuermer, C. A. (2005). Scaffolding microdomains and beyond: the function of reggie/flotillin proteins. *Cell. Mol. Life Sci.* 62, 2228–2240. doi: 10.1007/s00018-005-5166-4

Lee, Y. H., Kingston, A. W., and Helmann, J. D. (2012). Glutamate dehydrogenase affects resistance to cell wall antibiotics in *Bacillus subtilis*. *J. Bacteriol.* 194, 993–1001. doi: 10.1128/jb.06547-11

Liu, J., Tassinari, M., Souza, D. P., Naskar, S., Noel, J. K., Bohuszewicz, O., et al. (2021). Bacterial Vipp1 and PspA are members of the ancient ESCRT-III membrane-remodeling superfamily. *Cell* 184, 3660–3673.e18.

Lopez, D., and Kolter, R. (2010). Functional microdomains in bacterial membranes. *Genes Dev.* 24, 1893–1902. doi: 10.1101/gad.1945010

Manganelli, R., and Gennaro, M. L. (2017). Protecting from Envelope Stress: variations on the Phage-Shock-Protein Theme. *Trends Microbiol.* 25, 205–216. doi: 10.1016/j.tim.2016.10.001

Maxson, M. E., and Darwin, A. J. (2006). PspB and PspC of Yersinia enterocolitica are dual function proteins: regulators and effectors of the phage-shock-protein response. *Mol. Microbiol.* 59, 1610–1623. doi: 10.1111/j.1365-2958.2006.05047.x

McCullough, J., Clippinger, A. K., Talledge, N., Skowyra, M. L., Saunders, M. G., Naismith, T. V., et al. (2015). Structure and membrane remodeling activity of ESCRT-III helical polymers. *Science* 350, 1548–1551. doi: 10.1126/science.aad8305

McDonald, C., Jovanovic, G., Ces, O., and Buck, M. (2015). Membrane Stored Curvature Elastic Stress Modulates Recruitment of Maintenance Proteins PspA and Vipp1. *mBio* 6, e01188–15.

Mielich-Suss, B., and Lopez, D. (2015). Molecular mechanisms involved in *Bacillus subtilis* biofilm formation. *Environ. Microbiol.* 17, 555–565. doi: 10.1111/1462-2920.12527

Mielich-Suss, B., Schneider, J., and Lopez, D. (2013). Overproduction of flotillin influences cell differentiation and shape in *Bacillus subtilis*. *mBio* 4, e00719–13.

Nickels, J. D., Chatterjee, S., Stanley, C. B., Qian, S., Cheng, X., and Myles, D. A. A. (2017). The in vivo structure of biological membranes and evidence for lipid domains. *PLoS Biol.* 15:e2002214. doi: 10.1371/journal.pbio.2002214

Owen, D. M., and Gaus, K. (2013). Imaging lipid domains in cell membranes: the advent of super-resolution fluorescence microscopy. *Front. Plant Sci.* 4:503. doi: 10.3389/fpls.2013.00503

Petersohn, A., Brigulla, M., Haas, S., Hoheisel, J. D., Volker, U., and Hecker, M. (2001). Global analysis of the general stress response of *Bacillus subtilis*. *J. Bacteriol.* 183, 5617–5631. doi: 10.1128/jb.183.19.5617-5631.2001

Popp, P. F., Benjdia, A., Strahl, H., Berteau, O., and Mascher, T. (2020). The Epipeptide YydF Intrinsically Triggers the Cell Envelope Stress Response of Bacillus subtilis and Causes Severe Membrane Perturbations. *Front. Microbiol.* 11:151. doi: 10.3389/fmicb.2020.00151

Popp, P. F., Gumerov, V. M., Andrianova, E. P., Bewersdorf, L., Mascher, T., Zhulin, I. B., et al. (2021). Phyletic distribution and diversification of the Phage Shock Protein stress response system in bacteria and archaea. *bioRxiv* [preprint]. doi: 10.1101/2021.02.15.431232

Ravi, J., Anantharaman, V., Chen, S. Z., Datta, P., Aravind, L., and Gennaro, M. L. (2021). The Phage-shock-protein (PSP) Envelope Stress Response: discovery of Novel Partners and Evolutionary History. *BioRxiv* [preprint]. doi: 10.1101/2020.09.24.301986

Rivera-Milla, E., Stuermer, C. A., and Malaga-Trillo, E. (2006). Ancient origin of reggie (flotillin), reggie-like, and other lipid-raft proteins: convergent evolution of the SPFH domain. *Cell. Mol. Life Sci.* 63, 343–357. doi: 10.1007/s00018-005-5434-3

Salzer, U., and Prohaska, R. (2001). Stomatin, flotillin-1, and flotillin-2 are major integral proteins of erythrocyte lipid rafts. *Blood* 97, 1141–1143.

Sawant, P., Eissenberger, K., Karier, L., Mascher, T., and Bramkamp, M. (2016). A dynamin-like protein involved in bacterial cell membrane surveillance under environmental stress. *Environ. Microbiol.* 18, 2705–2720. doi: 10.1111/1462-2920.13110

Schindelin, J., Arganda-Carreras, I., Frise, E., Kaynig, V., Longair, M., Pietzsch, T., et al. (2012). Fiji: an open-source platform for biological-image analysis. *Nat. Methods* 9, 676–682. doi: 10.1038/nmeth.2019

Shaner, N. C., Lambert, G. G., Chammas, A., Ni, Y., Cranfill, P. J., Baird, M. A., et al. (2013). A bright monomeric green fluorescent protein derived from *Branchiostoma lanceolatum*. *Nat. Methods* 10, 407–409. doi: 10.1038/nmeth.2413

Simons, K., and Ikonen, E. (1997). Functional rafts in cell membranes. *Nature* 387, 569–572. doi: 10.1038/42408

Strahl, H., Burmann, F., and Hamoen, L. W. (2014). The actin homologue MreB organizes the bacterial cell membrane. *Nat. Commun.* 5:3442.

Stuermer, C. A., and Plattner, H. (2005). The 'lipid raft' microdomain proteins reggie-1 and reggie-2 (flotillins) are scaffolds for protein interaction and signalling. *Biochem. Soc. Symp.* 72, 109–118. doi: 10.1042/bss0720109

Subach, F. V., Patterson, G. H., Manley, S., Gillette, J. M., Lippincott-Schwartz, J., and Verkhusha, V. V. (2009). Photoactivatable mCherry for high-resolution two-color fluorescence microscopy. *Nat. Methods* 6, 153–159. doi: 10.1038/nmeth.1298

Tavernarakis, N., Driscoll, M., and Kyrpides, N. C. (1999). The SPFH domain: implicated in regulating targeted protein turnover in stomatins and other membrane-associated proteins. *Trends Biochem. Sci.* 24, 425–427. doi: 10.1016/s0968-0004(99)01467-x

Wiegert, T., Homuth, G., Versteeg, S., and Schumann, W. (2001). Alkaline shock induces the *Bacillus subtilis* sigma(W) regulon. *Mol. Microbiol.* 41, 59–71. doi: 10.1046/j.1365-2958.2001.02489.x

Willdigg, J. R., and Helmann, J. D. (2021). Mini Review: bacterial Membrane Composition and Its Modulation in Response to Stress. *Front. Mol. Biosci.* 8:634438. doi: 10.3389/fmolb.2021.634438

Wolf, D., Kalamorz, F., Wecke, T., Juszczak, A., Mader, U., Homuth, G., et al. (2010). In-depth profiling of the LiaR response of *Bacillus subtilis*. *J. Bacteriol.* 192, 4680–4693. doi: 10.1128/jb.00543-10

Yanisch-Perron, C., Vieira, J., and Messing, J. (1985). Improved M13 phage cloning vectors and host strains: nucleotide sequences of the M13mp18 and pUC19 vectors. *Gene* 33, 103–119. doi: 10.1016/0378-1119(85)90120-9

Yokoyama, H., and Matsui, I. (2020). The lipid raft markers stomatin, prohibitin, flotillin, and HflK/C (SPFH)-domain proteins form an operon with NfeD proteins and function with apolar polyisoprenoid lipids. *Crit. Rev. Microbiol.* 46, 38–48. doi: 10.1080/1040841x.2020.1716682

Yuan, C., Furlong, J., Burgos, P., and Johnston, L. J. (2002). The size of lipid rafts: an atomic force microscopy study of ganglioside GM1 domains in sphingomyelin/DOPC/cholesterol membranes. *Biophys. J.* 82, 2526–2535. doi: 10.1016/s0006-3495(02)75596-3

Zielinska, A., Savietto, A., De Sousa Borges, A., Martinez, D., Berbon, M., Roelofsen, J. R., et al. (2020). Flotillin-mediated membrane fluidity controls peptidoglycan synthesis and MreB movement. *Elife* 9:e57179.

Conflict of Interest: The authors declare that the research was conducted in the absence of any commercial or financial relationships that could be construed as a potential conflict of interest.

Publisher's Note: All claims expressed in this article are solely those of the authors and do not necessarily represent those of their affiliated organizations, or those of the publisher, the editors and the reviewers. Any product that may be evaluated in this article, or claim that may be made by its manufacturer, is not guaranteed or endorsed by the publisher.

Supplemental Material

An SPFH-domain protein required to link the phage-shock protein to the membrane in Bacillus subtilis

Abigail Savietto Scholz[1,2], Sarah Baur[1], Diana Wolf[3], Marc Bramkamp[1, 2*]

[1]Institute for General Microbiology, Christian-Albrechts-University of Kiel, Germany;

[2] Faculty of Biology, Ludwig-Maximilians-Universität München, Germany;

[3]Institute of Microbiology, Technische Universität Dresden, Germany.

**Correspondence:* Marc Bramkamp, Institute for General Microbiology, Christian-Albrechts-University, Germany. E-mail: bramkamp@ifam.uni-kiel.de

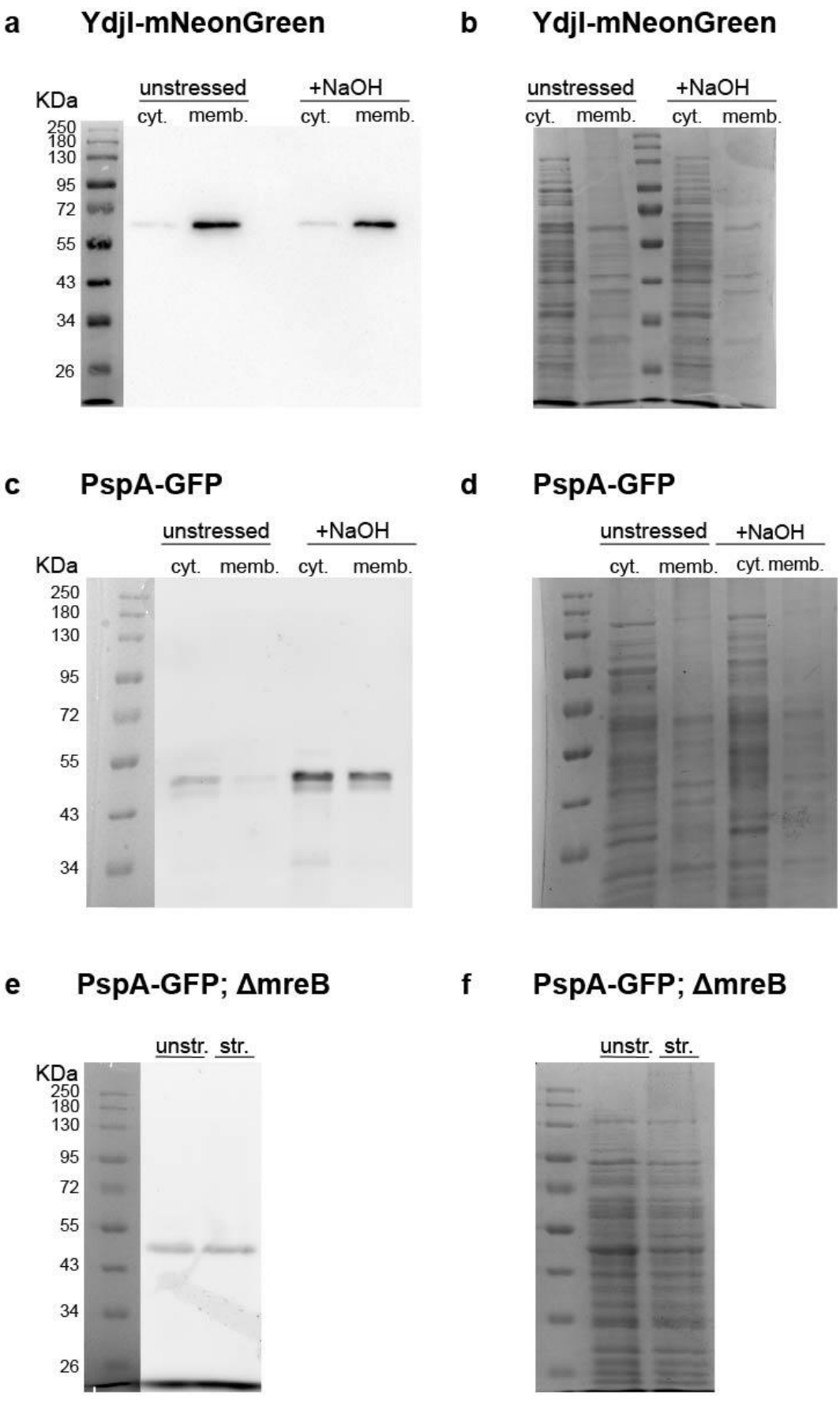
a
YdjI-mNeonGreen
KDa
unstressed
+NaOH
cyt.
memb.
cyt.
memb.
250
180
130
95
72
55
43
34
26
b
YdjI-mNeonGreen
unstressed
+NaOH
cyt.
memb.
cyt.
memb.
c
PspA-GFP
KDa
unstressed
+NaOH
cyt.
memb.
cyt.
memb.
250
180
130
95
72
55
43
34
d
PspA-GFP
unstressed
+NaOH
cyt.
memb.
cyt.
memb.
e
PspA-GFP; ΔmreB
KDa
unstr.
str.
250
180
130
95
72
55
43
34
26
f
PspA-GFP; ΔmreB
unstr.
str.

Figure S1. (A) Western-blot of strain YdjI-mNeonGreen (ASB033) showing cytosolic and membrane fractions under unstressed or stressed conditions (15mM NaOH). Blot was developed with HRP and excited for 90 seconds for visualization. **(B)** Coomassie staining of the corresponding SDS-PAGE gel blotted in A, as loading control. **(C)** In-gel fluorescence of SDS-PAGE containing cytosolic and membrane fractions of PspA-GFP (TSB2351), with and without stress condition (15 mM NaOH); Ex/Em: 488 nm / 526 nm. **(D)** Coomassie staining of the corresponding SDS-PAGE shown in C as loading controls. **(E)** In-gel fluorescence Δ*mreB pspA-gfp* grown with and without stress); Ex/Em: 488 nm / 526 nm. **(F)** Coomassie staining of the corresponding SDS-PAGE shown in E as loading controls.

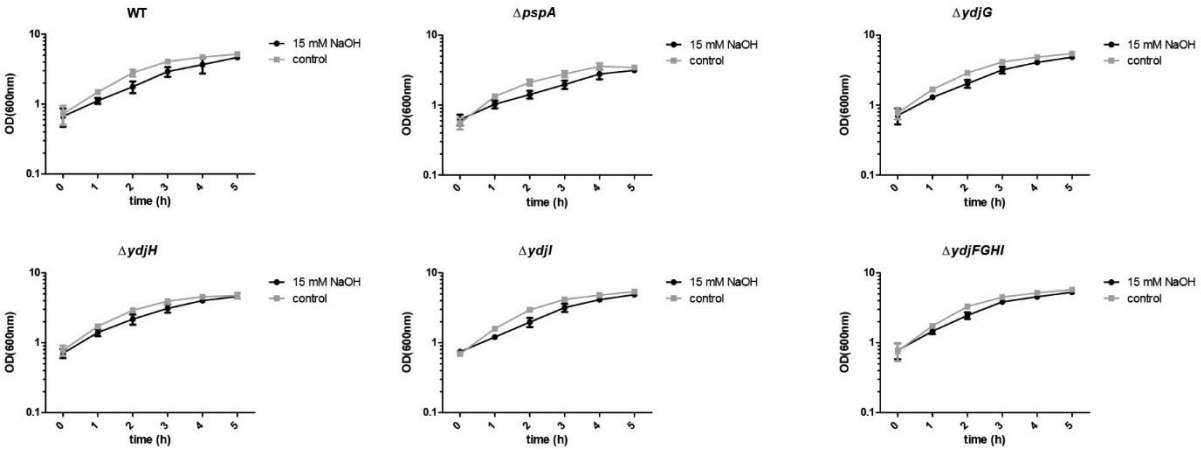

Figure S2. Growth curves of all mutant strains of proteins encoded *pspA-ydjGHI* operon in unstressed or alkali stress (15 mM NaOH) conditions. Error bars represent standard deviation of three independent biological replicates. No significant difference was found between the strains within the treatment and control groups ($p > 0.01$, Mann-Whitney Test).

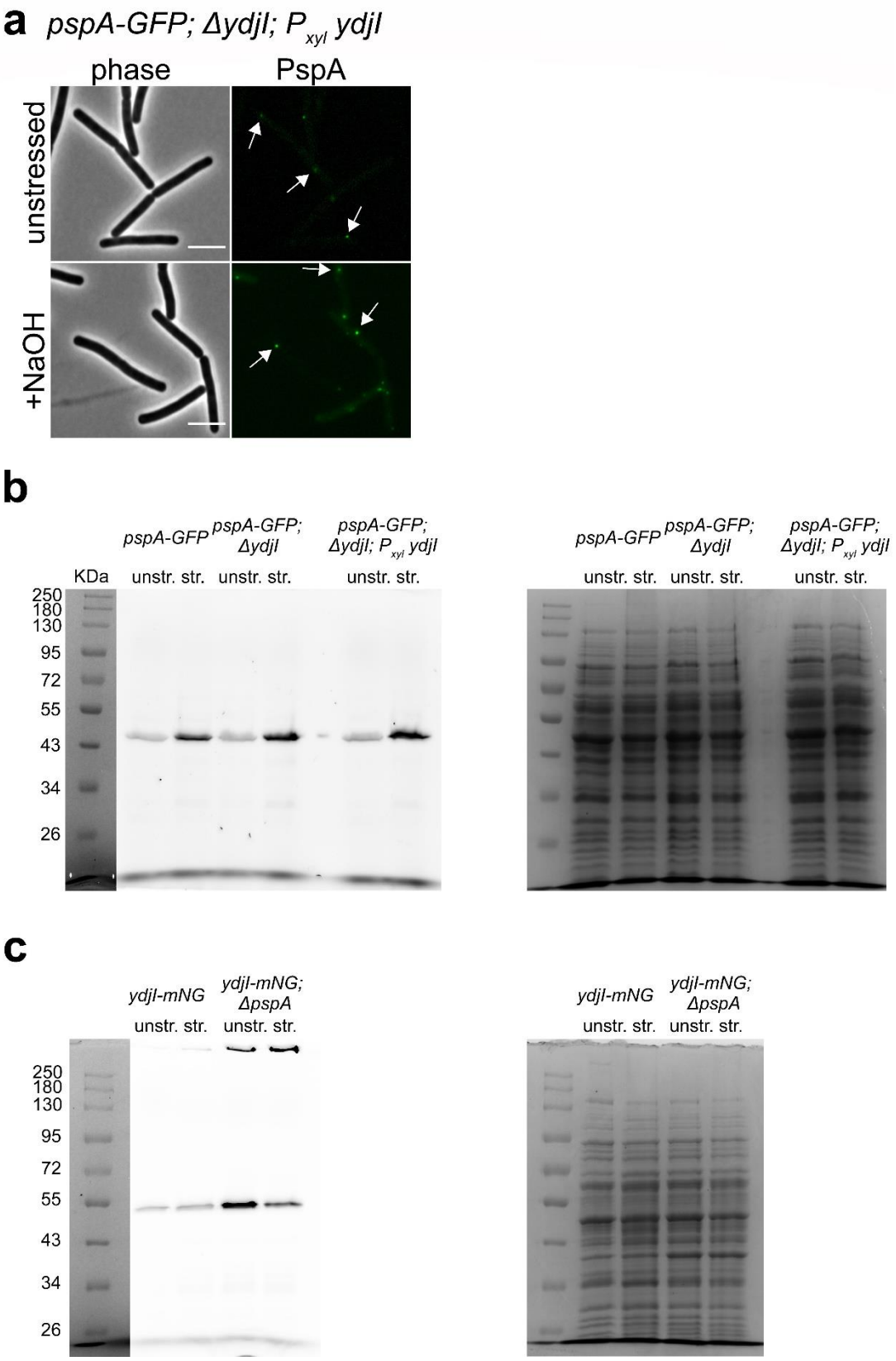
a
pspA-GFP; ΔydjI; P xyl ydjI
phase
PspA
unstressed
+NaOH
b
pspA-GFP
pspA-GFP; ΔydjI
pspA-GFP; ΔydjI; P xyl ydjI
KDa
unstr. str. unstr. str. unstr. str.
250
180
130
95
72
55
43
34
26
pspA-GFP
pspA-GFP; ΔydjI
pspA-GFP; ΔydjI; P xyl ydjI
unstr. str. unstr. str. unstr. str.
c
ydjI-mNG
ydjI-mNG; ΔpspA
unstr. str. unstr. str.
250
180
130
95
72
55
43
34
26
ydjI-mNG
ydjI-mNG; ΔpspA
unstr. str. unstr. str.

Figure S3. (A) Complementation of YdjI-mediated PspA focus formation. A *ydjI* deletion is complemented with an ectopic expression of *ydjI* from a xylose inducible promoter in a strain expressing *pspA-GFP* (strain ASB167). Cells were grown in BHI without additional xylose. This was sufficient for basal expression of the ectopic *ydjI*. Under these conditions PspA focus formation is readily complemented. Arrows point to PspA foci. Scale bars: 4 µm. **(B)** In gel fluorescence analysis of strain TSB2351 expressing *pspA*-GFP, *pspA*-GFP Δ*ydjI* (ASB162), and *pspA*-GFP Δ*ydjI* P_{xyl}-*ydjI* (ASB167) under unstressed or stressed conditions (15mM NaOH). A coomassie stained gel of the corresponding SDS-PAGE is shown as loading control. **(C)** In gel fluorescence analysis of strain ASB033 (*ydjI*-mNeonGreen) and strain ASB153 (*ydjI*-mNeonGreen Δ*pspA).* Note that in the strain deleted for *pspA* (ASB153) the expression of *ydjI* is upregulated. This is likely due to the loss of the Rho-independent terminator between the *pspA* and the *ydjG* genes. YdjI oligomers were observed in particular under stress conditions, as indicated by the blot signal at the top of the gel. These are apparently large protein complexes that are not denatured and do not enter the separating gel. A coomassie stained gel of the corresponding SDS-PAGE is shown as loading control.

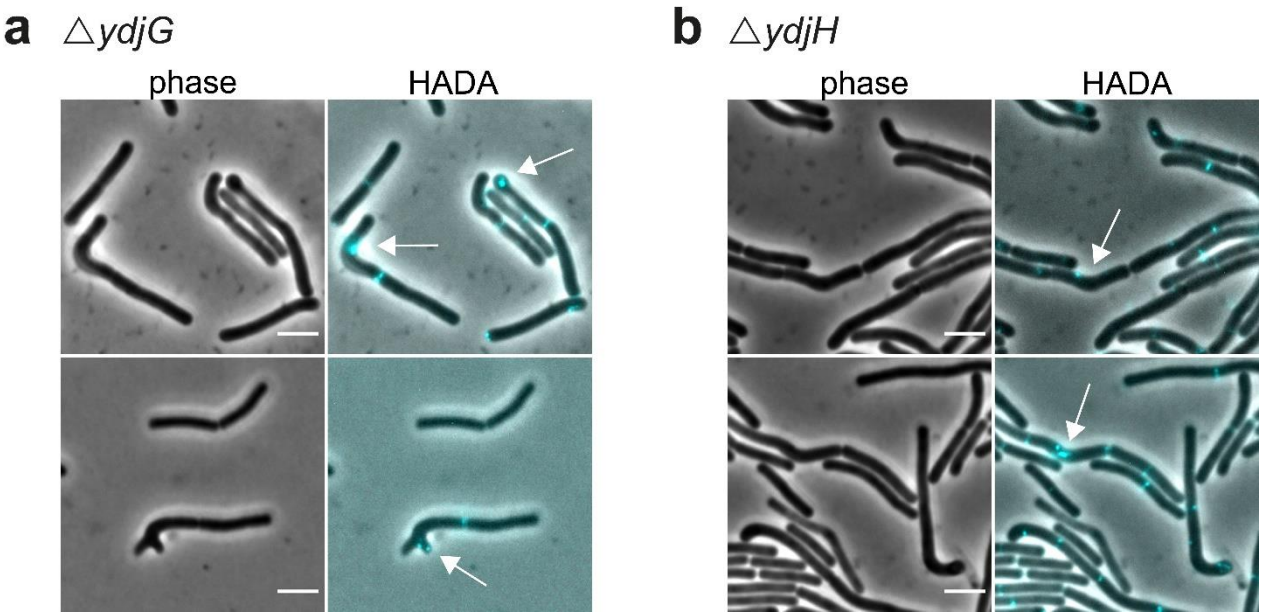

Figure S4. Peptidoglycan synthesis machinery is delocalized upon deletion of *ydjG* and *ydjH*. (A, B) Mutant YdjG (ASB054) and YdjH (ABS055) strains were grown in LB including 15 mM NaOH and stained with HADA as a peptidoglycan synthesis machinery probe. Exemplary images are shown in both panels. Arrows indicate miss-localization of peptidoglycan machinery and membrane cytoskeleton associated phenotype. Note that the phenotype in the *ydjG* mutant is more pronounced, indicating a stronger interaction of YdjG with cell-shape controlling machinery. Scale bars: 3 µm.

Supplemental Material Movies

Still images of cells shown in supplementary movies S1-8 are shown below. Cells were grown in LB medium and alkaline shock was induced by addition of 15 mM NaOH. Strains mutated in *mreB* were grown in LB supplemented with 25 mM $MgCl_2$ and 0.3 M sucrose to maintain rod-shaped morphology. For time lapse movies cells were mounted on agar pads with the indicated media and images were taken every 30 second for 5 minutes in total. Insets show the corresponding phase contrast image. Scale bar is always 2 µm.

Movie S1.

YdjI-mNeonGreen (unstressed):

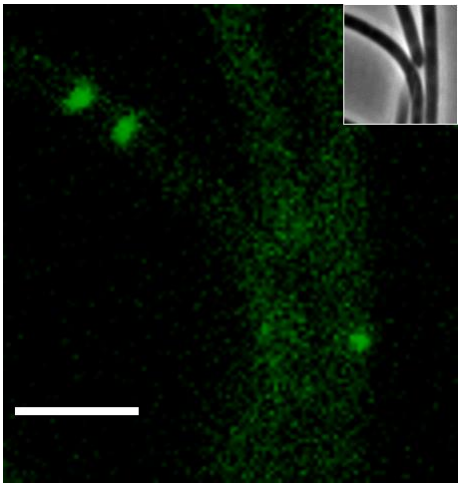

Movie S2

YdjI-mNeonGreen (NaOH):

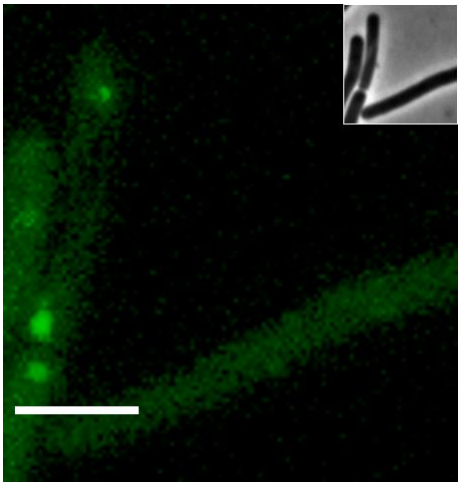

Movie S3

YdjI-mNeonGreen; Δ*mreB* (unstressed):

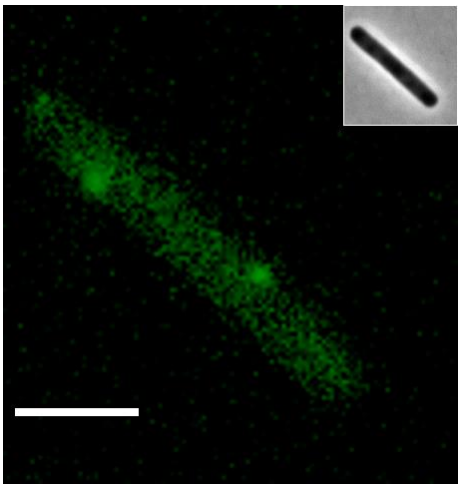

Movie S4

YdjI-mNeonGreen; Δ*mreB* (NaOH):

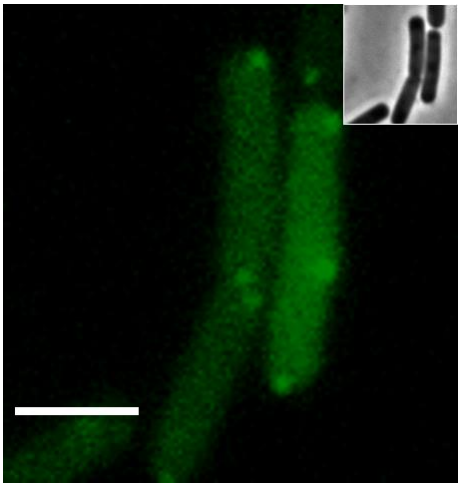

Movie S5

PspA-GFP (unstressed):

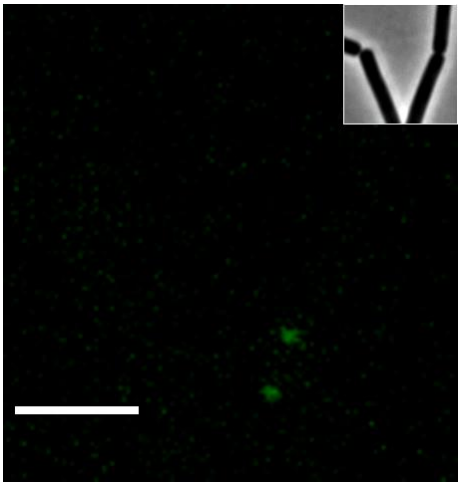

Movie S6

PspA-GFP (NaOH):

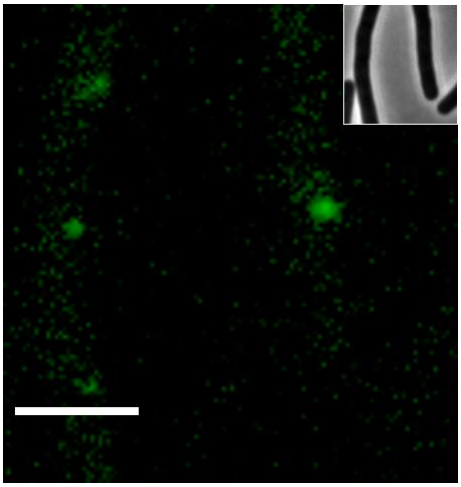

Movie S7

PspA-GFP; Δ*mreB* (unstressed):

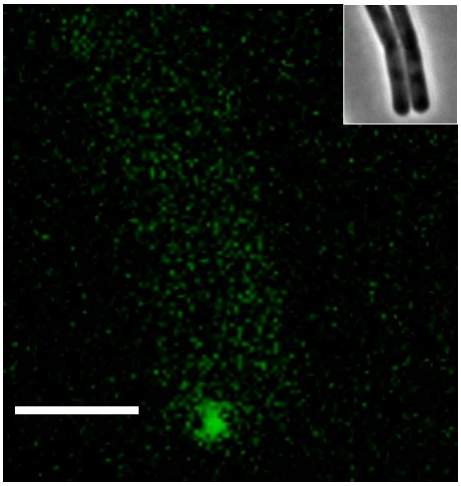

Movie S8

PspA-GFP; Δ*mreB* (NaOH):

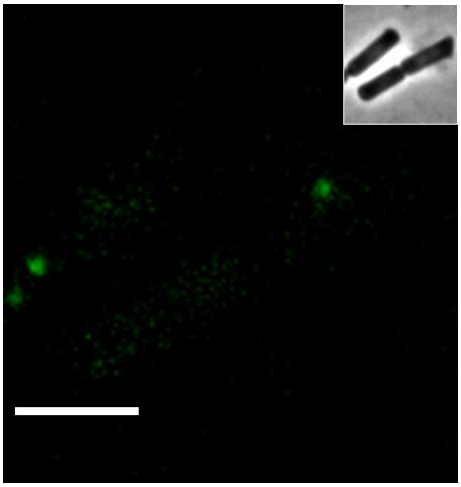

3. CONCLUDING DISCUSSION

The current understanding of bacterial SPFH-domain proteins and their roles in bacterial physiology is rapidly evolving. The commonly accepted hypothesis is that bacterial SPFH-domain proteins exist in liquid-ordered membrane domains and serve primarily as scaffolding proteins, allowing spatial and temporal membrane compartmentalization. It is thought that they have functions in the formation of the so-called functional membrane microdomains (FMM) which are defined as bacterial membrane platforms that resemble lipid rafts of eukaryotic cells in certain functional and structural aspects.

Here, we addressed the discrepancy between the implications of SPFH domain proteins as lipid raft organizers, the apparent limitations of this hypothesis and highlighted the advancements of our knowledge regarding other functions of SPFH-domain proteins found by this study. More specifically, we found that the bacterial SPFH-domain proteins from *B. subtilis* are important for the correct maintenance of membrane fluidity, which in turn affects important cellular features such as cell shape maintenance and MreB movement. This allowed us to attribute a function of bacterial SPFH-domain proteins towards membrane adaptation responsive to environmental changes and thus expand our knowledge about SPFH-domain proteins in bacteria. Furthermore, a third SPFH-domain protein, which contrary to the common knowledge does not reside in the expected Lo membrane region where usually other SPFH-domain proteins are found, was characterized here. This puts into question the current established knowledge regarding bacterial flotillins functioning as scaffolding proteins.

3.1 The limitations of the lipid raft model

Numerous studies on lipid biophysics, lipid sorting, and the effects of detergents on biological bilayers have led to the proposition of a specific type of membrane microdomain enriched in cholesterol and sphingolipids, later termed "lipid rafts." Considerable research has been conducted on the functional assumptions, localization, and associations of lipid rafts with proteins. This model has generally been embraced as a valuable framework for understanding cellular membrane organization. Nevertheless,

uncertainties persist regarding the existence of lipid rafts, and the model is not without its limitations and controversies.

One of the primary concerns lies in the lack of direct experimental evidence that firmly supports the existence of lipid rafts as distinct and stable entities in the plasma membrane. The most commonly used approaches to detect and isolate rafts are indirect, thereby subjected to various interpretations, particularly with regard to their resistance to solubilization by nonionic detergents and sensitivity to cholesterol depletion. Many studies on lipid biophysics, lipid sorting and effects of detergents on biological bilayers brought the argumentation for the existence of a particular type of membrane microdomain enriched in cholesterol and sphingolipids, later called and defined as “lipid rafts” (Pizzo *et al.*, 2002; Heerklotz, 2002; Edidin, 2003). Secondly, lipid rafts were demonstrated to be highly heterogenous in composition and properties, varying greatly depending on the cell type and isolation conditions. Furthermore, rafts have been difficult to be observed in living cells, and when evidence for their visualization emerged, their appearance was not always consistent (Anderson and Jacobson, 2002; Kenworthy, 2002), making it difficult to outline a universal definition of what constitutes a lipid raft. Third, the controversy over function is very obvious, with studies attributing to lipid rafts a wide range of roles in essential biological processes, from numerous signal transduction pathways, to cell adhesion, migration, synaptic transmission, Alzheimer amyloid formation, cytoskeleton organization, protein sorting, apoptosis, as well as a cellular entry point for toxins, bacteria and viruses (Naslavsky *et al.*, 1997; Brown and London, 1998; Simons and Toomre, 2000; Kovbasnjuk *et al.*, 2001; Harris and Siu, 2002; Simons and Ehehalt, 2002; Ehehalt *et al.*, 2003); while lipid rafts are believed to play roles in important cellular functions, the exact mechanism by which they function are not well understood and more research is needed to fully comprehend mechanistically their role in cell biology. Forth, the lipid raft model is relatively simple, considered a top-down view of membrane organization that does not fully capture the complex and dynamic nature of the plasma membrane.

In regards to their composition and isolation, the lipid rafts are thought to harbor lipids resistant to solubilization with nonionic detergents (as Triton X-100) and have therefore been associated with DRM (detergent-

resistant membrane) fractions that can be separated from soluble membrane isolates upon cold detergent treatment and centrifugation. It was implied that the Triton-resistant fraction is enriched in cholesterol and sphingolipids, and that GPI (glycosylphosphatidylinositol)-anchored proteins were described to acquire resistance to Triton as they move through the secretory pathway (Brown and Rose, 1992b). Therefore, it was suggested that these resistant components would together represent raft domains, implying that this extraction method allows for the detection of liquid-ordered phase (*Lo*) constituents *in vivo* (Schroeder *et al.*, 1994; Schroeder *et al.*, 1998). However, there are several reasons not to conclude that the detergent resistance indicates the presence of a protein in a microdomain prior to the addition of Triton X-100. Mechanistically, detergent solubilization involves the partitioning of individual detergent molecules into the lipid bilayer until they reach a particular threshold necessary to induce the formation of holes/pores, before micellar fragments are formed (Maire *et al.*, 2000). During this process, the lower temperature could cause alone nonphysiological rearrangements in the lipid bilayer, altering the organization of its components. As a result, structures from the original membrane, particularly proteins of interest, could be extracted from the resulting structures depending on their physical properties, rather than their lateral distribution in the living cell.

The detergent solubilization approach instead of arise results from differences in the detergent sensitivity of coexisting domains could be, for instance, due to differences in the detergent sensitivity of the two leaflets (Schroeder *et al.*, 1994; Schroeder *et al.*, 1998; Heerklotz, 2002; Prior *et al.*, 2003). Finally, detergent treatment has long been demonstrated to promote the formation of ordered domains in model bilayers, inducing segregation of components of the bilayer by reducing the already low levels of sphingolipids and cholesterol in the *Ld* phase. Studies on the mechanism of action of Triton conclude that the detergent-resistant membranes "*should not be assumed to resemble biological rafts in size, structure, composition or even existence*" (Heerklotz, 2002). This certainly does not disprove the lipid raft model; instead, it demonstrates that the content of detergent-resistant membranes cannot be considered to accurately reflect or support the existence of rafts. The DRM isolation method is, however, an useful tool for isolation of candidate proteins, but not without the need of further assays

to investigate potential protein-protein or protein-lipid interactions such as direct imaging or functional analysis of knockouts, i.e. (Tanaka *et al.*, 2004; Staneva *et al.*, 2005).

Proteins isolated in the insoluble fraction of Triton X-100, floating after sucrose centrifugation were termed flotillins (Bickel *et al.*, 1997). Some studies on the proteome of DRM fractions indicated that these membrane fractions were rich in proteins containing the PHB (prohibitin) domain, which are part of the SPFH protein family, including the flotillin proteins (Langhorst *et al.*, 2005; Browman *et al.*, 2007a; Donovan and Bramkamp, 2009; López and Kolter, 2010; Bach and Bramkamp, 2013; Bach and Bramkamp, 2015; Willdigg and Helmann, 2021). In a similar manner to eukaryotic membranes, bacterial membranes can also be fractionated yielding to DRM fractions, and several bacteria were found to encode flotillin-like proteins. Later on, bacterial flotillins have been associated with roles on formation of functional membrane microdomains (FMM) (Morrow and Parton, 2005; Zhao *et al.*, 2011; Mielich-süß, 2017) and were until now considered microdomain markers. However, the overall results comprised in both publications of this thesis put into question the initial hypothesis that flotillins and SPFH domain proteins are generally recruiting proteins to FMMs facilitating their interaction and oligomerization (Morrow and Parton, 2005; Zhao *et al.*, 2011). Here we demonstrated that not all SPFH containing proteins in *B. subtilis* are enriched in DRM fractions, neither can be directly associated to functional membrane microdomains. We have found that YdjI – the third SPFH/domain containing protein in *B. subtilis*, contrary to FloT and FloA, is enriched in the soluble protein fraction. This is reminiscent of studies with SPFH proteins from *E. coli*, in which the YqiK protein, one of the four SPFH proteins in *E.coli* and considered a *bona fide* flotillin in this bacterium, was found to be enriched in the detergent sensitive membrane fraction (Wessel *et al.*, 2022). Also, in line with the data presented in this thesis regarding SPFH protein's subcellular localization, Wessel and collaborators also confirmed that SPFH fluorescent fusion proteins showed distinct localization patterns. This has been also described some years ago by Dempwolff and collaborators, who observed only temporarily or no colocalization pattern of flotillins and other proteins co-eluted in DRM fractions (Dempwolff *et al.*, 2016). Altogether, it is possible to assume that

there is no *a priori* prediction that proteins within the membrane will exhibit similar behavior based on the presence of SPFH-domain.

3.2 The function of flotillins in controlling of membrane fluidity

In the Chapter 2.1, it was demonstrated that the flotillin-like proteins play in fact, a direct role in controlling membrane fluidity of *B. subtilis* in regards to growth condition. We could show that this particular physical role of flotillins in membrane organization, in turn, affects other important cellular aspects that only occur when membrane protein homeostasis is maintained. We found that together with a deletion of *pbp1*, a bifunctional glycosyl transferase/transpeptidase required for efficient cell division, the lack of flotillin proteins led to **(1)** extremely elongated cells, with loss of cell shape maintenance and **(2)** a severe delocalization of peptidoglycan synthesis machinery. Fundamentally, the cell wall synthesis machinery is regulated spatially within the cell. To properly coordinate the insertion of new PGs into the cell wall, PBPs activity should be well-regulated. During cell wall synthesis, the bacterial homolog of actin, MreB, organizes the spatial organization of the cytoskeleton. As PBP1 localizes to MreB and has been shown to physically interact with MreB (Carballido-López and Formstone, 2007; Kawai *et al.*, 2009), the dynamics of MreB protein in absence of flotillins were analyzed. It was found here, that the deletion of flotillins alone caused a **(3)** reduction of the MreB dynamics.

The predominantly physiological role in membrane organization for flotillins alone was further confirmed with *in vivo* observations that flotillin mutants presented an increase in the generalized polarization value (GP), a parameter used to detect the liquid ordering in the membrane of cells treated with the dye Laurdan, indicating that the membrane in absence of flotillins was rigidified. This result were in line with previously described by Bramkamp's group (Bach and Bramkamp, 2013). When these cells were treated with a membrane fluidizer, the GP was restored at normal levels, the elongated phenotype was reverted and the position of cell wall synthetic machinery was restored in the same position as for the wild-type cells. These results, altogether, indicate that in fact flotillins have a direct role in fluidizing the membrane rather than physically stabilizing membrane microdomains. Our *in vitro* experiments using NMR have shown that

FloT alone has a remarkable fluidizing effect on the entire acyl chain of membrane lipids, increasing the mobility of deuterated carbon. Our results using this approach demonstrated a particularly higher fluidization capability of FloT, when compared to the effects other proteins have when reconstituted into liposomes, such as plant remorins (Legrand *et al.*, 2019) or the membrane binding peptide of the nonreceptor tyrosine kinase protein Src (Scheidt and Huster, 2009), both known to promote membrane lipid modifications. Similar to the reduction in membrane fluidity observed in *B. subtilis* flotillin mutants, a study measuring fluorescence recovery after photobleaching (FRAP) of supported lipid bilayers (SLB) in the presence or absence of YqiK showed that IM lipid's lateral diffusion movement was decreased in absence of this flotillin-like protein from *E. coli* (Burdiel, 2018), thereby, supporting the notion that flotillins from other organisms may also play a role in maintaining membrane fluidity.

A possible biological interpretation for the function of flotillin proteins on the membrane fluidization reported in this thesis, is supported by several reports that describe that a sufficiently fluid membrane facilitates the synthesis of the peptidoglycan precursor Lipid II and its insertion into the membrane, consequently improving the recruitment and movement of MreB (Schirner *et al.*, 2015; Hussain *et al.*, 2018; Wong *et al.*, 2019). Moreover, it has been found that Lipid II prefers a more liquid, disordered state of the membrane (Ganchev et al., 2006; Witzke et al., 2016; Calvez et al., 2019).

The results in our study are also consistent with a recently reported observation that, when membrane fluidity is reduced by changing membrane fatty acid content, *B. subtilis* cells elongate and lose MreB organization (Gohrbandt *et al.*, 2022). Impairment of crucial cellular processes, including cell wall synthesis as showed in this thesis, was also observed by Gohrbandt and collaborators. The authors have recently demonstrated that the separation between the gel phase and fluid phase caused by a reduction in membrane fluidity does not affect the membrane's integrity. Instead, the lipid demixing cause the membrane proteins to be excluded from the gel phase areas, and are segregated into liquid membrane regions impairing not only protein functionality related to cell wall synthesis, but also including disturbances in processes such as cell division, chromosome segregation and energy production (Gohrbandt *et al.*, 2022). This would also elucidate several phenotypes of flotillin mutants already described in the literature, which comprises impairment in

membrane-bound processes such as sporulation (Donovan and Bramkamp, 2009), biofilm formation (Yepes *et al.*, 2012; Mielich-Süss and Lopez, 2015), motility (Dempwolff *et al.*, 2012a), and others.

The findings presented here, which highlight the role of SPFH-domain containing proteins, specifically flotillin-like proteins, in directly regulating membrane fluidity, are in line with phenotypic characterization already described in the literature on how these proteins may function in *B. subtilis* to adapt the membrane to various environmental conditions. These conditions include temperature fluctuations, osmotic stress, nutrient limitations, and antibiotic resistance (Dempwolff *et al.*, 2012b; Bach and Bramkamp, 2013). It has been suggested that NfeD-like proteins, encoded in the same operon as flotillins, play a potential role in maintaining membrane integrity during conditions of cellular stress (Dempwolff *et al.*, 2012a). Maintenance of physical parameters of the membrane such as fluidity is important for correct membrane protein homeostasis and guarantees that the membrane-associated processes are functional and occurring correctly in time and space.

In fact, flotillin proteins are long considered scaffolding proteins for formation of membrane compartmentalization, which is the result of the efficient separation of different states of liquid-ordered and disordered lipid domains within the membrane bilayer (López and Kolter, 2010; Bach and Bramkamp, 2013; Schneider *et al.*, 2015). It is important to understand that the packing behavior of the membrane is a significant physical aspect underpinning the molecular mechanisms of membrane regulation. Liquid membrane regions are characterized by phospholipids containing unsaturated chain fatty acids, whereas lipids with saturated acyl chains are tightly packed, resulting in a non-fluid gel phase in which lipid dynamics are restricted (Ernst *et al.*, 2016b; Chwastek *et al.*, 2020). As a result of this lipid mobility reduction, it has long been believed that membrane gel-like states cannot be found in living cells as they would not provide an adequate environment for the proper function of membrane proteins. Living membranes, however, can undergo liquid-liquid phase separation due to a certain degree of unsaturation in the acyl chain and the presence of hopanoids as sterol surrogates, as demonstrated recently by Gohrbandt and collaborators (Gohrbandt *et al.*, 2022). Membrane fluidity, in that sense, was here demonstrated to be also regulated by membrane proteins FloA and FloT in *B. subtilis* (Bach and Bramkamp, 2015) by a complete and effective

separation of states of liquid-ordered and disordered lipid domains and the effects on other membrane bound processes were demonstrated in this thesis.

3.3 Membrane adaptation to stress

This biophysical response caused by the bacterial flotillins FloA and FloT can also be related to the third SPFH-domain protein in *B. subtilis*, the YdjI protein. Their roles, as demonstrated in this thesis, illustrate the relative importance of SPFH-proteins from *B. subtilis* in modulating the membrane thereby promoting the resistance of cells to environmental stressors.

Similarly, ESCRT-III complexes are essential for membrane repair mechanisms, which are critical for maintaining cellular integrity when membranes are damaged due to various stresses or injuries (Jimenez *et al.*, 2014). The function of ESCRT-III proteins is highly regulated, and it requires specific interactions with a variety of partner proteins. These partners play essential roles in the assembly, localization, and activity of ESCRT-III complexes. The partnership between ESCRT-III proteins and their respective partners ensures the precise spatiotemporal control of membrane remodelling events and enables the cells to effectively respond to different cues (Colombo *et al.*, 2013; Camacho *et al.*, 2023). bacteria also encode ESCRIT-III homologs and the best studied is the phage-shock protein A (PspA) system described in *E.coli*, proposed to assemble in a carpet-like oligomeric structure in regions of membrane damage (Kobayashi *et al.*, 2007). A detailed analysis on the Psp system homologs among bacteria and archea demonstrated that certain proteins within the system remained conserved, like the core subunit PspA, while the associated protein may differ significantly between various bacterial species(Popp *et al.*, 2022). This variation implies that different bacteria have evolved diverse sets of associated proteins that interact with PspA to fulfil specific functions tailored to their unique cellular needs and environmental conditions.

In the Chapter 2.2 we wanted to unravel and characterize the YdjI protein and its association with the PspA system in *B. subtilis,* with the hypothesis that similarly to other ESCRIT-III like proteins that are dependent to protein association to bind to the membrane, YdjI could be the core associated protein necessary for the assembly of PspA to damaged membrane regions. A central

aim of our study (Scholz *et al.*, 2021) was to understand the subcellular localization and protein interactions within the sigma W regulated operon PspA-YdjGHI in *B. subtilis.*

It was found that the SPFH-domain protein YdjI forms distinct clusters at the membrane and co-localizes with PspA. The formation of PspA foci depends on the involvement of YdjI, YdjG, and YdjH. Nevertheless, it is worth noting that the co-localization of PspA clusters with YdjI complexes is not consistently observed, suggesting that the association between the Ydj and PspA may not be maintained throughout the entire membrane repair process. It is possible that once PspA recruitment and assembly are complete, YdjI oligomeric assembly disperses to other regions of the damaged membrane, while PspA acts to seal and remove the damaged areas via membrane scission.

We have also described the significance of other proteins, specifically YdjG and YdjH, in facilitating the membrane association of YdjI. When YdjG and YdjH were absent, severe cell morphological defects were observed, along with mislocalization of the peptidoglycan synthesis machinery. These discoveries indicate that YdjI's proper functioning and localization rely on the presence of YdjG and YdjH, and highlights the sensitivity of the cell wall synthesis machinery when this cellular membrane stress response system is compromised.

Comparatively, the dynamic membrane positioning of the PspA system in *E. coli* has been shown to rely on the bacterial cytoskeletal component MreB. The MreB protein, which dynamics is directly linked to the peptidoglycan synthesis, coordinates the elongasome during synthesis of lateral cell wall of rod-shaped bacteria (Egan *et al.*, 2020). Upon absence of MreB, the Psp response is triggered, but the cells lose their protection against membrane stress in *E. coli* (Engl *et al.*, 2009). This discovery strongly indicates that the bacterial cytoskeletal is essential for the protective role of PspA complexes. Our study demonstrated that the formation of YdjI and PspA clusters in *B. subtilis,* however, does not depend on the presence of the MreB cytoskeleton protein, but did displayed reduced cluster numbers in its absence. This suggests that while MreB is not essential for cluster formation, it may play a role in optimizing the process, since MreB absence is known to dissipate membrane potential leading to secondary effects such as changes in membrane homeostasis and membrane rigidification (Strahl *et al.*, 2014).

Interestingly, it was observed that YdjI is located in liquid disordered membrane regions, which contrasts with the localization pattern of typical bacterial flotillins, enriched in liquid ordered membrane regions (Bach and Bramkamp, 2013). Interestingly, the deletion of YdjI, similarly to the deletion of FloT, leads to a reduction in overall membrane fluidity. This implies a conserved role of SPFH domain proteins in modulating membrane fluidity, which is in line with the general roles of the sigma W regulon in controlling membrane fluidity in an effort to modulate diffusion of compounds across the membrane (Kingston *et al.*, 2011).

Increased membrane fluidity has been observed to aid in membrane repair by facilitating the recruitment and localization of stress-response related proteins to damaged areas. YdjI may play a role in modulating membrane fluidity to promote repair processes and enhance overall membrane adaptation. A higher local fluidity of the membrane allows for greater flexibility and mobility of the lipid bilayer, aiding in the sealing of impaired areas by facilitating small portions of damaged membrane to bulge or bend to be further scissed from the membrane. Membrane fusion and fission events, enabled by an optimal fluidity, can merge lipid bilayers or remove damaged portions to repair breaches in the membrane. Furthermore, fluidity supports the movement and recruitment of repair proteins such as the PspA-YdjGHI complex, and enzymes to the site of damage, facilitating tasks such as membrane resealing, remodelling, and the removal of damaged lipid molecules. Additionally, membrane fluidity contributes to the stability and proper organization of the bilayer by allowing lateral movement of lipids, proteins, and other components (Gohrbandt *et al.*, 2022). Overall, fluidity is essential for effective membrane repair processes as it enables necessary molecular rearrangements and protein interactions (Kingston *et al.*, 2011; Zielińska *et al.*, 2020).

In the context of antibiotic response, YdjI may modulate the recruitment and localization of PspA to the membrane, enhancing the cell's ability to cope with antibiotic-induced membrane stress. By facilitating the assembly of PspA at the membrane, YdjI may contribute to the defence against antibiotic-induced damage and acts again in maintaining membrane integrity. Moreover, the involvement of YdjI in membrane repair processes can help restore membrane functionality and fluidity after antibiotic exposure, promoting cell survival. Comparatively, the LiaRS two-component system of *B. subtilis* exhibits response to various cell envelope stress conditions, including agents that perturb the cell

envelope such as antimicrobial peptides (Popp *et al.*, 2020), as well as abiotic stresses such as heat and osmotic shock (Mascher *et al.*, 2004). LiaS activates the cognate response regulator LiaR, upon detection of cell envelope perturbations, consequently inducing the *liaIH* operon. LiaI, similarly to what YdjI does to PspA, recruits LiaH to the membrane in order to promote envelope protection and counteract damage induced by antibiotic (Domínguez-Escobar *et al.*, 2014).

LiaH is a homologue of the phage-shock protein A, with stablished roles in responding to induced filamentous phage infection, high osmolarity, heat shock, secretion stress and changes to membrane homeostasis (Brissette *et al.*, 1991; Adams *et al.*, 2003). LiaI is found in mobile membrane-associated clusters, while LiaH is distributed throughout the cytoplasm. However, under stress conditions, both proteins are significantly induced and localized in multiple distinct foci at the cytoplasmic membrane, similarly to the PspA-YdjI complex formation described here. Similarly to what occurs with PspA-YdjI, the membrane complex formation of LiaIH system is also not influenced by MreB nor associated with the inhibition of cell wall biosynthesis machinery by antibiotics (Domínguez-Escobar *et al.*, 2014). Instead, it can be triggered by antibiotics that disrupt the membrane-anchored steps of cell wall biosynthesis, while compounds inhibiting cytoplasmic or extracytoplasmic steps do not elicit this response.

OUTLOOK

In summary, the findings included in this thesis demonstrated that the SPFH-domain containing proteins, FloA and FloT from *B. subtilis* have a direct role in regulating membrane fluidity, which is essential for correct peptidoglycan synthesis and regulation of MreB dynamics under particular growth conditions. The impact of flotillin-like proteins on membrane fluidity demonstrated by this thesis is direct, resulting in an effective separation of membrane states. The membrane fluidity is affected by both temperature and growth conditions and membrane-bound processes such as correct cell shape maintenance, peptidoglycan synthesis machinery localization and MreB dynamics are restored by chemically fluidizing the membrane, when flotillins are absent. These results support the idea of the importance of membrane fluidity to preserve the membrane associated process. Besides the existing differences between FloA/T and YdjI, a remarkable similarity between them is the effect of *ydjI* deletion on membrane fluidity. YdjI deletion causes an increase in total GP values, similarly to flotillin deletion, showing that this protein is also involved in membrane fluidization. The molecular mechanism by which the SPFH-domain proteins in *B. subtilis* control membrane homeostasis by maintaining optimal membrane fluidity remains to be elucidated. Absence of FloA, FloT and YdjI on *B. subtilis* cells, probably has effects on lipid organization or in lipid synthesis causing a decrease in membrane fluidity. The study of *B. subtilis* cell membrane focusing on the exact mechanisms by which YdjI and flotillins control membrane homeostasis, holds significant potential to advance our understanding of membrane organization, repair mechanisms and stress response. By unravelling the intricate molecular interactions and regulatory networks involving YdjI and flotillins, we can gain deeper insights into the fundamental processes that govern membrane dynamics in this model organism. Moreover, understanding the interplay between other partners of the proteins here studied, sheds light on the importance of protein complexes in coordinating membrane dynamics in bacterial cells, contributing to the overall understanding of cellular membrane maintenance and regulation.

REFERENCES

Adams, H., Teertstra, W., Demmers, J., Boesten, R., and Tommassen, J. (2003) Interactions between phage-shock proteins in *Escherichia coli*. *J Bacteriol* **185**: 1174–1180.

Aguilar, P.S., Cronan, J.E., and Mendoza, D. De (1998) A *Bacillus subtilis* gene induced by cold shock encodes a membrane phospholipid desaturase. *J Bacteriol* **180**: 2194–2200.

Aguilar, P.S., Lopez, P., and Mendoza, D. De (1999) Transcriptional control of the low-temperature-inducible des gene, encoding the delta5 desaturase of *Bacillus subtilis*. *J Bacteriol* **181**: 7028–7033.

Alexander, V. (1999) Biological functions of carotenoids – diversity and evolution. *Biofactors* **10**: 99–104.

Altabe, S.G., Aguilar, P., Caballero, G.M., and Mendoza, D. de (2003) The *Bacillus subtilis* Acyl Lipid Desaturase Is a 5 Desaturase. *J Bacteriol* **185**: 3228–3231.

Anderson, R.G., and Jacobson, K. (2002) A role for lipid shells in targeting proteins to caveolae, rafts, and other lipid domains. *Science (80-)* **296**: 1821–1825.

Antelmann, H., Yamamoto, H., Sekiguchi, J., and Hecker, M. (2002) Stabilization of cell wall proteins in *Bacillus subtilis*: A proteomic approach. *Proteomics* **2**: 591–602.

Bach, J.N., and Bramkamp, M. (2013) Flotillins functionally organize the bacterial membrane. *Mol Microbiol* **88**: 1205–1217.

Bach, J.N., and Bramkamp, M. (2015) Dissecting the Molecular Properties of Prokaryotic Flotillins. .

Barria, C., Malecki, M., and Arraiano, C.M. (2013) Bacterial adaptation to cold. *Microbiology* **159**: 2437–2443.

Bartholomew, J.W., and Mittwer, T. (1952) The Gram Stain. *Bacteriol Rev* **16**: 1.

Beeby, M., Gumbart, J.C., Roux, B., and Jensen, G.J. (2013) Architecture and assembly of the Gram-positive cell wall. *Mol Microbiol* **88**: 664–672.

Belin, B.J., Busset, N., Giraud, E., Molinaro, A., Silipo, A., and Newman, Di.K. (2018) Hopanoid lipids: from membranes to plant–bacteria interactions. *Nat Rev Microbiol 2018 165* **16**: 304–315.

Bell, S.A., and Chappell, J. (2014) Now playing: farnesol in the biofilm. *Chem Biol* **21**: 1421–1422.

Berks, B.C. (1996) A common export pathway for proteins binding complex redox cofactors? *Mol Microbiol* **22**: 393–404.

Bernal-Cabas, M., Miethke, M., Antelo-Varela, M., Aguilar Suárez, R., Neef, J., Schön, L., *et al.* (2020) Functional association of the stress-responsive LiaH protein and the minimal TatAyCy protein translocase in *Bacillus subtilis*. *Biochim Biophys Acta - Mol Cell Res* **1867**.

Bickel, P.E., Scherer, P.E., Schnitzer, J.E., Oh, P., Lisanti, M.P., and Lodish, H.F. (1997) Flotillin and epidermal surface antigen define a new family of caveolae-associated integral membrane proteins. *J Biol Chem* **272**: 13793–13802.

Blobel, G. (1980) Intracellular protein topogenesis. *Proc Natl Acad Sci U S A* **77**: 1496–1500.

Bosak, T., Losick, R.M., and Pearson, A. (2008) A polycyclic terpenoid that alleviates oxidative stress. .

Bramkamp, M., and Lopez, D. (2015) Exploring the Existence of Lipid Rafts in Bacteria. *Microbiol Mol Biol Rev* **79**: 81–100.

Briggs, D.E.G., and Summons, R.E. (2014) Ancient biomolecules: their origins, fossilization, and role in revealing the history of life. *Bioessays* **36**: 482–490.

Brissette, J.L., Weiner, L., Ripmaster, T.L., and Model, P. (1991) Characterization and sequence of the *Escherichia coli* stress-induced psp operon. *J Mol Biol* **220**: 35–48.

Brocks, J.J., Logan, G.A., Buick, R., and Summons, R.E. Archean Molecular Fossils and the Early Rise of Eukaryotes. .

Browman, D.T., Hoegg, M.B., and Robbins, S.M. (2007a) The SPFH domain-containing proteins: more than lipid raft markers. *Trends Cell Biol* **17**: 394–402.

Browman, D.T., Hoegg, M.B., and Robbins, S.M. (2007b) The SPFH domain-containing proteins: more than lipid raft markers. *Trends Cell Biol* **17**: 394–402.

Brown, D.A., and London, E. (1998) Functions of Lipid Rafts in Biological Membranes. *Annu Rev Cell Dev Biol* **14**: 111–136.

Brown, D.A., and Rose, J.K. (1992a) Sorting of GPI-Anchored Proteins to Glycolipid-Enriched Membrane Subdomains during Transport to the Apical Cell Surface. *Cell* **66**: 533–544.

Brown, D.A., and Rose, J.K. (1992b) Sorting of GPI-anchored proteins to glycolipid-enriched membrane subdomains during transport to the apical cell surface. *Cell* **68**: 533–544.

Brown, S., Santa Maria Jr, J.P., and Walker, S. (2013) Wall Teichoic Acids of Gram-Positive Bacteria PG: peptidoglycan WTA: wall teichoic acid MRSA: methicillin-resistant Staphylococcus aureus. .

Camacho, A.C., Alfandari, D., Kozela, E., and Regev-Rudzki, N. (2023) Biogenesis of extracellular vesicles in protozoan parasites: The ESCRT complex in the trafficking fast lane? *PLoS Pathog* **19**.

Carballido-López, R., and Formstone, A. (2007) Shape determination in *Bacillus subtilis*. *Curr Opin Microbiol* **10**: 611–616.

Carballido-López, R., Formstone, A., Li, Y., Ehrlich, S.D., Noirot, P., and Errington, J. (2006) Actin Homolog MreBH Governs Cell Morphogenesis by Localization of the Cell Wall Hydrolase LytE. *Dev Cell* **11**: 399–409.

Chou, K.C., and Shen, H. Bin (2007) Recent progress in protein subcellular

location prediction. *Anal Biochem* **370**: 1–16.

Chwastek, G., Surma, M.A., Rizk, S., Ruci, M., Jambor, H., Sá Enz Correspondence, J., *et al.* (2020) Principles of Membrane Adaptation Revealed through Environmentally Induced Bacterial Lipidome Remodeling ll Principles of Membrane Adaptation Revealed through Environmentally Induced Bacterial Lipidome Remodeling. *CellReports* **32**: 108165.

Claessen, D., Emmins, R., Hamoen, L.W., Daniel, R.A., Errington, J., and Edwards, D.H. (2008) Control of the cell elongation-division cycle by shuttling of PBP1 protein in *Bacillus subtilis*. *Mol Microbiol* **68**: 1029–1046.

Colombo, M., Moita, C., Niel, G. Van, Kowal, J., Vigneron, J., Benaroch, P., *et al.* (2013) Analysis of ESCRT functions in exosome biogenesis, composition and secretion highlights the heterogeneity of extracellular vesicles. *J Cell Sci* **126**: 5553–5565.

Coskun, Ü., and Simons, K. (2011) Cell membranes: the lipid perspective. *Structure* **19**: 1543–1548.

Cozy, L.M., Phillips, A.M., Calvo, R.A., Bate, A.R., Hsueh, Y.-H., Bonneau, R., *et al.* (2012) SlrA/SlrR/SinR inhibits motility gene expression upstream of a hypersensitive and hysteric switch at the level of σ D in *Bacillus subtilis*. *Mol Microbiol* **83**: 1210–1228.

Cronan, J.E., and Gelmann, E.P. (1975) Physical properties of membrane lipids: biological relevance and regulation. *Bacteriol Rev* **39**: 232–256.

Cybulski, L.E., Martín, M., Mansilla, M.C., Fernández, A., and Mendoza, D. De (2010) Membrane thickness cue for cold sensing in a bacterium. *Curr Biol* **20**: 1539–1544.

Czárán, T.L., Hoekstra, R.F., and Pagie, L. (2002) Chemical warfare between microbes promotes biodiversity. .

Darwin, A.J. (2007) Regulation of the phage-shock-protein stress response in Yersinia enterocolitica. *Adv Exp Med Biol* **603**: 167–177.

Darwin, A.J., and Miller, V.L. (2001) The psp locus of Yersinia enterocolitica is required for virulence and for growth in vitro when the Ysc type III secretion system is produced. *Mol Microbiol* **39**: 429–445.

Dempwolff, F., and Graumann, P.L. (2014) Genetic links between bacterial dynamin and flotillin proteins. *Commun Integr Biol* **7**.

Dempwolff, F., Möller, H.M., and Graumann, P.L. (2012a) Synthetic Motility and Cell Shape Defects Associated with Deletions of Flotillin/Reggie Paralogs in *Bacillus subtilis* and Interplay of These Proteins with NfeD Proteins. .

Dempwolff, F., Schmidt, F.K., Hervás, A.B., Stroh, A., Rösch, T.C., Riese, C.N., *et al.* (2016) Super Resolution Fluorescence Microscopy and Tracking of Bacterial Flotillin (Reggie) Paralogs Provide Evidence for Defined-Sized Protein Microdomains within the Bacterial Membrane but Absence of Clusters Containing Detergent-Resistant Proteins. *PLoS Genet* **12**.

Dempwolff, F., Wischhusen, H.M., Specht, M., and Graumann, P.L. (2012b) The deletion of bacterial dynamin and flotillin genes results in pleiotrophic effects on cell division, cell growth and in cell shape maintenance. *BMC*

Microbiol **12**: 1.

Domínguez-Escobar, J., Chastanet, A., Crevenna, A.H., Fromion, V., Wedlich-Söldner, R., and Carballido-López, R. (2011) Processive movement of MreB-associated cell wall biosynthetic complexes in bacteria. *Science (80-)* **333**: 225–228.

Domínguez-Escobar, J., Wolf, D., Fritz, G., Höfler, C., Wedlich-Söldner, R., and Mascher, T. (2014) Subcellular localization, interactions and dynamics of the phage-shock protein-like Lia response in *Bacillus subtilis*. *Mol Microbiol* **92**: 716–732.

Donovan, C., and Bramkamp, M. (2009) Characterization and subcellular localization of a bacterial flotillin homologue. *Microbiology* **155**: 1786–1799.

Edidin, M. (2003) The state of lipid rafts. *Annu Rev Biophys Biomol Struct* **32**: 257–283.

Egan, A.J.F., Errington, J., and Vollmer, W. (2020) Regulation of peptidoglycan synthesis and remodelling. *Nat Rev Microbiol* **18**: 446–460.

Ehehalt, R., Keller, P., Haass, C., Thiele, C., and Simons, K. (2003) Amyloidogenic processing of the Alzheimer beta-amyloid precursor protein depends on lipid rafts. *J Cell Biol* **160**: 113–123.

Eiamphungporn, W., and Helmann, J.D. (2008) The *Bacillus subtilis* σM regulon and its contribution to cell envelope stress responses. *Mol Microbiol* **67**: 830–848.

Eijlander, R.T., Jongbloed, J.D.H., and Kuipers, O.P. (2009) Relaxed specificity of the *Bacillus subtilis* TatAdCd translocase in Tat-dependent protein secretion. *J Bacteriol* **91**: 196–202.

Emami, K., Guyet, A., Kawai, Y., Devi, J., Wu, L.J., Allenby, N., *et al.* (2017) RodA as the missing glycosyltransferase in *Bacillus subtilis* and antibiotic discovery for the peptidoglycan polymerase pathway. *Nat Microbiol* **2**.

Emanuelsson, O., Brunak, S., Heijne, G. von, and Nielsen, H. (2007) Locating proteins in the cell using TargetP, SignalP and related tools. *Nat Protoc* **2**: 953–971.

Engl, C., Jovanovic, G., Lloyd, L.J., Murray, H., Spitaler, M., Ying, L., *et al.* (2009) In vivo localizations of membrane stress controllers PspA and PspG in *Escherichia coli*. *Mol Microbiol* **73**: 382–396.

Ernst, R., Ejsing, C.S., and Antonny, B. (2016a) Homeoviscous Adaptation and the Regulation of Membrane Lipids. *J Mol Biol* **428**: 4776–4791.

Ernst, R., Ejsing, C.S., and Antonny, B. (2016b) Homeoviscous Adaptation and the Regulation of Membrane Lipids. *J Mol Biol* **428**: 4776–4791.

Escribá, P. V., and Nicolson, G.L. (2014) Membrane structure and function: relevance of lipid and protein structures in cellular physiology, pathology and therapy. *Biochim Biophys Acta* **1838**: 1449–1450.

Feng, X., Hu, Y., Zheng, Y., Zhu, W., Li, K., Huang, C.H., *et al.* (2014) Structural and Functional Analysis of *Bacillus subtilis* YisP Reveal a Role of its Product in Biofilm Production. *Chem Biol* **21**: 1557.

Fischer, W.W., Summons, R.E., and Pearson, A. (2005) Targeted genomic detection of biosynthetic pathways: anaerobic production of hopanoid biomarkers by a common sedimentary microbe. *Geobiology* **3**: 33–40.

Flores-Kim, J., and Darwin, A.J. (2016) The Phage Shock Protein Response. .

Foster, L.J., Hoog, C.L. De, and Mann, M. (2003) Unbiased quantitative proteomics of lipid rafts reveals high specificity for signaling factors. *Proc Natl Acad Sci* **100**: 5813–5818.

Frain, K.M., Robinson, C., and Dijl, J.M. van (2019) Transport of Folded Proteins by the Tat System. *Protein J 2019 384* **38**: 377–388.

Frickey, T., and Kannenberg, E. (2009) Phylogenetic analysis of the triterpene cyclase protein family in prokaryotes and eukaryotes suggests bidirectional lateral gene transfer. .

Fröbel, J., Rose, P., and Müller, M. (2012) Twin-arginine-dependent translocation of folded proteins. *Philos Trans R Soc B Biol Sci* **367**: 1029–1046.

Gabrielska, J., and Gruszecki, W.I. (1996) Zeaxanthin (dihydroxy-β-carotene) but not β-carotene rigidifies lipid membranes: a 1H-NMR study of carotenoid-egg phosphatidylcholine liposomes. *Biochim Biophys Acta - Biomembr* **1285**: 167–174.

García-Fernández, E., Koch, G., Wagner, R.M., Fekete, A., Stengel, S.T., Schneider, J., *et al.* (2017) Membrane Microdomain Disassembly Inhibits MRSA Antibiotic Resistance. *Cell* 1–14.

Garner, E.C., Bernard, R., Wang, W., Zhuang, X., Rudner, D.Z., and Mitchison, T. (2011) Coupled, circumferential motions of the cell wall synthesis machinery and MreB filaments in B. subtilis. *Science (80-)* **333**: 222–225.

Ghuysen, J.M. (1991) Serine beta-lactamases and penicillin-binding proteins. *Annu Rev Microbiol* **45**: 37–67.

Goffin, C., and Ghuysen, J.-M. (1998) Multimodular penicillin-binding proteins: an enigmatic family of orthologs and paralogs. *Microbiol Mol Biol Rev* **62**: 1079–1093.

Gohrbandt, M., Lipski, A., Grimshaw, J.W., Buttress, J.A., Baig, Z., Herkenhoff, B., *et al.* (2022) Low membrane fluidity triggers lipid phase separation and protein segregation in living bacteria. *EMBO J* e109800.

Goosens, V.J., Monteferrante, C.G., and Dijl, J.M. Van (2014a) The Tat system of Gram-positive bacteria. *Biochim Biophys Acta - Mol Cell Res* **1843**: 1698–1706.

Goosens, V.J., Monteferrante, C.G., and Dijl, J.M. Van (2014b) Co-factor Insertion and Disulfide Bond Requirements for Twin-arginine Translocase-dependent Export of the *Bacillus subtilis* Rieske Protein QcrA. *J Biol Chem* **289**: 13124–13131.

Gram, H. (1884) *Ueber die isolirte Färbung der Schizomyceten : in Schnitt-und Trockenpräparaten*. Theodor Fischer's medicinischer Buchhandlung, Berlin.

Green, David E., and G.V. (1971) Structure and Function of Biological

Membranes. *Colloid Morphol Behav Block Graft Copolym Springer, Boston, MA* 101–112.

Gueguen, E., Savitzky, D.C., and Darwin, A.J. (2009) Analysis of the Yersinia enterocolitica PspBC proteins defines functional domains, essential amino acids and new roles within the phage-shock-protein response. *Mol Microbiol* **74**: 619–633.

Guilhelmelli, F., Vilela, N., Albuquerque, P., Derengowski, L. da S., Silva-Pereira, I., and Kyaw, C.M. (2013) Antibiotic development challenges: The various mechanisms of action of antimicrobial peptides and of bacterial resistance. *Front Microbiol* **4**.

Guo, L., and Bramkamp, M. (2019) Bacterial dynamin-like protein DynA mediates lipid and content mixing. *FASEB J* **33**: 11746–11757.

Guo, L., Sattler, L., Shafqat, S., Graumann, P.L., and Bramkamp, M. (2022) A Bacterial Dynamin-Like Protein Confers a Novel Phage Resistance Strategy on the Population Level in *Bacillus subtilis*. *MBio* **13**.

Gupta, T.K., Klumpe, S., Gries, K., Heinz, S., Wietrzynski, W., Ohnishi, N., *et al.* (2021) Structural basis for VIPP1 oligomerization and maintenance of thylakoid membrane integrity. *Cell* **184**: 3643-3659.e23.

Harris, T.J., and Siu, C.H. (2002) Reciprocal raft-receptor interactions and the assembly of adhesion complexes. *Bioessays* **24**: 996–1003.

Härtner, T., Straub, K.L., and Kannenberg, E. (2005) Occurrence of hopanoid lipids in anaerobic Geobacter species. *FEMS Microbiol Lett* **243**: 59–64.

Hayhurst, E.J., Kailas, L., Hobbs, J.K., and Foster, S.J. (2008) Cell wall peptidoglycan architecture in *Bacillus subtilis*. .

Heerklotz, H. (2002) Triton promotes domain formation in lipid raft mixtures. *Biophys J* **83**: 2693–2701.

Heidrich, J., Thurotte, A., and Schneider, D. (2017) Specific interaction of IM30/Vipp1 with cyanobacterial and chloroplast membranes results in membrane remodeling and eventually in membrane fusion. *Biochim Biophys acta Biomembr* **1859**: 537–549.

Helmann, J.D. (2016) *Bacillus subtilis* extracytoplasmic function (ECF) sigma factors and defense of the cell envelope. *Curr Opin Microbiol* **30**: 122–132.

Henriques, A.O., and Moran, C.P. (2007) Structure, Assembly, and Function of the Spore Surface Layers. .

Hinderhofer, M., Walker, C. a, Friemel, A., Stuermer, C. a O., Möller, H.M., and Reuter, A. (2009) Evolution of prokaryotic SPFH proteins. *BMC Evol Biol* **9**: 10.

Hjort Ipsen, J., Karlström, G., Mourtisen, O.G., Wennerström, H., and Zuckermann, M.J. (1987) Phase equilibria in the phosphatidylcholine-cholesterol system. *BBA - Biomembr* **905**: 162–172.

Holthuis, J.C.M., and Menon, A.K. (2014) Lipid landscapes and pipelines in membrane homeostasis. *Nature* **510**: 48–57.

Höltje, J.V. (1998) Growth of the Stress-Bearing and Shape-Maintaining Murein

Sacculus of *Escherichia coli*. **62**: 181–203.

Hu, Y., Jia, S., Ren, F., Huang, C.H., Ko, T.P., Mitchell, D.A., *et al.* (2013) Crystallization and preliminary X-ray diffraction analysis of YisP protein from *Bacillus subtilis* subsp. subtilis strain 168. *Acta Crystallogr Sect F Struct Biol Cryst Commun* **69**: 77–79.

Hussain, S., Wivagg, C.N., Szwedziak, P., Wong, F., Schaefer, K., Izoré, T., *et al.* (2018) Mreb filaments align along greatest principal membrane curvature to orient cell wall synthesis. *Elife* **7**.

Inoue, Y., Togashi, N., and Hamashima, H. (2016) Farnesol-Induced Disruption of the Staphylococcus aureus Cytoplasmic Membrane. .

Isono, E. (2021) ESCRT Is a Great Sealer: Non-Endosomal Function of the ESCRT Machinery in Membrane Repair and Autophagy. *Plant Cell Physiol* **62**: 766–774.

Jamshad, M., Lin, Y.P., Knowles, T.J., Parslow, R.A., Harris, C., Wheatley, M., *et al.* (2011) Surfactant-free purification of membrane proteins with intact native membrane environment. *Biochem Soc Trans* **39**: 813–818.

Jimenez, A.J., Maiuri, P., Lafaurie-Janvore, J., Divoux, S., Piel, M., and Perez, F. (2014) ESCRT machinery is required for plasma membrane repair. *Science (80-)* **343**.

Joly, N., Engl, C., Jovanovic, G., Huvet, M., Toni, T., Sheng, X., *et al.* (2010) Managing membrane stress: The phage shock protein (Psp) response, from molecular mechanisms to physiology. *FEMS Microbiol Rev* **34**: 797–827.

Jones, L.J.F., Carballido-López, R., and Errington, J. (2001) Control of Cell Shape in Bacteria: Helical, Actin-like Filaments in *Bacillus subtilis*. *Cell* **104**: 913–922.

Jordan, S., Hutchings, M.I., and Mascher, T. (2008a) Cell envelope stress response in Gram-positive bacteria. *FEMS Microbiol Rev* **32**: 107–146.

Jordan, S., Hutchings, M.I., and Mascher, T. (2008b) Cell envelope stress response in Gram-positive bacteria. *FEMS Microbiol Rev* **32**: 107–146.

Junglas, B., Huber, S.T., Heidler, T., Schlösser, L., Mann, D., Hennig, R., *et al.* (2021) PspA adopts an ESCRT-III-like fold and remodels bacterial membranes. *Cell* **184**: 3674-3688.e18.

Junglas, B., Orru, R., Axt, A., Siebenaller, C., Steinchen, W., Heidrich, J., *et al.* (2020) IM30 IDPs form a membrane-protective carpet upon super-complex disassembly. *Commun Biol* **3**.

Junglas, B., and Schneider, D. (2018) What is Vipp1 good for? *Mol Microbiol* **108**: 1–5.

Kaiser, H.J., Lingwood, D., Levental, I., Sampaio, J.L., Kalvodova, L., Rajendran, L., and Simons, K. (2009) Order of lipid phases in model and plasma membranes. *Proc Natl Acad Sci U S A* **106**: 16645–16650.

Kannenberg, E.L., and Poralla, K. (1999) Hopanoid Biosynthesis and Function in Bacteria. *Naturwissenschaften 1999 864* **86**: 168–176.

Karnovsky, M.J., Kleinfeld, A.M., Hoover, R.L., and Klausner, R.D. (1982) The

Concept of Lipid Domains in Membranes. *J Cell Biol* **94**: 1–6.

Kawai, F., Shoda, M., Harashima, R., Sadaie, Y., Hara, H., and Matsumoto, K. (2004) Cardiolipin domains in *Bacillus subtilis* marburg membranes. *J Bacteriol* **186**: 1475–1483.

Kawai, Y., Daniel, R.A., and Errington, J. (2009) Regulation of cell wall morphogenesis in *Bacillus subtilis* by recruitment of PBP1 to the MreB helix. *Mol Microbiol* **71**: 1131–1144.

Kenworthy, A. (2002) Peering inside lipid rafts and caveolae. *Trends Biochem Sci* **27**: 435–437.

Keren, K. (2011) Cell motility: the integrating role of the plasma membrane. *Eur Biophys J* **40**: 1013–1027.

Keyzer, J. De, Does, C. Van Der, and Driessen, A.J.M. (2003) The bacterial translocase: A dynamic protein channel complex. *Cell Mol Life Sci* **60**: 2034–2052.

Kingston, A.W., Liao, X., and Helmann, J.D. (2013) Contributions of the σW, σM and σX regulons to the lantibiotic resistome of *Bacillus subtilis*. *Mol Microbiol* **90**: 502–518.

Kingston, A.W., Subramanian, C., Rock, C.O., and Helmann, J.D. (2011) A σW-dependent stress response in *Bacillus subtilis* that reduces membrane fluidity. *Mol Microbiol* **81**: 69–79.

Kobayashi, R., Suzuki, T., and Yoshida, M. (2007) *Escherichia coli* phage-shock protein A (PspA) binds to membrane phospholipids and repairs proton leakage of the damaged membranes. *Mol Microbiol* **66**: 100–109.

Koch, A.L. (2000) The bacterium's way for safe enlargement and division. *Appl Environ Microbiol* **66**: 3657–3663.

Koch, G., Wermser, C., Acosta, I.C., Kricks, L., Stengel, S.T., Yepes, A., and Lopez, D. (2017) Attenuating Staphylococcus aureus Virulence by Targeting Flotillin Protein Scaffold Activity. *Cell Chem Biol* **24**: 845-857.e6.

Komeili, A., Li, Z., Newman, D.K., and Jensen, G.J. (2006) Magnetosomes are cell membrane invaginations organized by the actin-like protein MamK. *Science* **311**: 242–245.

Kontnik, R., Bosak, T., Butcher, R.A., Brocks, J.J., Losick, R., Clardy, J., and Pearson, A. (2008) Sporulenes, heptaprenyl metabolites from *Bacillus subtilis* spores. *Org Lett* **10**: 3551–3554.

Kovbasnjuk, O., Edidin, M., and Donowitz, M. (2001) Role of lipid rafts in Shiga toxin 1 interaction with the apical surface of Caco-2 cells. *J Cell Sci* **114**: 4025–4031.

Lang, D.M., Lommel, S., Jung, M., Ankerhold, R., Petrausch, B., Laessing, U., *et al.* (1998) Identification of reggie-1 and reggie-2 as plasmamembrane-associated proteins which cocluster with activated GPI-anchored cell adhesion molecules in non-caveolar micropatches in neurons. *J Neurobiol* **37**: 502–523.

Langhorst, M.F., Reuter, A., and Stuermer, C.A.O. (2005) Scaffolding microdomains and beyond: the function of reggie/flotillin proteins.

Cell Mol Life Sci **62**: 2228–2240.

Langhorst, M.F., Solis, G.P., Hannbeck, S., Plattner, H., and Stuermer, C.A.O. (2007) Linking membrane microdomains to the cytoskeleton: Regulation of the lateral mobility of reggie-1/flotillin-2 by interaction with actin. *FEBS Lett* **581**: 4697–4703.

Laura Cueta Burdiel (2018) The effect of the synthesis and localization of ZipA, an essential component of the *Escherichia coli* divisome, on division and membrane dynamics. .

Legrand, A., Martinez, D., Grélard, A., Berbon, M., Morvan, E., Tawani, A., *et al.* (2019) Nanodomain Clustering of the Plant Protein Remorin by Solid-State NMR. *Front Mol Biosci* **6**: 107.

Lenarcic, R., Halbedel, S., Visser, L., Shaw, M., Wu, L.J., Errington, J., *et al.* (2009) Localisation of DivIVA by targeting to negatively curved membranes. *EMBO J* **28**: 2272–2282.

Levin, P.A., Fan, N., Ricca, E., Driks, A., Losick, R., and Cutting, S. (1993) An unusually small gene required for sporulation by Bacillus subtiiis. *Mol Microbiol* **9**: 761–771.

Li, Y., Gong, H., Zhan, R., Ouyang, S., Park, K.T., Lutkenhaus, J., and Du, S. (2021) Genetic analysis of the septal peptidoglycan synthase FtsWI complex supports a conserved activation mechanism for SEDS-bPBP complexes. *PLoS Genet* **17**.

Lingwood, D., and Simons, K. (2010) Lipid rafts as a membrane-organizing principle. *Science* **327**: 46–50.

Liu, G.Y., and Nizet, V. (2009) Color me bad: microbial pigments as virulence factors. *Trends Microbiol* **17**: 406–413.

Liu, J., Tassinari, M., Souza, D.P., Naskar, S., Noel, J.K., Bohuszewicz, O., *et al.* (2021) Bacterial Vipp1 and PspA are members of the ancient ESCRT-III membrane-remodeling superfamily. *Cell* **184**: 3660-3673.e18.

Liu, Y., Engelman, D.M., and Gerstein, M. (2002) Genomic analysis of membrane protein families: abundance and conserved motifs. *Genome Biol* **3**.

London, E., and Brown, D.A. (2000) Insolubility of lipids in Triton X-100: physical origin and relationship to sphingolipid/cholesterol membrane domains (rafts). *Biochim Biophys Acta - Biomembr* **1508**: 182–195.

López, C.S., Alice, A.F., Heras, H., Rivas, E.A., and Sánchez-Rivas, C. (2006) Role of anionic phospholipids in the adaptation of *Bacillus subtilis* to high salinity. *Microbiology* **152**: 605–616.

Lopez, D., and Koch, G. (2017) Exploring functional membrane microdomains in bacteria: an overview. *2Current Opin Microbiol* **36**: 76–84.

López, D., and Kolter, R. (2010) Functional microdomains in bacterial membranes. *Genes Dev* **24**: 1893–1902.

Maire, M. le, Champeil, P., and Moller, J.V. (2000) Interaction of membrane proteins and lipids with solubilizing detergents. *Biochim Biophys Acta* **1508**: 86–111.

Malanovic, N., and Lohner, K. (2016) Antimicrobial peptides targeting Gram-

positive bacteria. *Pharmaceuticals* **9**.

Manganelli, R., and Gennaro, M.L. (2017) Protecting from Envelope Stress: Variations on the Phage-Shock-Protein Theme. *Trends Microbiol* **25**: 205–216.

Mangiarotti, A., Genovese, D.M., Naumann, C.A., Monti, M.R., and Wilke, N. (2019) Hopanoids, like sterols, modulate dynamics, compaction, phase segregation and permeability of membranes. *Biochim Biophys Acta - Biomembr* **1861**.

Mascher, T., Zimmer, S.L., Smith, T.A., and Helmann, J.D. (2004) Antibiotic-inducible promoter regulated by the cell envelope stress-sensing two-component system LiaRS of *Bacillus subtilis*. *Antimicrob Agents Chemother* **48**: 2888–2896.

Maxson, M.E., and Darwin, A.J. (2006) PspB and PspC of Yersinia enterocolitica are dual function proteins: Regulators and effectors of the phage-shock-protein response. *Mol Microbiol* **59**: 1610–1623.

McCullough, J., Clippinger, A.K., Talledge, N., Skowyra, M.L., Saunders, M.G., Naismith, T. V., *et al.* (2015) Structure and membrane remodeling activity of ESCRT-III helical polymers. *Science (80-)* **350**: 1548–1551.

McMahon, H.T., and Boucrot, E. (2015) Membrane curvature at a glance. *J Cell Sci* **128**: 1065–1070.

Meer, G. Van, Voelker, D.R., and Feigenson, G.W. (2008) Membrane lipids: Where they are and how they behave. *Nat Rev Mol Cell Biol* **9**: 112–124.

Meeske, A.J., Riley, E.P., Robins, W.P., Uehara, T., Mekalanos, J.J., Kahne, D., *et al.* (2016) SEDS proteins are a widespread family of bacterial cell wall polymerases. *Nature* **537**: 634–638.

Meeske, A.J., Sham, L.-T., Kimsey, H., Koo, B.-M., Gross, C.A., Bernhardt, T.G., and Rudner, D.Z. (2015) MurJ and a novel lipid II flippase are required for cell wall biogenesis in *Bacillus subtilis*. *Proc Natl Acad Sci* **112**.

Mendoza, D. De, Klages Ulrich, A., and Cronan, J.E. (1983) Thermal regulation of membrane fluidity in *Escherichia coli*. Effects of overproduction of beta-ketoacyl-acyl carrier protein synthase I. *J Biol Chem* **258**: 2098–2101.

Mielich-süß, B. (2017) Elucidating structural and functional aspects of prokaryotic membrane microdomains. .

Mielich-Süss, B., and Lopez, D. (2015) Molecular mechanisms involved in *Bacillus subtilis* biofilm formation. *Environ Microbiol* **17**: 555–565.

Mielich-Süss, B., Schneider, J., and Lopez, D. (2013) Overproduction of Flotillin Influences Cell Differentiation and Shape in *Bacillus subtilis*. *Bacillus subtilis mBio* **4**: 719–732.

Miethke, M., Monteferrante, C.G., Marahiel, M.A., and Dijl, J.M. van (2013) The *Bacillus subtilis* EfeUOB transporter is essential for high-affinity acquisition of ferrous and ferric iron. *Biochim Biophys Acta - Mol Cell Res* **1833**: 2267–2278.

Mileykovskaya, E., and Dowhan, W. (2000) Visualization of phospholipid

domains in *Escherichia coli* by using the cardiolipin-specific fluorescent dye 10-N-nonyl acridine orange. *J Bacteriol* **182**: 1172–1175.

Milton R.J. Salton and Kwang-Shin Kim (1996) *Medical Microbiology. 4th edition. Chaper 2: Structure*. University of Texas Medical Branch at Galveston, Galveston (TX), .

Mirouze, N., Ferret, C., Cornilleau, C., and Carballido-López, R. (2018) Antibiotic sensitivity reveals that wall teichoic acids mediate DNA binding during competence in *Bacillus subtilis*. *Nat Commun 2018 91* **9**: 1–11.

Monteferrante, C.G., Miethke, M., Ploeg, R. Van Der, Glasner, C., and Dijl, J.M. Van (2012) Specific Targeting of the Metallophosphoesterase YkuE to the Bacillus Cell Wall Requires the Twin-arginine Translocation System. *J Biol Chem* **287**: 29789–29800.

Morrow, I.C., and Parton, R.G. (2005) Flotillins and the PHB domain protein family: Rafts worms and anaesthetics. *Traffic* **6**: 725–740.

Naslavsky, N., Stein, R., Yanai, A., Friedlander, G., and Taraboulos, A. (1997) Characterization of detergent-insoluble complexes containing the cellular prion protein and its scrapie isoform. *J Biol Chem* **272**: 6324–6331.

Neuhaus, F.C., and Baddiley, J. (2003) A Continuum of Anionic Charge: Structures and Functions of d-Alanyl-Teichoic Acids in Gram-Positive Bacteria. *Microbiol Mol Biol Rev* **67**: 686.

Neumann-Giesen, C., Falkenbach, B., Beicht, P., Claasen, S., Lüers, G., Stuermer, C.A.O., *et al.* (2004) Membrane and raft association of reggie-1/flotillin-2: role of myristoylation, palmitoylation and oligomerization and induction of filopodia by overexpression. *Biochem J* **378**: 509–518.

Nickels, J.D., Chatterjee, S., Stanley, C.B., Qian, S., Cheng, X., Myles, D.A.A., *et al.* (2017) The in vivo structure of biological membranes and evidence for lipid domains. *PLoS Biol* **15**.

Nickels, J.D., Poudel, S., Chatterjee, S., Farmer, A., Cordner, D., Campagna, S.R., *et al.* (2020) Impact of Fatty-Acid Labeling of *Bacillus subtilis* Membranes on the Cellular Lipidome and Proteome. *Front Microbiol* **11**: 914.

Ohtomo, Y., Kakegawa, T., Ishida, A., Nagase, T., and Rosing, M.T. (2014) Evidence for biogenic graphite in early archaean isua metasedimentary rocks. *Nat Geosci* **7**: 25–28.

Ooij, C. Van, and Losick, R. (2003) Subcellular Localization of a Small Sporulation Protein in *Bacillus subtilis*. *J Bacteriol* **185**: 1391.

Ourisson, G., and Albrecht, P. (1992) Hopanoids. 1. Geohopanoids: The Most Abundant Natural Products on Earth? *Acc Chem Res* **25**: 398–402.

Ourisson, G., Rohmer, M., and Poralla, K. (1987) Prokaryotic hopanoids and other polyterpenoid sterol surrogates. *Annu Rev Microbiol* **41**: 301–333.

Palmer, T., Sargent, F., and Berks, B.C. (2005) Export of complex cofactor-containing proteins by the bacterial Tat pathway. *Trends Microbiol* **13**: 175–180.

Pasquina-Lemonche, L., Burns, J., Turner, R.D., Kumar, S., Tank, R., Mullin, N., *et al.* (2020a) The architecture of the Gram-positive bacterial cell wall. *Nature* **294**.

Pasquina-Lemonche, L., Burns, J., Turner, R.D., Kumar, S., Tank, R., Mullin, N., *et al.* (2020b) The architecture of the Gram-positive bacterial cell wall. *Nat 2020 5827811* **582**: 294–297.

Pike, L.J. (2003) Lipid rafts: bringing order to chaos. *J Lipid Res* **44**: 655–667.

Pike, L.J. (2006) Rafts defined: a report on the Keystone symposium on lipid rafts and cell function. *J Lipid Res* **47**: 1597–1598.

Pizzo, P., Giurisato, E., Tassi, M., Benedetti, A., Pozzan, T., and Viola, A. (2002) Lipid rafts and T cell receptor signaling. *Eur J Immunol* **32**: 3082–3091.

Plessis, D.J.F. Du, Nouwen, N., and Driessen, A.J.M. (2011) The Sec translocase. *Biochim Biophys Acta - Biomembr* **1808**: 851–865.

Pohlschröder, M., Prinz, W.A., Hartmann, E., and Beckwith, J. (1997) Protein translocation in the three domains of life: variations on a theme. *Cell* **91**: 563–566.

Pop, O., Martin, U., Abel, C., and Müller, J.P. (2002) The twin-arginine signal peptide of PhoD and the TatAd/Cd proteins of *Bacillus subtilis* form an autonomous tat translocation system. *J Biol Chem* **277**: 3268–3273.

Popham, D.L., and Setlow, P. (1995) Cloning, nucleotide sequence, and mutagenesis of the *Bacillus subtilis* ponA operon, which codes for penicillin-binding protein (PBP) 1 and a PBP-related factor. *J Bacteriol* **177**: 326–335.

Popp, P.F., Benjdia, A., Strahl, H., Berteau, O., and Mascher, T. (2020) The Epipeptide YydF Intrinsically Triggers the Cell Envelope Stress Response of *Bacillus subtilis* and Causes Severe Membrane Perturbations. *Front Microbiol* **11**.

Popp, P.F., Gumerov, V.M., Andrianova, E.P., Bewersdorf, L., Mascher, T., Zhulin, I.B., *et al.* (2022) Phyletic Distribution and Diversification of the Phage Shock Protein Stress Response System in Bacteria and Archaea. .

Poralla, K., Härtner, T., and Kannenberg, E. (1984) Effect of temperature and pH on the hopanoid content of Bacillus acidocaldarius. *FEMS Microbiol Lett* **23**: 253–256.

Porrini, L., Cybulski, L.E., Altabe, S.G., Mansilla, M.C., and Mendoza, D. de (2014) Cerulenin inhibits unsaturated fatty acids synthesis in *Bacillus subtilis* by modifying the input signal of DesK thermosensor. *Microbiologyopen* **3**: 213–224.

Prabudiansyah, I., and Driessen, A.J.M. (2017) The Canonical and Accessory Sec System of Gram-positive Bacteria. *Curr Top Microbiol Immunol* **404**.

Prior, I.A., Muncke, C., Parton, R.G., and Hancock, J.F. (2003) Direct visualization of Ras proteins in spatially distinct cell surface microdomains. *J Cell Biol* **160**: 165–170.

Quinn, P.J. (2012) Lipid–lipid interactions in bilayer membranes: Married couples and casual liaisons. *Prog Lipid Res* **51**: 179–198.

Radeck, J., Fritz, G., and Mascher, T. (2017) The cell envelope stress response of *Bacillus subtilis*: from static signaling devices to dynamic regulatory network. *Curr Genet* **63**: 79–90.

Radeck, J., Gebhard, S., Orchard, P.S., Kirchner, M., Bauer, S., Mascher, T., and Fritz, G. (2016) Anatomy of the bacitracin resistance network in *Bacillus subtilis*. *Mol Microbiol* **100**: 607–620.

Raetz, C.R.H., and Dowhan, W. (1990) Biosynthesis and function of phospholipids in *Escherichia coli*. *J Biol Chem* **265**: 1235–1238.

Rajagopal, M., and Walker, S. (2015) Envelope Structures of Gram-Positive Bacteria. *Curr Top Microbiol Immunol* **404**: 1–44.

Ramamurthi, K.S., Lecuyer, S., Stone, H.A., and Losick, R. (2009) Geometric Cue for Protein Localization in a Bacterium. *Science* **323**: 1354.

Ravi, J., Anantharaman, V., Chen, S.Z., Datta, P., Aravind, L., and Gennaro, M.L. (2021) The Phage-shock-protein (PSP) Envelope Stress Response: Discovery of Novel Partners and Evolutionary History. *bioRxiv* .

Remaut, H., and Fronzes, R. (2014) Bacterial membranes: structural and molecular biology. .

Rexroth, S., Mullineaux, C.W., Ellinger, D., Sendtko, E., Rögner, M., and Koenig, F. (2011) The plasma membrane of the cyanobacterium Gloeobacter violaceus contains segregated bioenergetic domains. *Plant Cell* **23**: 2379–2390.

Riento, K., Frick, M., Schafer, I., and Nichols, B.J. (2009) Endocytosis of flotillin-1 and flotillin-2 is regulated by Fyn kinase. *J Cell Sci* **122**: 912–918.

Rivera-Milla, E., Stuermer, C.A.O., and Málaga-Trillo, E. (2006a) Ancient origin of reggie (flotillin), reggie-like, and other lipid-raft proteins: Convergent evolution of the SPFH domain. *Cell Mol Life Sci* **63**: 343–357.

Rivera-Milla, E., Stuermer, C.A.O., and Málaga-Trillo, E. (2006b) Ancient origin of reggie (flotillin), reggie-like, and other lipid-raft proteins: Convergent evolution of the SPFH domain. *Cell Mol Life Sci* **63**: 343–357.

Rizk, S., Henke, P., Santana-Molina, C., Martens, G., Gnädig, M., Nguyen, N.A., *et al.* (2021) Functional diversity of isoprenoid lipids in Methylobacterium extorquens PA1. *Mol Microbiol* **116**: 1064–1078.

Rodriguez-Boulan, E., and Nelson, W.J. (1989) Morphogenesis of the Polarized Epithelial Cell Phenotype. *Science (80-)* **245**: 718–725.

Rohmer, M., Bouvier, P., and Ourisson, G. (1979) Molecular evolution of biomembranes: structural equivalents and phylogenetic precursors of sterols. *Proc Natl Acad Sci U S A* **76**: 847–851.

Rudner, D.Z., and Losick, R. (2010) Protein Subcellular Localization in Bacteria. *Cold Spring Harb Perspect Biol* **2**.

Rueff, A.-S., Chastanet, A., Domínguez-Escobar, J., Yao, Z., Yates, J., Prejean, M.-V., *et al.* (2014) An early cytoplasmic step of peptidoglycan synthesis is associated to MreB in *Bacillus subtilis*. *Mol Microbiol* **91**: 348–362.

Sáenz, J.P., Grosser, D., Bradley, A.S., Lagny, T.J., Lavrynenko, O., Broda, M., and Simons, K. (2015) Hopanoids as functional analogues of cholesterol in

bacterial membranes. *Proc Natl Acad Sci* **112**.

Sáenz, J.P., Sezgin, E., Schwille, P., and Simons, K. (2012) Functional convergence of hopanoids and sterols in membrane ordering. *Proc Natl Acad Sci U S A* **109**: 14236–14240.

Salzberg, L.I., and Helmann, J.D. (2008) Phenotypic and transcriptomic characterization of *Bacillus subtilis* mutants with grossly altered membrane composition. *J Bacteriol* **190**: 7797–7807.

Salzer, U., and Prohaska, R. (2001) Stomatin, flotillin-1, and flotillin-2 are major integral proteins of erythrocyte lipid rafts. *Blood* **97**: 1141–1143.

Sawant, P., Eissenberger, K., Karier, L., Mascher, T., and Bramkamp, M. (2016) A dynamin-like protein involved in bacterial cell membrane surveillance under environmental stress. *Environ Microbiol* **18**: 2705–2720.

Scheffers, D.-J., and Tol, M.B. (2015) LipidII: Just Another Brick in the Wall? *PLoS Pathog* **11**: e1005213.

Scheidt, H.A., and Huster, D. (2009) Structure and dynamics of the myristoyl lipid modification of Src peptides determined by 2H solid-state NMR spectroscopy. *Biophys J* **96**: 3663–3672.

Schirner, K., Eun, Y.J., Dion, M., Luo, Y., Helmann, J.D., Garner, E.C., and Walker, S. (2015) Lipid-linked cell wall precursors regulate membrane association of bacterial actin MreB. *Nat Chem Biol* **11**: 38–45.

Schneider, J., Mielich-Süss, B., Böhme, R., and Lopez, D. (2015) In vivo characterization of the scaffold activity of flotillin on the membrane kinase KinC of *Bacillus subtilis*. *Microbiology* **161**: 1871–1887.

Scholz, A.S., Baur, S.S.M., Wolf, D., and Bramkamp, M. (2021) An Stomatin, Prohibitin, Flotillin, and HflK/C-Domain Protein Required to Link the Phage-Shock Protein to the Membrane in *Bacillus subtilis*. *Front Microbiol* **0**: 3156.

Schroeder, R., London, E., and Brown, D. (1994) Interactions between saturated acyl chains confer detergent resistance on lipids and glycosylphosphatidylinositol (GPI)-anchored proteins. *Proc Natl Acad Sci USA* **91**: 12130–12134.

Schroeder, R.J., Ahmed, S.N., Zhu, Y., London, E., and Brown, D.A. (1998) Cholesterol and sphingolipid enhance the Triton X-100 insolubility of glycosylphosphatidylinositol-anchored proteins by promoting the formation of detergent-insoluble ordered membrane domains. *J Biol Chem* **273**: 1150–1157.

Schuck, S., Honsho, M., Ekroos, K., Shevchenko, A., and Simons, K. (2003) Resistance of cell membranes to different detergents. *Proc Natl Acad Sci* **100**: 5795–5800.

Schulte, T., Paschke, K.A., Laessing, U., Lottspeich, F., and Stuermer, C.A.O. (1997) Reggie-1 and reggie-2, two cell surface proteins expressed by retinal ganglion cells during axon regeneration. *Development* **124**: 577–587.

Seel, W., Baust, D., Sons, D., Albers, M., Etzbach, L., Fuss, J., and Lipski, A. (2020) Carotenoids are used as regulators for membrane fluidity by Staphylococcus xylosus. *Sci Reports 2020 101* **10**: 1–12.

Sengupta, P., and Garrity, P. (2013) Sensing temperature. *Curr Biol* **23**.

Shivaji, S., and Prakash, J.S.S. (2010) How do bacteria sense and respond to low temperature? *Arch Microbiol* **192**: 85–95.

Shrivastava, R. (2019) Lipid trafficking across the Gram-negative cell envelope. *J Biol Chem* **294**: 14175–14184.

Siebenaller, C., and Schneider, D. (2023) Cyanobacterial membrane dynamics in the light of eukaryotic principles. *Biosci Rep* **43**.

Siegel, S., Liu, J., and Ton-That, H. (2016) Biogenesis of the Gram-positive bacterial cell envelope. *Curr Opin Microbiol* **34**: 31–37.

Siliakus, M.F., Oost, J. van der, and Kengen, S.W.M. (2017) Adaptations of archaeal and bacterial membranes to variations in temperature, pH and pressure. *Extremophiles* **21**: 651–670.

Simons, K., and Ehehalt, R. (2002) Cholesterol, lipid rafts, and disease. *J Clin Invest* **110**: 597–603.

Simons, K., and Ikonen, E. (1997) Functional rafts in cell membranes. *Nature* **387**: 569–572.

Simons, K., and Meer, G. Van (1988) Lipid sorting in epithelial cells. *Biochemistry* **27**: 6197–6202.

Simons, K., and Toomre, D. (2000) Lipid rafts and signal transduction. *Nat Rev Mol Cell Biol* **1**: 31–39.

Simons, K., and Vaz, W.L.C. (2004) Model Systems, Lipid Rafts, and Cell Membranes. *Annu Rev Biophys Biomol Struct* **33**: 269–95.

Singer, S.J., and Nicolson, G.L. (1972a) The Fluid Mosaic Model of the Structure of Cell Membranes. *Science (80-)* **175**.

Singer, S.J., and Nicolson, G.L. (1972b) The fluid mosaic model of the structure of cell membranes. *Science (80-)* **175**: 720–31.

Sjodt, M., Rohs, P.D.A., Gilman, M.S.A., Erlandson, S.C., Zheng, S., Green, A.G., *et al.* (2020) Structural coordination of polymerization and crosslinking by a SEDS-bPBP peptidoglycan synthase complex. *Nat Microbiol* **5**: 813–820.

Sohlenkamp, C., and Geiger, O. (2016) Bacterial membrane lipids: diversity in structures and pathways. *FEMS Microbiol Rev* **40**: 133–159.

Sohlenkamp, C., Schubotz, F., Villanueva, L., Nickels, J.D., Elkins, J.G., Poudel, S., *et al.* (2020) Impact of Fatty-Acid Labeling of *Bacillus subtilis* Membranes on the Cellular Lipidome and Proteome. .

Solis, G.P., Hoegg, M., Munderloh, C., Schrock, Y., Malaga-Trillo, E., Rivera-Milla, E., and Stuermer, C.A.O. (2007) Reggie/flotillin proteins are organized into stable tetramers in membrane microdomains. *Biochem J* **403**: 313.

Staneva, G., Seigneuret, M., Koumanov, K., Trugnan, G., and Angelova, M.I. (2005) Detergents induce raft-like domains budding and fission from giant unilamellar heterogeneous vesicles: a direct microscopy observation. *Chem Phys Lipids* **136**: 55–66.

Staroń, A., Finkeisen, D.E., and Mascher, T. (2011) Peptide antibiotic sensing and detoxification modules of *Bacillus subtilis*. *Antimicrob Agents Chemother* **55**: 515–525.

Strahl, H., Bürmann, F., and Hamoen, L.W. (2014) The actin homologue MreB organizes the bacterial cell membrane. *Nat Commun* **5**: 3442.

Subczynski, W.K., Markowska, E., Gruszecki, W.I., and Sielewiesiuk, J. (1992) Effects of polar carotenoids on dimyristoylphosphatidylcholine membranes: a spin-label study. *Biochim Biophys Acta - Biomembr* **1105**: 97–108.

Suutari, M., and Laakso, S. (1994) Microbial fatty acids and thermal adaptation. *Crit Rev Microbiol* **20**: 285–328.

Swoboda, J.G., Campbell, J., Meredith, T.C., and Walker, S. (2010) Wall Teichoic Acid Function, Biosynthesis, and Inhibition. *Chembiochem* **11**: 35.

Taguchi, A., Welsh, M.A., Marmont, L.S., Lee, W., Sjodt, M., Kruse, A.C., *et al.* (2019) FtsW is a peptidoglycan polymerase that is functional only in complex with its cognate penicillin-binding protein. *Nat Microbiol* **4**: 587–594.

Tanaka, T., Sano, R., Yamashita, Y., and Yamazaki, M. (2004) Shape changes and vesicle fission of giant unilamellar vesicles of liquid-ordered phase membrane induced by lysophosphatidylcholine. *Langmuir* **20**: 9526–9534.

Tavernarakis, N., Driscoll, M., and Kyrpides, N.C. (1999) The SPFH domain: Implicated in regulating targeted protein turnover in stomatins and other membrane-associated proteins. *Trends Biochem Sci* .

Taylor, R.F. (1984) Bacterial triterpenoids. .

Teeffelen, S. Van, Wang, S., Furchtgott, L., Huang, K.C., Wingreen, N.S., Shaevitz, J.W., and Gitai, Z. (2011) The bacterial actin MreB rotates, and rotation depends on cell-wall assembly. *Proc Natl Acad Sci U S A* **108**: 15822–15827.

Teixeira, V., Feio, M.J., and Bastos, M. (2012) Role of lipids in the interaction of antimicrobial peptides with membranes. *Prog Lipid Res* **51**: 149–177.

Thurotte, A., Br€, T., Mascher, T., and Schneider, D. (2017) Membrane chaperoning by members of the PspA/IM30 protein family. *Commun Integr Biol* **10**.

Tilburg, A.Y. van, Warmer, P., Heel, A.J. van, Sauer, U., and Kuipers, O.P. (2021) Membrane composition and organization of *Bacillus subtilis* 168 and its genome-reduced derivative miniBacillus PG10. *Microb Biotechnol* .

Trachtenberg, S. (2005) Mollicutes. *Curr Biol* **15**: R483–R484.

Turner, R.D., Ratcliffe, E.C., Wheeler, R., Golestanian, R., Hobbs, J.K., and Foster, S.J. (2010) Peptidoglycan architecture can specify division planes in Staphylococcus aureus. *Nat Commun* **1**.

Vereb, G., Szöllosi, J., Matkó, J., Nagy, P., Farkas, T., Vígh, L., *et al.* (2003) Dynamic, yet structured: The cell membrane three decades after the Singer-Nicolson model. *Proc Natl Acad Sci U S A* **100**: 8053–8058.

Vollmer, W., and Seligman, S.J. (2010) Architecture of peptidoglycan: more data and more models. *Trends Microbiol* **18**: 59–66.

Wachi, M., Doi, M., Tamaki, S., Park, W., Nakajima-Iijima, S., and Matsuhashi, M. (1987) Mutant isolation and molecular cloning of mre genes, which determine cell shape, sensitivity to mecillinam, and amount of penicillin-binding proteins in *Escherichia coli*. *J Bacteriol* **169**: 4935–4940.

Wagner, R.M., Kricks, L., and Lopez, D. (2017) Functional Membrane Microdomains Organize Signaling Networks in Bacteria. *J Membr Biol* **250**: 367–378.

Wallin, E., and Heijne, G. Von (1998) Genome-wide analysis of integral membrane proteins from eubacterial, archaean, and eukaryotic organisms. *Protein Sci* **7**: 1029–1038.

Weidel, W., and Pelzer, H. (1964) *Bagshaped Macromolecules - A new outlook on bacterial cell walls.* Adv Enzymol Relat Subj Biochem, .

Wendt, K., Poralla, K., and Schulz, G. (1997) Structure and function of a squalene cyclase. *Science* **277**.

Wessel, A.K., Yoshii, Y., Reder, A., Boudjemaa, R., Szczesna, M., Betton, J.-M., *et al.* (2022) *Escherichia coli* membrane microdomain SPFH protein HflC interacts with YajC and contributes to aminoglycoside and oxidative stress tolerance. *bioRxiv* 2022.07.25.501378.

Wiegert, T., Homuth, G., Versteeg, S., and Schumann, W. (2001) Alkaline shock induces the *Bacillus subtilis* σw regulon. *Mol Microbiol* **41**: 59–71.

Willdigg, J.R., and Helmann, J.D. (2021) Mini Review: Bacterial Membrane Composition and Its Modulation in Response to Stress. *Front Mol Biosci* **8**.

Wolf, D., Kalamorz, F., Wecke, T., Juszczak, A., Mäder, U., Homuth, G., *et al.* (2010) In-depth profiling of the LiaR response of bacillus subtilis. *J Bacteriol* **192**: 4680–4693.

Wong, F., Garner, E.C., and Amir, A. (2019) Mechanics and dynamics of translocating mreb filaments on curved membranes. *Elife* **8**.

Wunderlich, F., Ronai, A., Speth, V., Seelig, J., and Blume, A. (1975) Thermotropic Lipid Clustering in Tetrahymena Membranes. *Biochemistry* **14**: 3730–3735.

Yamaguchi, S., and Darwin, A.J. (2012) Recent findings about the Yersinia enterocolitica phage shock protein response. *J Microbiol* **50**: 1–7.

Yepes, A., Schneider, J., Mielich, B., Koch, G., García-Betancur, J.-C., Ramamurthi, K.S., *et al.* (2012) The biofilm formation defect of a *Bacillus subtilis* flotillin-defective mutant involves the protease FtsH. .

Yuan, J., Zweers, J.C., Dijl, J.M. Van, and Dalbey, R.E. (2010) Protein transport across and into cell membranes in bacteria and archaea. *Cell Mol Life Sci* **67**: 179–199.

Zhang, Y.M., and Rock, C.O. (2008) Membrane lipid homeostasis in bacteria. *Nat Rev Microbiol* **6**: 222–233.

Zhao, F., Zhang, J., Liu, Y.S., Li, L., and He, Y.L. (2011) Research advances on flotillins. *Virol J* **8**: 1–6.

Zielińska, A., Savietto, A., Borges, A. de S., Martinez, D., Berbon, M., Roelofsen, J.R., *et al.* (2020) Flotillin-mediated membrane fluidity controls peptidoglycan synthesis and mreb movement. *Elife* **9**: 1–21.

Zoued, A., Brunet, Y.R., Durand, E., Aschtgen, M.S., Logger, L., Douzi, B., *et al.* (2014) Architecture and assembly of the Type VI secretion system. *Biochim Biophys Acta - Mol Cell Res* **1843**.

ACKNOWLEDGMENTS

First of all, I want to thank Prof. Dr. Marc Bramkamp, for offering me the chance to work in this project in his lab and for your guidance through the years. Marc, I want to dearly thank you for being a supervisor who had unlimited time for discussions - scientific or not - and for sharing your enthusiasm and motivation, for your advices and for supporting me in any possible way.

I am also thankful to all members of my thesis committee for their interest in my topic and for their time. Especially, I would like to thank Prof Dr. Jörg Nickelsen, who agreed on being the second reviewer of my thesis. I am particularly thankful for all the helpful input of Prof. Dr. Jörg Nickelsen and Prof Dr. Thorben Cordes, members of my Thesis Advisory Committee in the course of my doctoral studies.

Moreover, I would like to thank all collaborators who I worked with over the years, especially Prof. Dr. Dirk-Jan Scheffers and Dr. Aleksandra Zielińska. Thank you for the productive meetings in Groningen or Munich – it was a great fun working with both of you.

I want to thank the German Academic Exchange Services (DAAD) for financially supporting my doctoral studies and especially Ms. Maria Salgado, my DAAD coordinator, for her efforts and availability to treat all funding related matters.

A thank you also goes to the former and current Programme coordinators of the LSM Graduate School Francisca Rosa Mendez, Nadine Hamze and Korbinian Dischinger, for all the hard work you put in to giving us students the best trainings and academic support.

I want to dearly thank the people I spent most time with in the past years - the present “northern” and past “southern” members of the lab - Manu, Giacomo, Helge, Fabian, Feng Peng, Kati, Lijun, Gustavo, Karin and Nadine, Dagmar, Holger and Ulrike. Our lab has an exceptional working atmosphere full of helpfulness, openness and interest, wherever it is located: in Munich or Kiel. Thank you all for building up and keeping this environment. I will miss working with all of you. Thank you also to the master students Tabea and Sarah.

I want to thank my CBI family, for still being around does not matter the distance. I am extremely grateful and lucky for having you since 2009. I am eternally grateful to my family – German and Brazilian – for all their unconditional support and for making my life better in every way. Finally, thank you Justus, for being a constant in my life and for all the love and happiness you and Vincent brought into my life.

CURRICULUM VITAE

Personal Information

Name: Abigail Savietto Scholz

Educational and Professional Experiences

2024-today **Clinical Project Manager of Oncology Imaging** at Clario

2022 – 2024 **Associate Clinical Project Manager** at Clario

2019 – 2022 **Doctoral student** in the group of Prof. Dr. Marc Bramkamp at CAU-Kiel
Supervisor: Prof. Dr Marc Bramkamp

2017 – 2022 **Doctoral Student** at Ludwig-Maximilians-Universität München (LMU)
Supervisor: Prof. Dr Marc Bramkamp

2016 – 2017 **Senior Microbiologist** at Colep Brazil Personal Care & Creams (São Paulo)

2014 – 2016 **MSc. in Applied Microbiology – São Paulo State University (UNESP, Rio Claro)**
Thesis title: Alkyl gallates derivatives used as antibacterial agents against citrus canker.
Supervisors: Dr. Dirk-Jan Scheffers (University of Groningen) and Dr. Henrique Ferreira (UNESP)

2015 – 2015 **Visitor Researcher** as Master's student at University of Groningen (The Netherlands)

2012 – 2013 **Young Talent** at the R&D Cosmetic Formulation Laboratory - Natura Cosméticos

2009 – 2013 **B.Sc and Licentiate in Biological Sciences São Paulo State University (UNESP, Rio Claro)**
Thesis title: Antibacterial activity of deodorant formulas containing natural deodorants actives.
Supervisor: Prof. Dr. Fernando Carlos Pagnocca

Publications

1. **Savietto, A.**, Polaquini, C.R., Kopacz, M. *et al.* Antibacterial activity of monoacetylated alkyl gallates against *Xanthomonas citri subsp. citri*. Arch Microbiol 200, 929–937 (2018). https://doi.org/10.1007/s00203-018-1502-6

2. Zielińska A, **Savietto A**, de Sousa Borges A, Martinez D, Berbon M, Roelofsen JR, Hartman AM, de Boer R, Van der Klei IJ, Hirsch AK, Habenstein B, Bramkamp M, Scheffers DJ. Flotillin-mediated membrane fluidity controls peptidoglycan synthesis and MreB movement. eLife. 2020 Jul 14;9:e57179. doi: 10.7554/eLife.57179. (Shared co-first authorship).
3. **Scholz AS**, Baur SSM, Wolf D and Bramkamp M (2021) An Stomatin, Prohibitin, Flotillin, and HflK/C-Domain Protein Required to Link the Phage-Shock Protein to the Membrane in *Bacillus subtilis*. Front. Microbiol. 12:754924. doi: 10.3389/fmicb.2021.754924

Academic Achievements and Prices

07/2017 -2022	Scholarship from DAAD (GSSP) – German Academic Exchange Service (Graduate School Scholarship Program) during doctoral studies.
2017-2022	Member of the LSM Gradute School, Life Sciences Muenchen
2014 - 2016	Scholarship from FAPESP (Research Support Foundation of São Paulo) during master's degree.
2015	Scholarship from BEPE FAPESP (International scholarship) during master's degree.
2010-2013	Board member at Tutorial Educational Program (PET), Brazilian Educational Ministry (SeSuMec).
2010-2012	Scholarship from SeSuMec as Educational Tutor (PET).
2011	Student representative of the standing Extension Committee of São Paulo State University.

Conferences

2020	3rd Bacterial Cell Biology Conference, Nassau, Bahamas
2019	Annual Conference of the Association for General and Applied Microbiology (VAAM), Mainz, Germany
2018	Cell Biology Meeting of the Association for General and Applied Microbiology (VAAM), Marburg, Germany

Languages

Portuguese	Native speaker
English	Fluent oral and written (Working language since 2014)
German	Level B 2.1